

# **Iterative Identification and Control Design for Robust Performance**

**Wee Sit LEE**

B.Eng. University of Singapore  
M.Sc. National University of Singapore

September 1994

*A thesis submitted for the degree of Doctor of Philosophy  
of The Australian National University*

Department of Systems Engineering  
Research School of Information Sciences and Engineering  
The Australian National University



## Declaration

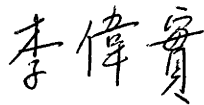
My doctoral studies were conducted under the guidance of Professor Brian D.O. Anderson and Dr. Iven M.Y. Mareels as supervisors, and Dr. Robert R. Bitmead as advisor. I also have the opportunity to work with Dr. Robert L. Kosut (from Integrated Systems Inc., USA) and Dr. Marco Campi (from Politecnico di Milano, Italy) during their visits to the Department of Systems Engineering, The Australian National University.

Most of the research results reported in this thesis have been published as academic papers in refereed journals, presented as conference papers, or have been submitted as academic papers to refereed journals. These papers are:

1. W.S.Lee, B.D.O.Anderson, R.L.Kosut, and I.M.Y.Mareels, On Adaptive Robust Control and Control-Relevant System Identification, *Proc. ACC'92 (Invited Session)*, 2834-2841, Chicago IL., Jun 1992.
2. W.S.Lee, B.D.O.Anderson, and I.M.Y.Mareels, New Algorithms for Adaptive Control, *Proc. IEAust CONTROL 92 Conference*, 97-108, Perth WA., Nov 1992.
3. W.S.Lee, B.D.O.Anderson, R.L.Kosut, and I.M.Y.Mareels, A New Approach to Adaptive Robust Control, *Int. J. Adaptive Control and Signal Processing*, Vol. 7, 183-211, (1993).
4. M.Campi, W.S.Lee, and B.D.O.Anderson, Filters for Internal Model Control Design for Unstable Plants, *Proc. IEEE CDC'93*, 1343-1348, San Antonio TX., Dec 1993.
5. W.S.Lee, B.D.O.Anderson, R.L.Kosut, and I.M.Y.Mareels, On Robust Performance Improvement through The Windsurfer Approach to Adaptive Robust Control, *Proc. IEEE CDC'93 (Invited Session)*, 2821-2827, San Antonio TX., Dec 1993.
6. M.Campi, W.S.Lee, and B.D.O.Anderson, New Filters for Internal Model Control Design, to appear in *Int. J. Robust and Nonlinear Control*, Vol. 4 (1994).
7. W.S.Lee, B.D.O.Anderson, I.M.Y.Mareels, and R.L.Kosut, On Some Practical Issues in System Identification for The Windsurfer Approach to Adaptive Control, *Proc. 10<sup>th</sup> IFAC Symposium on System Identification (Invited Session)*, 2, 165-170, Copenhagen, Denmark, Jul 1994.

8. W.S.Lee, B.D.O.Anderson, I.M.Y.Mareels, and R.L.Kosut, On Some Key Issues in The Windsurfer Approach to Adaptive Robust Control, (submitted to *Automatica*).

I hereby declare that the contents of this thesis are the results of original research except where appropriate referenced, and have not been submitted for a degree at any other university or educational institution. Roughly 70% of the work is my own.



Wee Sit LEE  
Department of Systems Engineering,  
Research School of Information Sciences and Engineering,  
The Australian National University,  
Canberra 0200, AUSTRALIA.

## Acknowledgements

I am indebted to Professor Brian D.O. Anderson and Dr. Iven M.Y. Mareels for their constructive criticism and guidance. I should also pay tribute to Iven for encouraging me to stay on and complete my Ph.D studies. I thank Dr. Robert R. Bitmead for valuable advice, and Professor John B. Moore, Head of the Department of Systems Engineering, for providing the stimulating academic environment. I should also thank Mr. James Ashton for advice on the use of computer software packages.

It is a pleasure to thank Dr. Robert L. Kosut and Dr. Marco Campi for very enjoyable collaborations, Professor Michel Gevers, Professor Paul M.J. Van den Hof, and Professor Bo Wahlberg for sharing their expert knowledge with me through technical advice and interesting discussions, and Dr. Duncan McFarlane and the Automation Technology Group of BHP Research for allowing me to experience industrial research at their Melbourne Laboratories.

I am grateful to the Graduate School of The Australian National University for the Ph.D Scholarship, and the Co-operative Research Centre of Robust and Adaptive System for the financial assistance and opportunities to gain industrial research experience.

To my dear Yin Hong, I could only say “wǒ ài nǐ” in the lack of better words to express my deepest appreciation for her selfless love and endless patience. I thank my mother, my brothers, and Karen for their understanding and supports. The close relationship with them has gone a long way to see me through the critical periods of my life.

Last but not least, I thank Ari Partanen (another iterator) for sharing with me his experience on the Zang-Bitmead-Gevers iterative scheme and the Sugar Cane Crushing Mill Project, and James Lam, Khiang Wee, Kok Lay, Meng Joo, Soon Huat, Sumeth, Zhuquan (a co-inventor of the Zang-Bitmead-Gevers iterative scheme), and all other friends who have involved in one way or another during the course of my studies.

## Abstract

In this thesis we are concerned with iterative identification and control design. We establish that, given an initial model which may represent the plant accurately only in the low frequency region, the iterative identification and control design paradigm propounded recently by Anderson and Kosut [1991] may achieve good closed-loop performance in the sense that the closed-loop system has a large bandwidth and good step responses.

We begin our investigation of the iterative identification and control design paradigm in the ideal situation where an infinite number of noiseless measurements are available for the plant input and output. The resulting iterative model approximation and control design procedure combines the Internal Model Control design method [Morari and Zafiriou 1989] and a control-relevant closed-loop model approximation procedure which employs Hansen's system identification framework [Hansen 1989]. This gives encouraging results that are supported by simulations. We then study the iterative identification and control design paradigm under realistic situations where only a finite number of noisy input-output measurements are available. At this stage we also consider plants that, other than having poles in the open left-half plane, may have one pole at the origin. This investigation provides further insights into the role of appropriate frequency weighting in the control-relevant closed-loop system identification procedure. It also supports the philosophy of iterative identification and control design.

Some crucial questions which arise in the iterative identification and control design methodology are examined in this thesis. This leads to further understanding of various mechanisms that may be helpful or harmful to the iterative identification and control design procedure. Furthermore, model validation methods are developed to improve the reliability of the closed-loop system identification procedure. The key conclusion is that, given a stable strictly proper model of a stable strictly proper plant, we can improve the performance robustness of the closed-loop system through iterative identification and control design if certain verifiable conditions are satisfied.

The applications of the iterative identification and control design paradigm is extended to the situation of unstable plants. This is achieved via a two step control design approach where the unstable plant is first stabilized by a strictly proper parallel output feedback

compensator. The iterative identification and control design methodology is then applied to the stabilized plant. Simulation results clearly demonstrated the advantages of the two step iterative identification and control design procedure in the situation of unstable plants.

Finally, the thesis concludes with a suggestion of future research directions.

# Contents

<b>1</b>	<b>Introduction</b>	<b>1</b>
1.1	Background and Motivation . . . . .	1
1.2	Review of Two Major Iterative Schemes . . . . .	6
1.2.1	Delft School's Approach . . . . .	7
1.2.2	Zang-Bitmead-Gevers Scheme . . . . .	14
1.3	A Glimpse of the Problems Concerned and Their Solutions . . . . .	17
1.4	Outline of the Thesis . . . . .	19
1.5	Point Summary of Thesis Contributions . . . . .	21
<b>2</b>	<b>Iterative Model Approximation and Control Design</b>	<b>23</b>
2.1	Two Main Control Design Approaches for Inexactly Known Plants . . . . .	24
2.2	Iterative Identification and Control Design - A New Paradigm . . . . .	26
2.3	An Adaptive $\mathcal{H}_\infty$ Model Matching Control Problem . . . . .	27
2.4	Closed-loop System Identification . . . . .	30
2.5	Internal Model Control Method . . . . .	36
2.6	Approximation of the $R_i^f$ Transfer Function . . . . .	44
2.7	Simulation Results . . . . .	50
2.8	Discussions . . . . .	57
<b>3</b>	<b>Iterative Identification and Control Design</b>	<b>59</b>
3.1	Frequency Weighted Identification Criterion . . . . .	60
3.2	Control Design for Type 1 Stable Plants . . . . .	64
3.3	Control-Relevant System Identification for Type 1 Stable Plants . . . . .	69
3.3.1	System Identification Criteria . . . . .	72
3.3.2	Signal Models . . . . .	72
3.3.3	Model Update Equations . . . . .	73
3.4	Iterative Algorithm for Stable Plants and Type 1 Stable Plants . . . . .	75

3.5	Simulation Results . . . . .	78
3.6	Summary . . . . .	86
<b>4</b>	<b>Some Key Issues in Iterative Identification and Control Design</b>	<b>88</b>
4.1	Introduction . . . . .	88
4.2	Nominal Performance Improvement and Robust Stability . . . . .	90
4.3	Properties of Good Models . . . . .	94
4.4	System Identification in the Iterative Identification and Control Design Approach . . . . .	97
4.4.1	Control-Relevant System Identification . . . . .	98
4.4.2	Accurate Identification of $R_0^f$ . . . . .	102
4.4.3	Practically Unbiased Estimation of $R_0^f$ . . . . .	107
4.5	Mechanisms that Influence Performance Robustness and Identification . . . . .	108
4.6	Identification and Validation of New Models . . . . .	111
4.6.1	A Frequency Domain Method for Model Validation . . . . .	112
4.6.2	A Time Domain Method for Model Validation . . . . .	113
4.6.3	Identification of A Better Model . . . . .	114
4.7	Robust Performance Improvement . . . . .	116
4.8	Simulation Results . . . . .	122
4.9	Summary . . . . .	133
<b>5</b>	<b>Iterative Identification and Control Design for Unstable Plants</b>	<b>135</b>
5.1	Introduction . . . . .	136
5.2	One Step Control Design Approach for Unstable Plants . . . . .	140
5.2.1	Outline of The One Step Control Design Approach . . . . .	140
5.2.2	Difficulties with The One Step Design Approach . . . . .	145
5.3	A Two Step Iterative Identification and Control Design Approach for Unstable Plants . . . . .	151
5.3.1	Outline of A Two Step Control Design Approach . . . . .	151
5.3.2	Design Guidelines for Parallel Feedback Stabilizer . . . . .	160
5.4	Simulation Results . . . . .	168
5.4.1	Example 1 . . . . .	169
5.4.2	Example 2 . . . . .	172
5.5	Summary and Discussions . . . . .	174
<b>6</b>	<b>Conclusions and Future Research Directions</b>	<b>192</b>



---

6.1	Conclusions . . . . .	192
6.2	Future Research Directions . . . . .	193
6.2.1	Immediate extensions . . . . .	194
6.2.2	Theoretical issues . . . . .	195
6.2.3	Practical investigations . . . . .	196
6.2.4	Model error characterization . . . . .	197
6.2.5	Adaptive control design framework . . . . .	197
6.3	Epilogue . . . . .	197
	<b>Appendices</b>	<b>199</b>
A	<b>Proof of Theorem 2.4.2 in Chapter 2</b>	<b>199</b>
B	<b>Proof of Theorem 2.6.1 in Chapter 2</b>	<b>202</b>
C	<b>Proof of Theorem 2.6.2 in Chapter 2</b>	<b>204</b>
D	<b>Proof of Theorem 3.2.2 in Chapter 3</b>	<b>205</b>
E	<b>Proof of Theorem 3.3.1 in Chapter 3</b>	<b>206</b>
F	<b>Proof of Theorem 4.7.2 in Chapter 4</b>	<b>208</b>
G	<b>Proof of Theorem 4.7.3 in Chapter 4</b>	<b>210</b>
H	<b>Programs and Information for Simulations</b>	<b>211</b>
	<b>Bibliography</b>	<b>227</b>

# Chapter 1

## Introduction

This thesis is concerned with a systematic study of iterative identification and control design. We establish in Section 1.1 that there is a need for iterative identification and control design procedures. Some general questions that are of interest to any iterative identification and control design procedure will also be presented. Recent developments in adaptive control and improved understanding of closed-loop system identification that have paved the road for iterative identification and control design are highlighted at the end of Section 1.1. We review in Section 1.2 two major iterative identification and control design schemes. In Section 1.3 we briefly explain how the questions posed in Section 1.1 for iterative identification and control design can be answered for a reference tracking problem where it is desirable that the closed-loop system has a large bandwidth and good step response. An outline of the thesis is given in Section 1.4 and a point summary of thesis contributions is provided in Section 1.5.

### 1.1 Background and Motivation

With reference to Figure 1.1, we consider the situation where it is desired to design a closed-loop system such that its output  $y$  will track a step reference input  $r$  in a well behaved manner. We assume that a model  $\bar{G}$  of the plant  $G$  is employed for designing the controller  $K$ . Obviously, step responses of the closed-loop system will depend on the **actual closed-loop transfer function**,

$$T = \frac{GK}{1 + GK} .$$

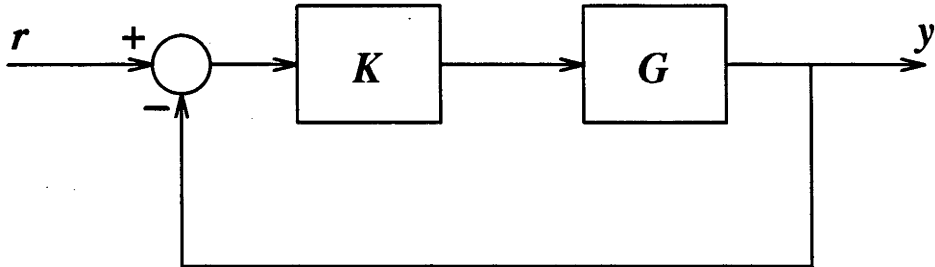


Figure 1.1: Closed-loop control system

Therefore, other than requiring  $T$  to be stable, it is desirable that  $T$  has a step response with small rise time, small settling time, small peak overshoot, and no steady-state error. In general, the control objectives that we have just mentioned are accomplished *indirectly* through designing the **designed closed-loop transfer function**,

$$\bar{T} = \frac{\bar{G}K}{1 + \bar{G}K} ,$$

on the basis of the model  $\bar{G}$  such that  $\bar{T}$  has a large bandwidth and small (or negligible) resonance peak in its frequency response. The set of performance specifications (either in time domain or frequency domain) that is achieved by the designed closed-loop system is termed the **nominal performance** of the closed-loop system. It is clear that the achieved performance of the actual closed-loop system (which involves  $G$  and  $K$ ) may not be the same as the performance of the designed closed-loop system (which involves  $\bar{G}$  and  $K$ ), especially when  $\bar{G}$  is a poor representation of  $G$ . To characterize the behaviour of the actual closed-loop transfer function  $T$  in terms of the behaviour of the designed closed-loop transfer function  $\bar{T}$ , we say that the closed-loop system has **robust performance** if the achieved performance of the actual closed-loop system is close to the performance of the designed closed-loop system. This is more demanding than the requirement of **robust stability** where stability of  $\bar{T}$  implies stability of  $T$ . (Precise definitions for robust stability, nominal performance, and robust performance will be provided in the sequel.)

In any closed-loop control system design problem, it is obvious that one would like to achieve *both* high nominal performance and good robust performance. To obtain this is not a trivial problem because, in general, the desired nominal performance and robust performance of the target closed-loop system may be incompatible with the accuracy of the available plant

model. In fact, it is usually *not known a priori* whether the specified requirements on the closed-loop system are achievable with the existing model. This is obviously different from the robust performance problem studied by robust control researchers, where the question of “What should be done if the existing model (and the associated bound on the modelling error that is assumed to be known by robust control researchers) does not allow the specified nominal performance and performance robustness to be attained *simultaneously* by the closed-loop system?” is left unanswered. Despite this shortcoming, it is undeniable that, starting with [Doyle and Stein 1981] and [Zames 1981], robust control research has in the last decade brought to the forefront of control engineering the many important concepts and tools for dealing with unavoidable model uncertainties. A good tutorial in robust control and  $\mathcal{H}_\infty$ -optimization was given recently by Kwakernaak [1993], and a historical review on robust control is given in [Dorato 1986].

We have noticed that in robust control, one seeks to guarantee stability robustness and performance robustness in the presence of significant modelling errors. However there are no attempts to actively reduce the modelling errors that may limit the nominal performance. Therefore, from the nominal performance point of view, robust control tends to result in conservative design. By taking the inherent shortcoming of robust control as a clue, one tends to jump to the conclusion that, by actively improving the model accuracy through on-line parameter estimation and making corresponding adjustment to the controller parameters, adaptive control will provide the route to high performance closed-loop control system. However, it is well known by now that traditional adaptive control [Goodwin and Sin 1984, Åström and Wittenmark 1989, Sastry and Bodson 1989] still has many practical difficulties [Ortega and Tang 1989, Bodson 1993], although significant progress was made in robust adaptive control in the last decade [Anderson *et al.* 1986, Åström and Wittenmark 1989, Sastry and Bodson 1989]. It is interesting to note that, although many researchers have realized that the underlying control design can play a major role in the performance robustness of an adaptive control system (especially when it is not known a priori that the desired nominal performance can be achieved with the assumed model structure), almost all of the robust adaptive controllers are robustified through modifications of the on-line parameter update schemes and no attempts were made to improve the robustness by modifying the underlying control design procedure. A possible reason for this is that, other than a few exceptions (see, for example, [Goodwin *et al.* 1985], [Tay *et al.* 1989], [Bitmead *et al.* 1990], and [Iglesias 1990]), robust control and adaptive control have been treated separately in their respective

framework and interactions between these techniques have been minimal. This results in the shortcoming that, in an attempt to attain certain specified closed-loop performance objectives through adaptation with a model whose structure is fixed a priori, (for example, by trying to match the closed-loop transfer function to a given reference model while paying no attention to the question of whether the desired nominal performance can be achieved robustly under the assumed model complexity), poor nominal performance or poor performance robustness are often the end results.

A further serious problem with traditional adaptive control is that *extreme transient excursions* are possible even when global convergence and asymptotic performance are guaranteed. These problems are very seldom discussed in the literature. Some of the exceptions are [Kosut *et al.* 1987], [Zang and Bitmead 1990], [Bodson 1993], and [Zang and Bitmead 1994]. The most serious criticism of adaptive control from a practical engineering point of view is perhaps, as it was pointed out by Ljung and Anderson [1984], that there is a lack of qualitative, or semi-quantitative, conceptual aids, especially those invoking frequency domain ideas, for designing adaptive control systems.

From the above short review, it is clear that the attitude taken by the traditional adaptive control community is too optimistic in the sense that it has relied too much on the assumed parametrized model structure being correct. On the other hand, the attitude taken by the robust control community is too pessimistic because it only attempts to accommodate, usually, the worst possible modelling errors, and has neglected the fact that characteristics of the plant could be learned while it is being controlled. We believe that these approaches should be able to complement each other and there should be natural ways in which they could be blended harmoniously. In the process of doing so, we hope to construct an engineering design framework for adaptive robust control. It is in this spirit that we are going to develop the new iterative identification and control design methodology.

Irrespective of the nominal performance and robust performance requirements that are problem specific, the central questions in the general area of iterative identification and control design are:

1. Given a (crude) model of a plant which is stabilized by a known controller (or equivalently, the plant is stabilized by a controller designed on the basis of the given model), is

- it possible to improve the nominal performance and robust performance of the closed-loop system through the iterative applications of a control design procedure and a system identification procedure?
2. In what way should a particular control design method be combined with a certain system identification procedure? This is a question of algorithm design and its answer will depend, in general, on the objective and performance measure of the target closed-loop system. In detail, this question could be decomposed into the next three questions.
    - (a) For a given control objective and performance measure, what is a suitable (or the best) control design method to be adopted?
    - (b) For a given control objective and performance measure, what is a suitable (or the best) system identification procedure?
    - (c) How could the selected control design method and system identification procedure be integrated such that they support each other in the manner that is most beneficial for achieving the overall control performance objective?
  3. For an iterative identification and control design approach that attempts to answer the last set of questions (given that a specific control performance objective is to be achieved), are there any performance limitations?

In this thesis we study the above issues for a new iterative identification and control design algorithm that is related to a reference tracking problem. Specifically, we would like to design a closed-loop system such that it has a sufficiently large bandwidth. Furthermore, it is desirable that the step response of the actual closed-loop system has no overshoot and little oscillations.

Although the iterative identification and control design methodology that we are going to study is not, from the traditional adaptive control point of view, an *on-line* adaptive control algorithm, it is, according to the definition given in [Zames and Wang 1992], an adaptive robust control paradigm. Furthermore, although Bitmead *et al.* [1990] has focussed on on-line adaptive control, their viewpoint is very similar to ours in iterative identification and control design.

Another feature of iterative identification and control design that we should mention is that the controller is fixed while a system identification experiment is being carried out. It is

therefore a linear systems problem, as opposed to the nonlinear systems problem in the traditional adaptive control scenario. This has the advantage of eliminating the peculiar behaviour of adaptive control that can be observed in ideal and non-ideal adaptive control systems [Anderson 1985, Mareels and Bitmead 1987, Bodson 1993]. Shimkin and Feuer [1988] have shown that, for traditional discrete-time adaptive control systems, if the parameters of the controller are updated only at the end of a block of data while the parameters are estimated (without controller updates) at every sample within the block of data, coupling between the system identification loop and the control loop is reduced and convergence can be proved for a number of adaptive control schemes.

We end this section by emphasizing that good understanding in the frequency domain behaviour of system identification methods only became available in the eighties through the works of Ljung and co-workers (see [Ljung 1985], [Wahlberg and Ljung 1986], [Ljung 1987] and the references therein). These have very quickly developed into the modern theory for the joint design of identification and control. (See for example, [Skelton 1985], [Gevers and Ljung 1986], [Hansen 1989], [Bitmead *et al.* 1990], [Liu and Skelton 1990], [Anderson and Kosut 1991], [Schrama and Van den Hof 1992], and [Schrama 1992a].) It is through these researches that the importance of appropriate treatments on system identification in closed-loop become appreciated and widely recognized. They have also paved the road for iterative identification and control design. For a good tutorial and historical perspective in joint design of identification and control, we refer to [Gevers 1993]. It is no doubt that these works will have long lasting impacts on forthcoming iterative identification and control design methodologies.

## 1.2 Review of Two Major Iterative Schemes

Iterative identification and control design has become a very active research area of control engineering in the last few years. This is evident from the following samples of publications: [Liu and Skelton 1990], [Zang *et al.* 1991, Zang *et al.* 1992, Partanen and Bitmead 1993c, Partanen *et al.* 1994], [Schrama and Van den Hof 1992, Schrama 1992a, Schrama 1992b, Van den Hof *et al.* 1993], [Anderson and Kosut 1991, Lee *et al.* 1993], and [Åström 1993]. At the current stage of development, two of these approaches have emerged as comparatively well studied. We briefly review in this section these two major iterative schemes, which

are known to the control community as the Delft School's approach and the Zang-Bitmead-Gevers scheme. As we concentrate on the broad pictures and main points, fine details and many recent developments in these schemes are inevitably omitted. For recent developments in the Delft School's approach, we refer to the journal "Selected Topics in Identification, Modelling and Control" (edited by Professor O.H. Bosgra and Professor P.M.J. Van den Hof) published by Delft University Press. Latest developments in the Zang-Bitmead-Gevers scheme are reported recently in [Partanen and Bitmead 1993c] and [Partanen *et al.* 1994].

### 1.2.1 Delft School's Approach

In the Delft School's approach [Schrama 1992a, Schrama 1992b, Van den Hof *et al.* 1993], the controller is designed by the method introduced by McFarlane and Glover [1990] and Bongers and Bosgra [1990]. Its overall control objective is described by the "four block"  $\mathcal{H}_\infty$ -optimal control problem, where the controller  $K$  in Figure 1.1 is designed to satisfy

$$\|T(G, K)\|_\infty \leq \gamma^{-1}$$

for a specific value of  $\gamma$ . Here

$$T(G, K) = \begin{bmatrix} GK/(1 + GK) & G/(1 + GK) \\ K/(1 + GK) & 1/(1 + GK) \end{bmatrix},$$

and  $G$  represents the plant transfer function. Schrama [1992b] has convincingly demonstrated that, ideally the overall control objective should be solved by *simultaneous* system identification and control design but, in practice, an iterative approach is necessary. The control design part of the Delft School's approach is accomplished at the  $i^{\text{th}}$  stage of iteration by designing a controller  $K_i$  such that

$$K_i = \arg \min_{\tilde{K}} \left\| T(\alpha_i G_i, \tilde{K}/\alpha_i) \right\|_\infty.$$

Observe that the model  $G_i$  used in the design of  $K_i$  is either obtained in the  $(i - 1)^{\text{th}}$  stage of iteration by performing a closed-loop system identification (to be described shortly) or given at the initial stage ( $i = 0$ ) of iteration by an open-loop system identification. The scalar variable  $\alpha_i$  is a nominal performance design parameter whose function will be highlighted shortly. The model  $G_{i+1}$  identified at the  $i^{\text{th}}$  stage of iteration will have a plant-model mismatch. In order that this mismatch is well tuned for achieving the overall control objective through



control re-design, the control-relevant system identification criterion is chosen as

$$G_{i+1} = \arg \min_{\tilde{G}} \left\| T(\alpha_i G, K_i/\alpha_i) - T(\alpha_i \tilde{G}, K_i/\alpha_i) \right\|_{\infty} .$$

Since it is infeasible to deal with  $\mathcal{H}_{\infty}$  system identification, an  $\mathcal{L}_2$  system identification problem,

$$G_{i+1} = \arg \min_{\tilde{G}} \left\| T(\alpha_i G, K_i/\alpha_i) - T(\alpha_i \tilde{G}, K_i/\alpha_i) \right\|_2 ,$$

is considered instead. The control-relevant closed-loop system identification problem formulated in the last equation is solved by recasting it into an open-loop system identification problem via a modified version of Hansen's system identification framework [Hansen 1989]. Specifically, instead of following [Hansen 1989] exactly, right coprime factorization as defined in [Vidyasagar 1985a] is employed by Schrama [1992b] and Van den Hof *et al.* [1993] to show that  $G$  can be identified through estimating the coprime factors ( $N$  and  $D$ ) in a fractional description of  $G$  (in the form of  $G = N/D$ ). They proceed as follows.

With reference to Figure 1.2, assume that the plant  $G$  is proper and is stabilized by the controller  $K_i = X_i/Y_i$ , where  $X_i$  and  $Y_i$  are coprime factors of  $K_i$ . Let  $G_x = N_x/D_x$  be an auxiliary proper transfer function that is also stabilized by  $K_i$ . (An obvious but may not be the best choice is  $G_x = G_i$ , where  $G_i$  is the model used to design  $K_i$  at the  $i^{\text{th}}$  stage of iteration.) The theory of Youla-parametrization then allows one to write

$$N = N_x + Y_i R , \quad (1.1)$$

and

$$D = D_x - X_i R , \quad (1.2)$$

where  $R$  is a stable proper transfer function. Furthermore, by defining an auxiliary signal

$$x = (D_x + K_i N_x)^{-1} (u + K_i y) ,$$

it can be shown that

$$y = N x + (1 + K_i G)^{-1} H e , \quad (1.3)$$

$$u = D x - K_i (1 + K_i G)^{-1} H e , \quad (1.4)$$

and

$$x = (D_x + K_i N_x)^{-1} r , \quad (1.5)$$

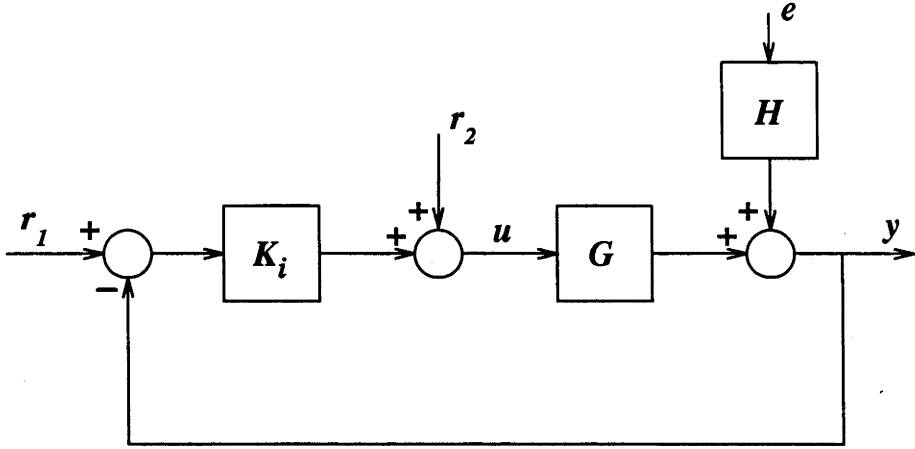


Figure 1.2: Iterative identification and control

where the signals  $u$  and  $y$  are measured (at the  $i^{\text{th}}$  stage of iteration) from the actual closed-loop system represented by Figure 1.2, and  $r = K_i r_1 + r_2$ . Observe that the auxiliary signal  $x$  can be generated by filtering known signals with known transfer functions.

Equation (1.5) clearly shows that  $x$  is uncorrelated with the noise disturbance  $e$  and hence equations (1.3) and (1.4) constitute a framework for performing open-loop system identification. Furthermore, it can be shown that

$$T(G, K_i) = \begin{bmatrix} N \\ D \end{bmatrix} \frac{1}{D_x + K_i N_x} \begin{bmatrix} K_i & 1 \end{bmatrix} .$$

By defining a parametrized set of models,

$$\mathcal{G} = \left\{ \tilde{G} : \tilde{G} = \frac{N(\theta)}{D(\theta)} \right\} ,$$

the following can be written

$$T(\tilde{G}(\theta), K_i) = \begin{bmatrix} N(\theta) \\ D(\theta) \end{bmatrix} \frac{1}{D_x + K_i N_x} \begin{bmatrix} K_i & 1 \end{bmatrix} .$$

Now it is easy to write

$$T(\alpha_i G, K_i/\alpha_i) = \begin{bmatrix} \alpha_i N \\ D \end{bmatrix} \frac{1}{D_x + K_i N_x} \begin{bmatrix} K_i/\alpha_i & 1 \end{bmatrix}$$

and

$$T(\alpha_i \tilde{G}(\theta), K_i/\alpha_i) = \begin{bmatrix} \alpha_i N(\theta) \\ D(\theta) \end{bmatrix} \frac{1}{D_x + K_i N_x} \begin{bmatrix} K_i/\alpha_i & 1 \end{bmatrix} .$$

To identify a plant  $G$ , Schrama [1992b] performs sine-wave experiments and measures the signals  $x$ ,  $y$ , and  $u$ . A frequency spectral analyzer is then employed to estimate frequency response of  $N$  and  $D$  over a set of discrete frequencies  $\Omega = \{\omega_i : i = 1, 2, \dots, M\}$ . These are then treated as the actual frequency responses for the coprime factors of the plant. Denote these frequency response samples as  $N(j\omega_i)$  and  $D(j\omega_i)$ , and define

$$J(\theta, j\omega_i) = \left\| \left[ \begin{array}{c} \alpha_i N(j\omega_i) \\ D(j\omega_i) \end{array} \right] - \left[ \begin{array}{c} \alpha_i N(\theta, j\omega_i) \\ D(\theta, j\omega_i) \end{array} \right] [D_i(j\omega_i) + K_i(j\omega_i)N_i(j\omega_i)]^{-1} \right\|^2,$$

the optimal parameter vector  $\theta^*$  is then obtained by solving the nonlinear optimization problem

$$\theta^* = \arg \min_{\theta} \sum_{i=1}^M J(\theta, j\omega_i) [1 + |K_i(j\omega_i)/\alpha_i|^2]$$

by Newton-Raphson method. The model is then updated as

$$G_{i+1}(\theta^*) = \frac{N(\theta^*)}{D(\theta^*)}$$

before the iteration process continues.

It is important to observe from equations (1.1) and (1.2) that both  $N$  and  $D$  are parametrized by a single stable transfer function  $R$ . If  $N$  and  $D$  are estimated independently in the presence of noise, their estimates may not be consistent in the sense that they may not be parametrized by a single stable transfer function like equations (1.1) and (1.2).

In [Van den Hof *et al.* 1993] the control-relevant system identification are considered in the time domain. The control-relevant system identification criterion adopted is

$$G_{i+1} = \arg \min_{\tilde{G}} \|T(G, K_i) - T(\tilde{G}, K_i)\|_2.$$

With reference to Figure 1.2, it can be seen that  $T(G, K_i)$  relates the signals in the actual closed-loop system as follows

$$\begin{bmatrix} y \\ u \end{bmatrix} = T(G, K_i) \begin{bmatrix} r_1 \\ r_2 \end{bmatrix}.$$

Corresponding to the last equation, we can write

$$\begin{bmatrix} \bar{y} \\ \bar{u} \end{bmatrix} = T(\tilde{G}, K_i) \begin{bmatrix} r_1 \\ r_2 \end{bmatrix}.$$

It is easy to observe that the effects of closed-loop mismatch  $T(G, K_i) - T(\tilde{G}, K_i)$  will be reflected by the error signals

$$\begin{bmatrix} \Delta_y \\ \Delta_u \end{bmatrix} = [T(G, K_i) - T(\tilde{G}, K_i)] \begin{bmatrix} r_1 \\ r_2 \end{bmatrix} ,$$

which can be re-written as

$$\begin{bmatrix} \Delta_y \\ \Delta_u \end{bmatrix} = \begin{bmatrix} (G - \tilde{G})/[(1 + GK_i)(1 + \tilde{G}K_i)] \\ -(G - \tilde{G})K_i/[(1 + GK_i)(1 + \tilde{G}K_i)] \end{bmatrix} r ,$$

where

$$r = K_i r_1 + r_2 .$$

From the point of view of control design, it is desirable to find a model  $G_{i+1}$  such that

$$G_{i+1} = \arg \min_{\tilde{G}} \left\| \begin{bmatrix} \Delta_y \\ \Delta_u \end{bmatrix} \right\|_2 ,$$

or

$$G_{i+1} = \arg \min_{\tilde{G}} \frac{1}{2\pi} \int_{-\pi}^{\pi} J_1(\tilde{G}, j\omega) \Phi_r(\omega) d\omega , \quad (1.6)$$

where

$$J_1(\tilde{G}, j\omega) = \left| \frac{G}{1 + GK_i} - \frac{\tilde{G}}{1 + \tilde{G}K_i} \right|^2 + \left| \frac{1}{1 + GK_i} - \frac{1}{1 + \tilde{G}K_i} \right|^2 ,$$

and  $\Phi_r(\omega)$  is the power spectral density of  $r = K_i r_1 + r_2$ . The problem is how to achieve this objective through estimating the coprime factors  $N$  and  $D$ . By noting that

$$\begin{bmatrix} N \\ D \end{bmatrix} = \begin{bmatrix} G/(1 + GK_i) \\ 1/(1 + GK_i) \end{bmatrix} (D_x + K_i N_x) ,$$

and if it would be able to construct a parametrization ( $N(\theta)$  and  $D(\theta)$ ) that satisfies

$$\begin{bmatrix} N(\theta) \\ D(\theta) \end{bmatrix} = \begin{bmatrix} \tilde{G}(\theta)/[1 + \tilde{G}(\theta)K_i] \\ 1/[1 + \tilde{G}(\theta)K_i] \end{bmatrix} (D_x + K_i N_x) , \quad (1.7)$$

then asymptotic estimate determined by

$$\theta^* = \arg \min_{\theta} \frac{1}{2\pi} \int_{-\pi}^{\pi} \begin{bmatrix} N - N(\theta) \\ D - D(\theta) \end{bmatrix}^* \begin{bmatrix} |L_1|^2 & 0 \\ 0 & |L_2|^2 \end{bmatrix} \begin{bmatrix} N - N(\theta) \\ D - D(\theta) \end{bmatrix} \Phi_x(\omega) d\omega$$

becomes

$$\theta^* = \arg \min_{\theta} \frac{1}{2\pi} \int_{-\pi}^{\pi} J_2(\theta, j\omega) \Phi_r(\omega) d\omega , \quad (1.8)$$

where

$$J_2(\theta, j\omega) = \left| \frac{G}{1 + GK_i} - \frac{\tilde{G}(\theta)}{1 + \tilde{G}(\theta)K_i} \right|^2 |L_1|^2 + \left| \frac{1}{1 + GK_i} - \frac{1}{1 + \tilde{G}(\theta)K_i} \right|^2 |L_2|^2 .$$

Comparing equation (1.8) with equation (1.6) clearly indicated that equation (1.8) represents a very flexible approximation criterion for control-relevant system identification.

It was pointed out by Van den Hof *et al.* [1993] that the coprime factors estimated by the above system identification procedure will depend strongly on the chosen  $N_x$  and  $D_x$ , and it is nontrivial to parametrize low order  $N(\theta)$  and  $D(\theta)$  such that the restriction (1.7) is satisfied and accurately estimates can be obtained. However, by taking advantage of the freedom in choosing  $N_x$  and  $D_x$ , they presented a normalization procedure in [Van den Hof *et al.* 1993] which allows a *normalized* coprime factors of  $G$  to be approximately identified in the sense that for these estimates ( $\hat{N}_n$  and  $\hat{D}_n$ ),  $\hat{N}_n^* \hat{N}_n + \hat{D}_n^* \hat{D}_n \sim 1$ . It is also shown in the same paper that the method has been applied to a mechanical servo system with very good results.

In the following we compare the salient features of the Delft School's approach to those of our approach.

- The bandwidth of the closed-loop system at the  $i^{\text{th}}$  stage of iteration is approximately given by the gain crossover frequency of  $\alpha_i G_i$ . Therefore  $\alpha_i$  serves as the tuning knob for exercising caution at the beginning of iteration (when the initial plant-model mismatch prevents the achievement of high nominal performance) and for increasing the nominal performance gradually when the model accuracy improves progressively through iteration. Its effects are similar to that of a design parameter  $\lambda_i$  used in the approach that we will develop in this thesis. It suffice to say at this point that, in our case,  $\lambda_i$  directly specifies the designed closed-loop bandwidth.
- The system identification criterion employed is induced naturally by the overall control objective and hence is control-relevant. It is more general than our control-relevant system identification criterion in the sense that it is a mixed sensitivity (or "four block") plant-model mismatch criterion, whereas we consider the complementary sensitivity (or "one block") plant-model mismatch criterion.
- The  $\mathcal{H}_\infty$  system identification problem formulated in the Delft School's approach is not solved in practice. Instead, they employ a least squares identification technique.

As will be shown in the sequel, we face the same difficulty with  $\mathcal{H}_\infty$  system identification and therefore also use a least squares system identification technique.

- As it was mentioned previously, Schrama [1992b] uses right coprime factorization to identify the plant indirectly through *separately* estimating the frequency response samples of the two stable coprime factors ( $N$  and  $D$ ) that are parametrized by a *single* stable transfer function  $R$ . We will use left coprime factorization approach like [Hansen 1989] to identifying the single stable transfer function  $R$  that parametrizes the plant. Although both approaches have the disadvantage of resulting in high order models, the approach adopted in [Schrama 1992b] may have the additional difficulty that the two estimated stable transfer functions may be inconsistent in the sense that they may not be expressible in terms of a single parametrizing transfer function like  $R$ . Other closed-loop system identification schemes are proposed recently by the Delft School's researchers to overcome this and other difficulties [Van den Hof and Schrama 1994]. One of these approaches, which identifies the normalized coprime factors of the plant [Van den Hof and Schrama 1993], was described in the above discussions.

- The Delft School's approach uses a powerful stability robustness test to check the newly designed controllers before they are implemented in the actual closed-loop. The robust stability test requires  $\mathcal{H}_\infty$  model uncertainty bounds. Schrama [1992b] constructs these uncertainty bounds by fitting a high order model to the frequency response samples of the plant.

In our case (see Chapter 4), instead of checking stability robustness analytically, *performance robustness* of the closed-loop is verified experimentally by time domain and frequency domain model validation methods while the designed closed-loop bandwidth is increased carefully.

- The Delft School's approach uses a **multi-pass** algorithm in the sense that, for a fixed nominal performance design parameter, system identification and control design are iterated until there are negligible changes in the consecutive models and controllers.

In our case, the **single pass** iteration will proceed by several control design steps (each with a slightly increased designed closed-loop bandwidth) between *single* identification steps (carried out when experimental performance robustness tests in time domain and frequency domain dictate that a model update is necessary).

- Schrama [1992b] has observed that, when a model leads to the design of a high

performance (both nominal and robust) closed-loop system, the frequency response of the model is often a poor representation of the plant under open-loop conditions.

Our simulation experience (see Chapters 3 to 5) does not support Schrama's observation. In fact, we often find that frequency responses of models approach the frequency response of the open-loop plant while the actual closed-loop performance is improved through iteration. However, because our simulations are performed for plants different from those used by Schrama, further works are necessary to clarify this issue.

## 1.2.2 Zang-Bitmead-Gevers Scheme

In the Zang-Bitmead-Gevers Scheme [Zang *et al.* 1991, Zang *et al.* 1992, Zang 1992, Partanen and Bitmead 1993*b*], an LQG method is employed for the design of controllers. With reference to Figure 1.1, the global (or overall) control objective to be achieved is the minimization of

$$J^{global} = E \sum_{t=1}^N \{ (y_t - r_t)^2 + \lambda u_t^2 \} .$$

The signals involved in the last equation are defined as before, except that the subscript  $t$  is used to denote the sampling time index. The design parameter is  $\lambda$ . Decreasing  $\lambda$  will allow the closed-loop tracking performance to improve at the expense of a large control energy.

Observe that the above global objective involves the actual closed-loop variables  $y_t$  and  $u_t$ . Since the global control objective depends on the unknown plant, it can only be achieved, as we have observed for other approaches, through iterative identification and control design. It was shown in [Zang 1992] that a control-relevant system identification criterion is, in this case, given by

$$J^{ident} = \sum_{t=1}^N \{ (y_t - y_t^c)^2 + \lambda (u_t - u_t^c)^2 \} ,$$

where  $u_t^c$  and  $y_t^c$  are, respectively, the designed control input and the designed closed-loop output that can be obtained through simulating the design closed-loop system that involves the current controller  $K_i$  and the current model  $G_i$ .

In order to employ standard least squares algorithms (for example, the algorithms available in MATLAB<sup>TM</sup>) to estimate a parametrized model  $G_{i+1}(\theta)$ , the last identification criterion

can be re-written such that the asymptotic estimate satisfies

$$G_{i+1}(\theta^*) = \arg \min_{\tilde{G}(\theta)} \frac{1}{2\pi} \int_{-\pi}^{\pi} J_3[\tilde{G}(\theta), j\omega] \Phi_r(\omega) d\omega ,$$

where

$$J_3[\tilde{G}(\theta), j\omega] = \left| \frac{K_i[G - \tilde{G}(\theta)]}{(1 + GK_i)[1 + \tilde{G}(\theta)K_i]} \right|^2 (1 + \lambda |K_i|^2) .$$

The above criterion can be compared with the following criterion for direct closed-loop system identification [Gevers 1993],

$$G_{i+1}(\theta^*) = \arg \min_{\tilde{G}(\theta)} \frac{1}{2\pi} \int_{-\pi}^{\pi} J_4[\tilde{G}(\theta), j\omega] \Phi_r(\omega) d\omega ,$$

where

$$J_4[\tilde{G}(\theta), j\omega] = \left| \frac{K_i[G - \tilde{G}(\theta)]}{(1 + GK_i)} \frac{L_i}{H_i(\theta)} \right|^2 ,$$

$L_i$  is a user choice data filter for tuning the model towards the modelling objective, and  $H_i(\theta)$  is an estimate for the noise model. By choosing an output error algorithm (with  $H_i(\theta) = 1$ ), we observe that criterion formulated in the Zang-Bitmead-Gevers fits into the direct closed-loop system identification framework if the data filter is selected such that

$$|L_i|^2 = \frac{1 + \lambda |K_i|^2}{|1 + \tilde{G}(\theta)K_i|^2} .$$

However, the parameter vector  $\theta$  is yet to be estimated and hence is not available. To avoid this difficulty, the parameter vector estimated in the  $(i - 1)^{\text{th}}$  stage is used instead. Therefore the data filter becomes

$$L_i(z) = D_i(z)[1 + G_i(z, \theta_{i-1}^*)K_i(z)]^{-1} ,$$

where the stable transfer function  $D_i(z)$  employed in the data filter is obtained by solving the spectral factorization problem

$$D_i(z)D_i^*(z^{-1}) = 1 + \lambda K_i(z)K_i^*(z^{-1}) .$$

At the  $i^{\text{th}}$  stage of iteration, a new model  $G_{i+1}$  is identified on the basis of data measured from the closed-loop that involves  $G$  and the latest controller  $K_i$  according to the method just described. Autoregressive models of the spectra  $\Phi_u(\omega)$ ,  $\Phi_{u^c}(\omega)$ ,  $\Phi_{y-\tau}(\omega)$ , and  $\Phi_{y^c-\tau}(\omega)$  are also estimated for later use (which we will describe shortly).



Although the effect of plant-model mismatch associated with  $G_i$  and  $G$  on closed-loop performance deterioration (especially the initial model  $G_0$ ) can be ameliorated in the controller design using  $G_i$  (by using a large value for  $\lambda$ , provided that  $G_i$  is stable), this method is not adopted in the Zang-Bitmead-Gevers scheme. They employ a local frequency weighted design criterion

$$J^{local} = E \sum_{t=1}^N \{ [F_1(z)(y_t^c - r_t)]^2 + \lambda [F_2(z)u_t^c]^2 \} .$$

(Here local means the design is carried out on the basis of the current model  $G_i$ , and  $y_t^c$  and  $u_t^c$  are designed quantities, as opposed to the actual quantities  $y_t$  and  $u_t$  that appeared in the global or overall objective.) The linear stable filters  $F_1(z)$  and  $F_2(z)$  are constructed from the autoregressive models  $\Phi_u(z)$ ,  $\Phi_{u^c}(z)$ ,  $\Phi_{y-r}(z)$ , and  $\Phi_{y^c-r}(z)$  such that:

$$\Phi_{y-r}(\omega) = |F_1(e^{j\omega})|^2 \Phi_{y^c-r}(\omega) ,$$

and

$$\Phi_u(\omega) = |F_2(e^{j\omega})|^2 \Phi_{u^c}(\omega) .$$

The controller  $K_i$  is designed to satisfy

$$K_i = \arg \min_{\tilde{K}} J^{local}(\tilde{K}) .$$

The objective of including the filters  $F_1$  and  $F_2$  is to bring the local control design objective at the  $i^{\text{th}}$  iterative stage to be more in line with the global control objective by taking into account the mismatch between the designed and actual closed-loop systems in the  $(i-1)^{\text{th}}$  stage.

In the following, key features of the Zang-Bitmead-Gevers scheme are compared to those of the Delft School's approach and ours.

- The control design method does not employ a user choice parameter like  $\lambda$  for exercising caution or increasing nominal performance (recall that the parameter  $\lambda$  is chosen only once and is held constant throughout the iteration). It relies on the filters  $F_1(z)$  and  $F_2(z)$  (which carries the information on closed-loop mismatch at the  $(i-1)^{\text{th}}$  iteration) to adjust the control design objective at the  $i^{\text{th}}$  iteration such that the controller will be tightened or detuned automatically for the local (or designed) performance to approximate the global (or overall) performance as close as possible while, hopefully,

performance robustness and stability robustness are maintained. This feature is the most important difference from other iterative schemes in the sense that the Zang-Bitmead-Gevers scheme is probably the one that needs minimum user intervention and is closest in spirit to on-line adaptive control. However this strategy also causes its tuning for performance and for accommodating modelling errors to be much less direct and transparent than the Delft School's approach and ours.

- The system identification criterion in this scheme is induced by the overall control objective. Furthermore, the control-relevant  $\mathcal{L}_2$  system identification problem formulated is solved *exactly* through a least squares technique. This is different from using a practical least squares procedure to approximate an ideal but infeasible  $\mathcal{H}_\infty$  objective that is practised by the Delft School and us.
- The system identification procedure in this scheme does not use coprime factorizations. The plant is identified directly from closed-loop input-output data. The advantages (as compared to those schemes that use coprime factorizations) are that the order of the identified model is under direct control of users, and low order models are usually obtained. However, it is impossible to obtain unbiased estimates by direct closed-loop identification under noisy conditions. Experimental design is described in [Partanen and Bitmead 1993b] for securing good estimates in this scheme.
- There is no robustness test (like the one used by the Delft School) or model validation steps (like those that we introduced) in the original scheme [Zang *et al.* 1991]. Recent developments in this scheme do, however, include a model validation step that incorporate user's a priori knowledge of the plant. It was applied to a sugar cane crushing process with success [Partanen and Bitmead 1993a].
- The original scheme uses a multi-pass algorithm in the sense of what we have described for the Delft School's approach. Recent refinements of the scheme [Partanen and Bitmead 1993c] have led to a single pass algorithm like ours.

### 1.3 A Glimpse of the Problems Concerned and Their Solutions

In this thesis we demonstrate that, when an existing model of the plant (due to the associated *high frequency* model uncertainties) does not allow the closed-loop system to have robust

performance while achieving a large bandwidth, it is possible to increase the closed-loop bandwidth progressively and to arrive at the desired specifications eventually through a new iterative identification and control design procedure, for which the philosophy was propounded in [Anderson and Kosut 1991].

In the face of significant high frequency model uncertainties and the desire to achieve a large closed-loop bandwidth, it is necessary to have a control design method that can trade off nominal performance with performance robustness before a sufficiently accurate model is made available. This problem of incompatible model accuracy and performance requirement is resolved by employing the Internal Model Control design method [Morari and Zafriou 1989]. The resulting controller can easily tune the bandwidth of the closed-loop system to suit the model at hand. This allows the closed-loop bandwidth to be widened progressively (and carefully), when better models are identified, so that the high frequency unmodelled dynamics associated with the models are not overly excited.

The other major component in the iterative identification and control design algorithm is an appropriate system identification procedure. For this purpose, a control-relevant system identification problem will be formulated. The corresponding closed-loop system identification task cannot be accomplished simply by direct applications of well known open-loop system identification procedures [Ljung 1987, Söderström and Stoica 1988]. A method for transforming a closed-loop system identification problem into an open-loop system identification problem pioneered by Hansen [1989] is helpful at this point. It will be demonstrated that, with due considerations given to the intended application, the resulting frequency weighted open-loop system identification procedure is tuned to deliver models that allow the bandwidth of the closed-loop system to be widened robustly through controller re-design.

It is important to emphasize that a suitable control design method and an appropriate system identification method are necessary but not sufficient for constructing a successful iterative identification and control design algorithm. It will be shown through analysis that before an improved model can be obtained through the control-relevant system identification procedure, it is necessary that a certain closed-loop output error has a sufficiently high signal-to-noise ratio. The last condition is satisfied only if the closed-loop system suffers a certain level of deterioration in its performance robustness. It should be emphasized that the converse is not necessarily true. In fact it will be revealed by analysis that although

there are three mechanisms that can lead to deterioration in performance robustness, robust performance may be recovered by re-identification and control re-design (before the closed-loop bandwidth is increased further) only if the performance robustness deterioration is caused mainly by an increase in the magnitude of a certain phase insensitive factor. For the purpose of assessing the validity of an existing model with respect to the closed-loop control objective and the signal-to-noise ratio required for good system identification, a time domain model validation method and a frequency domain model validation method will be developed. These model validation methods will also be employed to evaluate the quality of a newly identified model. The fidelity of these model validation procedures plays an important role in enhancing the reliability of the iterative identification and control design algorithm.

## 1.4 Outline of the Thesis

In Chapter 2 we introduce a new iterative identification and control design paradigm. We begin our study on the new design paradigm in the *ideal situation* where an infinite number of noiseless measurements are available for the plant input and output. Under these conditions, the system identification problem involved reduces to a *model (or rational function) approximation problem*. The main reason for investigating iterative model approximation and control design (as opposed to iterative identification and control design) is that, at this initial stage of investigation, we are more concerned with the concept of iterative identification and control design as applied to adaptive robust control, rather than the details. Simulation results for iterative *model approximation* and control design will be presented to illustrate the effectiveness of the new idea.

Encouraged by the simulation results of Chapter 2 under ideal conditions, we investigate in Chapter 3 the iterative identification and control design approach under realistic situations where only a finite number of noisy input-output measurements are available. We also explore further, at the beginning of Chapter 3, a control-relevant system identification criterion formulated in Chapter 2. This will provide further insights into the role of appropriate frequency weighting in the control-relevant system identification procedure adopted in the iterative identification and control design process. It will also be shown that the controller design equations and the control-relevant system identification procedure for stable plants can be applied without modifications to (Type 1 stable) plants that, other than having poles

in the open left-half plane, may have one pole at the origin. Two simulation examples will be employed to illustrate the applications of the new iterative identification and control design algorithm to a stable plant and a Type 1 stable plant.

In Chapter 4 we examine a number of crucial questions which arise in the iterative identification and control design methodology. Among the issues considered are:

- When can one re-design the controller and expand the closed-loop bandwidth, without re-identifying?
- When should one re-identify?
- What does one want to identify in the re-identification process?
- What can one identify in the re-identification process?
- How can an identified model be verified against the desired purpose?
- Will re-identification and controller re-designs always lead to improved closed-loop performance?

The key conclusion of Chapter 4 is that, given a stable strictly proper model of a stable strictly proper plant, we can improve the performance robustness of the closed-loop system through iterative identification and control design if the plant and the existing model has no unstable zeros within the designed closed-loop bandwidth and if the deterioration in performance robustness caused by increasing the closed-loop bandwidth results in a sufficiently high signal-to-noise ratio for a certain closed-loop output error. Situations that may cause the iterative identification and control design process to terminate prematurely are also indicated. A simulation example will be used to illustrate the results discussed in Chapter 4.

In Chapter 5 we extend the applications of iterative identification and control design to unstable plants. By employing a *two step approach*, where an unstable plant is first stabilized by a parallel feedback compensator, we show that it is possible to design *systematically* an overall closed-loop system that has good step responses with little overshoot by using the iterative identification and control design methodology. Specifically, similar to situations where the plant is stable or is Type 1 stable, we can design a system with a small initial

overall designed closed-loop bandwidth (after the plant is stabilized by a known parallel feedback compensator) such that high frequency unmodelled dynamics of the plant are not overly excited. Through iterative applications of a control-relevant closed-loop system identification procedure to the stabilized plant, the overall designed closed-loop bandwidth of the system can be widened progressively while maintaining good step responses with little overshoot. Two examples will be employed to illustrate the method.

In Chapter 6, we conclude the thesis with an indication of some possible further research directions.

Most of the theorem proofs are given in the appendices. Programs and information useful for performing simulations are summarized in Appendix H<sup>1</sup>.

## 1.5 Point Summary of Thesis Contributions

The main contributions of this thesis are summarized below.

- We establish the need of blending robust control and adaptive control harmoniously such that, in the face of significant initial modelling errors, a large nominal closed-loop bandwidth with good performance robustness may be achieved progressively.
- We formulate a control-relevant closed-loop system identification criterion for high performance robust reference tracking.
- We develop appropriate signal (or data) filtering that allows exact transformation of the control-relevant closed-loop system identification criterion for high performance robust reference tracking into a frequency weighted open-loop system identification procedure via Hansen's framework.
- We transform the adaptive robust control philosophy propounded by Anderson and Kosut [1991] into an iterative identification and control design procedure that involves

---

<sup>1</sup>Programs for performing simulations described in this thesis are available. Please write (or email) to Dr. Iven M.Y. Mareels, Department of Systems Engineering, The Australian National University, Canberra, ACT 0200, AUSTRALIA (Email: Iven.Mareels@anu.edu.au).

the Internal Model Control design method and the frequency weighted open-loop system identification procedure.

- We derive an unified set of equations for iterative identification and control design that involves a stable plant or a Type 1 stable plant.
- We establish the relation between the normalized variance of the identified model and the signal-to-noise ratio of the closed-loop output error. This relation leads to a better understanding of the interactions between performance robustness deterioration and successful closed-loop identification, and the mechanisms that may lead to premature terminations of the iterative identification and control design process.
- We establish the sufficient conditions that allow robust performance improvement through re-identification and re-design.
- We develop model validation methods that improve the reliability of the models identified through the iterative identification and control design procedure.
- We extend the applications of the iterative identification and control design methodology to unstable plants through embedding the iterative identification and control design procedure into a two step control design approach.

## Chapter 2

# Iterative Model Approximation and Control Design

In this chapter we introduce a new iterative identification and control design paradigm. In this preliminary investigation, we study the design paradigm in the *ideal situation* where an infinite number of noiseless measurements are available for the plant input and output. Under these conditions, the system identification problem reduces to a *model (or rational function) approximation problem*. This simplifies the analysis and allows us to concentrate on the essence of iterative identification and control design.

We review briefly, in Section 2.1, the design of adaptive control and robust control for *inexactly known* plants. We outline in Section 2.2 the background philosophy of the iterative identification and control design paradigm. In Section 2.3 we elaborate on the new idea by considering an adaptive model matching problem. A related *control-relevant closed-loop system identification problem* will also be formulated in this section. Section 2.4 is devoted to the application of Hansen's method [Hansen and Franklin 1988, Hansen *et al.* 1989, Hansen 1989] for performing closed-loop system identification. It is demonstrated that, with appropriate signal filtering, it is possible to transform the control-relevant closed-loop system identification problem into a *frequency weighted open-loop system identification problem* by Hansen's method. In order to facilitate systematic discussions, we outline the Internal Model Control method [Morari and Zafiriou 1989] for designing controllers in Section 2.5. In Section 2.6 we examine how to decompose the transfer function to be identified in the frequency weighted open-loop system identification problem into the product of an



unknown transfer function and a transfer function that is known by design.

For simplicity, we consider only stable plants and models. Simulation results for iterative *model approximation* and control design will be presented in Section 2.7. In Section 2.8 we review the reasons for the effectiveness of the new approach.

### Note

Although we are concerned with the simpler iterative model approximation and control design problem (where the noise disturbance is absent) in this chapter, we will formulate the corresponding iterative identification and control design problem (where a noise disturbance is present) with a  $\mathcal{H}_\infty$  system identification criterion as a direct consequence of an adaptive  $\mathcal{H}_\infty$  model matching control problem. As we do not know how to perform  $\mathcal{H}_\infty$  system identification with noisy measurements, we will perform least squares (instead of  $\mathcal{H}_\infty$ ) system identification with noisy measurements in Chapter 3. In the sequel, all the conditions that involve a  $\mathcal{L}_\infty$ -norm should be interpreted either with the understanding that noise disturbance is absent or, in situations where noise disturbance must be considered, with the understanding that a  $\mathcal{L}_2$ -norm is implied.

## 2.1 Two Main Control Design Approaches for Inexactly Known Plants

Consider an adaptive control system as shown in Figure 2.1, where  $G$  is the unknown transfer function of the plant. The time axis is divided into intervals such that during the  $i^{\text{th}}$  interval, the control input applied to the plant is obtained from  $K_i$ , where  $K_i$  denotes the transfer function of the controller designed on the basis of the model,  $G_i$ , obtained at the end of the  $(i - 1)^{\text{th}}$  time interval.

In an adaptive control problem, the ulterior objective for finding  $G_i$  (an estimate of  $G$  updated from  $G_{i-1}$ ) is to re-design a controller  $K_i$  which improves on  $K_{i-1}$ . For example, if  $T_d$  represents the desired closed-loop transfer function for a tracking problem, then we may

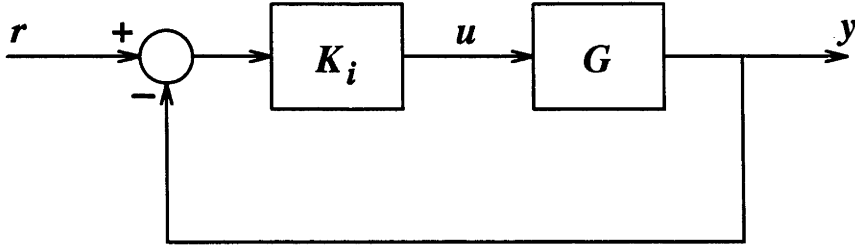


Figure 2.1: Adaptive control system

like to have

$$\left\| \frac{GK_i}{1 + GK_i} - T_d \right\|_{\infty} \leq \left\| \frac{GK_{i-1}}{1 + GK_{i-1}} - T_d \right\|_{\infty}, \quad \forall i.$$

Implicitly, this means we would like to minimize

$$\left\| \frac{GK_i}{1 + GK_i} - T_d \right\|_{\infty}$$

by selecting an appropriate  $K_i$ . Since the transfer function of the plant is unknown, we could only design  $K_i$  on the basis of the model,  $G_i$ , such that for example,

$$K_i = \arg \min_{\gamma} \left\| \frac{G_i \gamma}{1 + G_i \gamma} - T_d \right\|_{\infty}, \quad \forall i.$$

Here we invoked the *principle of certainty equivalence*. It is important to realize that

$$\left\| \frac{GK_i}{1 + GK_i} - T_d \right\|_{\infty}$$

is not necessarily small, even though

$$\left\| \frac{G_i K_i}{1 + G_i K_i} - T_d \right\|_{\infty}$$

is a minimum. This partly explains why traditional adaptive control systems [Åström and Wittenmark 1989, Goodwin and Sin 1984, Sastry and Bodson 1989], which invariably invoke the principle of certainty equivalence, may have *unsatisfactory* performance robustness.

In the robust control approach [Doyle 1984, Morari and Zafiriou 1989], a controller is designed on the basis of a nominal model for the plant with the associated parametric and unstructured model uncertainties explicitly taken into account. Therefore stability robustness is guaranteed and performance robustness is achieved sometimes. The *weakness* of this

approach is that it considers only the a priori information on the model, and neglects the fact that characteristics of the plant could be learned while it is being controlled. Therefore, the robust control approach tends to result in a conservative design in terms of performance. It is likely that *a posteriori* knowledge about the plant could be used to reduce the conservatism inherent in a robust control design.

## 2.2 Iterative Identification and Control Design - A New Paradigm

By considering how humans learn windsurfing, Anderson and Kosut [1991] made the following observations:

1. The human first learns to control over a limited bandwidth, and learning pushes out the bandwidth over which an accurate model of the plant is known.
2. The human first implements a low gain controller, and learning allows the loop to be tightened.

Based on these observations an iterative identification and control design philosophy is propounded in [Anderson and Kosut 1991]. It recognizes at the outset that the plant characteristics can differ greatly from the estimated model at any one time, particularly during the initial learning stage. In the new design paradigm, a low gain controller will first be implemented; and the control bandwidth will be small. Based on learning a frequency domain description of the plant operating in *closed-loop*, with the learning process progressively increasing the bandwidth over which the plant is accurately known, the controller gain can be increased appropriately over an increasing frequency band.<sup>1</sup> For details, refer to [Anderson and Kosut 1991]. Importantly, in the method suggested, the necessary closed-loop system identification task is transformed into an open-loop system identification problem through the use of coprime fractional representations as discussed in [Hansen *et al.* 1989] and [Hansen 1989].

It was pointed out by Owens and Skelton [1985] (see also [Skelton 1985] and [Skelton 1989]) that modelling (for control) and control design problems are inseparable. The problems

---

<sup>1</sup>This design paradigm is known to the control community as *the windsurfer approach*.

cannot be solved simultaneously and an iterative approach is necessary. It was re-confirmed recently by Schrama [1992a] that the best model for control design cannot be derived from open-loop experiments alone. The control task at hand dictates how system identification should be performed. Hence, a general solution to the combination of system identification and control design is necessarily iterative. A good historical perspective and tutorial in the *joint design of identification and control* is given recently by Gevers [1993]. It was also shown in [Zang *et al.* 1991] that an iterative approach for model refinement and control robustness enhancement can be developed for a  $\mathcal{H}_2$  control problem. Although the emphasis of [Schrama 1992a] is on the problem of modelling for control design, its approach is very similar to that of [Anderson and Kosut 1991] (see also [Schrama and Van den Hof 1992]). In the next section, we elaborate on the new design approach by considering a  $\mathcal{H}_\infty$  model matching problem in the context of adaptive control.

## 2.3 An Adaptive $\mathcal{H}_\infty$ Model Matching Control Problem

Let  $G$  be the unknown transfer function of the plant, and let  $T_d$  represent the desired closed-loop transfer function. We wish to achieve, through iterative system identification and control design, the minimization of the cost function

$$\left\| \frac{GK}{1 + GK} - T_d \right\|_\infty,$$

where  $K$  is the transfer function of a controller to be designed.

We begin by designing a controller  $K_0^0$  to stabilize a given initial model  $G_0$ , which may be obtained from an open-loop system identification exercise. Note that we use  $K_i^j$  to denote the  $j^{\text{th}}$  controller designed on the basis of the  $i^{\text{th}}$  model, which has a transfer function  $G_i$ . In general,  $L_i^j$  denotes a transfer function  $L$  that it is either specified or derived at the  $j^{\text{th}}$  control design iteration on the basis of the  $i^{\text{th}}$  model for the plant. We shall adopt a similar system of notations for signals generated by the closed-loop system. We will need the following definition:

**Definition 2.3.1** *If a controller  $K_i^j$  stabilizes not only the known model  $G_i$  but also the unknown plant  $G$ , we say that  $K_i^j$  **robustly stabilizes**  $G_i$ . We also say that the designed closed-loop system involving  $G_i$  and  $K_i^j$  has **robust stability**.*

Since there may be significant modelling error between  $G_0$  and  $G$ , the resulting controller  $K_0^0$  may not be able to achieve high nominal performance with a small value for

$$\left\| \frac{G_0 K_0^0}{1 + G_0 K_0^0} - T_d \right\|_{\infty}$$

while robustly stabilizing  $G_0$ . In general, we need to consider how to handle the question of securing robust stabilization of  $G_i$  by  $K_i^j$ . This is bound up with the question of selection of  $T_d$ . It is in fact to be expected that a sequence of  $T_d$  will be selected in such a way that the end control objective can be approached in stages. We shall therefore proceed as follows.

Associated with each of the models  $G_i$ ;  $i = 0, 1, 2, \dots$ , we design a sequence of controllers  $\{K_i^j$ ;  $j = 0, 1, 2, \dots\}$  such that

$$K_i^j = \arg \min_{\gamma} \left\| \frac{G_i \gamma}{1 + G_i \gamma} - (T_d)_i^j \right\|_{\infty}, \quad \forall j,$$

where the sequence of functions  $\{(T_d)_i^j$ ;  $j = 0, 1, 2, \dots\}$  is specified with  $(T_d)_i^{j+1}$ ;  $j = 0, 1, 2, \dots, f$  of wider bandwidth than  $(T_d)_i^j$ , and with  $(T_d)_i$  resulting in a controller  $K_i$  that robustly stabilizes  $G_i$ . A stage will be reached (say when  $j = f$ ) where the bandwidth of the designed closed-loop transfer function,  $\bar{T}_i^f = G_i K_i^f / (1 + G_i K_i^f)$ , cannot be increased further without causing the effects of the model uncertainties associated with  $G_i$  to be too significant. This occurs when the value of  $\|T_i^f - \bar{T}_i^f\|_{\infty}$  is no longer small, where  $T_i^f = G K_i^f / (1 + G K_i^f)$  is the actual closed-loop transfer function of the system.

At this stage it is necessary to improve the accuracy of the model. Ideally we would like to use the control input and plant output measurements to identify a new model,  $G_{i+1}$ , such that

$$G_{i+1} = \arg \min_{\theta} \left\| \frac{G K_{i+1}^0}{1 + G K_{i+1}^0} - \frac{\theta K_{i+1}^0}{1 + \theta K_{i+1}^0} \right\|_{\infty},$$

where  $\bar{T}_{i+1}^0 = G_{i+1} K_{i+1}^0 / (1 + G_{i+1} K_{i+1}^0)$  has the same bandwidth as  $\bar{T}_i^f = G_i K_i^f / (1 + G_i K_i^f)$ . However  $K_{i+1}^0$  is not available since its determination rests on the new model yet to be identified. In the absence of  $K_{i+1}^0$ , we find an updated model  $G_{i+1}$  such that

$$G_{i+1} = \arg \min_{\theta} \left\| \frac{G K_i^f}{1 + G K_i^f} - \frac{\theta K_i^f}{1 + \theta K_i^f} \right\|_{\infty}, \quad (2.1)$$

where  $K_i^f$  is the latest controller available.

**Remark 2.3.1** It is not straightforward to identify  $G$  directly from plant input-output measurements under closed-loop conditions such that criterion (2.1) is satisfied. The problems are:

1. Irrespective of the presence of noise, under closed-loop conditions, there are two deterministic relationships between the control input  $u$  and the plant output  $y$  when  $r = 0$ . These are

$$y = Gu \text{ ,}$$

and

$$y = -\frac{1}{K_i}u \text{ .}$$

It is therefore not clear which one of the above relationships will be identified. It suffices to say that this will depend on the excitation conditions induced by the external inputs to the closed-loop. For a more detailed discussion on this problem, we refer to [Partanen and Bitmead 1993b].

2. With noise disturbances, the plant output and control input are correlated under closed-loop conditions. Therefore when the effect of noise disturbance is not negligible, the estimated model will be biased.
3. Since the argument in criterion (2.1) is not affine in  $G_{i+1}$ , the problem of finding a  $G_{i+1}$  that satisfies criterion (2.1) is a non-convex optimization problem and hence is difficult.
4. If criterion (2.1) is rewritten as

$$G_{i+1} = \arg \min_{\theta} \left\| \frac{K_i^f}{1 + GK_i^f} \frac{G - \theta}{1 + \theta K_i^f} \right\|_{\infty} \text{ ,}$$

we observe that it involves an *unknown* frequency weighting.

We will show in the next section that these difficulties can be overcome through a system identification framework pioneered by Hansen (see [Hansen and Franklin 1988], [Hansen *et al.* 1989], and [Hansen 1989]).

**Remark 2.3.2** Equation (2.1) would be the formulation of a frequency weighted rational function approximation problem, provided that  $G$  were known. In the simulation example

(see Section 2.7), we shall take this approach by using a known transfer function for  $G$ . This serves as a benchmark test of the new iterative identification and control design methodology as it corresponds to performing system identification with an infinite number of noiseless measurements. In later chapters we shall deal with this problem in a realistic system identification setting when only a finite number of noisy input-output measurements are available.

Once  $G_{i+1}$  is found, we can continue to increase the closed-loop bandwidth by repeating the procedure described for  $G_i$  previously. However  $G_{i+1}$  should be used instead of  $G_i$ , and we specify a new sequence of functions  $\{(T_d)_{i+1}^j ; j = 0, 1, 2, \dots\}$  with  $(T_d)_{i+1}^0$  having the same bandwidth as  $(T_d)_i^f$ . The iterative process is continued until the end control objective is achieved or it is prematurely terminated because of, for example,

1. fundamental performance limitations due to right-half plane poles and zeros of the plant and/or models [Freudenberg and Looze 1985],
2. finite control energy and actuator limits.

## 2.4 Closed-loop System Identification

We review a method for closed-loop system identification developed by Hansen and co-workers [Hansen 1989, Hansen and Franklin 1988, Hansen *et al.* 1989]. We demonstrate in Theorem 2.4.2 that, with appropriate signal filtering, Hansen's method provides a suitable framework to deal with the **control-relevant closed-loop system identification problem** formulated in Section 2.3 (see equation (2.1)). For the sake of expository simplicity we shall consider only scalar plants. We begin with the following theorem<sup>2</sup>:

**Theorem 2.4.1** *Let  $K = X/Y$  be a coprime fractional representation of the proper transfer function for a controller, where  $X$  and  $Y$  are stable proper transfer functions. If  $N$  and  $D$  are stable proper transfer functions that satisfy the Bezout identity  $NX + DY = 1$ , then the*

---

<sup>2</sup>The stable proper transfer function  $R$  in this theorem is now known as the Dual Youla-parametrization [Van den Hof and Schrama 1994].

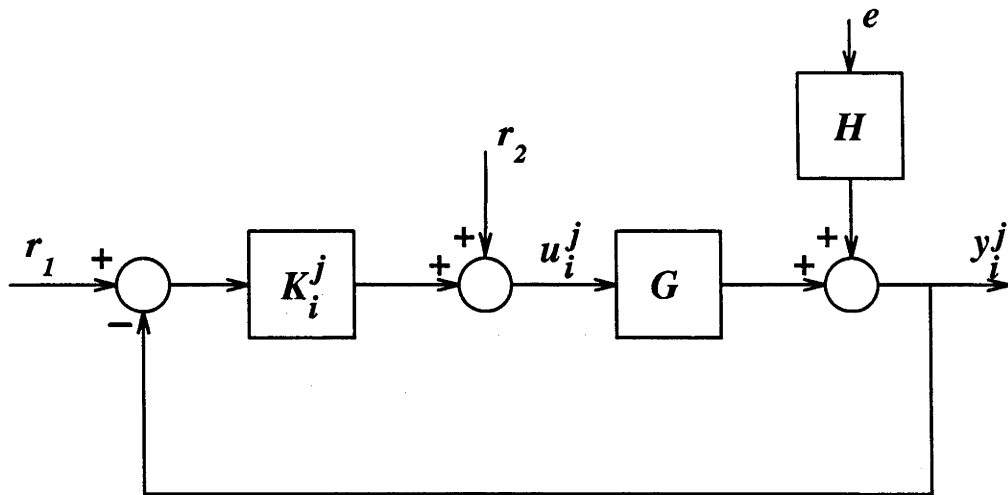


Figure 2.2: Closed-loop system

set of all plant transfer functions stabilized by  $K$  is precisely the set of elements in

$$\mathcal{G} = \left\{ \frac{N + RY}{D - RX} : R \text{ is a stable proper transfer function} \right\} .$$

Consider the feedback system shown in Figure 2.2, where  $y_i^j$  and  $u_i^j$  are respectively, the measured plant output and the control input,  $e$  is an unpredictable white noise disturbance, and  $r_1$  and  $r_2$  are user applied inputs. It is assumed that  $K_i^j$  (when  $j = f$ ) is a known stabilizing controller,  $G$  is inexactly known and possibly unstable, and, as is standard [Ljung 1987],  $H$  is imperfectly known, stable and inversely stable. The system identification problem is to obtain improved estimates of  $G$  and  $H$  from a finite interval of measured and known data  $\{y_i^f(t), u_i^f(t), r_1(t), r_2(t) : 0 \leq t \leq T_F\}$ , where  $y_i^f$  and  $u_i^f$  denote, respectively, the plant output and control input when  $G$  is controlled by  $K_i^f$ .

Following [Hansen 1989], we introduce the stable proper transfer functions  $X_i^f$ ,  $Y_i^f$ ,  $N_i$ , and  $D_i$  which satisfy  $K_i^f = X_i^f/Y_i^f$ ,  $G_i = N_i/D_i$ , and  $N_i X_i^f + D_i Y_i^f = 1$ . The interpretation is that  $G_i$  is a currently known (but imperfect) model of the plant which is stabilized by  $K_i^f$ . Applying Theorem 2.4.1 as shown in [Hansen *et al.* 1989] and [Hansen 1989], there exist stable proper transfer functions  $R_i^f$  and  $S_i^f$ , with  $S_i^f$  also inversely stable,





and

$$\beta = D_i y_i^f - N_i u_i^f . \quad (2.6)$$

However, as  $u_i^f = K_i^f (r_1 - y_i^f) + r_2$  and  $K_i^f = X_i^f / Y_i^f$ , equation (2.5) can be re-written as

$$\alpha = X_i^f r_1 + Y_i^f r_2 . \quad (2.7)$$

It is important to observe from equations (2.4), (2.6) and (2.7) that  $\alpha$  depends on the applied signals  $r_1$  and  $r_2$  operated on by known stable proper transfer functions  $X_i^f$  and  $Y_i^f$  respectively, and  $\beta$  depends on measured signals  $y_i^f$  and  $u_i^f$  operated by known stable proper transfer functions  $D_i$  and  $N_i$  respectively. Moreover,  $\alpha$  is *independent* of the transfer functions  $G$  and  $H$  and the noise disturbance  $e$ . Hence identification of  $G$  and  $H$  in closed-loop has been recast into identification of  $R_i^f$  and  $S_i^f$  in *open-loop*.

We shall next state a result which is highly relevant to solving the control-relevant closed-loop system identification problem.

**Theorem 2.4.2** *With reference to Figure 2.3, let the controller  $K_i^f$  stabilize the plant  $G$  and the model  $G_i = N_i / D_i$ , where  $N_i$  and  $D_i$  are stable proper transfer functions, and let  $K_i^f = X_i^f / Y_i^f$ , where  $X_i^f$  and  $Y_i^f$  are stable proper transfer functions satisfying the Bezout identity  $N_i X_i^f + D_i Y_i^f = 1$ .*

*Let  $G_{i+1}$  be another model of  $G$ , also stabilized by  $K_i^f$  and therefore having a description*

$$G_{i+1} = \frac{N_i + \widehat{R}_i^f Y_i^f}{D_i - \widehat{R}_i^f X_i^f} \quad (2.8)$$

*where  $\widehat{R}_i^f$  is a stable proper transfer function. Also define the filtered output error*

$$\xi_1 = Y_i^f (\beta - \widehat{R}_i^f \alpha) , \quad (2.9)$$

*where, with  $r_2 = 0$ ,*

$$\alpha = X_i^f r_1 ,$$

$$\beta = D_i y_i^f - N_i u_i^f ,$$

$$r_1 = \text{reference signal} ,$$

$$y_i^f = \text{plant output under the control of } K_i^f ,$$

$u_i^f = \text{plant input generated by } K_i^f$  .

Then the filtered output error can be expressed as

$$\xi_1 = \left( \frac{GK_i^f}{1 + GK_i^f} - \frac{G_{i+1}K_i^f}{1 + G_{i+1}K_i^f} \right) r_1 + w_i^f ,$$

where

$$w_i^f = \frac{1}{1 + GK_i^f} He$$

is the effect of the noise disturbance at the plant output attenuated by the sensitivity function of the actual closed-loop system.

### Proof

See Appendix A. □

**Remark 2.4.1** Observe that  $\xi_1$  is a frequency weighted error arising in the (open-loop) identification of  $R_i^f$  through an estimate  $\hat{R}_i^f$  (see equation (2.9)).

**Remark 2.4.2** By writing the signal  $\alpha = X_i^f r_1 + Y_i^f r_2$  as

$$\alpha = \frac{1}{D_i(1 + G_i K_i^f)} (K_i^f r_1 + r_2) ,$$

we can see immediately that  $r_2$  (as opposed to  $r_1$ ) may be a helpful probing signal for identifying  $R_i^f$  in the frequency range where the gain of the controller  $K_i^f$  is small.

**Remark 2.4.3** Note that in Theorem 2.4.2, it is necessary that  $K_i^f$  stabilizes  $G$  when the system identification procedure is carried out. This can be assured by increasing the closed-loop bandwidth smoothly and cautiously in the controller design stages (to be described in Section 2.6). We would always detect a gradual degradation of performance robustness (while stability is still being maintained and the system identification procedure is being carried out) before the closed-loop system loses stability.

Suppose that the value of

$$\left\| \frac{GK_i^f}{1 + GK_i^f} - \frac{G_i K_i^f}{1 + G_i K_i^f} \right\|_{\infty} \quad (2.10)$$

has become large. As it was described in Section 2.3, we want a new estimate of  $G$ , namely  $G_{i+1}$ , for which

$$\left\| \frac{GK_i^f}{1 + GK_i^f} - \frac{G_{i+1}K_i^f}{1 + G_{i+1}K_i^f} \right\|_{\infty} \quad (2.11)$$

is minimized. We are going to use the  $\hat{R}_i^f$  parametrization of  $G_{i+1}$ . By substituting equation (2.2) and equation (2.8) into expression (2.11), and noting that  $K_i^f = X_i^f/Y_i^f$ , we can conclude after simplification that

$$\left\| \frac{GK_i^f}{1 + GK_i^f} - \frac{G_{i+1}K_i^f}{1 + G_{i+1}K_i^f} \right\|_{\infty} = \left\| Y_i^f X_i^f (R_i^f - \hat{R}_i^f) \right\|_{\infty} \quad (2.12)$$

should be minimized.

**Remark 2.4.4** The right-hand side of equation (2.12) defines a **frequency weighted open-loop system identification problem**.

**Remark 2.4.5** Theorem 2.4.2 and equation (2.12) establish the connection between a control-relevant closed-loop system identification problem and a frequency weighted open-loop system identification problem.

By using equations (2.4), (2.9), and (2.12), we immediately see that the appropriate signal model for the frequency weighted open-loop system identification procedure is,

$$\beta_1 = R_i^f \alpha_1 + w_i^f, \quad (2.13)$$

where

$$\beta_1 = Y_i^f \beta, \quad (2.14)$$

and

$$\alpha_1 = Y_i^f \alpha. \quad (2.15)$$

**Remark 2.4.6** Observe that the results of this section are derived without assuming that the plant  $G$  or models  $G_i$  are stable, as opposed to the results that we are going to derive in the next section.

**Remark 2.4.7** Note that  $T_i^f = GK_i^f / (1 + GK_i^f)$  is the actual closed-loop transfer function of the system, and  $\bar{T}_i^f = G_i K_i^f / (1 + G_i K_i^f)$  is the designed closed-loop transfer function of the system. Therefore, using similar substitutions that resulted in equation (2.12), we can obtain

$$T_i^f - \bar{T}_i^f = Y_i^f X_i^f (R_i^f - \bar{R}_i^f) .$$

However, since  $\bar{R}_i^f$  is the parametrization of  $G_i$  in terms of  $X_i^f$ ,  $Y_i^f$ ,  $N_i$ , and  $D_i$ , and hence

$$\bar{R}_i^f \equiv 0 , \quad \forall f, \forall i ,$$

it follows that

$$T_i^f - \bar{T}_i^f = Y_i^f X_i^f R_i^f . \quad (2.16)$$

By comparing the argument of the  $\mathcal{H}_\infty$  norm given in expression (2.10) with the left hand side of equation (2.16), we see immediately that when the value of  $\|T_i^f - \bar{T}_i^f\|_\infty$  has become large; that is, when the closed-loop property of the actual system ( $T_i^f$ ) is significantly different from the closed-loop property of the designed system ( $\bar{T}_i^f$ ), the value of  $\|Y_i^f X_i^f R_i^f\|_\infty$  will be large.

**Remark 2.4.8** We observe that the effect of the noise disturbance on the filtered output error ( $\xi_1 = \beta_1 - \hat{R}_i^f \alpha_1$ ) is given by  $w_i^f$ , the effect of the noise disturbance at the plant output attenuated by the sensitivity function of the actual closed-loop system.

In order to further our discussions systematically, we digress to describe, in the next section, a control design method that will be employed in the controller design stage of the iterative identification and control design methodology. We will return to discuss the approximation of the  $R_i^f$  transfer function in Section 2.6.

## 2.5 Internal Model Control Method

In this section we outline the results of the Internal Model Control (IMC) method [Morari and Zafriou 1989] that are relevant to the control design stage of the iterative identification and control design methodology. Whenever possible, we refer to [Morari and Zafriou 1989] for proofs of these results. Firstly we make the following assumptions.

**Assumption 2.5.1 [Not Necessarily Stable Transfer Function]** *A not necessarily stable transfer function has  $k$  distinct poles in the open right-half plane, a pole of multiplicity  $l$  at the origin, and no zeros on the imaginary axis. Furthermore we denote the  $k$  poles of the not necessarily stable transfer function in the open right-half plane by  $p_1, p_2, \dots, p_k$ .*

**Assumption 2.5.2 [Stable Transfer Function]** *A stable transfer function has no poles in the closed right-half plane and no zeros on the imaginary axis.*

In the following, we will use the notations  $n_H$  and  $d_H$  to denote the numerator polynomial and the denominator polynomial of a rational transfer function  $H$ .

For a model that has a not necessarily stable strictly proper transfer function

$$G_i = \frac{n_{G_i}}{d_{G_i}},$$

we can write

$$n_{G_i} = \tilde{n}_{G_i} \prod_i (z_i - s), \quad \text{and} \quad d_{G_i} = s^l \tilde{d}_{G_i} \prod_{i=1}^k (p_i - s),$$

where the polynomials  $\tilde{n}_{G_i}$  and  $\tilde{d}_{G_i}$  have no zeros in the closed right-half plane, and all of  $z_i$  and  $p_i$  have positive real parts.

We can then write  $G_i = [G_i]_m [G_i]_a$ , with

$$[G_i]_m = \frac{\tilde{n}_{G_i} \prod_i (z_i^* + s)}{d_{G_i}}; \quad z_i^* \text{ is the complex-conjugate of } z_i,$$

and

$$[G_i]_a = \frac{\prod_i (z_i - s)}{\prod_i (z_i^* + s)}.$$

We also define an all pass transfer function

$$[D_i]_a = \frac{\prod_{i=1}^k (p_i - s)}{\prod_{i=1}^k (p_i^* + s)}$$

that is related to the poles of  $G_i$  in the open right-half plane.

We can now state the following result:

**Theorem 2.5.1** *With reference to Figure 2.4, let  $G_i$  be a not necessarily stable model (see Assumption 2.5.1) for the plant  $G$ . Assume that the collection of open right-half plane poles in the Laplace transform of the generalized input,  $\nu(t) = r(t) - d(t)$ , is a subset of  $\{p_1, p_2, \dots, p_k\}$ .<sup>1</sup> Denote these as  $p_1, \dots, p_{k'}$ , with  $0 \leq k' \leq k$ . Furthermore assume that  $\nu(s)$  has at least  $l$  poles at the origin.<sup>2</sup> Define*

$$B_\nu = \prod_{i=1}^{k'} \frac{p_i - s}{p_i^* + s},$$

*and factor  $\nu(s)$  into an all pass factor  $\nu_a(s)$  (which contains all the zeros of  $\nu(s)$  in the open right-half plane) and a minimum-phase factor  $\nu_m(s)$  (which includes all the poles of  $\nu(s)$  in the open right-half plane and at the origin). Then the controller*

$$K_i^j \stackrel{\text{def}}{=} \frac{Q_i^j}{1 - G_i Q_i^j}$$

*stabilizes the model  $G_i$  if*

$$Q_i^j = [D_i]_a ([G_i]_m B_\nu \nu_m)^{-1} \left\{ ([D_i]_a [G_i]_a)^{-1} B_\nu \nu_m \right\}_* F_i^j, \quad (2.17)$$

*where the IMC filter  $F_i^j$  is given by*

$$F_i^j = \frac{(\lambda_i^j)^{k+q-1+N} \left( \sum_{i=0}^{k+q-1} a_i s^i \right)}{(s + \lambda_i^j)^{k+q-1+N}},$$

*with  $N \geq n$ ;  $n$  is the relative degree of  $G_i$ , and  $q \geq l$  is the number of poles of  $\nu(s)$  at the origin. The constants  $a_0, a_1, \dots, a_{k+q-1}$  in the IMC filter  $F_i^j$  are determined from the constraints:*

$$F_i^j(s) = 1 \quad \text{at the } k \text{ poles, } s = p_1, p_2, \dots, p_k, \text{ in the open right-half plane,}$$

*and*

$$F_i^j(0) = 1, \quad \text{if } q > 0,$$

*and*

$$\frac{d^m F_i^j}{ds^m}(0) = 0 \quad \text{for } m = 1, 2, \dots, q-1 \text{ if } q > 1.$$

*(The operator  $\{\}_*$  in equation (2.17) denotes that after a partial fraction expansion of the operand, all terms involving the poles of  $[G_i]_a^{-1}$  are omitted.)*

<sup>1</sup>As noted in [Morari and Zafriou 1989], this assumption is necessary to make a well posed problem.

<sup>2</sup>As noted in [Morari and Zafriou 1989], this assumption is necessary for the closed-loop system to handle plant input disturbances whose Laplace transform may have poles at the origin.

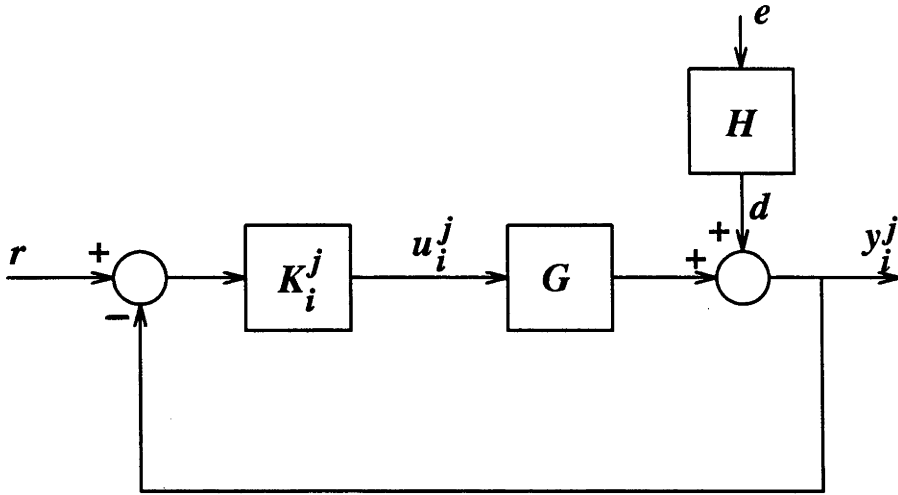


Figure 2.4: Closed-loop system

**Proof**

See Theorem 5.2-1 and Section 5.3.1 of [Morari and Zafiriou 1989]. □

**Remark 2.5.1** We must emphasize that  $K_i^j = Q_i^j / (1 - G_i Q_i^j)$ , with  $Q_i^j$  stable, does not stabilize  $G_i$  generally. However, since the transfer function  $Q_i^j$  in the IMC method is designed to satisfy the following conditions,

1.  $Q_i^j$  has no poles in the closed right-half plane, and
2.  $(1 - G_i Q_i^j) G_i$  has no poles in the closed right-half plane,

the controller  $K_i^j = Q_i^j / (1 - G_i Q_i^j)$  will stabilize  $G_i$  for all  $Q_i^j$  designed by the IMC method.

**Remark 2.5.2** In the IMC method, the relative degree  $N$  of the IMC filter is chosen to ensure that  $Q_i^j$  and  $K_i^j$  are proper. The design parameter  $\lambda_i^j$  is for adjusting the bandwidth of the designed closed-loop transfer function  $\bar{T}_i^j = G_i Q_i^j$ .



**Remark 2.5.3** We emphasize that the stabilization of  $G_i$  by  $K_i^j$  does not imply the stabilization of  $G$  by  $K_i^j$ .

For the discussion of robust stabilization, we need the following well known result.

**Theorem 2.5.2** *Let the plant  $G$  and the model  $G_i$  have the same number of poles in the open right-half plane. If  $K_i^j$  stabilizes  $G_i$ , then  $K_i^j$  stabilizes  $G$  if*

$$\|L_i \bar{T}_i^j\|_\infty < 1 . \quad (2.18)$$

where

$$\left| \frac{G(j\omega) - G_i(j\omega)}{G_i(j\omega)} \right| \leq L_i(\omega) ,$$

and

$$\bar{T}_i^j = \frac{G_i K_i^j}{1 + G_i K_i^j} .$$

### Proof

See Theorem 2.5-1 of [Morari and Zafriou 1989]. □

In the sequel, we shall call a plant (or a model) whose transfer function satisfies Assumption 2.5.2 as a stable plant (or a stable model). From Theorem 2.5.2 it is clear that if  $G_i$  and  $G$  are stable and if the mismatch between  $G_i$  and  $G$  is significant only in the high frequency region, then robust stabilization of  $G_i$  may be secured by designing a sufficiently small bandwidth for  $\bar{T}_i^j$ . To make precise the last statement, we consider the situation where  $K_i^j$  is designed on the basis of a stable  $G_i$  (for a stable  $G$ ) when the reference input is a step function. Under these conditions, Theorem 2.5.1 can be simplified as follows:

**Theorem 2.5.3** *With reference to Figure 2.4, let  $G_i$  be a stable proper model for a stable plant  $G$ . Let the reference input  $r$  to be a step function. Then the controller that stabilizes  $G_i$  is given by*

$$K_i^j = \frac{Q_i^j}{1 - G_i Q_i^j}$$

where

$$Q_i^j = [G_i]_m^{-1} F_i^j, \\ F_i^j = \left( \frac{\lambda_i^j}{s + \lambda_i^j} \right)^N; \quad \lambda_i^j > 0, \quad N \geq n,$$

$[G_i]_m$  is the minimum-phase factor of  $G_i$ , and  $n$  is the relative degree of  $G_i$ .

### Proof

Direct consequence of Theorem 2.5.1. □

**Remark 2.5.4** Since  $G_i$  is stable in Theorem 2.5.3, the only constraint on the IMC filter is  $F_i^j(0) = 1$ . This ensures that the output of the designed closed-loop system tracks a step reference input with zero steady state error. Observe that, under these conditions, the IMC filter takes the particularly simple form of  $F_i^j = [\lambda_i^j / (s + \lambda_i^j)]^N$ .

It follows from Theorem 2.5.3 that, when  $G_i$  is stable, the designed closed-loop transfer function is given by  $\bar{T}_i^j = F_i^j [G_i]_a$ , where  $[G_i]_a$  is the all pass factor of  $G_i$ . Since  $[G_i]_a$  does not affect  $|\bar{T}_i^j(j\omega)|$ , it is apparent that  $\lambda_i^j$  is the designed closed-loop bandwidth with a  $-3N$  dB attenuation. Furthermore, the form of  $F_i^j = [\lambda_i^j / (s + \lambda_i^j)]^N$  implies that  $|\bar{T}_i^j(j\omega)|$  is a monotonically decreasing function of  $\omega$  with  $\|\bar{T}_i^j\|_\infty = |\bar{T}_i^j(0)| = 1$ . Therefore it is obvious that, if  $L_i(\omega)$  is a continuous function with  $L_i(0) \neq 0$ , then by choosing a sufficiently small  $\lambda_i^f$ , the largest value of

$$|L_i(\omega) \bar{T}_i^j(j\omega)|$$

can be made to occur at  $\omega = 0$ . Under these conditions, Theorem 2.5.2 implies that  $K_i^j$  stabilizes  $G$  if

$$\left| \frac{G(0) - G_i(0)}{G_i(0)} \right| < 1.$$

Hence we have the following:

**Corollary 2.5.1** Let the plant  $G$  and the model  $G_i$  be stable, then the controller  $K_i^j$  designed by the method described in Theorem 2.5.3 robustly stabilizes  $G_i$  for a sufficiently small  $\lambda_i^j$  if

$$\left| \frac{G(0) - G_i(0)}{G_i(0)} \right| < 1.$$

**Remark 2.5.5** It is obvious that the condition

$$\left| \frac{G(0) - G_i(0)}{G_i(0)} \right| < 1$$

is not satisfied if  $G(0)$  and  $G_i(0)$  have different signs. In fact (as we will show in the next theorem), when  $G$  and  $G_i$  are stable, the controller designed by the method described in Theorem 2.5.3 may robustly stabilize  $G_i$  with a sufficiently small  $\lambda_i^j$  *only if*  $G(0)$  and  $G_i(0)$  have the same sign.

**Remark 2.5.6** The condition

$$\left| \frac{G(0) - G_i(0)}{G_i(0)} \right| < 1$$

given in Corollary 2.5.1 requires the relative error in  $G_i(0)$  to be smaller than 100%. This is stronger than it is necessary when  $G(0)$  and  $G_i(0)$  have the same sign. We will next show that, if  $G$  is stable and if  $K_i^j$  is designed by the method described in Theorem 2.5.3 to have a sufficiently small  $\lambda_i^j$ , it is necessary and *sufficient* to know the sign of  $G$  in order to stabilize  $G$ .

**Theorem 2.5.4** *With reference to Figure 2.4, let the stable strictly proper plant*

$$G(s) = \frac{n_G(s)}{d_G(s)}, \quad n_G(0) \neq 0,$$

*have a stable strictly proper model*

$$G_i = [G_i]_m [G_i]_a,$$

where

$$[G_i]_m = G_i(0) \left[ \frac{\tilde{n}_{G_i}(s) \prod_i (z_i^* + s)}{d_{G_i}(s)} \right], \quad G_i(0) \neq 0,$$

$$\frac{\tilde{n}_{G_i}(0)}{d_{G_i}(0)} = \frac{1}{\prod_i z_i^*} > 0,$$

$$[G_i]_a = \frac{\prod_i (z_i - s)}{\prod_i (z_i^* + s)}, \quad z_i \text{ is the } i^{\text{th}} \text{ unstable zero of } G_i,$$

and  $\tilde{n}_{G_i}$  and  $d_{G_i}$  have no zeros in the closed right-half plane.

If  $K_i^j$  is designed by the method described in Theorem 2.5.3 to have a sufficiently small  $\lambda_i^j$ , then  $K_i^j$  stabilizes  $G$  if and only if  $G_i(0)$  and  $G(0)$  have the same sign.

**Proof**

By using the method described in Theorem 2.5.3, we can obtain

$$K_i^j = \frac{[G_i]_m^{-1} \left( \frac{\lambda_i^j}{s + \lambda_i^j} \right)^N}{1 - [G_i]_a \left( \frac{\lambda_i^j}{s + \lambda_i^j} \right)^N} .$$

Since the transfer function

$$[G_i]_a \left( \frac{\lambda_i^j}{s + \lambda_i^j} \right)^N$$

is stable strictly proper and has an  $\mathcal{H}_\infty$ -norm

$$\left\| [G_i]_a \left( \frac{\lambda_i^j}{s + \lambda_i^j} \right)^N \right\|_\infty = 1$$

occurs at the origin, the transfer function

$$1 - [G_i]_a \left( \frac{\lambda_i^j}{s + \lambda_i^j} \right)^N$$

in the denominator of  $K_i^j$  is stable proper and has no zeros in the closed right-half plane other than at the origin. In fact, it can be shown that the last transfer function in the denominator of  $K_i^j$  has a simple zero at the origin. After some algebraic simplifications, we can write

$$K_i^j = \frac{(\lambda_i^j)^N d_{G_i}(s)}{G_i(0) s n_*(s) \tilde{n}_{G_i}(s)} ,$$

where the polynomial  $n_*(s)$  has no zeros in the closed right-half plane, and  $n_*(0) > 0$ .

The actual closed-loop system involving  $G$  and  $K_i^j$  therefore has the following characteristic polynomial,

$$G_i(0) s n_*(s) \tilde{n}_{G_i}(s) d_G(s) + (\lambda_i^j)^N d_{G_i}(s) n_G(s) . \quad (2.19)$$

As  $\lambda_i^j$  approaches zero, all but one pole of the actual closed-loop system approach the zeros of  $n_*(s)$ ,  $\tilde{n}_{G_i}(s)$ , and  $d_G(s)$ . The stability of the closed-loop system will therefore depend on the remaining actual closed-loop pole. Let  $s_0$  denote this remaining actual closed-loop pole that is approaching the origin. After approximating  $d_G(s)$  and  $n_G(s)$  in polynomial (2.19) by the constant term of their respective Taylor series expansions at the origin, we consider the first order polynomial,

$$s + \frac{(\lambda_i^j)^N d_{G_i}(0) G(0)}{n_*(0) \tilde{n}_{G_i}(0) G_i(0)} ,$$

whose zero is  $s_0$ . It is apparent from this first order polynomial that  $K_i^j$  stabilizes  $G$  for a sufficiently small  $\lambda_i^j > 0$  if and only if  $G_i(0)$  and  $G(0)$  have the same sign.

□

**Remark 2.5.7** In situations where the plant  $G$  is unstable (and presumably,  $G$  is represented by an unstable model  $G_i$ ), in addition to the constraint  $F_i^j(0) = 1$  imposed by the requirement of tracking a step reference input,  $F_i^j$  is constrained to be unity at the open right-half plant poles of  $G_i$  (see Theorem 2.5.1). Therefore, depending on the multiplicative model uncertainty bound  $L_i(\omega)$ , there may not exist a value for  $\lambda_i^j$  such that  $K_i^j$  robustly stabilizes  $G_i$ .

## 2.6 Approximation of the $R_i^f$ Transfer Function

In Section 2.4, we have shown that the closed-loop identification of  $G$  can be reformulated into an open-loop identification of the stable proper transfer function  $R_i^f$  that parametrizes  $G$  via the equation

$$G = \frac{N_i + R_i^f Y_i^f}{D_i - R_i^f X_i^f} .$$

In the following we shall, for simplicity, study situations where the plant  $G$  and the models  $G_i$  are stable. (Situations where the plant and models are not necessarily stable will be studied in later chapters.) We assume that the reference input is a step function and use the IMC method [Morari and Zafiriou 1989] to design controllers such that  $Q_i^j$  and  $K_i^j$  are bi-proper. This is accomplished by setting  $N = n$  for the IMC filter, where  $n$  is the relative degree of  $G_i$  (see Theorem 2.5.3). Specifically, the transfer function

$$Q_i^j = \frac{K_i^j}{1 + G_i K_i^j} \quad (2.20)$$

that parametrizes  $K_i^j$  is given by

$$Q_i^j = [G_i]_m^{-1} F_i^j , \quad (2.21)$$

with

$$F_i^j = \left( \frac{\lambda_i^j}{s + \lambda_i^j} \right)^n .$$

With the controller designed by the above procedure, we shall show that when  $j = f$ , the transfer function to be identified (namely,  $R_i^f$ ) is the product of a known stable proper transfer function and an unknown stable strictly proper transfer function. An analysis of the form of the unknown factor in  $R_i^f$  indicates how it can be sensibly approximated by a low-order transfer function.

Since the model  $G_i = N_i/D_i$  is stable, we may choose  $N_i = G_i$  and  $D_i = 1$  so that equation (2.2) becomes

$$G = G_i + \frac{R_i^f}{1 - R_i^f Q_i^f} . \quad (2.22)$$

Furthermore, the equations  $K_i^f = X_i^f/Y_i^f$  and  $N_i X_i^f + D_i Y_i^f = 1$  imply that

$$X_i^f = Q_i^f .$$

Notice also that

$$\bar{T}_i^f = G_i Q_i^f ,$$

and

$$Y_i^f = 1 - \bar{T}_i^f .$$

Let  $n_H$  and  $d_H$  denote, respectively, the numerator polynomial and the denominator polynomial of a rational transfer function  $H$ . By re-writing equation (2.22) as

$$R_i^f = \frac{G - G_i}{1 + Q_i^f (G - G_i)} , \quad (2.23)$$

we can obtain, after substituting equations (2.20) and (2.21) into equation (2.23) and performing some algebraic manipulations,

$$R_i^f = \{[G_i]_m d_{F_i^f}\} \left\{ \frac{d_{G_i} n_G - d_G n_{G_i}}{d_{K_i^f} d_G + n_{K_i^f} n_G} \right\} . \quad (2.24)$$

Note that equation (2.24) can also be written as

$$R_i^f = \tilde{R}_i^f \check{R}_i^f , \quad (2.25)$$

where

$$\tilde{R}_i^f = [G_i]_m d_{F_i^f}$$

is a *known* stable proper transfer function, and

$$\check{R}_i^f = \frac{d_{G_i} n_G - d_G n_{G_i}}{d_{K_i^f} d_G + n_{K_i^f} n_G} \quad (2.26)$$

is an *unknown* stable strictly proper transfer function that depends on the unknown transfer function  $G$ . Therefore the problem of identifying  $R_i^f$  has become one of identifying its unknown factor  $\check{R}_i^f$ . We shall summarize this important result in the following theorems.

**Theorem 2.6.1** *Let the controller  $K_i^f$  be designed as stated in Theorem 2.5.3 with  $N = n$ , where  $n$  is the relative degree of  $G_i$ , then the unknown stable strictly proper transfer function to be identified,*

$$R_i^f = \frac{G - G_i}{1 + Q_i^f (G - G_i)} ,$$

can be factorized as

$$R_i^f = \tilde{R}_i^f \check{R}_i^f ,$$

where  $\check{R}_i^f$  is an unknown stable strictly proper transfer function, and  $\tilde{R}_i^f$  is a known stable proper transfer function given by

$$\tilde{R}_i^f = [G_i]_m (s + \lambda_i^f)^n ,$$

where  $\lambda_i^f$  is the designed closed-loop system bandwidth (with a  $-3n$  dB attenuation) just before system identification is carried out.

### Proof

See Appendix B. □

**Remark 2.6.1** Note that the factorization of  $R_i^f$  given in Theorem 2.6.1 is naturally induced by the IMC design procedure.

**Remark 2.6.2** Observe from Theorem 2.6.1 that the poles of  $\check{R}_i^f$  are the poles of the actual closed-loop transfer function,  $T_i^f$ .

**Remark 2.6.3** It is important to note that  $\check{R}_i^f = 0$  if and only if  $G = G_i$ .

**Theorem 2.6.2** For the factorization  $R_i^f = \tilde{R}_i^f \check{R}_i^f$  given in Theorem 2.6.1, the order and the relative degree of the transfer function  $\check{R}_i^f$  are respectively, given by

$$\text{order of } \{\check{R}_i^f\} = \text{order of } \{G\} + \text{order of } \{G_i\} - (M + N) ,$$

and

$$\text{rel deg } \{\check{R}_i^f\} = \min(\text{rel deg } \{G\}, \text{rel deg } \{G_i\}) ,$$

where  $M$  is the number of common zeros in  $G$  and  $G_i$ , and  $N$  is the number of common poles in  $G$  and  $G_i$ .

### Proof

See Appendix C. □

**Remark 2.6.4** Observe that the order of  $\check{R}_i^f$  is constrained by the degree of the polynomial  $d_{K^f} d_G$ , which is an unknown (see equation (2.26)).

**Remark 2.6.5** The order of  $\check{R}_i^f$  would be large generically (see Theorem 2.6.2). However, as the control-relevant model approximation criterion is heavily frequency weighted, it may be necessary to update the model only in a “small” frequency range. Hence a low-order estimate for  $\check{R}_i^f$  may suffice. (For the case of system identification, consideration of excitation conditions in a “small” band of frequencies implies that only a few parameters may be estimated.) Since we are going to identify  $\check{R}_i^f$  (actually  $R_i^f$ ) and update  $G_i$  to  $G_{i+1}$  when the step response of the actual closed-loop system exhibits unacceptable oscillations and/or overshoot, we expect  $\check{R}_i^f$  to have complex-conjugate poles. Therefore a transfer function which can serve as an approximation of  $\check{R}_i^f$  is at least of second order. Moreover, since the smallest possible relative degree of a strictly proper transfer function is one and the relative degree of  $G$  is unknown, we have to assume that the relative degree of  $\check{R}_i^f$  could be one.



It was shown in equation (2.12) that the frequency weighted open-loop system identification problem is to find, using the signals  $\alpha$  and  $\beta$ ,

$$\widehat{R}_i^f = \arg \min_{\sigma} \|X_i^f Y_i^f (R_i^f - \sigma)\|_{\infty} . \quad (2.27)$$

If we define

$$\widehat{R}_i^f = \widetilde{R}_i^f \widetilde{R}_i^f, \quad (2.28)$$

where  $\widetilde{R}_i^f$  is an unknown second-order stable strictly proper transfer function, then by substituting equations (2.21), (2.25), and (2.28) into equation (2.27), we can show that the frequency weighted open-loop system identification problem becomes one of finding

$$\widetilde{R}_i^f = \arg \min_{\phi} \|(\lambda_i^f)^n Y_i^f (\widetilde{R}_i^f - \phi)\|_{\infty} . \quad (2.29)$$

Therefore, for the purpose of identifying  $\widetilde{R}_i^f$ , we can modify equation (2.13) appropriately to give the signal model

$$\beta_1 = \widetilde{R}_i^f \alpha_2 + w_i^f, \quad (2.30)$$

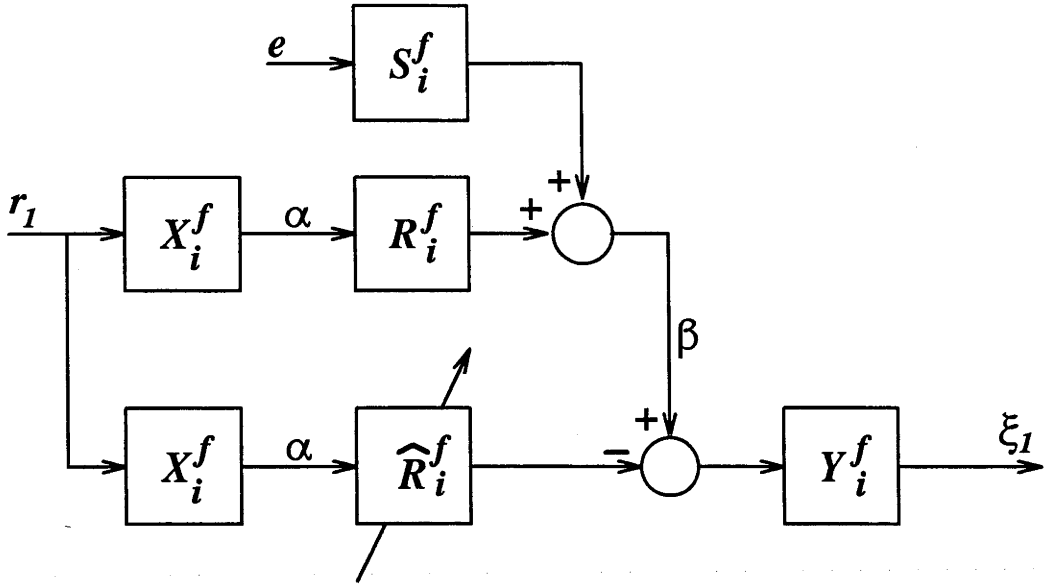
with

$$\alpha_2 = \widetilde{R}_i^f \alpha_1, \quad (2.31)$$

where  $\alpha_1$ ,  $\beta_1$  and  $w_i^f$  have been defined previously. The signals  $\beta_1$  and  $\alpha_2$  in the model described by equation (2.30) can easily be generated, using known filters, from the control input  $w_i^f$ , the measured output  $y_i^f$ , and the reference input  $r_1$ .

**Remark 2.6.6** Since  $Y_i^f = 1 - \widetilde{T}_i^f$  is the sensitivity function of the designed closed-loop system, we immediately see that the frequency shaping in the identification criterion given by equation (2.29) will force the updated model to have small modelling error in the range of frequencies where the designed sensitivity function cannot be made small by the controller  $K_i^f$ .

**Remark 2.6.7** From the signals defined in Theorem 2.4.2, we observed that  $R_i^f$ , the transfer function to be identified, is excited by the signal  $\alpha$ , where  $\alpha = X_i^f r_1$ . Therefore identification errors will be heavily weighted in the frequency range where the energy spectrum of  $\alpha$  is significant. In the current situation where  $G_i$  is stable, we have  $X_i^f = K_i^f / (1 + G_i K_i^f)$ . Since this is the transfer function between the reference input  $r_1$  and the control input  $w_i^f$ , the

Figure 2.5: Identification of  $R_i^f$ 

range of frequency where the energy spectrum of  $\alpha$  is significant is exactly where the control input  $u_i^f$  has appreciable energy induced by the reference input  $r_1$ . Therefore, for the system identification scheme presented, we automatically get the right frequency weighting for the input to  $R_i^f$ . (See [Hakvoort *et al.* 1994] and [Rivera 1991] for similar comments on direct identification of  $G$ .)

**Remark 2.6.8** When updating the model using the equation

$$G_{i+1} = G_i + \frac{\hat{R}_i^f}{1 - \hat{R}_i^f Q_i^f},$$

the order of the model may increase. To prevent the model order from increasing indefinitely, we use a frequency weighted balanced truncation scheme to reduce the order of  $G_{i+1}$ . Specifically we would like to find, ideally,

$$\hat{G}_{i+1} = \arg \min_{\eta} \left\| \frac{G_{i+1} K_i^f}{1 + G_{i+1} K_i^f} - \frac{\eta K_i^f}{1 + \eta K_i^f} \right\|_{\infty},$$

where  $\hat{G}_{i+1}$  is the reduced order model. In practice, we obtain approximately, under frequency weighted balanced truncation,

$$\hat{G}_{i+1} = \arg \min_{\eta} \left\| \frac{K_i^f (G_{i+1} - \eta)}{(1 + G_{i+1} K_i^f)^2} \right\|_{\infty}.$$

If the model is restricted to be of order  $m$ , the controller will be at most of order  $2m$  (see the controller design equations given in Theorem 2.5.3). In this way the controller complexity will be limited.

## 2.7 Simulation Results

We shall present some simulation results of applying iterative model approximation and control design (where the frequency weighted open-loop system identification procedure in the iterative identification and control design process is replaced by a corresponding frequency weighted rational function approximation procedure) to the control of a plant with the transfer function

$$G(s) = \frac{9}{(s+1)(s^2+0.06s+9)} .$$

By starting with an initial model whose transfer function is

$$G_0(s) = \frac{0.8}{s+1.2} ,$$

we will demonstrate that in the face of significant initial model uncertainties, it is possible to increase the closed-loop bandwidth through iterative model approximation and control design.

We first summarize the procedure in the following algorithm<sup>3</sup>:

### Step 1:

Set  $G_i = G_0$ , where  $G_0$  is the transfer function of an initial model of the plant.

### Step 2:

Factorize  $G_i$  as  $G_i = [G_i]_m [G_i]_a$ , where  $[G_i]_m$  is the minimum-phase factor of  $G_i$ , and  $[G_i]_a$  is the associated all pass factor of  $G_i$ .

---

<sup>3</sup>This provisional algorithm will be modified accordingly when the fine details of the iterative identification and control design methodology are described in the sequel.

**Step 3:**

For  $j = 0$ , find  $K_i^j = Q_i^j / (1 - G_i Q_i^j)$ , with  $Q_i^j = [G_i]_m^{-1} F_i^j$ , where

$$F_i^j = \left( \frac{\lambda_i^j}{s + \lambda_i^j} \right)^n ; \quad \lambda_i^j > 0 ,$$

$n$  is the relative degree of  $G_i$ , and  $\lambda_i^j$  is chosen such that  $K_i^j$  robustly stabilizes  $G_i$  in the sense that the step response of the actual closed-loop system has, at most, little oscillations and/or overshoot. Stop here if the robust stabilizing controller results in a closed-loop system which meets the specified bandwidth. Otherwise, proceed to the next step.

**Step 4:**

Let  $j = j + 1$  and set  $\lambda_i^j = \lambda_i^{j-1} + \epsilon$  for small  $\epsilon > 0$ , and re-design the controller  $K_i^j$  using the equations given in **Step 3**. Stop here if the design produces a robust stabilizing controller with the closed-loop system satisfying the specified bandwidth. Otherwise, repeat this step if  $K_i^j$  robustly stabilizes  $G_i$ ; else proceed to the next step. (The index  $j$  at the time to go to the next step has a value of  $f$ .)

**Step 5:**

By using the  $\check{R}_i^f$  calculated from the known  $G$ , perform frequency weighted rational function approximation to obtain

$$\tilde{R}_i^f = \arg \min_{\phi} \| (\lambda_i^f)^n Y_i^f (\check{R}_i^f - \phi) \|_{\infty} .$$

Then update the model using the following set of equations:

$$\tilde{R}_i^f = [G_i]_m d_{F_i^f} ,$$

$$\hat{R}_i^f = \tilde{R}_i^f \check{R}_i^f ,$$

and

$$G_{i+1} = G_i + \frac{\hat{R}_i^f}{1 - \hat{R}_i^f Q_i^f} .$$

**Step 6:**

If  $G_{i+1}$  is stable, find the reduced order model

$$\hat{G}_{i+1} = \arg \min_{\eta} \left\| \frac{K_i^f (G_{i+1} - \eta)}{(1 + G_{i+1} K_i^f)^2} \right\|_{\infty} .$$

Otherwise, stop here.

**Step 7:**

Set  $G_i = \hat{G}_{i+1}$  and return to **Step 2**.

**Remark 2.7.1** In the algorithm, rational function approximation has to be carried out when  $\|T_i^f - \bar{T}_i^f\|_{\infty}$  is no longer small. Broadly speaking, this will correspond to a significant difference between the designed nominal performance (depending on  $G_i$  and  $K_i^f$ ) and the actual performance (depending on  $G$  and  $K_i^f$ ). A user friendly test to identify this situation is via the visual comparison of the step responses of the actual and designed closed-loop systems. In particular, the observed actual step response may exhibit much more oscillations and/or overshoot than the designed values. This is not of course the same thing as guaranteeing that the  $\mathcal{H}_{\infty}$  error above has become large, but neither is it unrelated.

To be more precise, define the peak gain of a system, whose transfer function is  $F$  (and denote the corresponding unit impulse response by  $f$ ), by

$$\|f\|_1 = \sup_{\|w\|_{\infty} \neq 0} \frac{\|f * w\|_{\infty}}{\|w\|_{\infty}} ,$$

where  $*$  denotes the convolution operator. This is also equal to the *total variation* of the system's unit step response [Boyd and Barratt 1989] defined as the sum of all consecutive peak-to-valley differences in the unit step response. It can be shown [Boyd and Doyle 1987] that, if  $F$  is a stable strictly proper transfer function,

$$\|F\|_{\infty} \leq \|f\|_1 \leq 2n\|F\|_{\infty} ,$$

where  $n$  is the order of  $F$ . Now the peak gain,  $\|\tilde{t}_i^f\|_1$ , corresponds to the error in closed-loop transfer function  $\tilde{T}_i^f = T_i^f - \bar{T}_i^f$ . Since

$$\|\tilde{t}\|_1 \geq \|t_i^f\|_1 - \|\bar{t}_i^f\|_1 ,$$

it follows that, if the observed step response of  $T_i^f$  exhibits much more oscillations and/or overshoot than the designed step response of  $\bar{T}_i^f$ ,

$$\|t_i^f\|_1 \gg \|\bar{t}_i^f\|_1 ,$$

and hence,

$$\|\tilde{t}_i^f\|_1 \gg 0 .$$

Since the peak gain also provides a *loose* lower bound for the  $\mathcal{H}_\infty$  gain via the relationship  $\|f\|_1 \leq 2n\|F\|_\infty$ , it is likely that  $\|T_i^f - \bar{T}_i^f\|_\infty$  becomes large when the observed actual step response exhibits much more oscillations and/or overshoot than the desired one.

**Remark 2.7.2** The last remark explains why, in the simulation, the models are updated whenever the actual step response exhibits *unacceptable* oscillations and/or overshoot.

The simulation results are presented in Figure 2.6 and Figure 2.7.

We begin by designing a controller, on the basis of  $G_0(s) = 0.8/(s + 1.2)$ , for achieving a closed-loop bandwidth of 0.02 rad/s. The actual closed-loop unit step response is shown in Graph (a) of Figure 2.6. Since the closed-loop is well behaved, the designed closed-loop bandwidth is increased progressively by controller re-design. When the designed closed-loop bandwidth has reached 0.04 rad/s, the actual closed-loop unit step response is shown in Graph (b) of Figure 2.6. Note that this step response shows significant oscillations. By performing a frequency weighted rational function approximation for  $\check{R}_0^f$  with a  $\hat{R}_0^f$  whose order is two and relative degree is one (see Remark 2.6.5 for the rationale of this choice), we obtain

$$\hat{R}_0^f = \frac{-1.5117s + 2.5293}{s^2 + 0.0422s + 8.9688} .$$

The corresponding estimate for  $R_0^f$  is

$$\hat{R}_0^f = \frac{-1.2094s^2 + 1.9751s + 0.0809}{s^3 + 1.2422s^2 + 9.0194s + 10.7625} .$$

By using the above estimate for  $R_0^f$ , the model is updated to

$$G_1 = \left( \begin{array}{c} -0.4094s^4 + 1.5496s^3 \\ +9.7063s^2 + 8.9957s + 0.3444 \end{array} \right) / \left( \begin{array}{c} s^5 + 2.5427s^4 + 10.6541s^3 \\ +21.8522s^2 + 13.6265s + 0.5108 \end{array} \right) .$$

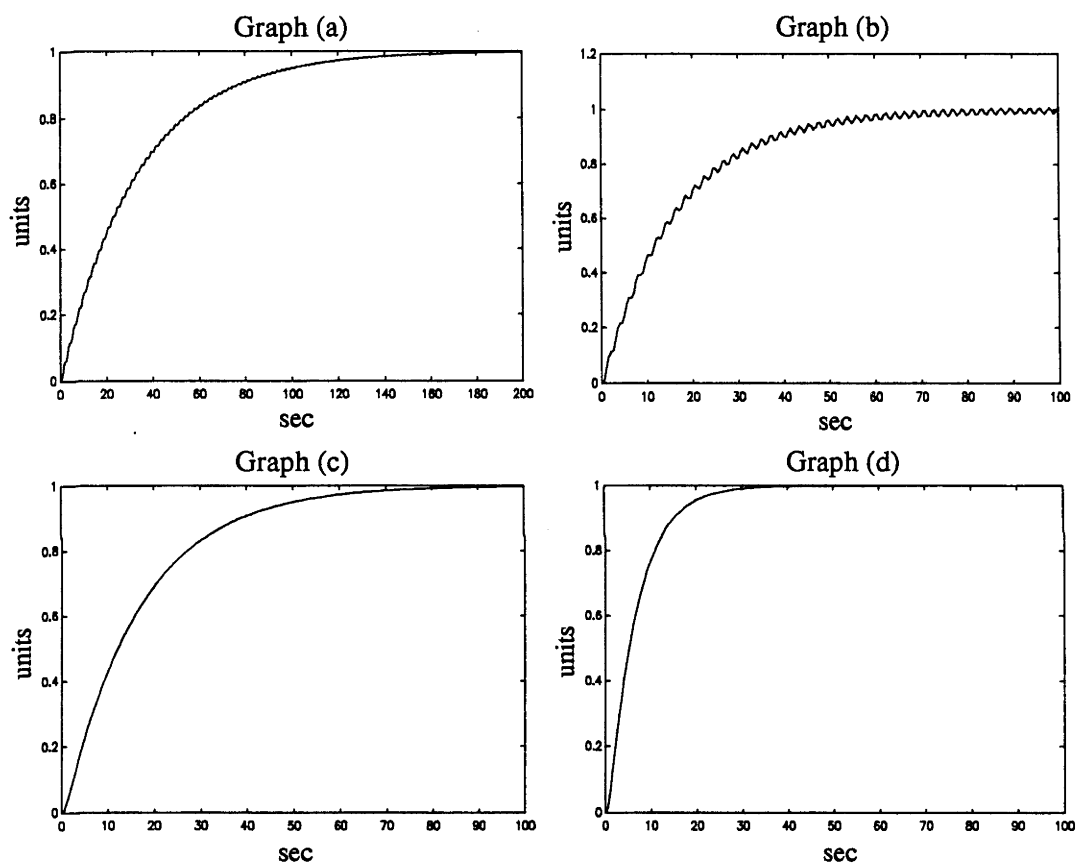


Figure 2.6: Step responses 1 of actual closed-loop system

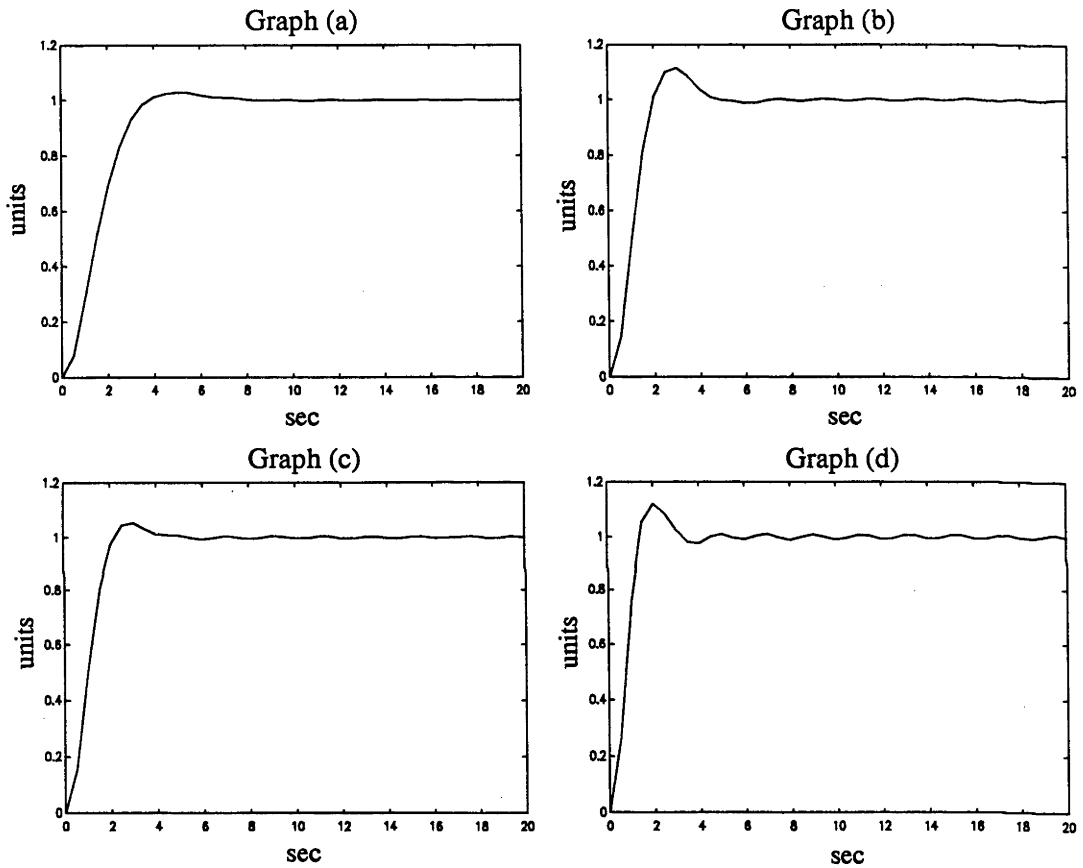


Figure 2.7: Step responses 2 of actual closed-loop system



After performing frequency weighted model reduction, we have

$$\hat{G}_1 = \frac{-0.4094s^2 + 2.0572s + 7.175}{s^3 + 1.3027s^2 + 8.9908s + 10.6411} .$$

We will set  $G_1 = \hat{G}_1$  for the next stage of iteration.

By keeping the designed closed-loop bandwidth at 0.04 rad/s, a controller is designed on the basis of  $G_1$ . The actual closed-loop unit step response is shown in Graph (c) of Figure 2.6. It is obvious that this step response is much better than the one shown in Graph (b). Graph (d) of Figure 2.6 shows the unit step response when the designed closed-loop bandwidth is increased to 0.1 rad/s. Graphs (a) and (b) of Figure 2.7 show the unit step responses when the designed closed-loop bandwidths are 0.5 rad/s and 1 rad/s respectively. Note that there is about 10% overshoot in the step response when the designed closed-loop bandwidth is 1 rad/s. Using the same procedure as before, we obtain

$$\hat{R}_1^f = \frac{-0.082031s - 0.91016}{s^2 + 0.6539s + 11.959} ,$$

$$\hat{R}_1^f = \left( \begin{array}{c} -0.033582s^4 - 0.73411s^3 \\ -4.9276s^2 - 10.757s - 6.5304 \end{array} \right) / \left( \begin{array}{c} s^5 + 1.9566s^4 + 21.802s^3 \\ +32.099s^2 + 114.48s + 127.26 \end{array} \right) ,$$

$$G_2 = \left( \begin{array}{c} -0.44296s^{10} - 4.3237s^9 \\ -11.459s^8 - 16.883s^7 \\ +257.85s^6 + 2042.6s^5 \\ +7485.1s^4 + 21325s^3 \\ +41969s^2 + 42357s + 16003 \end{array} \right) / \left( \begin{array}{c} s^{11} + 14.106s^{10} + 97.726s^9 \\ +572.45s^8 + 2392s^7 + 8230.1s^6 \\ +23162s^5 + 50342s^4 + 88762s^3 \\ +114100s^2 + 84389s + 25540 \end{array} \right) .$$

After performing frequency weighted model reduction, we have

$$\hat{G}_2 = \frac{-0.40612s^2 + 0.80196s + 6.3884}{s^3 + 1.0977s^2 + 8.882s + 9.3027} .$$

Before the iteration continues, we set  $G_2 = \hat{G}_2$ .

On the basis of  $G_2$ , a new controller is designed for a closed-loop bandwidth of 1 rad/s. The resulting unit step response is shown in Graph (c) of Figure 2.7. When the nominal closed-loop bandwidth is increased to 2 rad/s, the unit step response is shown in Graph (d) of Figure 2.7. This example clearly demonstrated that it is possible to increase the bandwidth of a closed-loop system by the iterative model approximation and control design procedure.

**Remark 2.7.3** We must emphasize that in these simulations, instead of performing frequency weighted open-loop system identification using input-output measurements obtained under

closed-loop conditions, we actually perform the corresponding frequency weighted rational function approximation

$$\hat{R}_i^f = \arg \min_{\phi} \|(\lambda_i^f)^n Y_i^f (\check{R}_i^f - \phi)\|_{\infty} ,$$

where  $\check{R}_i^f$  is obtained from the known  $G$ . The reasons for doing this are:

1. This serves as a benchmark in the sense that it corresponds to performing system identification with an infinite number of noiseless measurements.
2. We like to know how serious the problems may be due to employing a low-order approximation for  $\hat{R}_i^f$ . This is important for later system identification studies.
3. We are, at this stage, more concerned with the concept of iterative system identification and control design as applied to adaptive robust control.
4. Efficient algorithms for performing  $\mathcal{H}_{\infty}$  system identification are still lacking, and the corresponding theory is still not well understood [Helmicki *et al.* 1991, Parker and Bitmead 1987, Partington 1991].

In Chapter 3 to Chapter 5, we shall study the iterative identification and control design approach under realistic situations where only a finite number of noisy input-output data are available.

## 2.8 Discussions

We have reviewed in Section 2.1 the strength and weakness of both the traditional adaptive control and the robust control design methods. These methods should be able to complement each other and there should be natural ways in which they could blend harmoniously. We suggested that one way is through the iterative identification and control design philosophy propounded by Anderson and Kosut [1991]. We have shown, by simulation, that by starting with a (crude) initial model of the plant and a (small bandwidth) robustly stabilizing controller, the bandwidth of the closed-loop system can be increased progressively through an iterative control-relevant model approximation and control design procedure. We highlight the following points which underpin the success of the approach:

- The use of control-relevant frequency weighting in the model approximation criterion.
- Updating of the model when the effects of its errors are no longer small in the closed-loop response. This will ensure that model uncertainties are emphasized in the correct range of frequencies.
- When the model has no poles at the origin, the controller designed by the IMC method for a step reference input always has an integrator. Therefore it is insensitive to model uncertainties at low frequencies, provided the gain of the model at low frequencies is of the right sign.
- The controller designed by using the IMC method induces a natural factorization, namely  $R_i^f = \tilde{R}_i^f \check{R}_i^f$ , in the parametrization,  $R_i^f$ , of the plant. This enables the model approximation problem (and in later chapters, the system identification problem) to be solved effectively.

In conclusion, we emphasize that only stable plants and models are considered in this first study. We address the following issues in the sequel:

- Iterative identification and control design with finite number of noisy input-output measurements.
- Signal conditions that are necessary for successful model updates, and possible limitations imposed by unstable zeros of plants and/or models.
- Reliable model validation procedures that are in line with the objective of iterative identification and control design.
- Extension of the method to deal with unstable plants and models.

## Chapter 3

# Iterative Identification and Control Design

In Chapter 2 we introduced and discussed an iterative identification and control design approach for the closed-loop system as shown in Figure 3.1 under ideal conditions where an infinite number of noiseless input-output measurements are available. We also prepared the reader for what changes are in store when using  $\mathcal{L}_2$  identification techniques. Encouraged by the simulation results of Section 2.7, we investigate in this chapter the iterative identification and control design approach in more realistic situations when only a finite number of noisy input-output measurements are available. We explore further, in Section 3.1, the control-relevant system identification criterion formulated in Section 2.3 and highlight its similarity to a frequency weighted closed-loop model reduction problem that was investigated in [Anderson and Liu 1989]. This comparison and a concrete example will provide further insights into the role of appropriate frequency weighting in the control-relevant system identification procedure adopted in the iterative identification and control design process. Sections 3.2 and 3.3 are devoted to extending the iterative identification and control design procedure developed in Chapter 2 for stable plants to (Type 1 stable) plants that, other than having poles in the open left-half plane, may have one pole at the origin. Particularly, it is shown in Sections 3.2 and 3.3 respectively, that the controller design equations and the control-relevant system identification procedure for stable plants can be applied without modifications to Type 1 stable plants. The iterative identification and control algorithm that is applicable to stable plants and Type 1 stable plants will be discussed in Section 3.4. Two simulation examples in Section 3.5 illustrate the results. We conclude this chapter in Section 3.6.

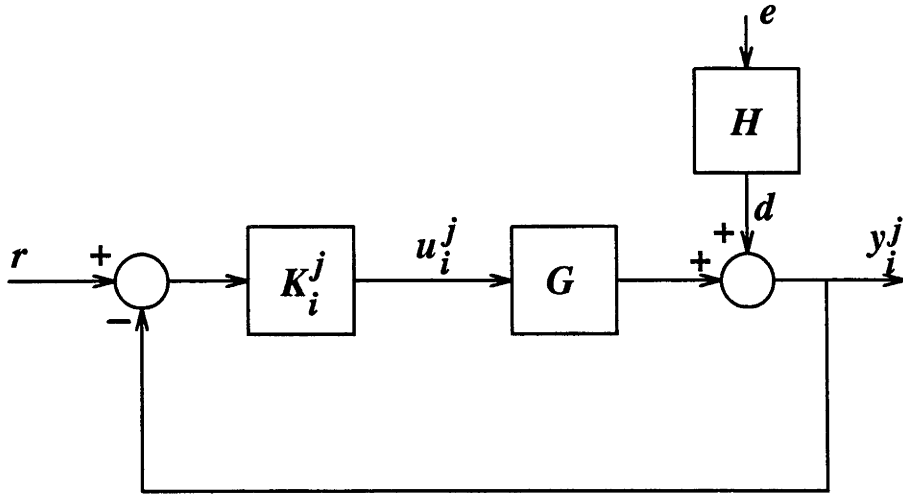


Figure 3.1: Closed-loop system

### 3.1 Frequency Weighted Identification Criterion

We studied in Chapter 2 the iterative identification and control design approach for stable plants under ideal conditions where an infinite number of noiseless input-output measurements are available. Under these conditions the iterative identification and control design problem has become an iterative *model approximation* and control design problem where the required updated model was obtained by solving the rational function approximation problem

$$G_{i+1} = \arg \min_{\theta} \left\| \frac{GK_i^f}{1 + GK_i^f} - \frac{\theta K_i^f}{1 + \theta K_i^f} \right\|_{\infty} \quad (3.1)$$

for a known  $G$ . In the *iterative identification* and control design problem to be discussed in this and all of the following chapters, as opposed to the iterative model approximation and control design problem, we are dealing with a system identification problem where  $G$  is an unknown transfer function and only a finite number of noisy input-output measurements in closed-loop configuration are available. Despite this apparent difference, we observe that equation (3.1) is similar to the criterion developed by Anderson and Liu [1989] in the controller reduction problem based on closed-loop transfer function considerations, except that their plant and reduced-order controller are replaced, respectively, by our controller and estimated model. As observed by Anderson and Liu [1989], there is a reduced weighting placed on the range of frequencies where the loop-gain is large. This is very appealing as

it agrees with the well known fact that, for a stable closed-loop system, model errors are more tolerable in the range of frequencies where the loop-gain is large. More importantly, as we shall explain below, this system identification criterion will enable us to find a new model which allows us to design a closed-loop system with a larger bandwidth than what the original model would permit.

If we rewrite equation (3.1) into the following form

$$G_{i+1} = \arg \min_{\theta} \left\| \left( \frac{1}{1 + GK_i^f} \right) \left( \frac{\theta K_i^f}{1 + \theta K_i^f} \right) \left( \frac{G - \theta}{\theta} \right) \right\|_{\infty}, \quad (3.2)$$

it can be seen immediately that the argument that is minimized is the product of the actual sensitivity function,  $1/(1 + GK_i^f)$ , and the designed complementary-sensitivity-function weighted multiplicative model error

$$\left( \frac{G_{i+1} K_i^f}{1 + G_{i+1} K_i^f} \right) \left( \frac{G - G_{i+1}}{G_{i+1}} \right).$$

It appears that the frequency weighting function in equation (3.2), which involves the unknown actual sensitivity function, cannot be implemented in the system identification procedure. However, as we have discussed in Section 2.4, by recasting the control relevant closed-loop system identification into a frequency weighted open-loop system identification problem, we obtain a system identification criterion which is equivalent to equation (3.2) but involves only known frequency weighting functions. Specifically, we have shown in equation (2.12) that

$$\left\| \frac{GK_i^f}{1 + GK_i^f} - \frac{G_{i+1}K_i^f}{1 + G_{i+1}K_i^f} \right\|_{\infty} = \left\| Y_i^f X_i^f (R_i^f - \hat{R}_i^f) \right\|_{\infty},$$

where  $R_i^f$  is the unknown stable proper transfer function that parametrizes  $G$ , and  $X_i^f$  and  $Y_i^f$  are stable proper transfer functions known by design. Therefore, for the purpose of understanding the effects of the system identification criterion on the identified model, we can treat the frequency weighting function in equation (3.2) as a known quantity.

Recall that, as described in Section 2.3, we were using the model  $G_i$  to design a sequence of controllers  $\{K_i^j; j = 0, 1, 2, \dots, f\}$  such that the closed-loop system has an increasing bandwidth. At the stage where  $j = f$ , the closed-loop bandwidth has become so large that the high frequency modelling errors between  $G_i$  and  $G$  have a significant effect on the corresponding closed-loop transfer functions. Any attempt to increase the closed-loop

bandwidth further will cause the magnitude of the designed complementary-sensitivity-function weighted multiplicative model error,

$$\left( \frac{G_i K_i^f}{1 + G_i K_i^f} \right) \left( \frac{G - G_i}{G_i} \right),$$

to become too large at certain frequencies such that the system may lose performance robustness or even stability robustness. Therefore, the gain of the controller  $K_i^f$  will be limited, and the actual sensitivity function,  $1/(1 + GK_i^f)$ , will be large beyond the existing limited closed-loop bandwidth. From equation (3.2) we notice that it is exactly in this range of frequencies, where the actual sensitivity function has large magnitude, that our system identification criterion will penalize the designed complementary-sensitivity-function weighted multiplicative model error of the new model  $G_{i+1}$ . We could therefore expect  $G_{i+1}$  to have smaller model uncertainties, as compared to  $G_i$ , near and beyond the edge of the closed-loop bandwidth that can be achieved with  $G_i$ . This will allow us to design a sequence of controllers  $\{K_{i+1}^f; j = 0, 1, 2, \dots\}$  that can lead to larger closed-loop bandwidth than it was possible with  $G_i$ . This explains why we say that the frequency weighting in criterion (3.2) is control-relevant.

To illustrate the above discussions, consider an example where the plant has a transfer function

$$G = \frac{9}{(s+1)(s^2 + 0.06s + 9)},$$

and an initial model has the transfer function

$$G_0 = \frac{1}{s+1}.$$

By using the IMC method [Morari and Zafriou 1989], we can design a strictly proper controller of the form

$$K = \frac{\lambda^2(s+1)}{s(s+2\lambda)}$$

by setting the relative degree of the IMC filter as  $N = n + 1$  (see Theorem 2.5.3), where, in this example,  $n = 1$  is the relative degree of  $G_0$ . (We shall explain in Section 3.2 why a strictly proper controller, instead of a bi-proper controller, is preferred.)

It can be shown that the designed closed-loop transfer function is given by

$$\bar{T} = \frac{\lambda^2}{(s+\lambda)^2}.$$

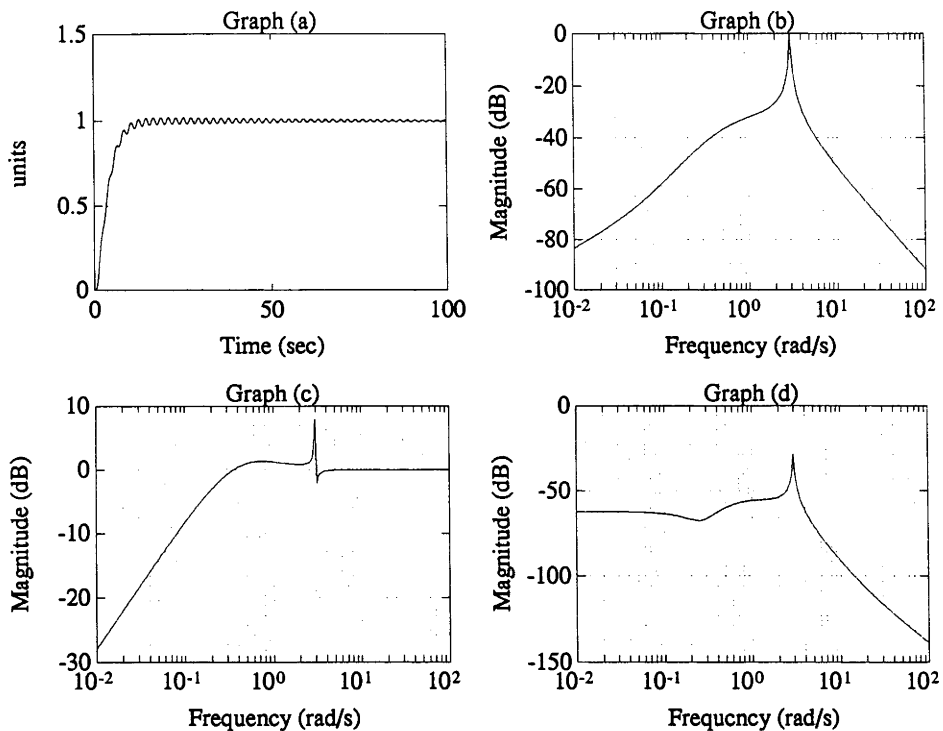


Figure 3.2: Frequency weighted multiplicative model errors

Therefore,  $\lambda$  is the nominal  $-6$  dB bandwidth of the closed-loop system. As  $\lambda$  is increased to  $0.5$  rad/s, the actual closed-loop unit step response (as shown in Graph (a) of Figure 3.2) has excessive oscillations which differs significantly from the design step response because the model uncertainties associated with  $G_0$  are no longer insignificant. This is apparent in Graph (b) of Figure 3.2, which shows the magnitude of the designed complementary-sensitivity-function weighted multiplicative model error of  $G_0$ . We have also shown the actual sensitivity function in Graph (c) of Figure 3.2, which indicates that, if it is incorporated into the system identification criterion (for which the procedure is already given in Sections 2.4 and 2.6), the designed complementary-sensitivity-function weighted multiplicative error in the new model  $G_1$  will be penalized in the range of frequencies near and beyond the existing closed-loop bandwidth of  $0.5$  rad/s. It can be seen from Graph (d) of Figure 3.2, which shows the designed complementary-sensitivity-function weighted multiplicative error of the new model  $G_1$ , that this is indeed the case. Therefore, the new model  $G_1$  will allow us to increase the closed-loop bandwidth beyond  $0.5$  rad/s.



## 3.2 Control Design for Type 1 Stable Plants

It is well known that a large class of practical systems involves plants which, except for a pole at the origin, have all poles in the open left-half plane. These plants include electro-mechanical actuators for position control systems and level control systems in industrial processes like, for example, sugar cane crushing mills. Therefore, it is desirable to show that the iterative and control design approach that we have proposed for stable plants is also applicable to these plants. Specifically, we make the following assumption:

**Assumption 3.2.1 [Type 1 Stable Transfer Function]** *A Type 1 stable transfer function is strictly proper and, other than possibly having one pole at the origin, have no poles on the rest of the closed right-half plane and no zeros on the imaginary axis.*

In the sequel, we shall denote plants and models that satisfy Assumption 3.2.1 by *Type 1 stable plants* and *Type 1 stable models*, respectively. In this section we shall discuss control design for Type 1 stable plants. Control-relevant system identification for Type 1 stable plants will be discussed in the next section.

A standing assumption in this and the following chapters is:

**Assumption 3.2.2 [Strictly Proper Controllers]** *In the controller design stage, the transfer function  $Q_i^j$  that parametrizes the controller  $K_i^j$  is designed to be strictly proper.*

**Remark 3.2.1** The reason for requiring  $Q_i^j$ , and hence  $K_i^j = Q_i^j / (1 - G_i Q_i^j)$ , to be strictly proper is that this is a necessary condition for robustness in the presence of high-frequency parasitics or singular perturbation [Kokotovic *et al.* 1986].

**Remark 3.2.2** A large relative degree for  $Q_i^j$  will lead to a large relative degree in the designed closed-loop transfer function  $\bar{T}_i^j = G_i Q_i^j$ . In this situation, the large phase lag associated with  $\bar{T}_i^j$  at the high frequency region may cause the designed closed-loop system to have poor transient responses. In order to have good transient responses, while requiring

$Q_i^j$  to be strictly proper, we let  $Q_i^j$  have relative degree one in the sequel by setting  $N = n + 1$  in the IMC filter  $F_i^j$  (see Theorem 2.5.1), where  $n$  is the relative degree of  $G_i$ .

In the following, we will use the notations  $n_H$  and  $d_H$  to denote the numerator polynomial and the denominator polynomial of a rational transfer function  $H$ . For a not necessarily stable model (see Assumption 2.5.1)

$$G_i = \frac{n_{G_i}}{d_{G_i}}$$

we can write

$$n_{G_i} = \tilde{n}_{G_i} \prod_i (z_i - s), \quad \text{and} \quad d_{G_i} = s^l \tilde{d}_{G_i} \prod_{i=1}^k (p_i - s),$$

where the polynomials  $\tilde{n}_{G_i}$  and  $\tilde{d}_{G_i}$  have no zeros in the closed right-half plane, and all of  $z_i$  and  $p_i$  have positive real parts.

We can then write  $G_i = [G_i]_m [G_i]_a$ , where

$$[G_i]_m = \frac{\tilde{n}_{G_i} \prod_i (z_i^* + s)}{d_{G_i}}; \quad z_i^* \text{ is the complex-conjugate of } z_i,$$

and

$$[G_i]_a = \frac{\prod_i (z_i - s)}{\prod_i (z_i^* + s)}.$$

Furthermore, we can use coprime fractional representations to write  $G_i = N_i/D_i$ , with the stable proper transfer functions  $D_i$  and  $N_i$  defined as

$$D_i = \frac{d_{G_i}}{q_s}, \quad \text{and} \quad N_i = \frac{n_{G_i}}{q_s},$$

where  $q_s$  is a polynomial with no zeros in the closed right-half plane and has the same degree as  $d_{G_i}$ . Then we have  $N_i = [N_i]_m [N_i]_a$ , with

$$[N_i]_m = \frac{\tilde{n}_{G_i} \prod_i (z_i^* + s)}{q_s}, \quad [N_i]_a = [G_i]_a,$$

and

$$[D_i]_m = \frac{s^l \tilde{d}_{G_i} \prod_{i=1}^k (p_i^* + s)}{q_s}, \quad [D_i]_a = \frac{\prod_{i=1}^k (p_i - s)}{\prod_{i=1}^k (p_i^* + s)}.$$

Note that

$$[G_i]_m = \frac{[N_i]_m}{D_i}.$$

These notations will also be used in the next section.

The following results are direct consequences of Theorem 2.5.1 for stable plants and Type 1 stable plants, respectively, when the relative degree for the IMC filter  $F_i^j$  is set to  $N = n + 1$ , where  $n$  is the relative degree of  $G_i$ .

**Corollary 3.2.1** *With reference to Figure 3.1, let  $G_i$  be a stable strictly proper model for a stable plant  $G$ . Let the reference input  $r$  to be a step function. Then the controller that stabilizes  $G_i$  is given by*

$$K_i^j = \frac{Q_i^j}{1 - G_i Q_i^j}$$

where

$$Q_i^j = [G_i]_m^{-1} F_i^j, \\ F_i^j = \left( \frac{\lambda_i^j}{s + \lambda_i^j} \right)^{n+1}; \quad \lambda_i^j > 0,$$

$[G_i]_m$  is the minimum-phase factor of  $G_i$ , and  $n$  is the relative degree of  $G_i$ .

**Remark 3.2.3** Observe that Corollary 3.2.1 is a special case of Theorem 2.5.3 with  $N = n + 1$ .

**Corollary 3.2.2** *With reference to Figure 3.1, let  $G_i$  be a Type 1 stable model for a Type 1 stable plant  $G$ . Let the reference input  $r$  to be a step function. Then the controller that stabilizes  $G_i$  is given by*

$$K_i^j = \frac{Q_i^j}{1 - G_i Q_i^j}$$

where

$$Q_i^j = [G_i]_m^{-1} F_i^j, \\ F_i^j = \left( \frac{\lambda_i^j}{s + \lambda_i^j} \right)^{n+1}; \quad \lambda_i^j > 0,$$

$[G_i]_m$  is the minimum-phase factor of  $G_i$ , and  $n$  is the relative degree of  $G_i$ .

**Remark 3.2.4** The results of Corollary 3.2.1 and Corollary 3.2.2 imply that the controller design equations for stable plant situations can be applied without modifications to Type 1 stable plant situations when the reference input is a step function.

**Remark 3.2.5** The design parameter  $\lambda_i^j$  is the bandwidth of the designed closed-loop transfer function  $\bar{T}_i^j = G_i K_i^j / (1 + G_i K_i^j)$  with an attenuation of  $-3(n+1)$  dB.

**Remark 3.2.6** It can easily be shown that, whenever the model  $G_i$  does not have a pole at the origin, the controller  $K_i^j$  designed by the IMC method for a step reference input will have a pole at the origin. This ensure that the output of the designed closed-loop system tracks a step reference input with zero steady state error.

We shall now show that, under very mild conditions, it is possible to initialize the iterative identification and control design approach for Type 1 stable plants with low gain robust stabilizing controllers.

By using Taylor series expansions of the appropriate functions at the origin and Routh-Hurwitz criterion [Franklin *et al.* 1986], we can easily prove the following theorems.

If it is known a priori that the plant has a pole at the origin, then we have:

**Theorem 3.2.1** *Let a plant be*

$$G(s) = \frac{n_G(s)}{s \tilde{d}_G(s)},$$

where  $\tilde{d}_G(s)$  has no zeros in the closed right-half plane and  $n_G(0) \neq 0$ . Let the initial model of the plant be

$$G_0(s) = \frac{\kappa}{s},$$

then a controller designed by the method given in Corollary 3.2.2,

$$K_0^0(s) = \frac{(\lambda_0^0)^2}{\kappa(s + 2\lambda_0^0)}, \quad \lambda_0^0 > 0,$$

robustly stabilizes  $G_0(s)$  for sufficiently small  $\lambda_0^0$  if

$$\kappa \quad \text{and} \quad \frac{n_G(0)}{\tilde{d}_G(0)}$$

have the same sign.

**Proof**

Similar to the proof of the next theorem. □

Sometimes it may not be known a priori that the plant has a pole at the origin, and it is inaccurately modelled as a first order lag. In this case we have:

**Theorem 3.2.2** *Let a plant be*

$$G(s) = \frac{n_G(s)}{s\tilde{d}_G(s)},$$

where  $\tilde{d}_G(s)$  has no zeros in the closed right-half plane and  $n_G(0) \neq 0$ . Let the initial model of the plant be

$$G_0(s) = \frac{\kappa}{s + (1/\tau)}; \quad \tau > 0,$$

then a controller designed by the method given in Corollary 3.2.2,

$$K_0^0(s) = \frac{(\lambda_0^0)^2[s + (1/\tau)]}{\kappa s(s + 2\lambda_0^0)}, \quad \lambda_0^0 > 0,$$

robustly stabilizes  $G_0(s)$  if

$$\kappa \quad \text{and} \quad \frac{n_G(0)}{\tilde{d}_G(0)}$$

have the same sign, and if

$$\lambda_0^0 > \frac{1}{2\tau}$$

is suitably small.

**Proof**

See Appendix D. □

**Remark 3.2.7** From the last theorem, we observe that the low frequency mis-modelling (as measured by  $1/\tau$ ) of the plant  $G(s)$  by the initial model  $G_0(s)$  (with respect to the pole of  $G(s)$  at the origin) imposes a limit on the smallest value that the initial closed-loop bandwidth  $\lambda_0^0$  can possibly take. Under this condition, an initial robust stabilizing controller may not be found if there are also significant high frequency modelling errors.

### 3.3 Control-Relevant System Identification for Type 1 Stable Plants

We shall first consider plants that are not necessarily stable (as defined in Assumption 2.5.1). It was shown in Section 2.4 that, if the controller  $K_i^f$  in Figure 3.1 (with  $j = f$ ) robustly stabilizes  $G_i$ , then by using the coprime fractional representations  $G_i = N_i/D_i$ ,  $K_i^f = X_i^f/Y_i^f$ , and the equation  $N_i X_i^f + D_i Y_i^f = 1$ , we have

$$X_i^f = \frac{K_i^f}{D_i + N_i K_i^f}, \quad (3.3)$$

and

$$Y_i^f = \frac{1}{D_i + N_i K_i^f}. \quad (3.4)$$

Furthermore, there exist stable proper transfer functions  $R_i^f$  such that

$$G = \frac{N_i + R_i^f Y_i^f}{D_i - R_i^f X_i^f}. \quad (3.5)$$

Thus, by Hansen's method [Hansen 1989], the control-relevant closed-loop system identification problem for  $G$  can be transformed into a frequency weighted open-loop system identification problem for  $R_i^f$  and with the model updated via

$$G_{i+1} = \frac{N_i + \widehat{R}_i^f Y_i^f}{D_i - \widehat{R}_i^f X_i^f},$$

where  $\widehat{R}_i^f$  is an estimate of  $R_i^f$  obtained by employing the procedure described in Section 2.4.

The next theorem shows that  $R_i^f$  is the product of a known stable proper transfer function and an unknown stable strictly proper transfer function. We follow the notations of Theorem 2.5.1.

**Theorem 3.3.1** *Consider a not necessarily stable  $G_i$  with possibly one pole at the origin (that is,  $l \leq 1$ ). Let a controller with relative degree one be designed according to Theorem 2.5.1 (by setting  $N = n + 1$ , where  $n$  is the relative degree of the model  $G_i$ ) for a step reference input (that is  $q = 1$ ), then the unknown stable strictly proper transfer function to be identified,*

$$R_i^f = \frac{D_i^2(G - G_i)}{1 + D_i X_i^f(G - G_i)},$$

can be factorized as

$$R_i^f = \tilde{R}_i^f \check{R}_i^f, \quad (3.6)$$

where

$$\check{R}_i^f = (s + \lambda_i^f)^{k+1} \left[ \prod_{i=1}^k (p_i^* + s) \right] \frac{d_{G_i} n_G - d_G n_{G_i}}{d_G d_{K_i^f} + n_G n_{K_i^f}}$$

is an unknown stable strictly proper transfer function to be identified, and

$$\tilde{R}_i^f = D_i [N_i]_m (s + \lambda_i^f)^n$$

is a stable proper transfer function known by design.

### Proof

See Appendix E. □

**Remark 3.3.1** Note that

1. For a Type 1 stable  $G_i$ , by setting  $k = 0$  in the results of Theorem 3.3.1, we have

$$\check{R}_i^f = \frac{(s + \lambda_i^f)(d_{G_i} n_G - d_G n_{G_i})}{d_G d_{K_i^f} + n_G n_{K_i^f}}$$

and

$$\tilde{R}_i^f = D_i [N_i]_m (s + \lambda_i^f)^n.$$

2. For a stable  $G_i$ , other than setting  $k = 0$  in the results of Theorem 3.3.1, we can set  $q_s = d_{G_i}$  so that  $D_i = 1$  and  $[N_i]_m = [G_i]_m$ . Under these conditions, we have

$$\check{R}_i^f = \frac{(s + \lambda_i^f)(d_{G_i} n_G - d_G n_{G_i})}{d_G d_{K_i^f} + n_G n_{K_i^f}}$$

and

$$\tilde{R}_i^f = [G_i]_m (s + \lambda_i^f)^n.$$

Observe that these factorizations are obtained when  $Q_i^f$  and  $K_i^f$  have relative degree one, as opposed to the one given in Theorem 2.6.1 where  $Q_i^f$  and  $K_i^f$  are bi-proper transfer functions.

**Remark 3.3.2** When  $G_i$  is stable or is Type 1 stable and when the reference input is a step function, (that is,  $k = 0$ ,  $l \leq 1$ , and  $q = 1$ ), and when  $Q_i^f$  and  $K_i^f$  have relative degree one, it can be proved (by using steps similar to the proof of Theorem 2.6.2) that the order and the relative degree of the transfer function  $\check{R}_i^f$  are respectively, given by

$$\text{order of } \{\check{R}_i^f\} = \text{order of } \{G\} + \text{order of } \{G_i\} - (M + N) + 1 ,$$

and

$$\text{rel deg } \{\check{R}_i^f\} = \min(\text{rel deg } \{G\}, \text{rel deg } \{G_i\}) ,$$

where  $M$  is the number of common zeros in  $G$  and  $G_i$ , and  $N$  is the number of common poles in  $G$  and  $G_i$ .

**Remark 3.3.3** Although Hansen's approach enables us to obtain an unbiased estimate of the transfer function  $\check{R}_i^f$ , it should be noted that  $\check{R}_i^f$  has more parameters to be estimated than  $G$ . Furthermore, since the order of  $\check{R}_i^f$  (hence the number of parameters to be identified in  $\check{R}_i^f$ ) increases while the magnitude of  $\check{R}_i^f$  decreases with the stages of iteration, we would expect that the system identification problem will become harder as the iteration process progresses under noisy conditions. (Recall that it is because we want to perform the identification more efficiently that  $R_i^f$  is factorized into  $R_i^f = \tilde{R}_i^f \check{R}_i^f$ , where  $\tilde{R}_i^f$  is known by design, so that less parameters need to be estimated.) There is an obvious analogy in the windsurfing situation. The better is the skill of a windsurfer, the harder it will be for him/her to improve his/her skill further. In fact, it will take a long time under extreme conditions to improve his/her skill. In the system identification problem for  $\check{R}_i^f$ , the interpretation is that strong probing signals and long record of measurements are necessary to achieve even slight improvement if the closed-loop system already has good performance and large bandwidth.

We shall next show that the control-relevant system identification procedure for stable plants applies without modifications to Type 1 stable plants. We shall consider respectively, the criteria for system identification, the signal models for system identification, and the model update equations.



### 3.3.1 System Identification Criteria

If we define  $\hat{R}_i^f = \tilde{R}_i^f \check{R}_i^f$  as in equation (2.28), then criterion (2.27) for frequency weighted open-loop system identification becomes

$$\hat{R}_i^f = \arg \min_{\phi} \left\| X_i^f Y_i^f \tilde{R}_i^f (\check{R}_i^f - \phi) \right\|_{\infty} . \quad (3.7)$$

Since the controller  $K_i^f$  designed by the IMC method is parametrized by  $Q_i^f$  via  $K_i^f = Q_i^f / (1 - G_i Q_i^f)$ , we can rewrite equations (3.3) and (3.4) respectively as  $X_i^f = Q_i^f / D_i$  and  $Y_i^f = (1 - G_i Q_i^f) / D_i$ .

When  $G_i$  is stable (that is,  $k = 0$  and  $l = 0$ ), we have  $D_i = 1$  and  $\tilde{R}_i^f = [G_i]_m (s + \lambda_i^f)^n$ . In this case, equation (3.7) becomes

$$\hat{R}_i^f = \arg \min_{\phi} \left\| Q_i^f (1 - G_i Q_i^f) [G_i]_m (s + \lambda_i^f)^n (\check{R}_i^f - \phi) \right\|_{\infty} ,$$

or after simplification,

$$\hat{R}_i^f = \arg \min_{\phi} \left\| \frac{(\lambda_i^f)^{n+1}}{s + \lambda_i^f} (1 - G_i Q_i^f) (\check{R}_i^f - \phi) \right\|_{\infty} . \quad (3.8)$$

When  $G_i$  is Type 1 stable (that is,  $k = 0$  and  $l = 1$ ), we have  $\tilde{R}_i^f = D_i [N_i]_m (s + \lambda_i^f)^n$ , and  $[N_i]_m = D_i [G_i]_m$ . In this case, although  $D_i \neq 1$ , it can be shown by direct substitutions that equation (3.7) can be rewritten again as

$$\hat{R}_i^f = \arg \min_{\phi} \left\| \frac{(\lambda_i^f)^{n+1}}{s + \lambda_i^f} (1 - G_i Q_i^f) (\check{R}_i^f - \phi) \right\|_{\infty} .$$

Therefore the common criterion for identifying  $\check{R}_i^f$ , in both stable plant and Type 1 stable plant situations, is given by equation (3.8).

### 3.3.2 Signal Models

Now consider the signal model for the purpose of identifying  $\check{R}_i^f$ . Similar to the signal model that we have derived in Section 2.6, the appropriate signal model for identifying  $\check{R}_i^f$  can be shown to be given by

$$\beta_1 = \check{R}_i^f \alpha_2 + w_i^f , \quad (3.9)$$

where

$$\alpha_2 = \tilde{R}_i^f Y_i^f X_i^f r ,$$

$$\beta_1 = Y_i^f (D_i y_i^f - N_i u_i^f) ,$$

and  $w_i^f = (1 + GK_i^f)^{-1} H e$  is the the effect of the noise disturbance on the filtered output error,  $\xi_1 = \beta_1 - \tilde{R}_i^f \alpha_2$ .

When  $G_i$  is stable, it is easy to show by appropriate substitutions that

$$\alpha_2 = \frac{(\lambda_i^f)^{n+1}}{s + \lambda_i^f} (1 - G_i Q_i^f) r , \quad (3.10)$$

and

$$\beta_1 = (1 - G_i Q_i^f) (y_i^f - G_i u_i^f) . \quad (3.11)$$

When  $G_i$  is Type 1 stable, since  $\tilde{R}_i^f = D_i [N_i]_m (s + \lambda_i^f)^n$ ,  $Y_i^f = (1 - G_i Q_i^f) / D_i$ , and  $X_i^f = Q_i^f / D_i$ , we have again by substitutions,

$$\alpha_2 = \frac{(\lambda_i^f)^{n+1}}{s + \lambda_i^f} (1 - G_i Q_i^f) r ,$$

and

$$\beta_1 = (1 - G_i Q_i^f) (y_i^f - G_i u_i^f) .$$

Therefore the common signal model for the purpose of identifying  $\check{R}_i^f$ , in both stable plant and Type 1 stable plant situations, is given by equations (3.9), (3.10), and (3.11). The corresponding block diagram is given in Figure 3.3.2.

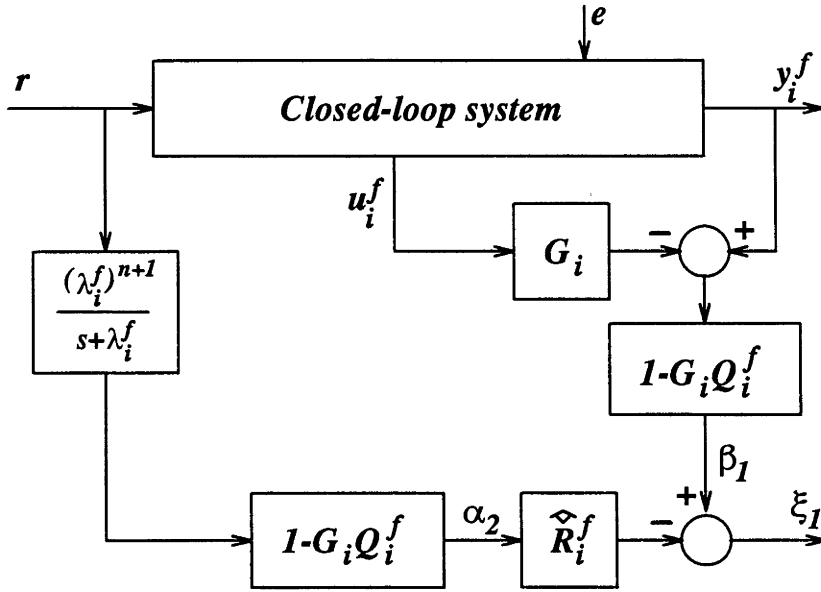
### 3.3.3 Model Update Equations

Now consider the model update equations. When  $G_i$  is stable, the model update equation is

$$G_{i+1} = G_i + \frac{\tilde{R}_i^f}{1 - \hat{R}_i^f Q_i^f} .$$

In this case, by using the equations  $\hat{R}_i^f = \tilde{R}_i^f \tilde{R}_i^f$ ,  $\tilde{R}_i^f = [G_i]_m (s + \lambda_i^f)^n$ ,  $Q_i^f = [G_i]_m^{-1} F_i^f$ , and  $F_i^f = [\lambda_i^f / (s + \lambda_i^f)]^{n+1}$ , we can rewrite the model update equation as

$$G_{i+1} = G_i + \frac{(s + \lambda_i^f)^{n+1} [G_i]_m \tilde{R}_i^f}{(s + \lambda_i^f) - (\lambda_i^f)^{n+1} \tilde{R}_i^f} . \quad (3.12)$$

Figure 3.3: Identification of  $\tilde{R}_i^f$ 

When  $G_i$  is Type 1 stable, the model update equation is

$$G_{i+1} = \frac{N_i + \hat{R}_i^f Y_i^f}{D_i - \hat{R}_i^f X_i^f}.$$

By noting that  $X_i^f = Q_i^f/D_i$  and  $Y_i^f = (1 - G_i Q_i^f)/D_i$ , the last model update equation can also be written as

$$G_{i+1} = G_i + \frac{\hat{R}_i^f}{D_i^2 - \hat{R}_i^f Q_i^f}.$$

Since in this case we have  $\hat{R}_i^f = \tilde{R}_i^f \tilde{R}_i^f$ ,  $\tilde{R}_i^f = D_i [N_i]_m (s + \lambda_i^f)^n$ ,  $Q_i^f = [G_i]_m^{-1} F_i^f$ , and  $F_i^f = [\lambda_i^f / (s + \lambda_i^f)]^{n+1}$ , therefore the model update equation becomes

$$G_{i+1} = G_i + \frac{(s + \lambda_i^f)^{n+1} [G_i]_m \tilde{R}_i^f}{(s + \lambda_i^f) - (\lambda_i^f)^{n+1} \tilde{R}_i^f}.$$

Note that the last equation is the same as equation (3.12). Therefore equation (3.12) is the common model update equation in both stable plant and Type 1 stable plant situations.

**Remark 3.3.4** When updating the model using the equation

$$G_{i+1} = G_i + \frac{(s + \lambda_i^f)^{n+1} [G_i]_m \tilde{R}_i^f}{(s + \lambda_i^f) - (\lambda_i^f)^{n+1} \tilde{R}_i^f},$$

the order of the model may increase. To prevent the model order from increasing indefinitely during a sequence of iteration, we use a frequency weighted balanced truncation scheme [Anderson and Liu 1989] to reduce the order of  $G_{i+1}$  at the end of each identification. Specifically, we would like, ideally, to find

$$\hat{G}_{i+1} = \arg \min_{\eta} \left\| \frac{G_{i+1}K_i^f}{1 + G_{i+1}K_i^f} - \frac{\eta K_i^f}{1 + \eta K_i^f} \right\|_{\infty},$$

where  $\hat{G}_{i+1}$  is the reduced order model. In practice, we obtain approximately, under frequency weighted balanced truncation,

$$\hat{G}_{i+1} = \arg \min_{\eta} \left\| \frac{K_i^f(G_{i+1} - \eta)}{(1 + G_{i+1}K_i^f)^2} \right\|_{\infty}.$$

### 3.4 Iterative Algorithm for Stable Plants and Type 1 Stable Plants

Before the simulation results are presented in Section 3.5, we summarize the algorithm for iterative identification and control design with respect to stable plants and Type 1 stable plants.

#### Step 1:

Set  $G_i = G_0$ , where  $G_0$  is the transfer function of an initial model of the stable plant or Type 1 stable plant.

#### Step 2:

Factorize  $G_i$  as  $G_i = [G_i]_m [G_i]_a$ , where  $[G_i]_m$  is the minimum-phase factor of  $G_i$  with a relative degree of  $n$ , and  $[G_i]_a$  is the associated all pass factor of  $G_i$ .

**Step 3:**

For  $j = 0$ , find  $K_i^j = Q_i^j / (1 - G_i Q_i^j)$ , with  $Q_i^j = [G_i]_m^{-1} F_i^j$ , where the parameter  $\lambda_i^j$  in the transfer function

$$F_i^j = \left( \frac{\lambda_i^j}{s + \lambda_i^j} \right)^{n+1}$$

is chosen such that  $K_i^j$  robustly stabilizes  $G_i$  and the step response of the actual closed-loop system (modulo the effects of the noise disturbance) has, at most, little oscillations and/or overshoots. Stop here if such a robust stabilizing controller cannot be found. (This may happen if the pole of the plant at the origin is incorrectly modelled. See Remark 3.2.7) Also stop here if the robust stabilizing controller results in a closed-loop system which meets the specified bandwidth. Otherwise, proceed to the next step.

**Step 4:**

Let  $j = j + 1$  and set  $\lambda_i^j = \lambda_i^{j-1} + \epsilon$  for small  $\epsilon > 0$ , and re-design the controller  $K_i^j$  using the equations given in **Step 3**. Stop here if the design produces a robust stabilizing controller with the closed-loop system satisfying the specified bandwidth. Otherwise, repeat this step if  $K_i^j$  robustly stabilizes  $G_i$ ; else proceed to the next step. (We assume that it is necessary to proceed to the next step when  $j = f$ .)

**Step 5:**

Perform frequency weighted open-loop system identification to obtain  $\hat{R}_i^f$ . For this purpose, we apply an algorithm such as least squares to obtain an estimate  $\check{R}_i^f$  of  $\check{R}_i^f$  which satisfies  $\beta_1 = \check{R}_i^f \alpha_2 + w_i^f$ . This depends on using the signals

$$\alpha_2 = \frac{(\lambda_i^f)^{n+1}}{s + \lambda_i^f} (1 - G_i Q_i^f) r \quad ,$$

and

$$\beta_1 = (1 - G_i Q_i^f) (y_i^f - G_i u_i^f) \quad .$$

(We actually used discrete-time samples of  $\beta_1$  and  $\alpha_2$  and an output error parameter estimation algorithm to construct a strictly causal discrete-time estimate for  $\hat{R}_i^f$ , from which a continuous-time strictly proper  $\tilde{R}_i^f$  was obtained. This are facilitated by the `oe.m` file and the `contin.m` file of MATLAB™ System Identification Toolbox [Ljung 1988].) Using  $\tilde{R}_i^f$ , the model is updated via the following equation:

$$G_{i+1} = G_i + \frac{(s + \lambda_i^f)^{n+1} [G_i]_m \tilde{R}_i^f}{(s + \lambda_i^f) - (\lambda_i^f)^{n+1} \tilde{R}_i^f}.$$

**Step 6:**

If  $G_{i+1}$  is stable or is Type 1 stable, find the reduced order model

$$\hat{G}_{i+1} = \arg \min_{\eta} \left\| \frac{K_i^f (G_{i+1} - \eta)}{(1 + G_{i+1} K_i^f)^2} \right\|_{\infty}.$$

Otherwise, stop here.

**Step 7:**

Set  $G_i = \hat{G}_{i+1}$  and return to **Step 2**.

**Remark 3.4.1** It is important to ensure that the input is sufficiently exciting when we are carrying out a system identification experiment.

**Remark 3.4.2** Under noisy conditions, the signals to be used in the system identification process should be appropriately low-pass filtered. In a discrete-time implementation, this can be accomplished by an anti-aliasing filter.

**Remark 3.4.3** The algorithm used to obtain an estimate  $\tilde{R}_i^f$  of  $\check{R}_i^f$  cannot be expected to give an optimal  $\mathcal{H}_{\infty}$  estimate. But efficient algorithms for performing  $\mathcal{H}_{\infty}$  system identification are still lacking, and the corresponding theory is still not well understood [Helmicki *et al.* 1991, Parker and Bitmead 1987, Partington 1991].

**Remark 3.4.4** Since the stability robustness of the closed-loop system for each  $\lambda_i^j$  has to be checked by using step response tests, the above algorithm is not an on-line procedure. In fact, at this stage of our development, the iterative identification and control design algorithm under discussion is an off-line procedure.

## 3.5 Simulation Results

With reference to Figure 3.1, we shall present two simulation examples in this section. Example 1 illustrates the application of the iterative identification and control design approach to a stable plant. The plant and initial model employed in this example are the same as those in the simulation example of Chapter 2, where we investigated the idea of iterative identification and control design through an iterative model approximation and control design procedure. We shall compare the results of this example with the results obtained in the simulation example of Chapter 2. In Example 2 we shall show that the iterative identification and control design approach can be applied with equal success to a Type 1 stable plant. In the following examples, we have  $H(s) = 1$  and  $e$  is a noise disturbance with zero mean and has a constant energy density of 0.0025 within the bandwidth of interest. In all of the simulation results presented, the graphs on the left show the noisy unit step responses of the actual closed-loop systems, and those on the right show the corresponding low-pass filtered signals. Bandwidths of the low-pass filters are ten times that of the designed closed-loop systems.

### Example 1

In this example, the stable plant has a transfer function

$$G(s) = \frac{9}{(s+1)(s^2+0.06s+9)}$$

The simulation results are presented in Figures 3.4, 3.5, and 3.6. We start with an initial model which has the transfer function

$$G_0 = \frac{0.8}{s+1.2}$$

Graphs (a) and (b) of Figure 3.4 show the responses of the actual closed-loop system with a designed closed-loop bandwidth of 0.1 rad/s. Note that there are no overshoot or oscillations

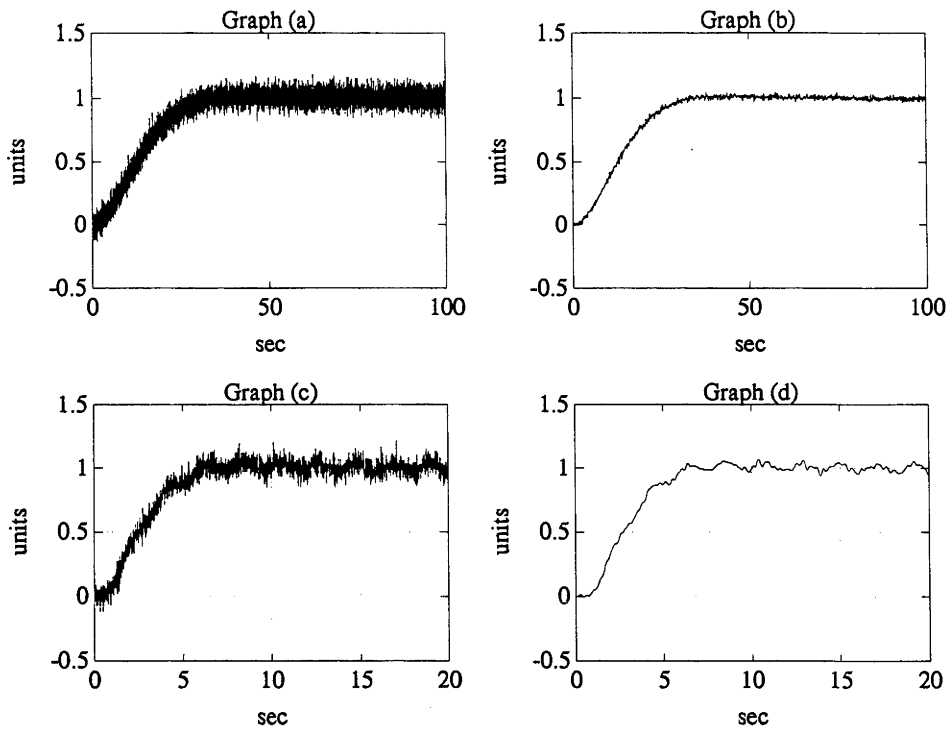


Figure 3.4: Simulation results 1 for Example 1

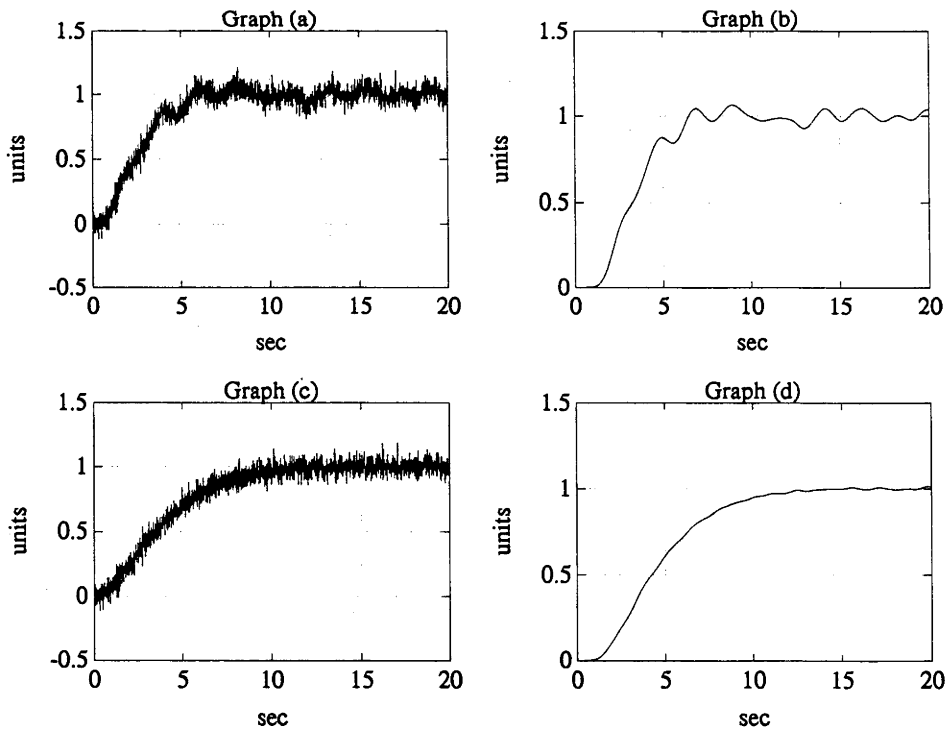


Figure 3.5: Simulation results 2 for Example 1



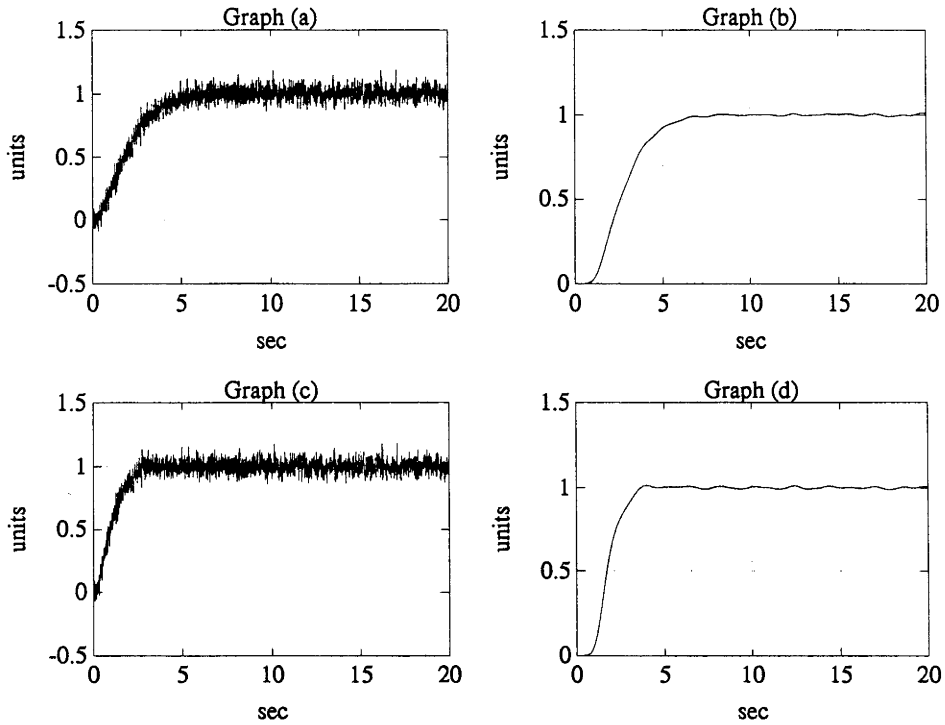


Figure 3.6: Simulation results 3 for Example 1

for the response in Graph (b). Graphs (c) and (d) of Figure 3.4 are for a designed closed-loop bandwidth of 0.5 rad/s. The response in Graph (d) is oscillatory and any attempt to increase the designed closed-loop bandwidth further is likely to lead to instability. At this stage, it is necessary to improve the accuracy of the model if we wish to increase the designed closed-loop bandwidth further. To ensure that the signals are sufficiently exciting, we superimpose on the unit step input at least  $(N/2) + 1$  low amplitude sinusoids (not harmonically related) that spread across ten times the designed closed-loop bandwidth prior to system identification. Here  $N$  is the number of parameters to be identified. The amplitudes of the sinusoids are such that each of their effects at the actual closed-loop output is just perceptible. This requires the sinusoids to be introduced one by one on the step input so that the marginal change at the closed-loop output causing by each of them could be detected. The frequencies of the sinusoids that we have introduced are 0.501 rad/s, 1.123 rad/s, 3.013 rad/s, 3.541 rad/s, and 4.37 rad/s. The corresponding amplitudes are 0.05, 0.1, 0.05, 0.5, and 1.0. The responses are shown in Graphs (a) and (b) of Figure 3.5.

To estimate  $\check{R}_0^f$ , we use a low-pass data filter with a bandwidth of 5 rad/s. A third order

model structure is selected for  $\hat{R}_0^f$  by specifying the model structure parameter as  $Nn = [3 \ 3 \ 1]$ . (Note that the noise model in the output error algorithm is unity.) Using these settings, we obtain

$$\hat{R}_0^f = \frac{-0.90396s^2 - 0.49698s + 3.997}{s^3 + 0.58707s^2 + 8.5803s + 5.0335} ,$$

$$\hat{R}_0^f = \left( \begin{array}{c} -0.72316s^3 - 0.75917s^2 \\ +2.9988s + 1.5988 \end{array} \right) \Bigg/ \left( \begin{array}{c} s^4 + 1.7871s^3 + 9.2848s^2 \\ +15.33s + 6.0401 \end{array} \right) ,$$

and

$$G_1 = \left( \begin{array}{c} 0.076836s^6 - 0.12047s^5 \\ +9.5183s^4 + 27.334s^3 \\ +26.069s^2 + 9.8166s + 1.208 \end{array} \right) \Bigg/ \left( \begin{array}{c} s^7 + 3.9871s^6 + 14.892s^5 \\ +39.427s^4 + 53.772s^3 \\ +35.895s^2 + 10.809s + 1.0926 \end{array} \right) .$$

After performing frequency weighted model reduction, we obtain

$$\hat{G}_1 = \frac{-0.05586s^2 - 0.016156s + 8.7487}{s^3 + 0.95932s^2 + 8.9233s + 8.3058} .$$

We set  $G_1 = \hat{G}_1$  before the iteration is continued.

The updated model  $G_1$  is used to re-design a closed-loop system such that the designed bandwidth is 0.5 rad/s, and the resulting responses are shown in Graphs (c) and (d) of Figure 3.5. By comparing Graph (d) of Figure 3.5 to that of Figure 3.4, we observe that the response no longer has oscillations. We also notice that the rise time in Graph (d) of Figure 3.5 is about twice of that in Graph (d) of Figure 3.4. Since both of  $G_0$  and  $G_1$  have the same relative degree of  $n = 1$ , we would expect Graph (d) of Figure 3.4 and Graph (d) of Figure 3.5 to be similar to the unit step response of the designed closed-loop transfer function  $[0.5/(s + 0.5)]^2$ . By comparing with the computed unit step response of the transfer function  $[0.5/(s + 0.5)]^2$ , we have verified that Graph (d) of Figure 3.5 is very close to the desired one. If we continue to increase the designed closed-loop bandwidth of the system, we obtain the responses shown in Figure 3.6 where Graphs (a) and (b) are for a designed closed-loop bandwidth of 1 rad/s, and Graphs (c) and (d) are for a designed closed-loop bandwidth of 2 rad/s.

The frequency responses of  $G$ ,  $G_0$ , and  $G_1$  are presented in Figure 3.7. Notice that, compared to  $G_0$ , the updated model  $G_1$  has effectively captured the effects of the poorly damped resonance of the plant.

We can compare the results in Figures 3.4 to 3.6 with those given in Figures 2.6 and 2.7 for the iterative model approximation and control design algorithm discussed in Chapter 2.

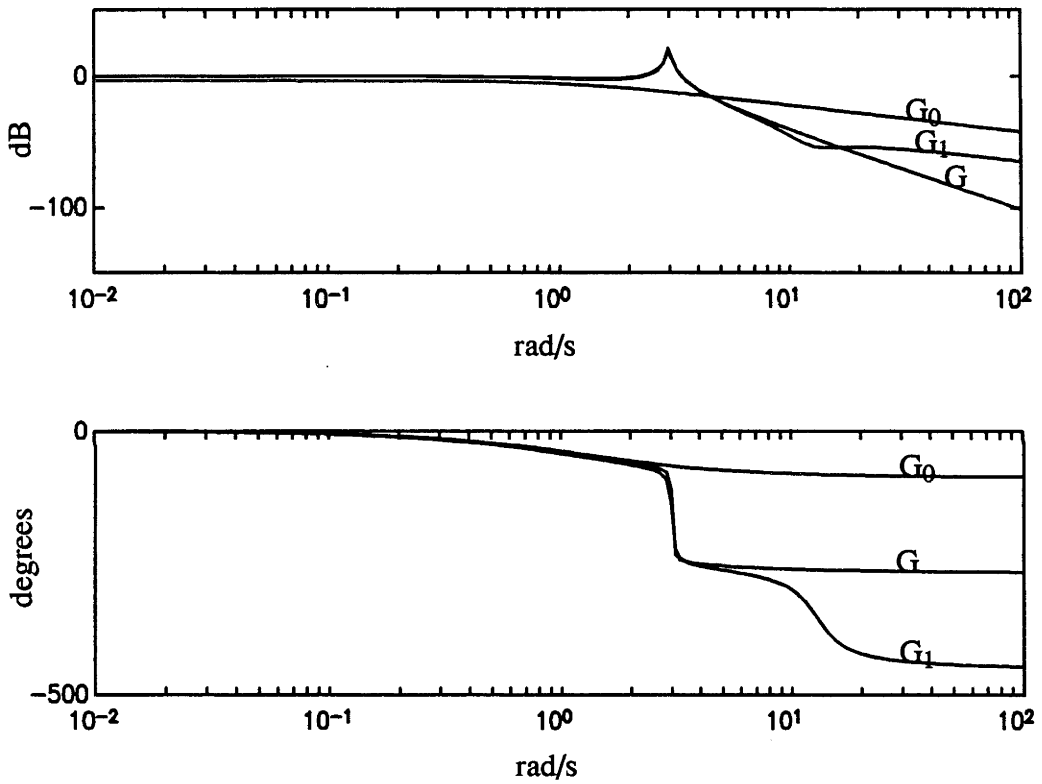


Figure 3.7: Frequency responses of models and plant

Recall that Figures 2.6 and 2.7 are obtained under noiseless conditions using rational function approximations (in the  $\mathcal{H}_\infty$  sense) of the plant instead of identified models. It is also important to emphasize that, instead of strictly proper controllers, bi-proper controllers are employed in the procedure described in Chapter 2.

**Remark 3.5.1** All else being equal, we would expect the noiseless situations to give better results than that of the noisy situations. However, by comparing the results given in Figures 3.4 to 3.6 with those given in Figures 2.6 and 2.7, we observed that, overall, the results given in Figures 3.4 to 3.6 appear better than those given in Figures 2.6 and 2.7. We attribute this to the fact that strictly proper controllers are less sensitive to high frequency model uncertainties, and hence require less frequent model updates when we attempt to increase the designed closed-loop bandwidth of the system. This is important because, as we have mentioned before, under noisy conditions, the system identification process is becoming progressively difficult and it is advantageous to be able to have infrequent but accurate model updates.

### Example 2

In this example we consider a system with

$$G(s) = \frac{9(-s + 2)}{s(s^2 + 0.06s + 9)} .$$

The plant  $G(s)$  has an unstable zero.

The simulation results are presented in Figures 3.8, 3.9, and 3.10. We start with an initial model which has the transfer function

$$G_0 = \frac{1.6}{s} .$$

Graphs (a) and (b) of Figure 3.8 show the responses of the actual closed-loop system with a designed bandwidth of 0.1 rad/s. There are no overshoot or oscillations for the response in Graph (b). Graphs (c) and (d) of Figure 3.8 are for a designed closed-loop bandwidth of 0.5 rad/s. The response in Graph (d) is oscillatory and any attempt to increase the nominal closed-loop bandwidth further is likely to lead to instability. At this stage, it is

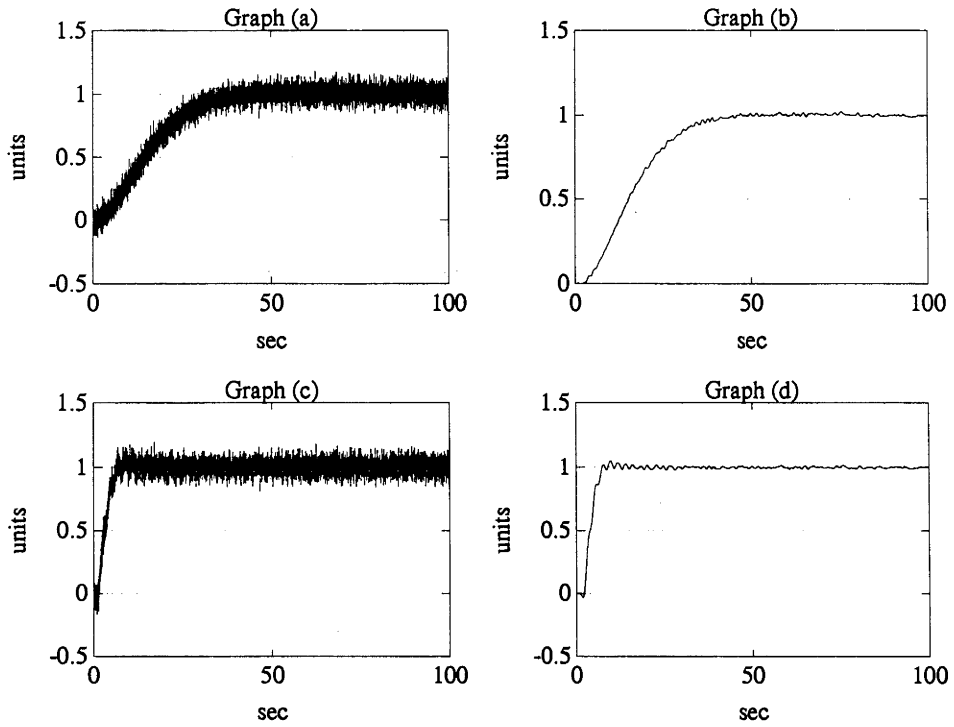


Figure 3.8: Simulation results 1 for Example 2

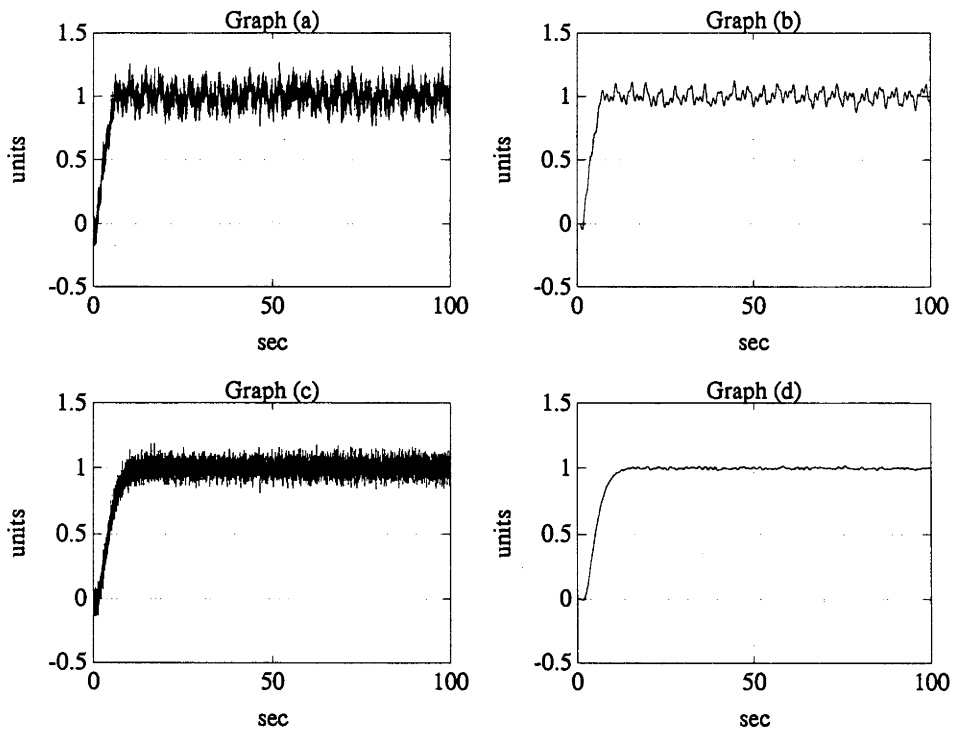


Figure 3.9: Simulation results 2 for Example 2

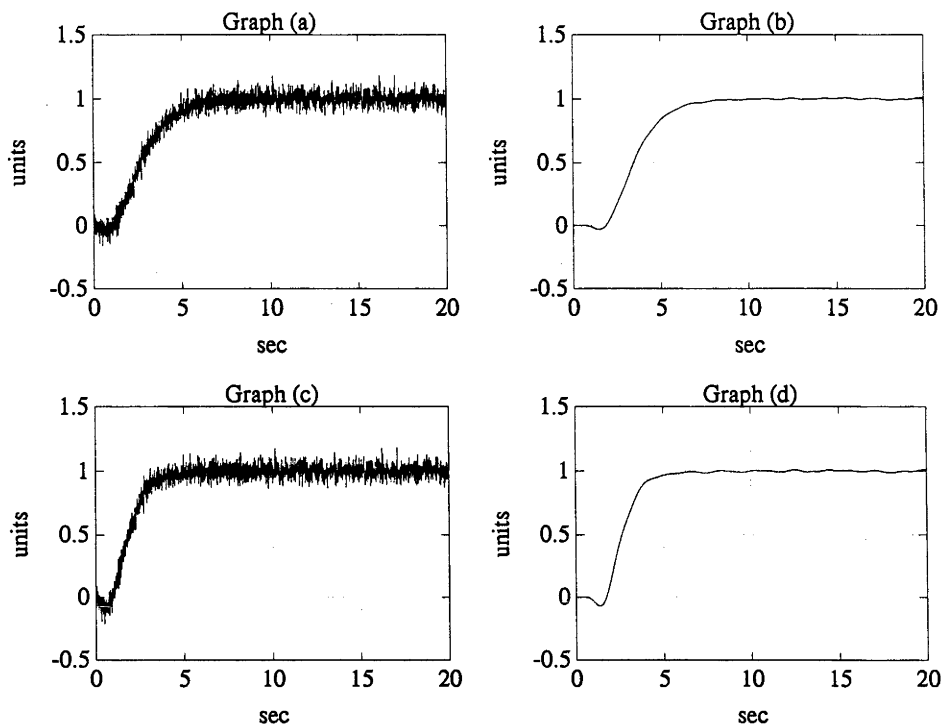


Figure 3.10: Simulation results 3 for Example 2

necessary to improve the accuracy of the model if we wish to increase the designed closed-loop bandwidth further. To ensure that the signals are sufficiently exciting, low amplitude sinusoids in the relevant frequency range are superimposed on the unit step input just prior to system identification (as we have described in Example 1). The frequencies of the sinusoids that we have introduced are 0.501 rad/s, 1.123 rad/s, 3.013 rad/s, 3.541 rad/s, and 4.37 rad/s. The corresponding amplitudes are 0.05, 0.1, 0.02, 0.25, and 0.5. The responses are shown in Graphs (a) and (b) of Figure 3.9.

To estimate  $\check{R}_0^f$ , we use a low-pass data filter with a bandwidth of 5 rad/s. A third order model structure is selected for  $\hat{R}_0^f$  by specifying the model structure parameter as  $N_n = [3 \ 3 \ 1]$ . Using these settings, we obtain

$$\hat{R}_0^f = \frac{-0.73975s^2 - 7.5262s + 2.9606}{s^3 + 1.1079s^2 + 8.7273s + 6.7902},$$

$$\hat{R}_0^f = \left( \begin{array}{c} -1.1836s^3 - 12.634s^2 \\ -1.2841s + 2.3685 \end{array} \right) \bigg/ \left( \begin{array}{c} s^4 + 1.1079s^3 \\ +8.7232s^2 + 6.7902s \end{array} \right),$$

and

$$G_1 = \left( \begin{array}{c} 0.41639s^4 - 10.653s^3 \\ +7.5384s^2 + 22.58s + 5.4322 \end{array} \right) \bigg/ \left( \begin{array}{c} s^5 + 1.6079s^4 + 9.4621s^3 \\ +13.033s^2 + 2.655s \end{array} \right)$$

After performing frequency weighted model reduction, we obtain

$$\hat{G}_1 = \frac{0.41639s^3 - 10.701s^2 + 8.4984s + 23.494}{s^4 + 1.5194s^3 + 9.1507s^2 + 12.197s}$$

We set  $G_1 = \hat{G}_1$  before the iteration is continued.

The updated model  $G_1$  is used to re-design a closed-loop system with a designed closed-loop bandwidth of 0.5 rad/s, and the responses are shown in Graphs (c) and (d) of Figure 3.9. By comparing Graph (d) of Figure 3.9 to that of Figure 3.8, we observe that the response no longer has oscillations. If we continue to increase the designed closed-loop bandwidth of the system, we obtain the responses shown in Figure 3.10 where Graphs (a) and (b) are for a designed closed-loop bandwidth of 1 rad/s, and Graphs (c) and (d) are for a designed closed-loop bandwidth of 2 rad/s.

### 3.6 Summary

We have studied in this Chapter the iterative identification and control design approach for stable plants and Type 1 stable plants. Simulation examples are employed to illustrate the approach and encouraging results are obtained for both stable plant and Type 1 stable plant situations. In particular, we would like to highlight the following points:

- We have illustrated that the frequency weighted open-loop system identification procedure embedded in the iterative identification and control design algorithm is relevant to achieving improved control design.
- We have shown that the control design equations and control-relevant system identification procedure developed for stable plants can be applied without modifications to Type 1 stable plants.
- We have illustrated the applications of the iterative identification and control design algorithm to a stable plant and a Type 1 stable plant by simulation examples. These

simulation examples have clearly shown that, starting with an initial (crude) model of a plant, the iterative identification and control design procedure is a viable methodology for improving progressively the performance of a closed-loop system.

- Comparison of the results obtained in Example 1 with those obtained in Chapter 2 indicated that strictly proper controllers are less sensitive to high frequency model uncertainties, and hence require less frequent model updates when we attempt to increase the designed closed-loop bandwidth of the system through the iterative identification and control design process. System identification, under noisy conditions, becomes the harder the larger the control bandwidth is. It is therefore advantageous to have infrequent model updates that are able to improve model accuracy significantly rather than frequent marginal model improvements.



## Chapter 4

# Some Key Issues in Iterative Identification and Control Design

### 4.1 Introduction

A practical iterative identification and control design algorithm was presented in Chapter 3. The objective is to increase the bandwidth of a closed-loop system, if possible, to a specified value, given that the initial model of the plant may involve significant error in the high frequency region. Furthermore, as the closed-loop bandwidth is being increased, the closed-loop frequency response is to be kept approximately flat in the passband so that the closed-loop transient response is not too oscillatory or having excessive peak overshoot. It was demonstrated in Chapter 3 by simulations that the bandwidth of a closed-loop system can be increased by iterative applications of the Internal Model Control (IMC) method (see [Morari and Zafriou 1989]) and a system identification method pioneered by Hansen (see, for example, [Hansen 1989]). In this chapter we examine a number of crucial questions which arise in the iterative identification and design methodology that we have investigated in Chapters 2 and 3. Among the issues considered are the following:

- When can one re-design the controller and expand the closed-loop bandwidth, without re-identifying?
- When should one re-identify?

- What does one want to identify in the re-identification process?
- What can one identify in the re-identification process?
- How can an identified model be verified against the desired purpose?
- Will re-identification always lead to improved closed-loop performance?

Although attention is restricted to stable strictly proper plants with no finite zeros on the imaginary axis, the results obtained are also applicable to strictly proper plants with no finite zeros on the imaginary axis and may have a simple pole at the origin<sup>1</sup>. (Extension of the iterative identification and control design methodology to unstable plants will be considered in Chapter 5.) The key conclusion in this chapter is that, given a stable strictly proper model for a stable strictly proper plant, we can improve the performance robustness of the closed-loop system through iterative identification and control design if the plant and the existing model have no unstable zeros within the designed closed-loop bandwidth and if the deterioration in performance robustness caused by increasing the closed-loop bandwidth resulted in a sufficiently high signal-to-noise ratio for a certain closed-loop output error. Situations that may cause the iterative identification and control design process to terminate prematurely are also indicated. A simulation example will be used to illustrate the results discussed in this chapter.

The structure of this chapter is as follows. In Section 4.2 we shall show that for the iterative identification and control design algorithm discussed in Section 3.4, it is safe to increase the designed closed-loop bandwidth gradually if the plant is stabilized by the existing controller. Section 4.2 also introduces some of the key concepts and notations that will be useful in the subsequent discussions. Properties of good models for iterative identification and control design are established in Section 4.3. The control-relevant system identification procedure embedded in the iterative identification and control design process is analysed further in Section 4.4. Conditions necessary for identifying a good model and methods for verifying experimentally that an identified model is suitable for the desired purpose (or otherwise) will be given. In Section 4.5 we study mechanisms that may influence the iterative identification and control design process. Situations that may lead to the premature termination of the iterative process will be indicated. In Section 4.6 two methods for model

---

<sup>1</sup>We have shown in Chapter 3 that control design equations and system identification equations for stable plants can be applied without modifications to (Type 1) stable plants that may have a simple pole at the origin.

validation will be described. A procedure for the identification of a better model while avoiding the potential danger of causing instability in the actual closed-loop system will then be suggested. Conditions under which the performance robustness of a closed-loop system can be improved through iterative identification and control design will be discussed in Section 4.7. In Section 4.8 we outline the iterative identification and control design algorithm which incorporates the model validation steps that we have discussed. A simulation example ends this section. We conclude the chapter in Section 4.9.

## 4.2 Nominal Performance Improvement and Robust Stability

In this section it is shown that we can increase the designed closed-loop bandwidth of the system, while maintaining the stability of the actual closed-loop system, if the increment is sufficiently small. Although the concepts of nominal performance and robust performance has been broadly defined in a Section 1.1, to facilitate analysis, we introduce towards the end of this section precise definitions of nominal performance and robust performance that are relevant to the iterative identification and control design methodology under considerations.

For ease of reference, we shall outline in the following the IMC design method when the reference input is a step function. Although the IMC method is generally applicable to the case where the plant and the models are not necessarily stable, we shall restrict our study in this chapter to the case where the plant and the models are stable.

Consider a closed-loop system as shown in Figure 4.1 where  $G$  is the transfer function of a stable strictly proper plant. A sequence of models (identified from data obtained under closed-loop condition) will usually be involved in the iterative identification and control design approach. We therefore use  $G_i$  to denote the  $i^{\text{th}}$  member in the sequence of stable strictly proper models  $\{G_0, G_1, G_2, \dots\}$ . On the basis of  $G_i$  a finite sequence of controllers  $\{K_i^0, K_i^1, \dots, K_i^f\}$  is designed such that, while keeping the closed-loop frequency responses approximately flat within the pass bands, the corresponding closed-loop bandwidths form an increasing sequence  $\{\lambda_1^0, \lambda_i^1, \dots, \lambda_0^f\}$ . Note that we shall in general use  $K_i$  to denote one of the controllers in the sequence  $\{K_i^0, K_i^1, \dots, K_i^f\}$  when it is immaterial to the discussion which particular controller is involved. (We shall also apply the same system of notations to

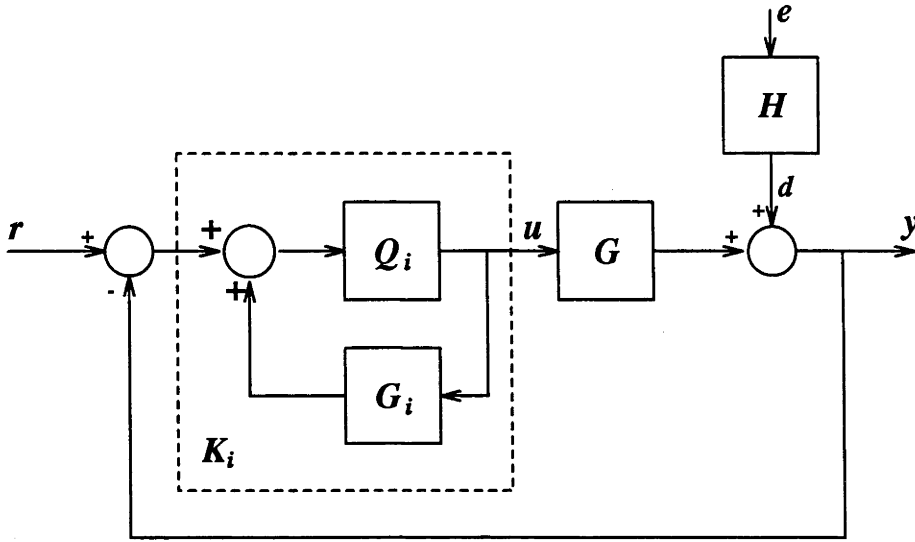


Figure 4.1: Internal model control structure

other transfer functions.) Figure 4.1 shows that

$$K_i = \frac{Q_i}{1 - G_i Q_i} , \quad (4.1)$$

with  $Q_i$  defined in the IMC method by

$$Q_i = [G_i]_m^{-1} F_i , \quad (4.2)$$

where  $[G_i]_m$  is the *minimum-phase factor* of  $G_i$ , and

$$F_i = \left( \frac{\lambda_i}{s + \lambda_i} \right)^{n+1} ; \quad \lambda_i > 0 \quad (4.3)$$

is a suitable IMC filter when the model is stable and when the reference input is a step function. The integer  $n$  is the relative degree of  $G_i$ . The design parameter  $\lambda_i$  must be chosen such that the actual closed-loop transfer function

$$T_i = \frac{G K_i}{1 + G K_i} \quad (4.4)$$

is stable.

It can be shown easily that the designed closed-loop transfer function  $\bar{T}_i = G_i K_i / (1 + G_i K_i)$  can be written as

$$\bar{T}_i = G_i Q_i \quad (4.5)$$

or

$$\bar{T}_i = F_i[G_i]_a, \quad (4.6)$$

where  $[G_i]_a$  is the all pass factor associated with  $G_i$ .

**Remark 4.2.1** Since  $[G_i]_a(j\omega)$  does not affect the magnitude of  $\bar{T}_i(j\omega)$ , it is clear that  $|\bar{T}_i(j\omega)|$  is flat in its passband. Also recall that  $\lambda_i$  is the designed closed-loop bandwidth with an attenuation of  $-3(n+1)$  dB.

**Remark 4.2.2** Note that the system becomes open-loop when  $\lambda_i$  approaches zero. Since  $G$  is stable, it is always possible to make  $T_i$  stable by choosing a sufficiently small  $\lambda_i$ .

Although the designed closed-loop transfer function  $\bar{T}_i$  is always well behaved, the actual closed-loop transfer function  $T_i$  may become unstable when  $\lambda_i$  is too large. That is, the closed-loop system may lose robust stability when  $\lambda_i$  is increased excessively. (Robust stability is defined in Definition 2.3.1.) Since the objective of the iterative identification and control design methodology is to increase the closed-loop bandwidth to a specified value, we would naturally ask the following question:

---

*When can the closed-loop bandwidth be increased **with safety**; that is, **without losing robust stability**, while retaining the use of the model  $G_i$ ?*

---

To answer the above question, we noted from Chapters 2 and 3 that if  $T_i$  (corresponding to  $\lambda_i$ ) is stable, then there exists a strictly proper transfer function  $R_i$  such that

$$G = G_i + \frac{R_i}{1 - Q_i R_i}.$$

It can then easily be shown that

$$\tilde{T}_i = Q_i (1 - \bar{T}_i) R_i, \quad (4.7)$$

where  $\tilde{T}_i = T_i - \bar{T}_i$  is the error in the closed-loop transfer function induced by the error in the model  $G_i$  when the designed closed-loop bandwidth is  $\lambda_i$ .

Suppose that the designed closed-loop bandwidth is increased to  $\lambda'_i > \lambda_i$ , then corresponding to  $\lambda'_i$  we can write

$$\tilde{T}'_i = Q'_i (1 - \bar{T}'_i) R'_i ,$$

where

$$R'_i = \frac{R_i}{1 + [G_i]_m^{-1} (F'_i - F_i) R_i} .$$

Since  $Q'_i$  and  $\bar{T}'_i$  are stable by design, therefore  $\tilde{T}'_i$  and  $T'_i$  are stable if and only if  $R'_i$  is stable. However,  $R'_i$  is stable if  $(\lambda'_i - \lambda_i) > 0$  is *sufficiently small*. Hence we have the following conclusion:

---

**C1** We can increase the designed closed-loop bandwidth **cautiously** if the existing closed-loop system has robust stability.

---

**Remark 4.2.3** Note that even when  $T_i$  is stable, its response to the reference input could be significantly different from that of  $\bar{T}_i$  if, relative to the frequencies where  $G_i$  has significant errors,  $\lambda_i$  is not sufficiently small. To address this issue, we need precise definitions of nominal performance and robust performance that are relevant to the iterative identification and control design methodology under considerations.

**Definition 4.2.1** For any two closed-loop systems designed by the IMC design method, we say that the one with a larger value of  $\lambda_i$  has a better **nominal performance**.

**Definition 4.2.2** We say that, with respect to the given reference input  $r$  and a specified finite (usually suitably small)  $\sigma > 0$ , the closed-loop system has **robust performance** with designed closed-loop bandwidth  $\lambda_i$  if and only if

$$J_i \stackrel{\text{def}}{=} \|v_i\|_2^2 \leq \sigma ,$$

where  $v_i = \tilde{T}_i r$  is the **tracking error**.

**Remark 4.2.4** It is implicitly assumed in Definition 4.2.2 that the control design method has invoked the internal model principle [Francis and Wonham 1976] (which is incorporated in the IMC design method). Otherwise,  $\sigma$  may not be finite.

**Remark 4.2.5** Robust performance clearly implies robust stability but not necessarily otherwise.

**Remark 4.2.6** It is important to note that a closed-loop system may have high nominal performance (large  $\lambda_i$ ) but poor robust performance ( $J_i > \sigma$ ), and vice versa.

**Remark 4.2.7** For a model with significant modelling errors in the high frequency region, the closed-loop system can be designed to have good robust performance if the designed closed-loop bandwidth is sufficiently small.

**Remark 4.2.8** While  $\lambda_i$  is being increased, a stage can be reached (before the occurrence of instability) where, because of the modelling errors associated with  $G_i$  making a significant contribution to  $J_i$ , the performance robustness has deteriorated beyond an acceptable level. At this stage the designed closed-loop bandwidth is  $\lambda_i = \lambda_i^f$  and it cannot be increased further before a more accurate model  $G_{i+1}$  is identified.

### 4.3 Properties of Good Models

In Section 4.2 we have concluded that when performance robustness of the closed-loop system has deteriorated beyond an acceptable level, it is necessary to identify a model better than the existing one before the designed closed-loop bandwidth can be increased further.

It is clear from Section 4.2 that we can increase the designed closed-loop bandwidth as long as the closed-loop system has robust performance. Therefore it is natural that, when

the closed-loop system loses robust performance, we attempt to seek a new model that will allow robust performance of the closed-loop system to be restored through controller re-design (while the designed closed-loop bandwidth remains unchanged). This prompts us to ask the following question:

---

*What **WOULD WE LIKE** to identify, in order that, with the new model, robust performance of the closed-loop system can be improved through controller re-design?*

---

Before we proceed to answer this question, we observe that each cycle of the iterative identification and control design procedure involves an existing model  $G_i$  and an updated model  $G_{i+1}$ . Since every stage of the iteration proceeds in a similar fashion, it suffices to discuss only the stage where  $i = 0$ . Therefore we shall denote the existing model by  $G_0$  and the updated model by  $G_1$ . This system of notations will carry over to all transfer functions and signals involved in the following discussions. We also need the following definition.

**Definition 4.3.1** *The critical frequency corresponding to a pole (or a zero) is numerically equal to the distance of the pole (or the zero) from the origin.*

Suppose that  $G_1$  is identified when  $\lambda_0$  has reached  $\lambda_0^f$ . A new controller  $K_1^0$  will then be designed on the basis of  $G_1$  such that  $\lambda_1^0$  has the same value as  $\lambda_0^f$ . Obviously we would like  $J_1^0 = \|\tilde{T}_1^0 r\|_2^2$  to be small. By using equations (4.1) to (4.5), with appropriate adjustments made to the notations, we can write  $\tilde{T}_1^0 = T_1^0 - \bar{T}_1^0$  as

$$\tilde{T}_1^0 = \frac{\left(\frac{G-G_1}{G_1}\right) \bar{T}_1^0}{1 + \left(\frac{G-G_1}{G_1}\right) \bar{T}_1^0} (1 - \bar{T}_1^0) . \quad (4.8)$$

Clearly it is necessary that  $\tilde{T}_1^0$  be stable. Since  $G - G_1$  is unknown, therefore we conclude that



**C2** We **WOULD LIKE** to obtain a model  $G_1$  for  $G$  of sufficient accuracy such that

$$\left\| \left( \frac{G - G_1}{G_1} \right) \bar{T}_1^0 \right\|_\infty < 1.$$

This ensures the stability of  $\tilde{T}_1^0$  (see equation 4.8), and hence the stability of  $T_1^0$ .

Furthermore we observe that the magnitude of the designed sensitivity function  $1 - \bar{T}_1^0$  in the right hand side of equation (4.8) could approach a magnitude significantly greater than one if  $G_1$  has unstable zeros with critical frequencies smaller than the passband of  $\bar{T}_1^0 = F_1^0[G_1]_a$ . In order that  $\tilde{T}_1^0$  has a small magnitude, we require in addition to the above robust stability condition that

**C3** We **WOULD LIKE** to obtain a model  $G_1$  for  $G$  of sufficient accuracy such that

$$\left| \left[ \frac{G(j\omega) - G_1(j\omega)}{G_1(j\omega)} \right] \bar{T}_1^0(j\omega) \right|$$

is sufficiently small for all frequencies above the lesser of the passband of  $\bar{T}_1^0$  and the smallest critical frequency corresponding to the unstable zeros of  $\bar{T}_1^0$ .

**Remark 4.3.1** Note that the unstable zeros of  $\bar{T}_1^0$  are those of  $G_1$  which, in a situation with good identification, will be at least approximately those of the plant  $G$ .

**Remark 4.3.2** If  $G_1$  has unstable zeros located within the passband of  $\bar{T}_1^0$ , it is likely that there is a range of frequency within the passband of  $\bar{T}_1^0$  where the magnitude of the designed sensitivity function  $1 - \bar{T}_1^0$  is significantly greater than one. It has the following consequences:

1. There is a range of frequency within the passband of  $\bar{T}_1^0$  where the designed system has poor disturbance rejection and the measurement noise is not well attenuated.
2. Since the magnitude of the designed sensitivity function is the inverse of the distance of the open-loop frequency response curve from the critical point of stability at  $-1 + j0$ , the designed system may have poor stability margins and transient response if the magnitude of the designed sensitivity function is excessively large near the edge of the system passband.

Therefore, purely from the point of view of control design, we may not want to increase the designed closed-loop bandwidth  $\lambda_1$  beyond  $\lambda_0^f$  if  $G_1$  is found to have unstable zeros with critical frequencies within the passband of  $\bar{T}_0^f$ .

#### 4.4 System Identification in the Iterative Identification and Control Design Approach

Notwithstanding the fact that we have established in the last section properties of a good model for iterative identification and control design, it is important to ask the following question:

---

*What CAN WE identify by using the system identification procedure embedded in the iterative identification and control design approach?*

---

In this section we answer the last question in three steps. In Section 4.4.1 we outline the control-relevant closed-loop system identification problem that we have formulated in Chapter 2. We state a key theorem that relates the control-relevant closed-loop system identification problem to a frequency weighted open-loop system identification problem, where a stable transfer function,  $R_0^f$ , that parametrizes the plant is to be identified. This

is a special case of Theorem 2.4.2 when the plant and the model involved are stable. In Section 4.4.2 we show that it is possible to identify  $R_0^f$  accurately only if the signal-to-noise ratio of a certain closed-loop output error resulting from the existing controller is high. Furthermore, by recognizing the relation between the signal component of the closed-loop output error and deterioration in robust performance, we can restate the conditions necessary for obtaining an accurate estimate of  $R_0^f$  in terms of the level of deterioration in robust performance against the effect of noise disturbance. In Section 4.4.3 we show how to verify indirectly that an estimate of  $R_0^f$  is unbiased.

#### 4.4.1 Control-Relevant System Identification

It was indicated at the end of Section 4.2 that when the designed closed-loop bandwidth has reached a certain value denoted by  $\lambda_0^f$ , the robust performance measure  $J_0^f = \|v_0^f\|_2^2$  associated with the closed-loop system designed on the basis of  $G_0$  would become excessively large. It was shown in Section 4.3 that at this stage, we would like to identify a new model  $G_1$  such that

$$\left| \left[ \frac{G(j\omega) - G_1(j\omega)}{G_1(j\omega)} \right] \bar{T}_1^0(j\omega) \right|$$

is sufficiently small in an appropriate frequency range. Unfortunately it is not clear how to process input-output measurements to determine  $G_1$  so that this condition is naturally or automatically satisfied. To overcome this difficulty we shall use input-output measurements and possibly the reference input of the stable closed-loop system as shown in Figure 4.2 to identify  $G_1$  such that

$$\left\| \left( \frac{GK_0^f}{1 + GK_0^f} - \frac{G_1K_0^f}{1 + G_1K_0^f} \right) r \right\|_2^2$$

is minimized. It was shown in Chapter 2 that this control-relevant closed-loop identification problem can be transformed into an open-loop identification problem by employing Hansen's framework of identification (see [Hansen 1989]). We shall state this result again in the following as special case of Theorem 2.4.2 when the plant  $G$  and the model  $G_0$  are stable.

**Theorem 4.4.1** *Let  $K_0^f = Q_0^f / (1 - G_0Q_0^f)$  stabilize  $G$  and  $G_0$ , where  $Q_0^f$  is a stable strictly proper transfer function, so that  $G$  can be parametrized by a stable strictly proper transfer*

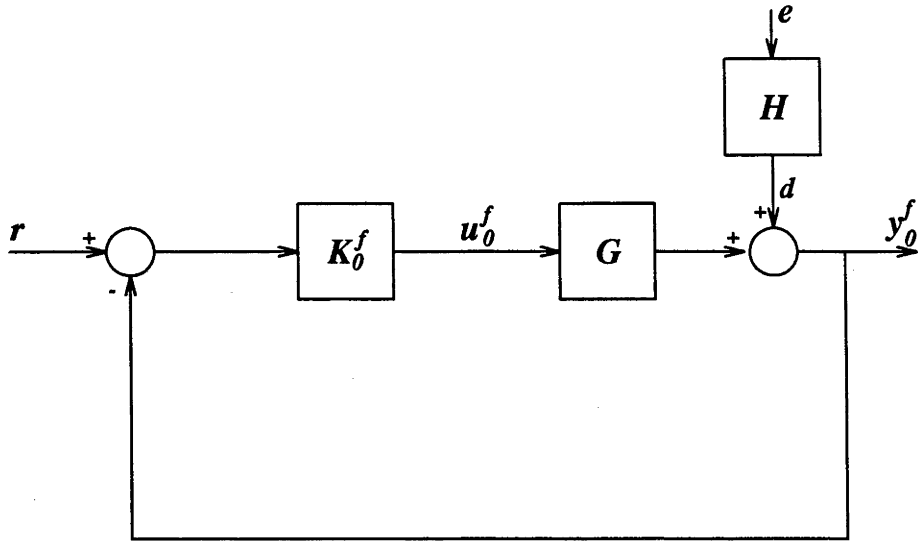


Figure 4.2: Closed-loop system just before identification

function  $R_0^f$  via

$$G = G_0 + \frac{R_0^f}{1 - R_0^f Q_0^f} .$$

Let

$$G_1 = G_0 + \frac{\hat{R}_0^f}{1 - \hat{R}_0^f Q_0^f} \quad (4.9)$$

be another model stabilized by  $K_0^f$ , where  $\hat{R}_0^f$  is a strictly proper stable estimate of  $R_0^f$ .

Also define the filtered output error

$$\xi_1 = (1 - \bar{T}_0^f) (\beta - \hat{R}_0^f \alpha) , \quad (4.10)$$

where  $\alpha = Q_0^f r$ ,  $\beta = y_0^f - G_0 u_0^f$ , and  $u_0^f$  and  $y_0^f$  are, respectively, the input and output of the plant resulting from the application of  $K_0^f$ . Then  $\xi_1$  can be expressed as

$$\xi_1 = \left( \frac{G K_0^f}{1 + G K_0^f} - \frac{G_1 K_0^f}{1 + G_1 K_0^f} \right) r + w_0^f , \quad (4.11)$$

where

$$w_0^f = (1 - T_0^f) H e \quad (4.12)$$

is the effect of the noise disturbance,  $e$ , on the actual closed-loop output.

**Remark 4.4.1** If we define  $H = S_0^f / (1 - R_0^f Q_0^f)$ , where  $S_0^f$  is a proper stable and inversely stable transfer function, then the actual closed-loop system has Hansen's open-loop representation

$$\beta = R_0^f \alpha + S_0^f e . \quad (4.13)$$

**Remark 4.4.2** From Theorem 4.4.1 it is clear that minimizing

$$\left\| \left( \frac{GK_0^f}{1 + GK_0^f} - \frac{G_1 K_0^f}{1 + G_1 K_0^f} \right) r + w_0^f \right\|_2^2$$

with respect to  $G_1$  is equivalent to minimizing  $\left\| (1 - G_0 Q_0^f) (\beta - \hat{R}_0^f \alpha) \right\|_2^2$  with respect to  $\hat{R}_0^f$ , provided that  $G_1$  is updated according to  $G_1 = G_0 + [\hat{R}_0^f / (1 - \hat{R}_0^f Q_0^f)]$ .

**Remark 4.4.3** Since the "input"  $\alpha$  in equation (4.13) is independent of the noise disturbance  $e$ , identifying  $R_0^f$  (and  $S_0^f$ ) is an *open-loop* identification problem.

We can summarise the above discussions as follows:

---

**C4** We can transform the problem of identifying  $G$  in closed-loop into a problem of identifying

$$R_0^f = \frac{G - G_0}{1 + Q_0^f (G - G_0)}$$

in open-loop.

---

It was shown in Section 3.3 that for stable plants, the frequency weighted open-loop system identification problem can be solved effectively by factorizing  $R_0^f$  as  $R_0^f = \tilde{R}_0^f \check{R}_0^f$ , where  $\tilde{R}_0^f$  is a stable proper transfer function known by design and  $\check{R}_0^f$  is an unknown stable strictly proper transfer function. After  $\check{R}_0^f$  is estimated via  $\tilde{\check{R}}_0^f$ , we can update the model via

$$G_1 = G_0 + \frac{(s + \lambda_0^f)^{n+1} [G_0]_m \tilde{\check{R}}_0^f}{(s + \lambda_0^f) - (\lambda_0^f)^{n+1} \tilde{\check{R}}_0^f} . \quad (4.14)$$

The equation that describes the open-loop identification of  $\check{R}_0^f$  was shown in Section 3.3 to be

$$\beta_1 = \check{R}_0^f \alpha_2 + w_0^f ,$$

where

$$\beta_1 = (1 - \bar{T}_0^f)(y_0^f - G_0 u_0^f) ,$$

$$\alpha_2 = (1 - \bar{T}_0^f) \frac{(\lambda_0^f)^{n+1}}{s + \lambda_0^f} r ,$$

and

$$w_0^f = (1 - \bar{T}_0^f) S_0^f e .$$

Usually data filters are employed to shape the bias-distribution of the estimates (which is due to under-modelling) such that the model error is small in the appropriate frequency range [Ljung 1987]. If we filter each of the signals  $\beta_1$  and  $\alpha_2$  by the data filter  $L$ , the signal model for identifying  $\check{R}_0^f$  becomes

$$\bar{\beta} = \check{R}_0^f \bar{\alpha} + \Psi_0^f e ,$$

where

$$\bar{\beta} = L \beta_1 ,$$

$$\bar{\alpha} = L \alpha_2 ,$$

and

$$\Psi_0^f = L(1 - \bar{T}_0^f) S_0^f .$$

We shall identify  $\check{R}_0^f$  and  $\Psi_0^f$  by the prediction error method (see [Ljung 1987]) as shown in Figure 4.3. Note that  $\check{R}_0^f$  and  $\Psi_0^f$  are independently parametrized through the Box-Jenkins model structure.

**Remark 4.4.4** From the above discussions, it is clear that we can either identify  $R_0^f$  directly or indirectly through identifying  $\check{R}_0^f$ . Furthermore, since  $R_0^f = \tilde{R}_0^f \check{R}_0^f$  and  $\hat{R}_0^f = \tilde{R}_0^f \hat{\check{R}}_0^f$ , where  $\tilde{R}_0^f$  is a *known* stable bi-proper transfer function (see Theorem 3.3.1), all discussions involving  $R_0^f$  and  $\hat{R}_0^f$  can be rephrased in terms of  $\check{R}_0^f$  and  $\hat{\check{R}}_0^f$ , and vice versa. *In practice*, since the order of  $\check{R}_0^f$  is smaller than that of  $R_0^f$ , it is *more efficient* to identify  $R_0^f$  indirectly through identifying  $\check{R}_0^f$ .



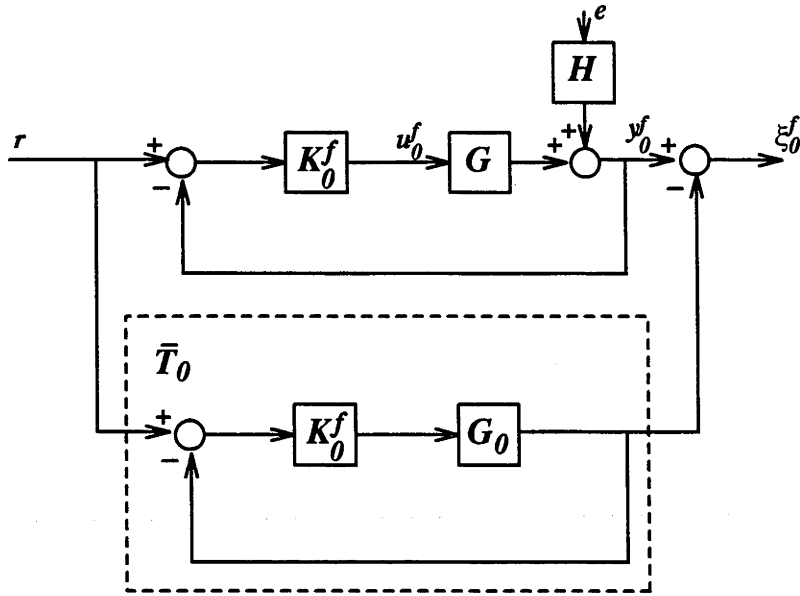


Figure 4.4: Closed-loop output error

Now we can use the fact that  $y_0^f = T_0^f r + (1 - T_0^f) H e$  to write

$$\xi_0^f = v_0^f + w_0^f \tag{4.16}$$

where

$$v_0^f = \bar{T}_0^f r \tag{4.17}$$

**Remark 4.4.5** Note that the tracking error  $v_0^f$  cannot be measured directly. It can only be estimated from the closed-loop output error  $\xi_0^f$ .

It is apparent that  $v_0^f$  is the signal component in  $\xi_0^f$  that carries the useful information about the existing modelling errors under closed-loop condition, and  $w_0^f$  is the noise component in  $\xi_0^f$  that will be a hindrance to the determination of  $\hat{R}_0^f$ . Therefore we can draw an immediate conclusion:



---

**C5** We can identify  $R_0^f$  only if the signal-to-noise ratio associated with the closed-loop output error resulting from the existing controller  $K_0^f$  is high.

---

We shall next show that the normalized variance for an unbiased estimate of  $R_0^f$  will be asymptotically small in the frequency range where the signal-to-noise ratio associated with the closed-loop output error is sufficiently high.

By substituting equations (4.16) and (4.17) into equation (4.15) and noting from equation (4.7) that  $\tilde{T}_0^f = Q_0^f (1 - \bar{T}_0^f) R_0^f$ , we can write

$$\hat{R}_0^f = \arg \min_{\rho} \left\| Q_0^f (1 - \bar{T}_0^f) (R_0^f - \rho) r + w_0^f \right\|_2^2 .$$

In practice we use sampled input-output data to estimate a discrete time model for  $\hat{R}_0^f$  before converting it to a continuous time transfer function. We shall assume that errors involved in this conversion are negligible. Following [Ljung 1987], we can write the variance of an unbiased estimate of  $R_0^f$  approximately as

$$\mathbf{E} \left( \left| \hat{R}_0^f(j\omega) - R_0^f(j\omega) \right|^2 \right) \sim \frac{m}{M} \frac{\Phi_{w_0^f}(\omega)}{\left| Q_0^f(j\omega) (1 - \bar{T}_0^f(j\omega)) \right|^2 \Phi_r(\omega)} ,$$

where  $\Phi_{w_0^f}(\omega)$  is the power spectral density of  $w_0^f$ , under the condition that the order of the discrete time model for  $\hat{R}_0^f$  (denoted by  $m$ ) and the number of data (denoted by  $M$ ) are large and the ratio  $m/M$  is small.

Since  $\Phi_{v_0^f}(\omega) = \left| Q_0^f(j\omega) [1 - \bar{T}_0^f(j\omega)] R_0^f(j\omega) \right|^2 \Phi_r(\omega)$  is the power spectral density of  $v_0^f$ , we can write the normalized variance of  $\hat{R}_0^f$  as

$$\mathbf{E} \left( \left| \frac{\hat{R}_0^f(j\omega) - R_0^f(j\omega)}{R_0^f(j\omega)} \right|^2 \right) \sim \frac{m}{M} \frac{\Phi_{w_0^f}(\omega)}{\Phi_{v_0^f}(\omega)}$$

for the frequencies where  $R_0^f(j\omega) \neq 0$ .

**Remark 4.4.6** For a finite number of data, the normalized variance of  $\widehat{R}_0^f$  can be small only in the frequency range where the signal-to-noise ratio associated with the closed-loop output error is sufficiently high. Furthermore, observe that the normalized variance of  $\widehat{R}_0^f$  is asymptotically inversely proportional to the number of data. This implies that, to achieve a certain normalized variance, the longer the data record we have the smaller the signal-to-noise ratio can be.

**Remark 4.4.7** Since  $R_0^f = \widetilde{R}_0^f \check{R}_0^f$  and  $\widehat{R}_0^f = \widetilde{R}_0^f \widehat{\check{R}}_0^f$ , it is obvious that

$$\mathbf{E} \left( \left| \frac{\widehat{\check{R}}_0^f(j\omega) - \check{R}_0^f(j\omega)}{\check{R}_0^f(j\omega)} \right|^2 \right) \sim \frac{m}{M} \frac{\Phi_{w_0^f}(\omega)}{\Phi_{v_0^f}(\omega)}$$

for the frequencies where  $\check{R}_0^f(j\omega) \neq 0$ .

We now summarise the above discussion as follows:

---

**C6** We can obtain an unbiased estimate of  $R_0^f$  with a small asymptotic normalized variance in a certain frequency range  $\omega_1 \leq \omega \leq \omega_2$  if and only if

1. the structure of the model set used in the estimation of  $R_0^f$  is sufficiently general,
2. the condition

$$\frac{\Phi_{v_0^f}(\omega)}{\Phi_{w_0^f}(\omega)} \geq \mu, \quad \text{for } \omega_1 \leq \omega \leq \omega_2$$

is satisfied for a sufficiently large  $\mu > 0$ .

---

It is clear that nothing comes for free, and it is prudent to ask the following question:

*What is the price that we have to pay, in terms of system performance, before a sufficiently high signal-to-noise ratio of the closed-loop output error can be achieved?*

We shall next show that it is necessary to have a certain level of deterioration in robust performance (relative to the effect of noise disturbance) before the closed-loop output error can achieve a sufficiently high signal-to-noise ratio.

By using equations (4.12) and (4.17) we can deduce that,

$$\frac{\Phi_{v_0^f}(j\omega)}{\Phi_{w_0^f}(j\omega)} \geq \mu, \quad \text{for } \omega_1 \leq \omega \leq \omega_2; \quad \omega_1 \geq 0$$

if and only if

$$|\tilde{T}_0^f(j\omega)|^2 \Phi_r(\omega) > \mu \left| [1 - T_0^f(j\omega)] H(j\omega) \right|^2 \Phi_e(\omega), \quad \text{for } \omega_1 \leq \omega \leq \omega_2 \quad (4.18)$$

where  $\Phi_e(\omega)$  is the power spectral density of the noise disturbance  $e$ . Upon integration we get

$$\frac{1}{\pi} \int_{\omega_1}^{\omega_2} |\tilde{T}_0^f(j\omega)|^2 \Phi_r(\omega) d\omega > \frac{\mu}{\pi} \int_{\omega_1}^{\omega_2} \left| [1 - T_0^f(j\omega)] H(j\omega) \right|^2 \Phi_e(\omega) d\omega .$$

By Parseval's theorem, and note that  $\omega_1 \geq 0$ , we can write

$$J_0^f = \frac{1}{2\pi} \int_{-\infty}^{\infty} |\tilde{T}_0^f(j\omega)|^2 \Phi_r(\omega) d\omega > \frac{1}{\pi} \int_{\omega_1}^{\omega_2} |\tilde{T}_0^f(j\omega)|^2 \Phi_r(\omega) d\omega .$$

Therefore

$$J_0^f > \frac{\mu}{\pi} \int_{\omega_1}^{\omega_2} \left| [1 - T_0^f(j\omega)] H(j\omega) \right|^2 \Phi_e(\omega) d\omega .$$

Now we can restate the conditions necessary for the estimation of  $R_0^f$  as follows:

**C7** *We can obtain an unbiased estimate of  $R_0^f$  with a small asymptotic normalized variance in a certain frequency range of interest ( $\omega_1 \leq \omega \leq \omega_2; \omega_1 \geq 0$ ) only if*

1. *the structure of the model set used in the estimate of  $R_0^f$  is sufficiently general,*

2. there is a certain level of deterioration in robust performance bounded from below by

$$\frac{\mu}{\pi} \int_{\omega_1}^{\omega_2} \left| [1 - T_0^f(j\omega)] H(j\omega) \right|^2 \Phi_e(\omega) d\omega$$

for a sufficiently large  $\mu > 0$ .

**Remark 4.4.8** It is obvious that a problem is ill-posed if the value of  $\sigma$  that specifies the tolerable level of deterioration in robust performance (see Definition 4.2.2) does not satisfy the inequality

$$\frac{1}{\pi} \int_{\omega_1}^{\omega_2} \left| [1 - T_0^f(j\omega)] H(j\omega) \right|^2 \Phi_e(\omega) d\omega < \frac{\sigma}{\mu}$$

for a sufficiently large  $\mu > 0$ .

#### 4.4.3 Practically Unbiased Estimation of $R_0^f$

In Section 4.4.2 we have shown that the normalized variance of  $\widehat{R}_0^f$  can be small if the signal-to-noise ratio associated with the closed-loop output error is sufficiently high. However normalized variance can be used as a measure of the quality of an estimate if and only if the estimate is unbiased. It is therefore necessary to verify that  $\widehat{R}_0^f$  is a practically unbiased estimate (or an unfalsified model as discussed in [Ljung *et al.* 1991]) of  $R_0^f$ . In this subsection we shall show that it is possible to verify indirectly that  $\widehat{R}_0^f$  is a practically unbiased estimate of  $R_0^f$  by verifying that  $G_1 K_0^f / (1 + G_1 K_0^f)$  is a practically unbiased estimate of  $G K_0^f / (1 + G K_0^f)$ .

We shall begin by considering

$$\xi_1 = \left( \frac{G K_0^f}{1 + G K_0^f} - \frac{G_1 K_0^f}{1 + G_1 K_0^f} \right) r + \frac{1}{1 + G K_0^f} H e .$$

Clearly if  $G_1 K_0^f / (1 + G_1 K_0^f)$  is a practically unbiased estimate of  $G K_0^f / (1 + G K_0^f)$ , then the power spectral density of  $\xi_1$  should reflect the effects of the noise disturbance only. We can perform this verification experimentally after  $G_1$  is obtained (as we shall describe in Section 4.6). Now recall that, if it is necessary to update the model  $G_0$ , the magnitude of

$$\frac{G K_0^f}{1 + G K_0^f} - \frac{G_0 K_0^f}{1 + G_0 K_0^f} = Q_0^f (1 - \bar{T}_0^f) R_0^f$$

must be significant in a certain frequency range  $[\omega_1, \omega_2]$ . Therefore, before the model  $G_0$  is updated, both the magnitude of the frequency weighting  $Q_0^f (1 - \bar{T}_0^f)$  and the magnitude of  $R_0^f$  cannot be small in  $[\omega_1, \omega_2]$ . Since we can write

$$\frac{GK_0^f}{1 + GK_0^f} - \frac{G_1K_0^f}{1 + G_1K_0^f} = Q_0^f (1 - \bar{T}_0^f) (R_0^f - \hat{R}_0^f) ,$$

it can be deduced easily that if  $G_1K_0^f/(1 + G_1K_0^f)$  is a practically unbiased estimate of  $GK_0^f/(1 + GK_0^f)$  in  $[\omega_1, \omega_2]$ , then  $\hat{R}_0^f$  is a practically unbiased estimate of  $R_0^f$  in  $[\omega_1, \omega_2]$ . We can therefore conclude that:

---

**C8** We can verify that  $\hat{R}_0^f$  is a practically unbiased estimate of  $R_0^f$  in  $[\omega_1, \omega_2]$  by verifying experimentally that  $G_1K_0^f/(1 + G_1K_0^f)$  is a practically unbiased estimate of  $GK_0^f/(1 + GK_0^f)$  in  $[\omega_1, \omega_2]$ .

---

## 4.5 Mechanisms that Influence Performance Robustness and Identification

In this section we shall study mechanisms that influence performance robustness of systems designed by the IMC method. We shall show that there are three mechanisms that may lead to deterioration in robust performance. However only one of them will contribute to the high signal-to-noise ratio needed for a successful estimation of  $R_0^f$ . These observations allow us to deduce situations where the iterative identification and control design process may continue or may terminate prematurely.

Recall that in Section 4.4.2 we have shown that a certain level of deterioration in robust performance is necessary before we can attempt to find a good estimate of  $R_0^f$ . However we should ask

---

Does it mean that, irrespective of the causes, deterioration in robust performance is always helpful to the identification of  $R_0^f$ ?

---

The answer is *obviously no*, as we shall elaborate now.

With appropriate substitutions in equations (4.17) and (4.12) respectively, we can obtain

$$v_0^f = \frac{\left(\frac{G-G_0}{G_0}\right) \bar{T}_0^f}{1 + \left(\frac{G-G_0}{G_0}\right) \bar{T}_0^f} (1 - \bar{T}_0^f) r \quad (4.19)$$

and

$$w_0^f = \frac{1}{1 + \left(\frac{G-G_0}{G_0}\right) \bar{T}_0^f} (1 - \bar{T}_0^f) He . \quad (4.20)$$

Since  $J_0^f = \|v_0^f\|_2^2$  we observe that, disregarding changes in disturbance suppression ability, deterioration in robust performances is governed by the value of

$$J_0^f = \frac{1}{2\pi} \int_{-\infty}^{\infty} \Phi_{v_0^f}(\omega) d\omega .$$

We therefore conclude from the right-hand side of equation (4.19) that, for a given reference input, there are three factors that contribute to  $J_0^f$  through  $\Phi_{v_0^f}(\omega)$ :

1. The effect of the term  $[(G - G_0)/G_0]\bar{T}_0^f$  in the *numerator* is independent of the phase angle of  $[(G - G_0)/G_0]\bar{T}_0^f$ . We shall call this the **phase insensitive factor**.
2. The effect of the term  $1 + [(G - G_0)/G_0]\bar{T}_0^f$  in the *denominator* depends on the gain and phase margins of  $[(G - G_0)/G_0]\bar{T}_0^f$ . We shall call this the **stability margin factor**.
3. The effect of the term  $1 - \bar{T}_0^f$  depends on the existence of unstable zeros of  $G_0$  within the passband of  $\bar{T}_0^f = F_0^f[G_0]_a$ . We shall call this the **unstable zeros dependent factor**.

By using equations (4.19) and (4.20) we can write the signal-to-noise ratio associated

with the closed-loop output error as

$$\frac{\Phi_{v_0^f}(\omega)}{\Phi_{w_0^f}(\omega)} = \frac{\left| \left[ \frac{G(j\omega) - G_0(j\omega)}{G_0(j\omega)} \right] \bar{T}_0^f(j\omega) \right|^2}{|H(j\omega)|^2} \frac{\Phi_r(\omega)}{\Phi_e(\omega)}$$

The last equation indicates that for a given reference input and noise disturbance scenario, only an increase in the magnitude of the phase insensitive factor can increase the signal-to-noise ratio of the closed-loop output error.

**Remark 4.5.1** When the stability margin factor or the unstable zeros dependent factor are the main causes of deterioration in robust performance, it may be difficult to obtain an accurate estimate of  $R_0^f$ . This may lead to premature termination of the iterative identification and control design process. In particular, when the existing model  $G_0$  has unstable zeros within the passband of the designed closed-loop transfer function  $T_0^f$ , the designed sensitivity (unstable zeros dependent factor) may have large magnitude in a certain frequency region. This fundamental limit in control performance (as discussed in [Freudenberg and Looze 1985]) will cause deterioration in designed and robust performances with no improvement in the signal-to-noise ratio associated with the closed-loop output error. We emphasize that the above discussions *do not* imply that unstable zeros of the model that are within the designed closed-loop bandwidth will *always* lead to premature termination of the iterative process, although we have experienced such situations in simulations. It must be pointed out that there are situations where unstable zeros of the model do not cause the iterative process to terminate prematurely (see the simulation example in Section 4.8).

We shall now summarise the above discussions as follows:

---

## C9

1. *There are three factors that can cause the performance robustness to deteriorate. They are namely, the phase insensitive factor, the stability margin factor, and the unstable zeros dependent factor. Among these factors, only the phase insensitive factor alone can contribute to improving the signal-to-noise ratio associated with the closed-loop output error.*

2. *When the unstable zeros dependent factor or the stability margin factor are the main causes of deterioration in robust performance, the signal-to-noise ratio associated with the closed-loop output error may be poor and it may be difficult to obtain a practically unbiased estimate of  $R_0^f$  with a small asymptotic normalized variance. This may cause subsequent difficulties in continuing the iterative identification and control design process.*

**Remark 4.5.2** From equation (4.19) it is clear that  $\Phi_{v_0^f}(\omega)$  cannot be large in the frequency range where the designed sensitivity function has small magnitude. This implies that the frequency range  $[\omega_1, \omega_2]$  emphasized in Section 4.4 cannot be well below  $\lambda_0^f$ .

**Remark 4.5.3** From the definitions of the phase insensitive factor and the stability margins factor, we can deduce that it is possible to estimate  $R_0^f$  accurately only in the frequency range where the designed complementary-sensitivity-function weighted multiplicative modelling error has large magnitude and small phase lag. This implies that the frequency range  $[\omega_1, \omega_2]$  cannot be well above  $\lambda_0^f$  (where  $\bar{T}_0^f$  has small magnitude and large phase lag).

## 4.6 Identification and Validation of New Models

In Section 4.4.2 we have shown that under noisy conditions, the accuracy of the identified model can be improved by increasing the signal-to-noise ratio associated with the closed-loop output error. It was also shown that this is equivalent to having a certain level of deterioration in robust performance relative to the effect of noise disturbance. It is clearly undesirable from the control point of view for robust performance to deteriorate too seriously, while on the other hand it is necessary to have a sufficiently high signal-to-noise ratio in the closed-loop output error before identification can successfully be carried out. Furthermore it is important to ensure that a model with the right properties is identified. We would therefore like to ask the following practical questions:



- 
1. *When should we try to identify a better model?*
  2. *Have we actually identified a good model for our purpose?*
- 

Before we can answer these questions we need methods for validating an identified model. In Section 4.6.1 we shall describe a frequency domain method for model validation. In Section 4.6.2 we shall give a time domain method for model validation. In Section 4.6.3 we shall first state some of the facts regarding the two methods of model validation that we have observed from simulations. (One of these simulations will be presented in Section 4.8.) We will then suggest a procedure for identifying a better model.

#### 4.6.1 A Frequency Domain Method for Model Validation

In the following we shall present a model validation method in the frequency domain. It should be emphasized that the model validation procedure is designed with the closed-loop control objective in mind.

Recall that, given the existing model  $G_0$ , it is necessary to identify an improved model  $G_1$  when  $J_0^f = \|v_0^f\|_2^2$  is excessively large. Evidently  $\xi_0^f$  could be large (implying undesirable performance) with one or both of  $v_0^f$  and  $w_0^f$  large. If the former is larger, there is a potential to reduce it by improved model identification. But this will only work (in a particular frequency band  $[\omega_1, \omega_2]$ ) if the signal-to-noise ratio is sufficiently high. Specifically, when only finite durations of input-output measurements are available for identifying  $R_0^f$  (which parametrizes  $G$ ), it was shown in Section 4.4.2 that the normalized variance of  $\hat{R}_0^f$  will be small only if the signal-to-noise ratio,  $\Phi_{v_0^f}(\omega)/\Phi_{w_0^f}(\omega)$ , associated with  $\xi_0^f = v_0^f + w_0^f$  is sufficiently high. Obviously, then one needs to estimate power spectra for  $w_0$  and  $v_0$  (or more precisely  $\xi_0$ ). We shall proceed as follows.

From  $v_0 = (T_0 - \bar{T}_0) r$  and  $\xi_0 = v_0 + w_0$  we observe that when  $r = 0$ , the sole contributor

to  $\xi_0$  is  $w_0$ . Therefore we can compute  $\Phi_{w_0}(\omega)$  after measuring  $\xi_0$  with  $r = 0$ . When  $r \neq 0$ , we have  $\xi_0 = v_0 + w_0$ . Assuming that  $v_0$  and  $w_0$  are uncorrelated (which follows if  $r$  and  $e$  are uncorrelated, a typical situation), then  $\Phi_{\xi_0}(\omega) = \Phi_{v_0}(\omega) + \Phi_{w_0}(\omega)$ . By visual comparison of  $\Phi_{\xi_0}(\omega)$  with  $\Phi_{w_0}(\omega)$ , we evaluate the significance of  $\Phi_{v_0}(\omega)$  with respect to  $\Phi_{w_0}(\omega)$ . If  $\Phi_{\xi_0^f}(\omega)$  is significantly larger than  $\Phi_{w_0^f}(\omega)$  in a frequency band spanning one decade and centred around  $\lambda_0^f$  (when the designed closed-loop bandwidth is  $\lambda_0^f$ ), the model  $G_0$  is invalidated for the design of closed-loop systems with bandwidths larger than or equal to  $\lambda_0^f$ .

The method just described can also be used to validate  $G_1$  after it is identified (both before and after model reduction is performed). We simply replace  $G_0$  by  $G_1$ , while retaining  $K_0^f$ , in the simulation of the designed closed-loop response to the reference input. This allows us to compute  $\xi_1$  and its power spectrum  $\Phi_{\xi_1}(\omega)$ . By visually comparing  $\Phi_{\xi_1}(\omega)$  with  $\Phi_{w_0^f}(\omega)$ , we have good confidence that  $G_1$  is a reliable model of  $G$  (when the designed closed-loop bandwidth is  $\lambda_0^f$ ) if  $\Phi_{\xi_1}(\omega)$  is comparable to  $\Phi_{w_0^f}(\omega)$  up to  $\lambda_0^f$ .

#### 4.6.2 A Time Domain Method for Model Validation

We shall now describe a time domain model validation method. This is useful both for establishing that  $G_0$  should be rejected (that is, as a flag for re-identification) as well as for validating a new model,  $G_1$ , replacing  $G_0$ .

Referring to Figure 4.3 and equation (4.10), we notice that  $e_\beta = L\xi_1$  when  $\hat{\Psi}_0^f = 1$ , where  $e_\beta$  is the prediction error (also known as the residual). We also observe from equation (4.14) that  $G_1 = G_0$  when  $\tilde{R}_0^f = 0$ , and from equation (4.11) that  $\xi_1 = \xi_0^f$  when  $G_1 = G_0$ . Therefore we have  $e_\beta = L\xi_0^f$  when  $\hat{\Psi}_0^f = 1$  and  $\tilde{R}_0^f = 0$ . This suggests that  $G_0$  should be rejected if the cross-correlation of the prediction error  $e_\beta$  with the future values of "input"  $\bar{\alpha}$  exceed its  $(3\sigma)$  confidence limits when  $\hat{\Psi}_0^f = 1$  and  $\tilde{R}_0^f = 0$ . This reasoning is independent of the true  $\Psi_0^f$ . See [Ljung 1987] and [Ljung 1988] for more details of model validation by residual analysis. (Actually it is also easy to apply the same method to validate a pair of newly identified  $\tilde{R}_0^f$  and  $\hat{\Psi}_0^f$  before  $\tilde{R}_0^f$  is used to calculate  $G_1$ . We simply check that the auto-correlation function of  $e_\beta$  for non-zero delays as well as the cross-correlation of  $e_\beta$  with the future values of  $\bar{\alpha}$  are within their respective confidence intervals.)

### 4.6.3 Identification of A Better Model

The methods of model validation described in Sections 4.6.1 and 4.6.2 were compared critically through many simulation studies. (An example of these simulations will be presented in Section 4.8.) The main observations from these simulations are:

- Correlation function estimates and power spectrum estimates are both useful for model validation where the goodness of fit is based on a closed-loop control criterion.
- Correlation function estimates are more sensitive than power spectrum estimates in the sense that the former tend to invalidate a model before identifying a better model is necessary and possible. This *does not imply* that the correlation method is useless. On the contrary, it suggests that the correlation method is useful for detecting incipient model errors.
- Power spectrum estimates not only suggest when a model becomes inadequate but they also indicate the frequency range in which the signal-to-noise ratio is high for identification.
- It was shown in Section 4.5 that a closed-loop system designed on the basis of models with unstable zeros within the closed-loop bandwidth may result in a poor signal-to-noise ratio for system identification when the closed-loop output error  $\xi_0^f$  becomes large. This may impose limitations on the achievable accuracy in closed-loop system identification. (Recall the effect of the unstable zeros dependent factor discussed in Remark 4.5.1.)

On the other hand, consideration of the equation

$$\xi_0^f = (T_0^f - \bar{T}_0^f)r + \frac{1}{1 + GK_0^f}He$$

reveals that, for a given closed-loop modelling error  $T_0^f - \bar{T}_0^f$ , the closed-loop output error  $\xi_0^f$  can also become large from the contribution of the noise disturbance if the plant  $G$  has unstable zeros within the closed-loop bandwidth. This again may result in a poor signal-to-noise ratio for system identification.

In general, we do not know a priori whether  $G$  has unstable zeros within the closed-loop bandwidth. We can only attempt to deduce this information from the

zeros of the identified models. Specifically, let  $\omega_z$  be the minimum critical frequency corresponding to the unstable zeros of  $G_0$ , simulation experience confirmed that it may be difficult to identify a model better than  $G_0$  if  $\lambda_0^f \geq \omega_z/2$ . It should be remarked that this is reminiscent of design tradeoffs discussed in [Freudenberg and Looze 1985].

- In general we should update  $G_0$  if
  1. both methods of model validation suggest that it is necessary to do so, and
  2.  $\lambda_0^f < \omega_z/2$ , where  $\omega_z$  is the minimum critical frequency corresponding to the unstable zeros of  $G_0$ .

We are now ready to suggest a procedure for identifying a better model. Note that in the frequency range where the current model  $G_0$  has significant modelling errors, the signal-to-noise ratio of the closed-loop output error can be increased by increasing the magnitude of the reference input or by increasing the designed closed-loop bandwidth. If practical operation constraints do not allow the magnitude of the reference input to be increased, then the signal-to-noise ratio of the closed-loop output error can only be increased by increasing the designed closed-loop bandwidth. This, however, has the potential danger of causing instability in the actual closed-loop system if the designed closed-loop bandwidth is increased excessively. To avoid this danger, we shall proceed as follows:

1. Reduce the rate of increasing the designed closed-loop bandwidth  $\lambda_0$  once the correlation method for model validation has invalidated  $G_0$ .
2. Attempt to identify  $R_0^f$  (when  $\lambda_0 = \lambda_0^f$ ) as soon as the power spectrum method for model validation suggests that  $\xi_0^f$  has a sufficiently high signal-to-noise ratio, provided that  $\lambda_0^f < \omega_z/2$ , where  $\omega_z$  is the minimum critical frequency corresponding to the unstable zeros of  $G_0$ .
  - (a) Use the collected data to identify a set of models by experimenting with the likely model structures. Perform model verification on each of these models.
  - (b) If an identified model is found to be sufficiently accurate, accept it for the next stage of control design. Otherwise, increase the designed closed-loop bandwidth slightly, collect a new set of measurements and repeat the procedures of model estimation and verification.

- (c) Repeat the last two steps until a sufficiently accurate model is obtained and verified.
3. Terminate the iterative identification and control design procedure if  $\lambda_0^f \geq \omega_z/2$  and  $\xi_0^f$ , although unacceptably large, does not facilitate the identification of a better model.

## 4.7 Robust Performance Improvement

Now we know what can be identified and how an identified model can be validated. We have also indicated in Section 4.3 what we would like to identify. It is therefore logical to ask:

---

*How does the object which we CAN identify relate to the object which we WOULD LIKE to identify?*

---

The answer is that the objects are virtually the same, although it is not obvious. What we can identify is couched in terms of  $R_0^f$ , and what we would like to identify is couched in terms of  $G_1$ . We need to connect these characterizations. In this section we shall show that provided that certain conditions are satisfied, the controller designed on the basis of the model  $G_1$  updated through an estimate of  $\hat{R}_0^f$  can improve the performance robustness of the system.

Recall from equation (4.18) that just before we attempt to update the model  $G_0$  through identifying  $R_0^f$ , it is necessary that

$$|\tilde{T}_0^f(j\omega)|^2 \Phi_r(\omega) > \mu |1 - T_0^f(j\omega)| H(j\omega)|^2 \Phi_e(\omega), \quad \text{for } \omega_1 \leq \omega \leq \omega_2$$

for a sufficiently large  $\mu > 0$ . Furthermore it is also necessary that  $|\tilde{T}_0^f(j\omega)|$  in the above inequality is mainly contributed by the phase insensitive factor before an accurate estimate of  $R_0^f$  can be obtained. This implies that in order to improve the robust performance through

identification and re-design, it is necessary that the phase insensitive factor (which is also the designed complementary-sensitivity-function weighted multiplicative modelling error) associated with the updated model  $G_1$  and the re-designed controller  $K_1^0$  (while keeping  $\lambda_1^0 = \lambda_0^f$ ) be small in the frequency range  $[\omega_1, \omega_2]$ . Hence it is relevant to consider the magnitude of the ratio

$$\frac{\frac{G-G_1}{G_1} \bar{T}_1^0}{\frac{G-G_0}{G_0} \bar{T}_0^f}$$

in the frequency range  $[\omega_1, \omega_2]$ .

Before the main results are presented in Theorems 4.7.2 and 4.7.3, we shall state a result (which follows directly from the remarks for stable plant after Theorem 3.3.1) that is relevant to the choice of the relative degree of  $\hat{R}_0^f$ , and establish two lemmas that will be used in the proof of Theorem 4.7.2.

**Theorem 4.7.1** *Let the controller  $K_0^f$  and the proper stable transfer function  $Q_0^f$  designed by the IMC method described in Section 4.2, then the relative degree of*

$$R_0^f = \frac{G - G_0}{1 + Q_0^f (G - G_0)}$$

is given by

$$\text{rel deg}\{R_0^f\} = \min(\text{rel deg}\{G\}, \text{rel deg}\{G_0\}) .$$

**Remark 4.7.1** The relative degree of the strictly proper plant  $G$  is usually unknown. It is therefore necessary to allow, in the identification of  $R_0^f$ , the relative degree of  $\hat{R}_0^f$  to take the smallest possible value of one.

It is easy to establish the following:

**Lemma 4.7.1** *Suppose that  $G_0$  has relative degree  $n \geq 1$ , and  $Q_0^f = [G_0]_m^{-1} F_0^f$ , where  $[G_0]_m$  is the minimum phase factor of  $G_0$ , and*

$$F_0^f = \left( \frac{\lambda_0^f}{s + \lambda_0^f} \right)^{n+1}, \quad \lambda_0^f > 0 .$$

Let  $\widehat{R}_0^f$  have relative degree  $q \geq 1$  and let  $G_1$  be updated according to

$$G_1 = G_0 + \frac{\widehat{R}_0^f}{1 - Q_0^f \widehat{R}_0^f},$$

then

1.  $G_1$  has a relative degree  $k$ , where

$$\begin{aligned} k &\geq n; && \text{if } q = n, \text{ and} \\ k &= \min(n, q); && \text{otherwise,} \end{aligned}$$

2. by using the IMC filter

$$F_1^0 = \left( \frac{\lambda_0^f}{s + \lambda_0^f} \right)^{k+1}; \quad \lambda_0^f > 0,$$

$Q_1^0 = [G_1]_m^{-1} F_1^0$  will have the same relative degree as  $Q_0^f$ ,

3. if, in addition to the above conditions,  $G_1$  has no zeros on the imaginary axis and  $G_0$  has no poles on the imaginary axis, then  $Q_1^0/Q_0^f$  is bounded on the imaginary axis. In particular, there exists a finite  $\delta$  such that

$$\sup_{\omega_1 \leq \omega \leq \omega_2} \left| \frac{Q_1^0(j\omega)}{Q_0^f(j\omega)} \right| = \delta$$

**Remark 4.7.2** Result 1 in Lemma 4.7.1 indicates that we have some control over the relative degree of  $G_1$  through choosing the relative degree of  $\widehat{R}_0^f$  in identification.

**Remark 4.7.3** Although Lemma 4.7.1 is stated for the case where  $Q_0^f$  and  $Q_1^0$  have relative degree one, it can be seen easily that similar results for cases where  $Q_0^f$  and  $Q_1^0$  are bi-proper, or have relative degree larger than one, can be established.

**Remark 4.7.4** It will be clear from Theorem 4.7.2 that it is undesirable for  $\delta$  to become excessively large.

**Remark 4.7.5** Since all poles of  $G_0$  that are also poles of  $G$  are always retained by a well identified  $G_1$ , it is clear that poles of  $G_0$  that are also poles of  $G$ , even if they are near the imaginary axis, will not cause  $\delta$  to assume excessively large value.

**Remark 4.7.6** Zeros of  $G_1$  near the imaginary axis for  $\omega_1 \leq \omega \leq \omega_2$  may not appear as zeros of  $G_0$ . However these zeros would be zeros of the plant  $G$  if  $G_1$  is a well identified model of  $G$  for  $\omega_1 \leq \omega \leq \omega_2$ . This would happen only if we increase the closed-loop bandwidth to the frequency range where the plant has (stable or unstable) zeros near the imaginary axis; and the controller has *excessively large* gain. Therefore we can prevent  $\delta$  from being excessively large by observing well known design guidelines.

**Remark 4.7.7** If  $G_0$  has poles near to the imaginary axis for  $\omega_1 \leq \omega \leq \omega_2$  which are not poles of the plant  $G$ , then a well identified model  $G_1$  for  $G$  will either have no poles at these locations or will have approximate pole zero cancellations at these locations. In these situations,  $\delta$  may become excessively large. It is therefore *important to verify* that an identified model (such as  $G_0$ ) has no unnecessary poles near the imaginary axis.

**Lemma 4.7.2** If  $G_0$  and  $G_1$  are stable strictly proper models of the plant  $G$ , and  $\bar{T}_0^f = G_0 Q_0^f$  is the closed-loop transfer function, where  $Q_0^f$  is designed by the IMC method, then there exist a finite  $\eta$  such that

$$\sup_{\omega_1 \leq \omega \leq \omega_2} \left| \left[ \frac{G_1(j\omega) - G_0(j\omega)}{G_0(j\omega)} \right] \bar{T}_0^f(j\omega) \right| = \eta .$$

### Proof

Clearly the transfer function  $G_1 - G_0$  is proper and stable. Also from the facts that  $\bar{T}_0^f = G_0 Q_0^f$ , and the  $Q_0^f$  designed by the IMC method is proper and stable, it is easy to conclude that

$$\left( \frac{G_1 - G_0}{G_0} \right) \bar{T}_0^f = (G_1 - G_0) Q_0^f$$

is proper and stable. Hence

$$\left( \frac{G_1 - G_0}{G_0} \right) \bar{T}_0^f$$

is bounded on the imaginary axis and there exist a finite  $\eta$  such that

$$\sup_{\omega_1 \leq \omega \leq \omega_2} \left| \left[ \frac{G_1(j\omega) - G_0(j\omega)}{G_0(j\omega)} \right] \bar{T}_0^f(j\omega) \right| = \eta .$$

□



**Remark 4.7.8** It will be clear from Theorem 4.7.2 that it is undesirable for  $\eta$  to become excessively large.

**Remark 4.7.9**  $\eta$  may become excessively large if  $G_1$  has poles near the imaginary axis for  $\omega_1 \leq \omega \leq \omega_2$  which are not poles of  $G_0$ , and if  $\lambda_0^f$  is very near to the critical frequencies of these poles. However this is impossible because if  $G_1$  is a well identified model of the plant  $G$ , then  $G$  would have poles near to  $\pm j\lambda_0^f$  which are not poles of  $G_0$ . Under these conditions, the actual closed-loop system  $T_0^f$  would be unstable or almost unstable. Furthermore,  $\lambda_0^f$  cannot be close to the zeros of  $G_0$  near the imaginary axis for  $\omega_1 \leq \omega \leq \omega_2$  because this will result in a controller with an excessively large gain in that frequency range. Hence by ensuring that the actual closed-loop system  $T_0^f$  is far from instability (recall the guidelines given at the end of Section 4.6.3) and by observing well known controller design guidelines, we automatically prevent  $\eta$  from taking excessively large values.

**Theorem 4.7.2** *Let  $G_0$  be a stable strictly proper model for the plant  $G$ . Suppose that  $G$  is stabilized by the controller  $K_0^f$  designed according to the IMC method described in Section 4.2 and hence has the description*

$$G = G_0 + \frac{R_0^f}{1 - Q_0^f R_0^f} \quad (4.21)$$

where

$$Q_0^f = [G_0]_m^{-1} F_0^f \quad (4.22)$$

and

$$[G_0]_m = \text{minimum-phase factor of } G_0.$$

Let  $G_1$  be a stable strictly proper model for  $G$  updated according to

$$G_1 = G_0 + \frac{\hat{R}_0^f}{1 - Q_0^f \hat{R}_0^f} \quad (4.23)$$

where  $\hat{R}_0^f$  is an estimate of  $R_0^f$ .

Suppose that

1.  $K_1^0$  is designed according to the IMC method with  $\lambda_1^0 = \lambda_0^f$ , and

2. conditions set out in Lemma 4.7.1 is satisfied,

then, for each  $\omega$  in  $[\omega_1, \omega_2]$  such that  $R_0^f(j\omega) \neq 0$ ,

$$\frac{\left| \left[ \frac{G(j\omega) - G_1(j\omega)}{G_1(j\omega)} \right] \bar{T}_1^0(j\omega) \right|^2}{\left| \left[ \frac{G(j\omega) - G_0(j\omega)}{G_0(j\omega)} \right] \bar{T}_0^f(j\omega) \right|^2} < \delta^2 (1 + \eta)^2 \left| \frac{\hat{R}_0^f(j\omega) - R_0^f(j\omega)}{R_0^f(j\omega)} \right|^2$$

where

$$\delta = \sup_{\omega_1 \leq \omega \leq \omega_2} \left| \frac{Q_1^0(j\omega)}{Q_0^f(j\omega)} \right|.$$

### Proof

See Appendix F. □

From Theorem 4.7.2 we observe immediately that if

$$\left| \frac{\hat{R}_0^f - R_0^f}{R_0^f} \right|^2 \ll \frac{1}{\delta^2 (1 + \eta)^2}$$

in the frequency range  $[\omega_1, \omega_2]$ , then the phase insensitive factor associated with  $G_1$  and  $\bar{T}_1^0$  will be much smaller in magnitude than that associated with  $G_0$  and  $\bar{T}_0^f$  in the same frequency range. We shall now prove a stronger result.

**Theorem 4.7.3** Assume that

$$\left| \frac{\hat{R}_0^f(j\omega) - R_0^f(j\omega)}{R_0^f(j\omega)} \right|^2 \ll \frac{1}{\delta^2 (1 + \eta)^2} \left| \left[ \frac{G(j\omega) - G_0(j\omega)}{G_0(j\omega)} \right] \bar{T}_0^f(j\omega) \right|^{-2}$$

for  $\omega_1 \leq \omega \leq \omega_2$ , then the tracking error  $v_1^0$  resulting from  $T_1^0$  (with  $\lambda_1^0 = \lambda_0^f$ ) designed on the basis of

$$G_1 = G_0 + \frac{\hat{R}_0^f}{1 - Q_0^f \hat{R}_0^f}$$

has a power spectrum approximately given by

$$\Phi_{v_1^0}(\omega) \approx \left| \left[ \frac{G(j\omega) - G_1(j\omega)}{G_1(j\omega)} \right] \bar{T}_1^0(j\omega) \right|^2 \left| 1 - \bar{T}_1^0(j\omega) \right|^2 \Phi_r(\omega)$$

for  $\omega_1 \leq \omega \leq \omega_2$ .

**Proof**

See Appendix G. □

Theorems 4.7.2 and 4.7.3 together show that if the phase insensitive factor associated with  $G_0^f$  and  $\bar{T}_0^f$  was the main reason for poor robust performance, then the pair  $G_1$  and  $\bar{T}_1^0$ , with a much smaller magnitude of phase insensitive factor, will attain a much better robust performance if  $G_1$  has no unstable zeros in the pass band of  $\bar{T}_1^0$ . We therefore have the following conclusion, which should be read in conjunction with conclusions C7 and C9:

---

**C10** *If a practically unbiased estimate  $\hat{R}_0^f$  for  $R_0^f$  with a sufficiently small normalized variance can be obtained over the frequency range  $\omega_1 \leq \omega \leq \omega_2$ , with  $\hat{R}_0^f$  and  $G_1$  satisfying the constraints stated in Lemmas 4.7.1 and 4.7.2, then it is possible to achieve robust performance improvement through controller re-design if the unstable zeros of  $G_1$  are outside the designed closed-loop passband.*

---

## 4.8 Simulation Results

In this section, we first outline the iterative identification and design algorithm which incorporates the model validations steps that we have discussed. We then show by a simulation example that, through the iterative identification and control design approach, it is possible to increase the bandwidth of a closed-loop system to its fundamental limits imposed by the unstable zeros of the plant, despite that the initial model has significant modelling errors in the high frequency region. In the process, we illustrate how the methods and procedure recommended in Section 4.6 can be applied.

The modified iterative algorithm is as follows:

**Step 1:**

Set  $G_i = G_0$ , where  $G_0$  is the transfer function of an initial stable model of the stable plant.

**Step 2:**

Factorize  $G_i$  as  $G_i = [G_i]_m [G_i]_a$ , where  $[G_i]_m$  is the minimum-phase factor of  $G_i$  with a relative degree  $n$ , and  $[G_i]_a$  is the all pass factor of  $G_i$ .

**Step 3:**

For  $j = 0$ , find  $K_i^j = Q_i^j / (1 - G_i Q_i^j)$ , with  $Q_i^j = [G_i]_m^{-1} F_i^j$ , where the parameter  $\lambda_i^j$  in the transfer function

$$F_i^j = \left( \frac{\lambda_i^j}{s + \lambda_i^j} \right)^{n+1}$$

is chosen such that the closed-loop system has robust stability.

**Step 4:**

Perform model validation on the existing model by the time domain method (with  $\tilde{R}_i^f = 0$  and  $\hat{\Psi}_i^f = 1$ ) and the frequency domain method. If the existing model is validated by both model validation methods, the closed-loop system has robust performance. Stop here if the closed-loop system also meets the specified bandwidth. Otherwise, proceed to the next step.

**Step 5:**

Let  $j = j + 1$  and set  $\lambda_i^j = \lambda_i^{j-1} + \epsilon$  for small  $\epsilon > 0$ , and re-design the controller  $K_i^j$  using the equations given in **Step 3**. Then do one of the following:

1. Stop here if the design produces a closed-loop system that has robust performance with the specified bandwidth.
2. (a) Repeat **Step 5** if the closed-loop system has robust performance (by model validation tests) but  $\lambda_i^j$  is smaller than the specified bandwidth.  
 (b) Repeat **Step 5** with a smaller  $\epsilon$  and monitor the result of the frequency domain model validation test carefully if the closed-loop system fails the time domain model validation test but passes the frequency domain model validation test.
3. Proceed to the next step if the closed-loop system fails both model validation methods. Hopefully, the signal-to-noise ratio associated with the closed-loop output error is sufficiently large at this stage for securing a better model. We assume that at this stage  $j = f$ .

### Step 6:

Perform frequency weighted open-loop system identification to obtain  $\hat{R}_i^f$  and  $\hat{\Psi}_i^f$ . For this purpose, we apply the prediction error method with the Box-Jenkins model structure as it was described towards the end of Section 4.4.1. The objective is to obtain the estimates  $\check{R}_i^f$  and  $\check{\Psi}_i^f$ , where  $\check{R}_i^f$  and  $\check{\Psi}_i^f$  satisfy  $\bar{\beta} = \check{R}_i^f \bar{\alpha} + \Psi_i^f e$ . (Note that the identification of  $\check{R}_i^f$  and  $\check{\Psi}_i^f$  includes validating the estimated  $\hat{R}_i^f$  and  $\hat{\Psi}_i^f$  by the time domain model validation method.) This depends on using the signals

$$\bar{\alpha} = L(1 - \bar{T}_i^f) \frac{(\lambda_i^f)^{n+1}}{s + \lambda_i^f} r ,$$

and

$$\bar{\beta} = L(1 - \bar{T}_i^f)(y_i^f - G_i u_i^f) ,$$

where  $L$  is an appropriate data filter. (We actually used discrete-time samples of  $\bar{\beta}$  and  $\bar{\alpha}$  and experiments with the Box-Jenkins algorithm to construct a strictly causal estimate for  $\check{R}_i^f$ ).

**Step 7:**

After converting the validated  $\tilde{R}_i^f$  to a continuous-time strictly proper  $\tilde{R}_i^f$  (using one of the discrete-time to continuous-time model conversion methods given in well known system identification tool boxes, like for example the System Identification Toolbox of *MATLAB*<sup>TM</sup>), we update the model via

$$G_{i+1} = G_i + \frac{(s + \lambda_i^f)^{n+1} [G_i]_m \tilde{R}_i^f}{(s + \lambda_i^f) - (\lambda_i^f)^{n+1} \tilde{R}_i^f}.$$

Then do one of the following:

1. If  $G_{i+1}$  is stable, and if it passes the frequency domain model validation test<sup>2</sup>, find the reduced order model

$$\hat{G}_{i+1} = \arg \min_{\eta} \left\| \frac{K_i^f (G_{i+1} - \eta)}{(1 + G_{i+1} K_i^f)^2} \right\|_{\infty}.$$

The order of  $\hat{G}_{i+1}$  is to be chosen such that  $\hat{G}_{i+1}$  also passes the frequency domain model validation test.

2. If  $G_{i+1}$  is unstable, or if  $G_{i+1}$  fails the frequency domain model validation test, it may be necessary to increase  $\lambda_i^f$  slightly (so that the closed-loop output error's signal-to-noise ratio may improve through further performance robustness deterioration), collect a new set of data and return to **Step 6**, or to terminate the iterative process prematurely.

*Specific guidelines for carrying out Step 5 to Step 7 are given at the end of Section 4.6.3.*

**Step 8:**

Set  $G_i = \hat{G}_{i+1}$  and return to **Step 2**.

---

<sup>2</sup>Sometimes  $\tilde{R}_i^f$  may have passed the time domain model validation test marginally. To be cautious, we usually perform the frequency model validation test on  $G_{i+1}$  after it is computed from  $\tilde{R}_i^f$ .

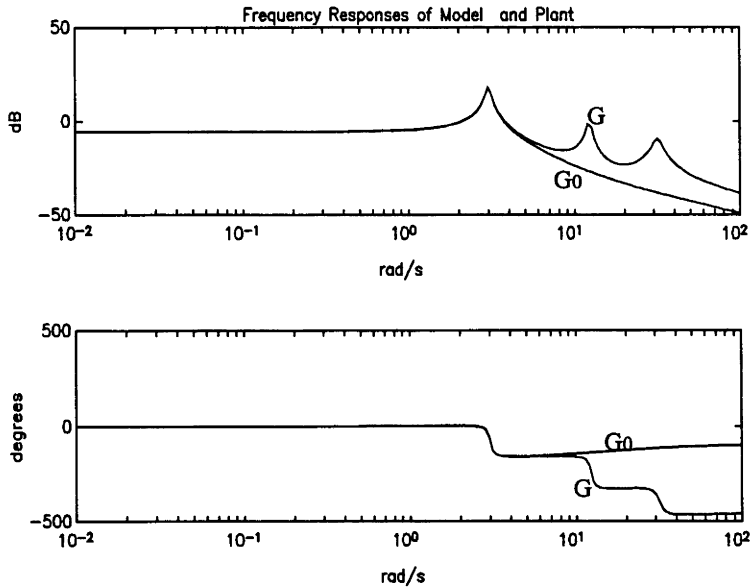


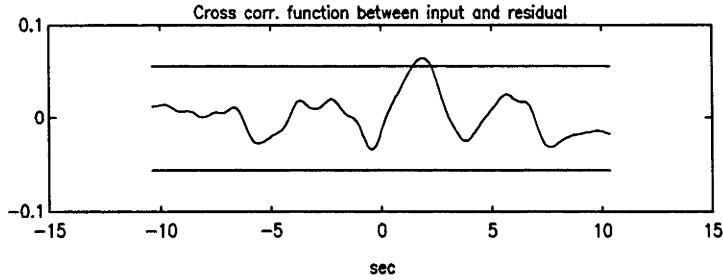
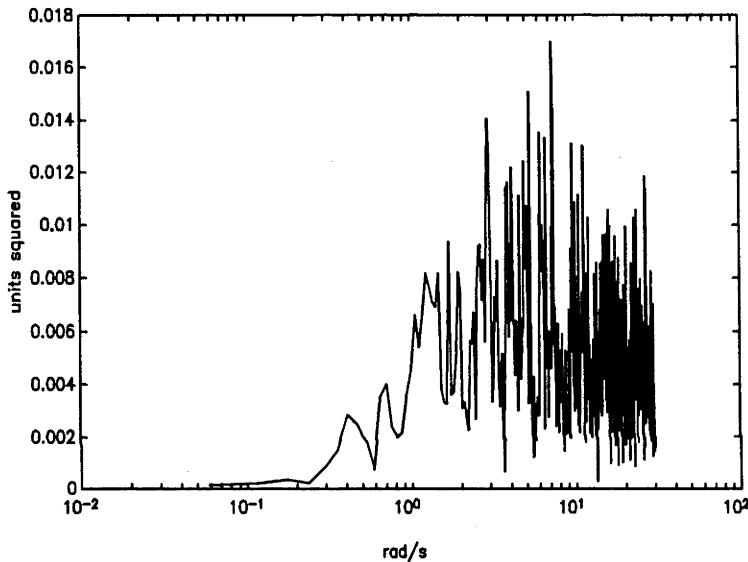
Figure 4.5: Frequency response of model  $G_0$

### Example

In the following, the plant involved is a simulated flexible link robot arm (only one of the degrees of freedom for the robot arm is considered here) whose transfer function  $G$  has poles at  $-0.0996 \pm j3.0017$ ,  $-0.3339 \pm j12.131$ ,  $-1.845 \pm j31.481$ , zeros at  $s = -13.162$ ,  $-10.646 \pm j12.27$ ,  $s = 7.169 \pm j11.54$ , and  $G(0) = 0.5196$ .

The initial model  $G_0$  is an open-loop description of  $G$  up to and including its first resonant frequency (see Figure 4.5).  $G_0$  has a pair of poles at  $-0.0903 \pm j3.0027$ , a zero at  $s = -13.31$ , and  $G_0(0) = 0.5188$ . We would like to achieve, by iterative identification and control design, a closed-loop system with a bandwidth that is as large as possible and has approximately unity gain in the passband.

We start by designing controllers (using the IMC method) on the basis of  $G_0$  such the designed closed-loop bandwidth is increased progressively. Performance robustness of the closed-loop system is monitored carefully while the designed closed-loop bandwidth increases. When the designed closed-loop bandwidth is increased to 1.5 rad/s, the method of correlations (see Figure 4.6) shows that  $G_0$  is not a good model of  $G$  whereas the method of power spectra (compare Figure 4.7 and Figure 4.8) shows that the tracking error is still insignificant. In fact, we are unable to identify a better model than  $G_0$  at this stage. This

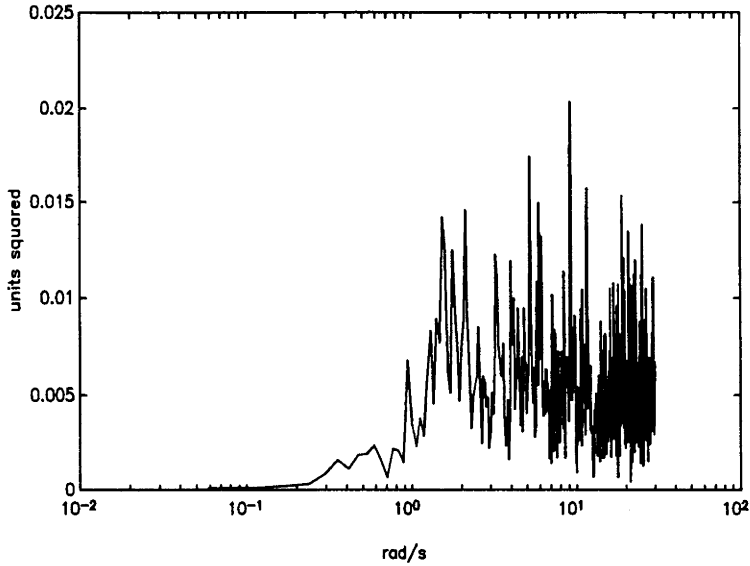
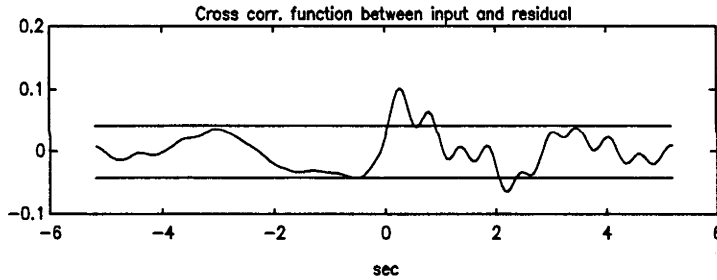
Figure 4.6: Validating  $G_0$  ( $\lambda_0 = 1.5$  rad/s)Figure 4.7:  $\Phi_w(\omega)$  when  $\lambda_0$  is 1.5 rad/s

is not surprising because, although we have a large number (4000 pairs) of input-output data, comparison of Figure 4.7 (power spectrum of noise disturbance) and Figure 4.8 (power spectrum of signal plus noise disturbance) indicates that the signal-to-noise ratio of the closed-loop output error is negligible<sup>3</sup>. However, as it was suggested at the end of Section 4.6.3, the rate of increasing the designed closed-loop bandwidth is reduced at this stage.

When the designed closed-loop bandwidth has reached 3 rad/s, the method of correlations (see Figure 4.9) and the method of power spectra (compare Figure 4.10 and Figure 4.11) both indicate that  $G_0$  is not a good model. In particular, comparison of Figure 4.10 and Figure 4.11 indicates that the closed-loop output error has a high signal-to-noise ratio at around 12 rad/s.

<sup>3</sup>Recall from conclusion C7 that we have to pay a price, in terms of deterioration in robust performance, for a high signal-to-noise ratio in the closed-loop output error

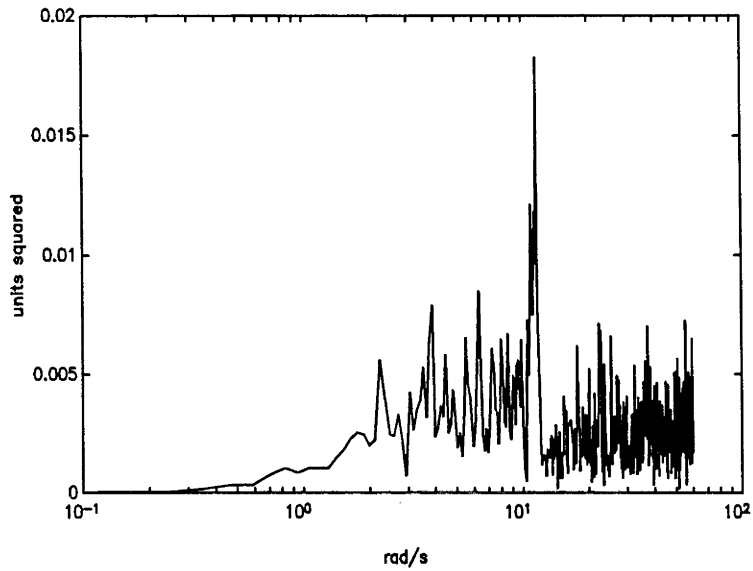
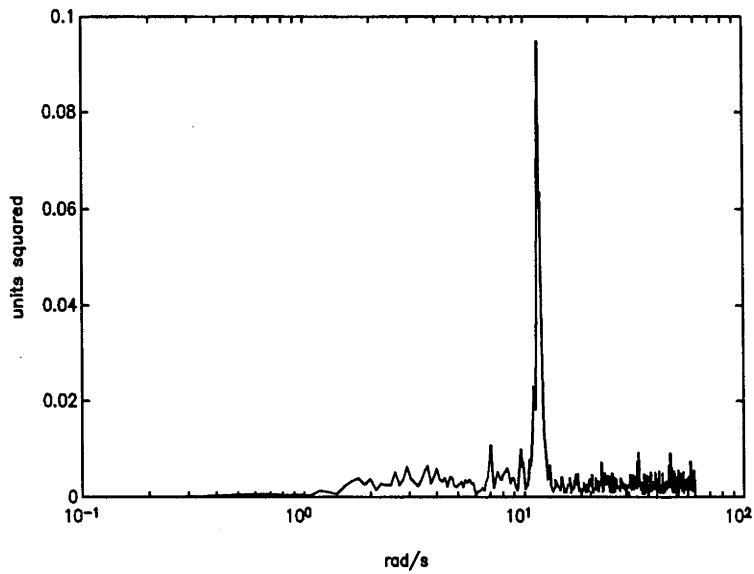


Figure 4.8:  $\Phi_\xi(\omega)$  when  $\lambda_0$  is 1.5 rad/sFigure 4.9: Validating  $G_0$  ( $\lambda_0^f = 3$  rad/s)

To identify  $\tilde{R}_0^f$ , we use Box-Jenkins method instead of output error method because we now have methods for model validation and hence can take advantage of the more general noise model in Box-Jenkins method. We use a low-pass data filter with a bandwidth of 12/,rad/s. A fourth order model structure for  $\tilde{R}_0^f$  and a fifth order noise model structure for  $\hat{\Psi}_0^f$  are selected by setting  $Nn = [4\ 5\ 5\ 4\ 1]$ . The identified  $\tilde{R}_0^f$  and  $\hat{\Psi}_0^f$  are validated by the method of correlations (see Figure 4.12) before  $\tilde{R}_0^f$  is used to update the model. The results are

$$\tilde{R}_0^f = \left( \begin{array}{c} 3.5508s^3 - 10.4014s^2 \\ -440.1311 + 198.1459 \end{array} \right) / \left( \begin{array}{c} s^4 + 8.5368s^3 + 1120.6515s^2 \\ +1586.672s + 133700.08 \end{array} \right),$$

$$\hat{R}_0^f = \left( \begin{array}{c} 1.249s^5 + 16.7129s^4 \\ -164.619s^3 - 2601.482s^2 \\ +5045.107s + 2783.073 \end{array} \right) / \left( \begin{array}{c} s^6 + 8.7174s^5 + 1131.217s^4 \\ +1866.101s^3 + 144099.841s^2 \\ +38465s + 1206563 \end{array} \right),$$

Figure 4.10:  $\Phi_w(\omega)$  when  $\lambda_0^f$  is 3 rad/sFigure 4.11:  $\Phi_\xi(\omega)$  when  $\lambda_0^f$  is 3 rad/s

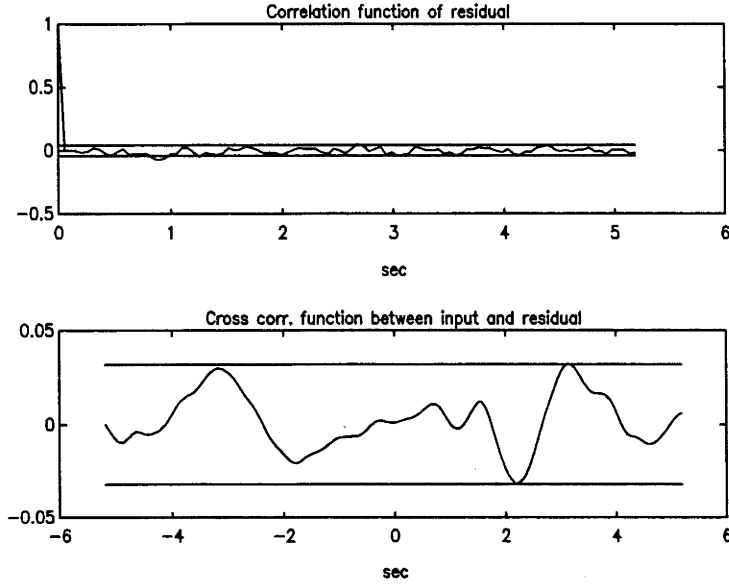


Figure 4.12: Validating  $\hat{R}_0^f$  and  $\hat{\Psi}_0^f$  ( $\lambda_0^f = 3$  rad/s)

and

$$G_1 = \left( \begin{array}{c} 1.6007s^6 + 29.2s^5 + 331.5s^4 \\ +3895.31s^3 + 60854.9s^2 \\ +794905.8s + 1877894.7 \end{array} \right) / \left( \begin{array}{c} s^7 + 11.72s^6 + 1125.41s^5 \\ 5347.59s^4 + 153387.8s^3 \\ +470541.4s^2 + 1357383.2s \\ +36035.7 \end{array} \right)$$

After performing frequency weighted model reduction, we obtain

$$\hat{G}_1 = \left( \begin{array}{c} 1.6008s^5 + 24.534s^4 \\ +259.96s^3 + 3137.56s^2 \\ +51707.2s + 644176.2 \end{array} \right) / \left( \begin{array}{c} s^6 + 8.8023s^5 + 1099.75s^4 \\ +2141.62s^3 + 147144.93s^2 \\ +41588.11s + 1236149.5 \end{array} \right)$$

After the resulting  $\hat{G}_1$  is validated by the method of power spectra (compare Figure 4.13 and Figure 4.10), we set  $G_1 = \hat{G}_1$  before the iteration is continued. This  $G_1$  has poles at  $s = -0.0903 \pm j3.0027$ ,  $-0.3836 \pm j12.08$ ,  $-3.9272 \pm j30.36$ , zeros at  $-13.31$ ,  $-7.809 \pm j10.94$ ,  $6.801 \pm j11.003$ , and  $G_1(0) = 0.5211$ . Figure 4.14 shows the frequency response of  $G_1$ . Using  $G_1$ , it is possible to increase the designed closed-loop bandwidth to 12 rad/s before it is necessary to identify a better model. At this stage, the method of correlations (see Figure 4.15) and the method of power spectra (compare Figure 4.16 and Figure 4.17) both indicate that  $G_1$  is not a good model. At this stage, the iterative identification and control design process has to be terminated because we are unable to identify a better model despite considerable efforts and numerous attempts.

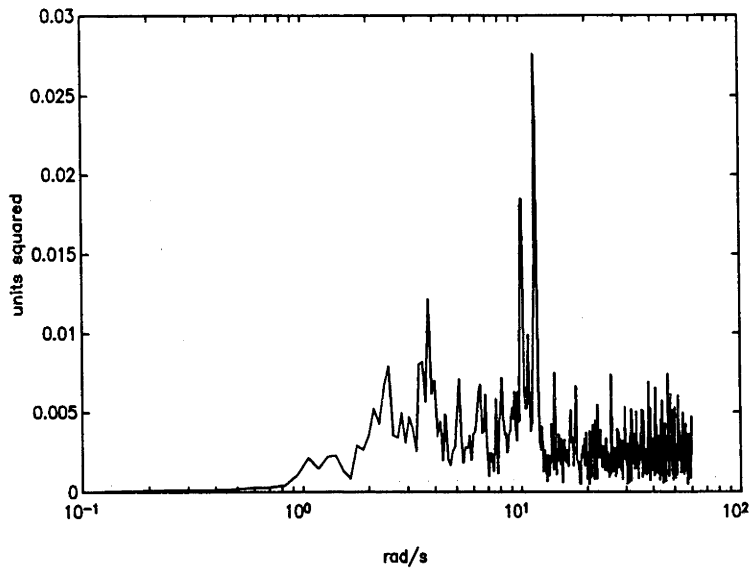


Figure 4.13:  $\Phi_{\xi_1}(\omega)$  when  $\lambda_0^f$  is 3 rad/s

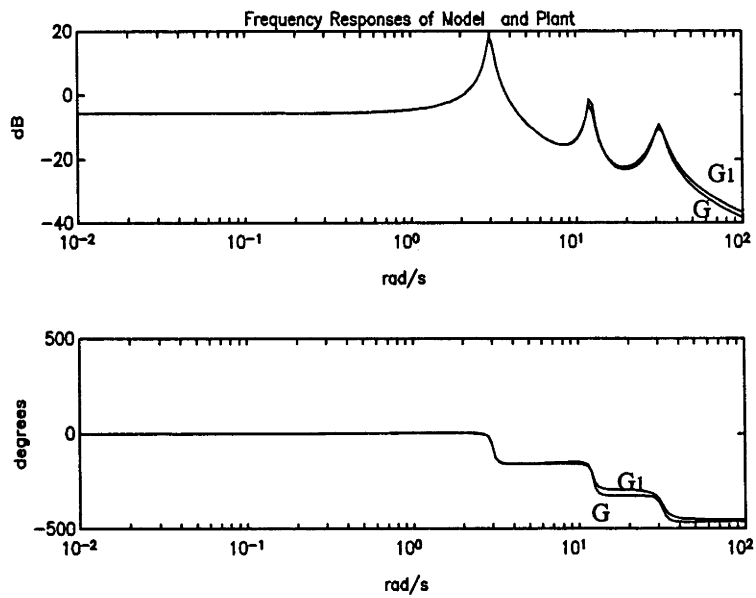


Figure 4.14: Frequency response of model  $G_1$

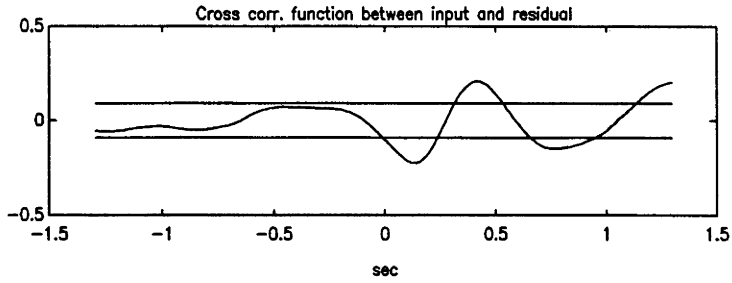


Figure 4.15: Validating  $G_1$  ( $\lambda_1^f = 12$  rad/s)

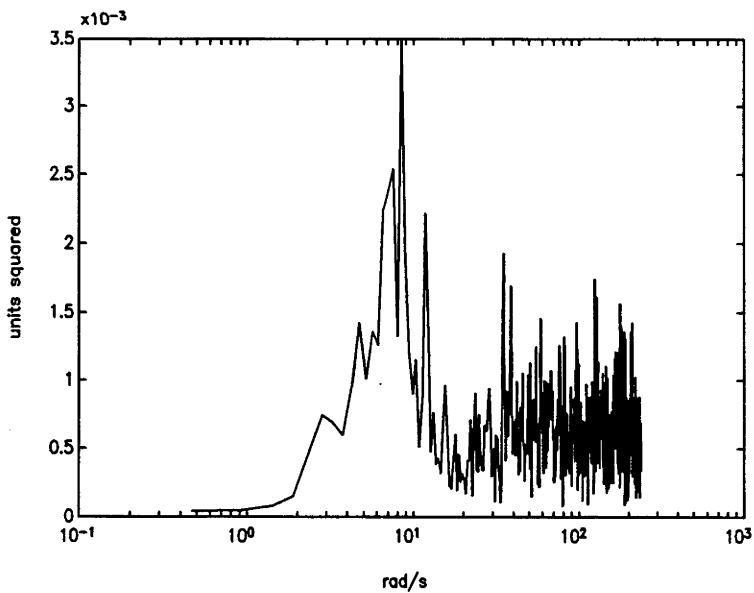


Figure 4.16:  $\Phi_w(\omega)$  when  $\lambda_1^f$  is 12 rad/s

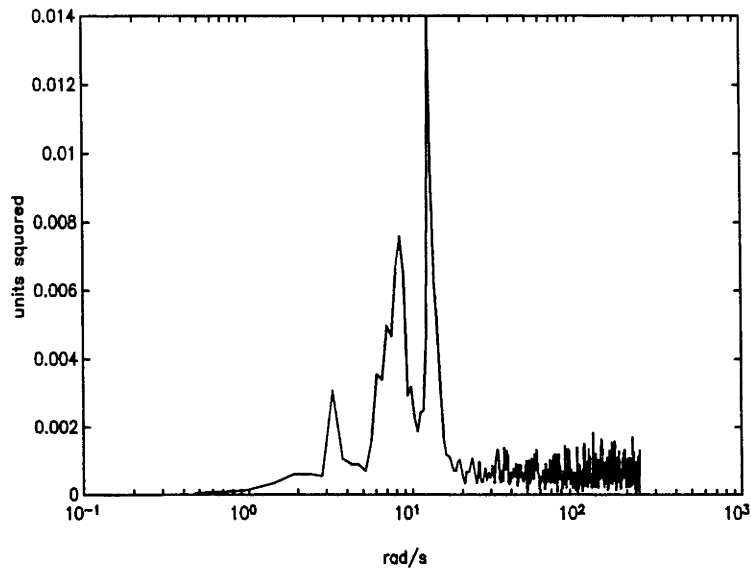


Figure 4.17:  $\Phi_\xi(\omega)$  when  $\lambda_1^f$  is 12 rad/s

**Remark 4.8.1** Notice that the designed closed-loop bandwidth (12 rad/s) is close to the critical frequency corresponding to the *unstable zeros* of  $G_1$  (at  $s = 9.098 \pm j12.07$ ) and  $G$  (at  $s = 7.169 \pm j11.54$ ). From the view point of control design, it follows from [Freudenberg and Looze 1985] that, due to the unstable zeros of  $G_1$  and  $G$ , *both* the designed and the actual closed-loop systems have reached their fundamental performance limitations (hence it is *not* a premature termination of iteration). This simulation example clearly demonstrated that, for this iterative identification and control design methodology, good control performance and good identified models go hand in hand.

## 4.9 Summary

We have examined in this chapter a number of crucial questions which arise in the iterative identification and control design approach for the case of stable plants with no zeros on the imaginary axis. Among the issues that we have clarified are:

- When can one re-design the controller and expand the closed-loop bandwidth, without re-identifying?

- When should one re-identify?
- What does one want to identify in the re-identification procedure?
- What can one identify in the re-identification procedure?

In order to check whether an identified model is actually good for our purpose, we have presented two methods for validating an identified model experimentally before it is employed in controller re-design.

The main conclusion of this chapter is that, given a stable strictly proper model of a stable strictly proper plant, it is possible to improve the robust performance of a closed-loop system through the iterative identification and control design approach if

- the deterioration in performance robustness caused by increasing the closed-loop bandwidth is mainly contributed by the phase insensitive factor,
- the deterioration in performance robustness caused by increasing the closed-loop bandwidth resulted in a sufficiently high signal-to-noise ratio associated with the closed-loop output error, and
- the designed closed-loop bandwidth has not approached the minimum critical frequency corresponding to the unstable zeros of the plant or the existing model.

## Chapter 5

# Iterative Identification and Control Design for Unstable Plants

In this chapter we shall extend the applications of iterative identification and control design to unstable plants. We show that by employing a *two step approach*, where an unstable plant is first stabilized by a parallel feedback compensator, it is possible to design *systematically* an overall closed-loop system that has good step responses with little overshoots by using the iterative identification and control design methodology. Furthermore, this approach easily preserves the simplicity in designing the IMC filter and tuning the overall designed closed-loop bandwidth with a single design parameter. Specifically, similar to situations where the plant is stable or is Type 1 stable, we can design a system with a small initial overall designed closed-loop bandwidth (after the plant is stabilized by a known parallel feedback compensator) such that high frequency unmodelled dynamics of the plant are not overly excited. Through iterative applications of a control-relevant closed-loop system identification procedure and the standard IMC design method (discussed in Chapters 3 and 4) to the stabilized plant, the overall designed closed-loop bandwidth of the system can be widened progressively while maintaining good step responses with little overshoot. Two examples are employed to illustrate the method.



## 5.1 Introduction

It has been shown in the last two chapters that the IMC method [Morari and Zafiriou 1989] is a simple and effective technique for designing the underlying control law in a new approach of iterative identification and control design when the plant is stable or is Type 1 stable. The control objective is to design a closed-loop system with a specified (or as large as possible) bandwidth in the face of model uncertainties. In essence the approach starts with designing a controller such that the designed closed-loop system has a small bandwidth. The performance of the corresponding actual closed-loop system for a step reference input is monitored through closed-loop model validation methods discussed in Section 4.6. If the performance robustness of the closed-loop system is confirmed and if the designed closed-loop bandwidth is smaller than the specified one, a new controller will be designed such that it results in an increase of the designed closed-loop bandwidth. It is obvious that, in this connection, it is desirable to have a single design parameter which can be interpreted as the designed closed-loop bandwidth. In the case of stable plants, the IMC method is found to have the desirable attribute that we have just mentioned. Specifically, the bandwidth of the designed closed-loop system is given by the bandwidth of a simple IMC filter with a single design parameter (see Remark 3.2.5 and [Morari and Zafiriou 1989]). However, if the plant is unstable, the aforementioned single design parameter can no longer be interpreted as the designed closed-loop bandwidth *even if the plant does not have unstable zeros*. This poses a problem if the IMC method is to be used in the iterative identification and control design method when the plant is unstable. Motivated by the problems discussed above, Campi *et al.* [1994] have studied the design of a new filter when the IMC method is applied to situations where the plant involved has no unstable zeros and has one or two unstable poles.

Although the IMC filter design proposed by Campi *et al.* [1994] resulted in improved step responses for the IMC filter, it requires the tuning of two parameters to achieve a specified designed closed-loop bandwidth and tradeoff between the magnitude of the *inevitable* overshoot and the recovery time (after the overshoot has occurred) in the step response. Furthermore it will be shown later that, if the model has unstable poles and zeros, unstable zeros at *undesirable* locations and different from those of the model may be introduced into the controller by the **one step iterative identification and control design approach** where, in an attempt to apply the iterative identification and control design approach *directly* to unstable plants, the IMC design method [Morari and Zafiriou 1989, Campi *et al.* 1994] is employed

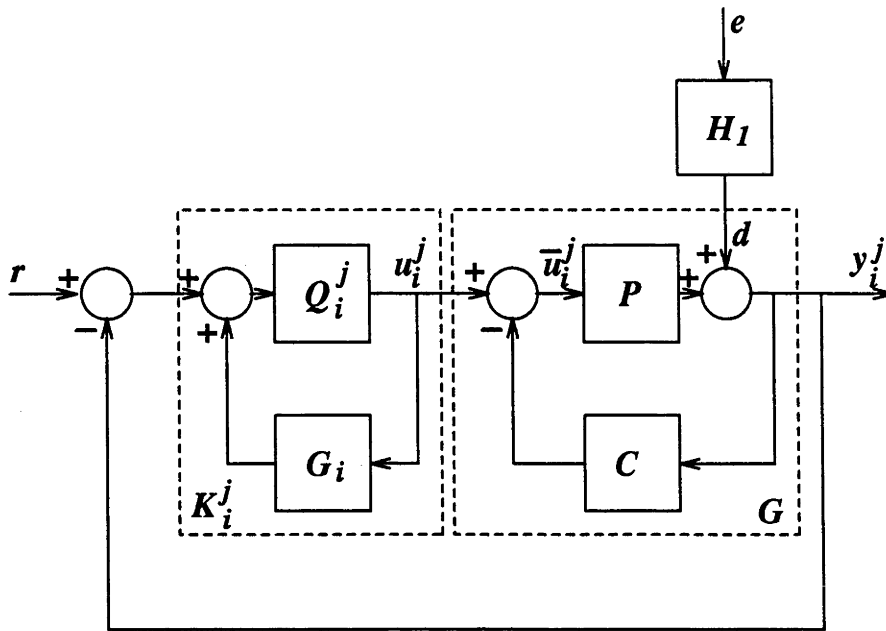


Figure 5.1: Closed-loop system structure for the two step approach

to design controllers directly for unstable plants.

It is well known [Freudenberg and Looze 1985] that open-loop unstable zeros impose a fundamental limit on closed-loop control performance. It is therefore important that control design methods do not introduce unnecessary performance limiting open-loop unstable zeros through the controllers. Furthermore it was also indicated in Section 4.5 that unstable zeros in the designed closed-loop transfer function may hinder closed-loop system identification. Hence the precaution that we have just mentioned has special significance in iterative identification and control design procedures, like the one that we are considering, which attempt to improve the closed-loop performance over an extended frequency range.

In this chapter we study a **two step iterative identification and control design approach** when the plant is unstable. The resulting overall closed-loop system will take the structure depicted in Figure 5.1, where  $r$  is the reference input and  $e$  is the unknown noise disturbance. The objective is to increase the overall closed-loop bandwidth progressively while good step responses are maintained. In the first step, the unstable plant  $P$  is stabilized by a parallel feedback compensator  $C$ . Thus even if  $P$  is imperfectly known, sufficient must be known about it to allow solution of a  $C$ . Typically this means having a good model for  $P$  at least

over a frequency band including the instability. In the second step, we apply the iterative identification and control design procedure to the stabilized plant  $G = P/(1 + CP)$ . That is, a sequence of series controllers,  $\{K_i^j ; j = 0, 1, 2, \dots\}$  is designed on the basis of a sequence of improving stable models,  $\{G_i ; i = 0, 1, 2, \dots\}$ , obtained by identifying the *stabilized* plant  $G$ . Since the IMC design method is employed only in the second step, where controllers are designed on the basis of stable models for a stabilized plant  $G$ , the two step iterative identification and control design approach completely avoids the problems that plague the one step control design approach.

**Remark 5.1.1** Observe that it is necessary to perform the first step, where  $C$  is designed to stabilize  $P$ , once only.

**Remark 5.1.2** Observe that when the plant is stable, it is not necessary to design  $C$  and we proceed immediately to the second step. This is similar to the situation where someone else has stabilized an unstable plant  $P$  before giving us the stabilized plant  $G$ . Note that in the latter situation we may not be told about the stabilization method, and hence will have no knowledge of, for example, the stabilizing compensator  $C$ . In either of the above situations, we would have performed the second step of the two step iterative identification and control design approach exactly as it was described in Chapters 3 and 4.

**Remark 5.1.3** Observe that in the second step, we are applying the iterative identification and control design procedure to the stabilized plant depicted in Figure 5.2. It does not matter whether  $C$  is designed by us or by someone else, we can start the iterative identification and design phase (by designing  $K_0^0$ ) as long as we are given a reasonable stable initial model  $G_0$  of the stabilized plant  $G$ . Note that this is equivalent to the situation where

$$y = Gu + He ,$$

with

$$G = \frac{P}{1 + CP} ,$$

and

$$H = \frac{H_1}{1 + CP} .$$

We note from Figures 5.1 and 5.2 that, since the noise disturbance  $e$  cannot affect the input to the stabilized plant  $u_i^j$  (which is *not* the input  $\tilde{u}_i^j$  of the unstable plant) before the

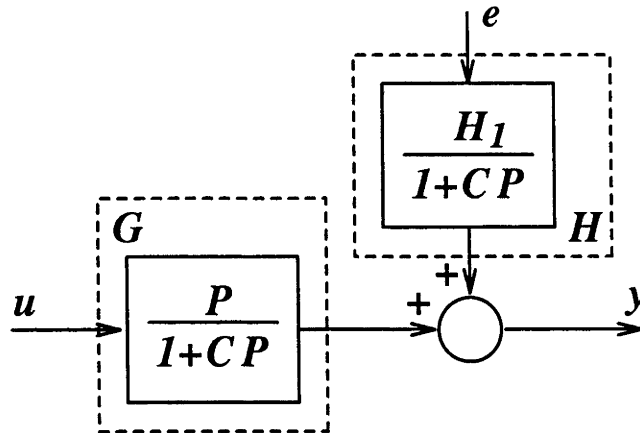


Figure 5.2: Stabilized plant before starting the iterative phase

major loop is closed by cascading  $G$  and  $K_i^j$ , Hansen's approach [Hansen 1989] can be applied to transform the closed-loop identification of  $G$  into a frequency weighted open-loop identification problem<sup>1</sup> as described in Chapters 3 and 4.

**Remark 5.1.4** The fundamental limits imposed by the plant's unstable poles on the area under the logarithmic magnitude of the sensitivity function are well known [Freudenberg and Looze 1985]. We shall not engage ourselves into more detail discussions on these issues other than to recognize the possibility that, in the process of stabilizing an unstable plant, the effects of noise disturbance at the plant output may be accentuated and hence may cause the problem of identifying  $G$  to become more difficult. This effect will depend on the choice of  $C$ , and will be studied elsewhere. However, it is important to emphasize that this is, in principle, a different issue from the legitimacy of applying Hansen's method. That is, stabilization of  $P$  by  $C$  (in the first design step) *does not* preclude the application of Hansen's method to transform the closed-loop identification of  $G$  (in the second design step) into an open-loop system identification problem, which involved only the signals  $u_i^j(t)$ ,  $y_i^j(t)$ , and  $r(t)$  (but not the  $\tilde{u}_i^j(t)$  that is within the minor loop formed by  $P$  and  $C$ ).

This chapter is structured as follows. In Section 5.2 we discuss difficulties related to the one step design approach when the plant is unstable. A two step iterative identification and control design approach for overcoming these difficulties is presented in Section 5.3. Two

<sup>1</sup>This is possible because it involves only the signals  $u_i^j(t)$  and  $y_i^j(t)$  that are outside the minor loop formed by  $P$  and  $C$ , and does not involve the signal  $\tilde{u}_i^j(t)$  that is inside the minor loop.

simulation examples are given in Section 5.4. We conclude and highlight two important future research problems in Section 5.5.

## 5.2 One Step Control Design Approach for Unstable Plants

In Section 5.2.1 we highlight the key features of the one step iterative identification and control design approach, where the IMC design method is employed to design controllers directly for unstable plants [Morari and Zafiriou 1989, Campi *et al.* 1994]. In Section 5.2.2 we show by simple examples that there are some problems when the one step design approach is applied to unstable plants.

### 5.2.1 Outline of The One Step Control Design Approach

In this subsection we briefly outline robust control design methods described in [Morari and Zafiriou 1989] and [Campi *et al.* 1994], where the IMC design method is employed to design controllers for unstable plants directly. To differentiate these methods from those where the unstable plant is first stabilized by a compensator before a performance-oriented controller is designed for the stabilized plant (like for example, the method to be discussed in Section 5.3), we shall call any such method a **one step control design approach**.

In the one step approach we are concerned with the design of a series controller,  $K$ , situated within a control loop which involves a partially known (not necessarily stable) plant  $P$ . Let  $\bar{P}$  be a model of the plant  $P$ . The controller  $K$  is parametrized in terms of a stable transfer function  $Q$  as shown in the IMC structure given in figure 5.3. We notice from Figure 5.3 that designing the controller

$$K = \frac{Q}{1 - \bar{P}Q} \quad (5.1)$$

is equivalent to designing its parametrization  $Q$ . The associated designed closed-loop transfer function is easily evaluated as  $\bar{T} = \bar{P}Q$ .

**Remark 5.2.1** Note that in the IMC design method, not only  $Q$  has to be stable, but it is also necessary that  $(1 - \bar{P}Q)\bar{P}$  is stable. It is proved in [Morari and Zafiriou 1989] that these

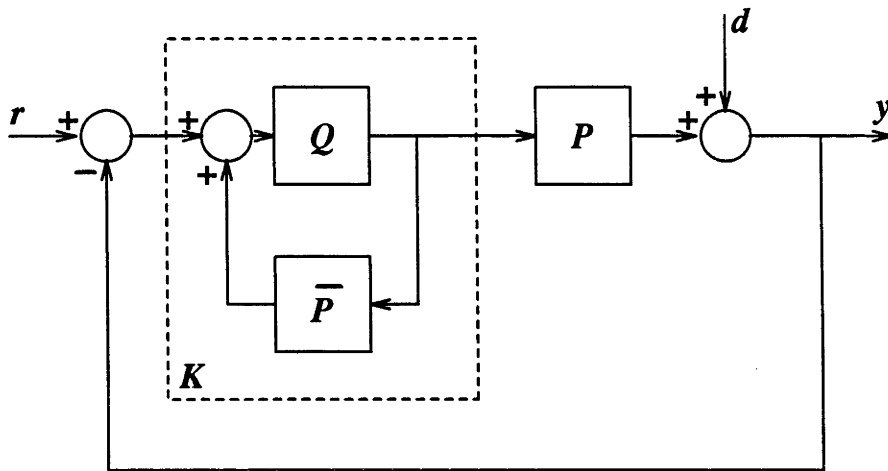


Figure 5.3: Internal model control structure

conditions ensure that the controller  $K$  defined by equation (5.1) results in a stable designed closed-loop system.

Since the plant  $P$  is only partially known in terms of its model  $\bar{P}$ , any practical design method must take into account the discrepancies between  $P$  and  $\bar{P}$ . In the IMC design method, this is achieved by specializing  $Q$  as the product of two transfer functions

$$Q = \tilde{Q}F ,$$

such that  $\tilde{Q}$  and  $F$  can be designed separately. The transfer function  $\tilde{Q}$  is designed with respect to the model  $\bar{P}$  such that, if  $P = \bar{P}$ , the objective

$$\|r - y\|_2^2 = \int_0^\infty [r(t) - y(t)]^2 dt$$

is minimized, where  $r(t) - y(t)$  is the error signal resulting from some known reference input  $r$  and unknown disturbance  $d$ . At this stage, one is not concerned with the model uncertainties involved in  $\bar{P}$  and/or the properness of the resulting controller as these will be taken care of by designing an appropriate IMC filter  $F$ . Specifically, a strictly proper stable filter  $F$  with an appropriate relative degree is employed to produce a proper or strictly proper  $Q = \tilde{Q}F$ . Furthermore it can be shown that, when the generalized input,  $v(t) = r(t) - d(t)$ , is a step function and if  $\tilde{Q}$  is designed by a method to be described shortly (in Theorem 5.2.1), the gain magnitude of the designed closed-loop transfer function (which is also the designed complementary-sensitivity function) is given by that of  $F$ . If the *unknown but bounded*

multiplicative model uncertainties are sufficiently small in the low frequency range (where the controller must have sufficiently large gain for the stabilization of  $\bar{P}$ ), we can secure robust stability of the closed-loop system by specifying an *appropriate* bandwidth for  $F$  (which has to be smaller than the frequencies where the effect of the multiplicative unstructured model uncertainties is significant).

**Remark 5.2.2** It is important to emphasize that we have assumed that the unknown but bounded multiplicative unstructured model uncertainties are sufficiently small in the frequency range where the controller must have sufficiently large gain magnitude for the stabilization of  $\bar{P}$ . Otherwise, it is impossible to find an appropriate bandwidth for  $F$  such that  $\bar{P}$  and  $P$  are stabilized simultaneously.

**Remark 5.2.3** When the uncertainties of the plant  $P$  permit its poles to migrate across the  $j\omega$ -axis,  $|\bar{P}^{-1}(j\omega)[P(j\omega) - \bar{P}(j\omega)]\bar{T}(j\omega)|$  would be unbounded when the poles of  $P$  are on the  $j\omega$ -axis. In this situation, we cannot ensure that using the IMC design method (which relies on the sufficient condition for robust stability, namely  $\|\bar{P}^{-1}[P - \bar{P}]\bar{T}\|_\infty < 1$ ) results in a closed-loop system with robust stability.

A general result related to the design of controllers by the IMC method was given in Theorem 2.5.1. We summarize the facts we need for the subsequent discussions in the next theorem. Note that because the discussions in this chapter involve an unstable plant, the corresponding stabilized plant, and their respective models, we have adopted a system of notations slightly different from that of the previous chapters. Specifically, we use  $P$  and  $\bar{P}$  to denote the unstable plant and its model;  $G$  and  $G_i$  are reserved, respectively, for the stabilized plant and the  $i^{\text{th}}$  model of the stabilized plant.

**Theorem 5.2.1** *With reference to Figure 5.3, suppose that  $\bar{P}$  has no poles on the imaginary axis, except those at the origin, and has no zeros on the imaginary axis. Let  $\bar{P}$  have  $k$  poles,  $p_1, \dots, p_k$ , in the open right-half plane and a pole of multiplicity  $l$  at the origin. Assume that the collection of open right-half plane poles in the Laplace transform of the generalized input,  $\nu(t) = r(t) - d(t)$ , is a subset of  $\{p_1, \dots, p_k\}$ .<sup>2</sup> Denote these as  $p_1, \dots, p_k$ , with*

<sup>2</sup>As noted in [Morari and Zafriou 1989], this assumption is necessary to make a well posed problem.

$0 \leq k' \leq k$ . Furthermore assume that  $\nu(s)$  has at least  $l$  poles at the origin.<sup>3</sup>

Define

$$B_{\bar{P}} = \prod_{i=1}^k \frac{p_i - s}{p_i^* + s}, \quad (5.2)$$

and factor  $\bar{P}$  into an all pass factor  $\bar{P}_a$  (which contains all the zeros of  $\bar{P}$  in the open right-half plane) and a minimum-phase factor  $\bar{P}_m$  (which includes all the poles of  $\bar{P}$  in the open right-half plane and at the origin) such that

$$\bar{P}(s) = \bar{P}_m(s)\bar{P}_a(s).$$

Similarly, define

$$B_\nu = \prod_{i=1}^{k'} \frac{p_i - s}{p_i^* + s}, \quad (5.3)$$

and factor  $\nu(s)$  such that

$$\nu(s) = \nu_m(s)\nu_a(s),$$

where  $\nu_m(s)$  is a minimum-phase factor that includes all the poles of  $\nu(s)$  in the open right-half plane and at the origin, and  $\nu_a(s)$  is an all pass factor that contains all the zeros of  $\nu(s)$  in the open right-half plane. Then the controller parametrization  $\tilde{Q}$  which minimizes the objective

$$\|r - y\|_2^2 = \int_0^\infty [r(t) - y(t)]^2 dt = \frac{1}{2\pi} \int_{-\infty}^\infty |r(j\omega) - y(j\omega)|^2 d\omega = \|(1 - \bar{P}\tilde{Q})\nu\|_2^2$$

is given by

$$\tilde{Q} = B_P(\bar{P}_m B_\nu \nu_m)^{-1} \left\{ (B_P \bar{P}_a)^{-1} B_\nu \nu_m \right\}_* \quad (5.4)$$

where the operator  $\{\cdot\}_*$  denotes that after a partial fraction expansion of the operand all terms involving the poles of  $\bar{P}_a^{-1}$  are omitted.

It was shown in [Campi *et al.* 1994] that, when the model is unstable, the standard design of the IMC filter  $F$  described in Theorem 2.5.1 (which is discussed in detail by Morari and Zafiriou [1989]) will lead to an IMC filter that has very large overshoot in the IMC filter's step response. Since the design closed-loop transfer function can be shown to have the form

$$\bar{T} = F \bar{P}_a \tilde{Q}_{nm},$$

<sup>3</sup>As noted in [Morari and Zafiriou 1989], this assumption is necessary for the closed-loop system to handle plant input disturbances whose Laplace transform may have poles at the origin.



where  $F$  is the IMC filter,  $\bar{P}_a$  is the all pass factor of the model  $\bar{P}$ , and  $\tilde{Q}_{nm}$  is a non-minimum phase transfer function that depends on the unstable poles and unstable zeros of  $\bar{P}$ , we could expect the transient response of the design closed-loop system to be at least as bad as that of the IMC filter. (Unstable zeros of  $\bar{P}$  and  $\tilde{Q}_{nm}$  may introduce extra phase lag into the the design closed-loop transfer function, for which  $F$  is one of the factors. This may cause the step response of the designed closed-loop transfer function to have even bigger overshoot than that of  $F$ .) Furthermore, the designed closed-loop bandwidth is no longer directly specified by the single design parameter of the standard IMC filter. These facts will cause difficulties in the use of the IMC design method in the iterative identification and control design approach where it is desirable that the designed closed-loop system has step response with little overshoot and there is a single design parameter that specifies directly the designed closed-loop bandwidth.

A new method for designing the IMC filter that can alleviate these difficulties was proposed by Campi *et al.* [1994]. However, it should be noted that the new IMC filter suggested by Campi *et al.* [1994] requires an additional design parameter (other than the one for specifying the designed closed-loop bandwidth) to tradeoff the magnitude of the overshoot and the recovery time after the overshoot has occurred in the step response of the IMC filter. Furthermore, the IMC filter design method described assumed for the analysis that the unstable plant and its model have no unstable zeros.

We shall show by an example in Section 5.2.2 that, when the model has unstable real poles and zeros, controllers designed by the one step design approach (using either of the IMC filter design methods in [Morari and Zafiriou 1989] or [Campi *et al.* 1994]) may introduce unstable zeros (other than those of the model) into the key transfer functions of the designed closed-loop systems. These additional unstable zeros may impose unnecessary limitations on the closed-loop performance achievable through the iterative identification and control design methodology.

**Remark 5.2.4** We shall see in Section 5.2.2 that the above difficulty will not occur when the unstable model has no finite unstable zeros.

However, this is still not the main problem with the one step design approach. More strikingly, we shall show by a second example that, even in the absence of unstable zeros

in the model  $\bar{P}$ , step responses of the closed-loop system designed by the one step design approach for unstable models can have *unacceptably large* overshoot when the designed closed-loop bandwidth is limited by the presence of high frequency unmodelled dynamics.

### 5.2.2 Difficulties with The One Step Design Approach

We first show by using a simple example that, when the model  $\bar{P}$  has unstable poles and zeros, unstable zeros other than those of the model may be introduced into some performance deciding transfer functions designed by the one step control design approach described in [Morari and Zafiriou 1989] and [Campi *et al.* 1994].

Consider an unstable model with the transfer function

$$\bar{P} = \frac{s - 1}{(s + 0.5)(s - 2)} .$$

According to the procedure outlined in Section 5.2.1, we first calculate

$$\tilde{Q} = B_{\bar{P}}(\bar{P}_m B_{\nu} \nu_m)^{-1} \left\{ (B_{\bar{P}} \bar{P}_a)^{-1} B_{\nu} \nu_m \right\}_* ,$$

which gives, for a step reference input,

$$\tilde{Q} = \frac{(s + 0.5)(s - 2)(7s - 2)}{(s + 1)(s + 2)} .$$

We can write  $\tilde{Q}$  as

$$\tilde{Q} = \bar{P}_m^{-1} \tilde{Q}_{nm} ,$$

where

$$\bar{P}_m = \frac{s + 1}{(s + 0.5)(s - 2)}$$

is the minimum-phase factor of  $\bar{P}$ , and

$$\tilde{Q}_{nm} = \frac{7s - 2}{s + 2}$$

is a non-minimum-phase factor resulting from the  $\{\cdot\}_*$  operation.

Note that the non-minimum-phase factor  $\tilde{Q}_{nm}$  has a gain magnitude greater than one for all frequencies and has a phase lag approaching  $2\pi$  for high frequencies. Furthermore, irrespective of the method by which the IMC filter is designed, the unstable zeros of  $\tilde{Q}_{nm}$

must appear as the unstable zero of  $Q = \tilde{Q}F$ ,  $K = Q/(1 - \bar{P}Q)$ , the designed open-loop transfer function  $L = K\bar{P}$ , and the designed closed-loop transfer function  $\bar{T} = F\tilde{Q}_{nm}\bar{P}_a$ . This implies that, even though the IMC filter proposed by Campi *et al.* [1994] provides good step response, the designed closed-loop system may have small stability margins and will have poor transient response if the designed closed-loop bandwidth is comparable or larger than  $2/7$  rad/s (corresponding to the unstable zero in  $\tilde{Q}_{nm}$ ).

**Remark 5.2.5** Fundamental limits imposed by open-loop unstable zeros on closed-loop performance are well known [Freudenberg and Looze 1985]. They are also discussed in, for example, [Doyle *et al.* 1992] and [Middleton and Goodwin 1990].

**Remark 5.2.6** It was indicated in Section 4.5 (where  $\tilde{Q}_{nm}$  can be treated as unity) that the undesirable phase lag of the all pass factor  $\bar{P}_a$  may hinder closed-loop system identification through increasing the designed sensitivity function in the designed closed-loop bandwidth. By comparing the frequency characteristics of  $\tilde{Q}_{nm}$  and  $\bar{P}_a$  in the above example, we observe that  $\tilde{Q}_{nm}$  could have more adverse effects than  $\bar{P}_a$  on closed-loop system identification.

**Remark 5.2.7** For the above reasons, it is important that factors like  $\tilde{Q}_{nm}$  (especially those that have zeros nearer to the origin than the unstable zeros of the model) are not introduced unnecessarily into the designed closed-loop transfer function.

It should be observed that the additional unstable zero in  $\tilde{Q}$  comes from the operation  $\{\cdot\}_*$  when the model has unstable poles and zeros. In general, consider the situation where the model has an unstable real pole at  $s = p$ ;  $p > 0$ , and an unstable real zero at  $s = z$ ;  $z > 0$ . It can be shown easily that, for a step input, we have

$$\left\{ \left( \frac{s+p}{-s+p} \right) \left( \frac{s+z}{-s+z} \right) \frac{1}{s} \right\}_* = \frac{z+3p}{p-z} \left[ \frac{-s+z_*}{s(-s+p)} \right],$$

with the zero at

$$z_* = \frac{p(p-z)}{z+3p}.$$

Therefore this zero is unstable if  $p > z$ . Note that for the purpose of increasing the closed-loop bandwidth, the unstable zero at  $z_*$  may impose limitations more severe than those imposed

by the unstable zero of the model at  $s = z$  if  $0 < z_* < z$  [Middleton and Goodwin 1990]. Simple algebra shows that  $0 < z_* < z$  occurs when  $\sqrt{5} - 2 < z/p < 1$ .

The above analysis suggests that the problem of introducing an additional unstable zero into the key transfer functions of the closed-loop system exists when the operation  $\{\cdot\}_*$  is performed on a model with a certain distribution of unstable real poles and zeros. We can overcome this problem if the operation  $\{\cdot\}_*$  is performed only on stable models. This prompted us to study, in Section 5.3, a two step control design approach where the standard IMC design method is applied to design series controllers (on the basis of stable models) after an unstable plant is stabilized by a parallel feedback compensator.

We shall now present an example which is representative of a more practical situation than the previous one. The forthcoming example shows that, even in benign situations where the unstable model has no unstable zeros, step responses of the closed-loop system designed by the one step design approach can have *unacceptably large* overshoot when the designed closed-loop bandwidth is limited by the presence of high frequency unmodelled dynamics.

Consider the model

$$\bar{P}(s) = \frac{0.1}{-s + 0.1}$$

of an unstable plant

$$P(s) = \frac{0.1(s - 4)}{(s - 0.1)(s^2 + 0.2s + 4)}$$

We shall design the controller  $K$  (refer to Figure 5.3) by the one step design approach. In particular we shall design the IMC filter by the method proposed in [Campi *et al.* 1994], which will result in an IMC filter with better characteristics than those designed by the method of [Morari and Zafiriou 1989].

By using the method given in Theorem 5.2.1, we can calculate on the basis of  $\bar{P}$ ,

$$\tilde{Q} = \frac{-s + 0.1}{0.1}$$

According to the guidelines given in [Campi *et al.* 1994], in order for  $Q = \tilde{Q}F$  to be strictly proper, the IMC filter for this example should take the form

$$F(s) = \frac{\mu(s + \alpha)}{(s + \gamma)(s + \lambda)(s + 10\lambda)}$$

Furthermore, the designed closed-loop transfer function will, in view of the minimum-phase property of  $\bar{P}$ , be identical with  $F(s)$ . There are two tuning parameters  $\lambda$  and  $\gamma$  in this filter.

The constants  $\mu$  and  $\alpha$  are determined from the two interpolation constraints:  $F(p) = 1$ , where  $p = 0.1$  is the unstable pole of  $\bar{P}$ , and  $F(0) = 1$  for a step reference input. The salient features of this IMC filter is as follows:

1. The bandwidth of this IMC filter is specified by  $\lambda$ .
2. The step response of this filter *always* has an overshoot. The magnitude of the overshoot reduces *monotonically* for increasing  $\lambda$ .
3. The resonance peak in the frequency response of  $F$  can be made small by requiring  $\gamma \ll p \ll \lambda$ . Decreasing the resonance peak in the frequency response of  $F$  will help to improve the stability robustness of the closed-loop system to high frequency unmodelled dynamics.
4. Although we can decrease the resonance peak in the frequency response by decreasing  $\gamma$ , the time to recovery after an overshoot has occurred in the step response of  $F$  increases *monotonically* for decreasing  $\gamma$ . Furthermore, the settling time of the step response is determined predominantly by  $\gamma$ , and can be estimated as  $5/\gamma$  seconds. A compromise in choosing a value for  $\gamma$  is therefore necessary. This can usually be achieved for some  $\gamma \in [0.02\lambda, 0.2\lambda]$ .

In order to keep the overshoot in the step response of the closed-loop system to not more than 10% of the magnitude of the step input, we attempt to design  $F$  for  $\lambda = 5p$  (see [Middleton and Goodwin 1990] for a discussion of this choice). We have discovered that it is impossible to design  $K$  for this choice of  $\lambda = 0.5$  such that  $P$  is stabilized (note that  $\bar{P}$  is always stabilized by  $K$ ). After searching over the two dimensional parameter space of  $\lambda$  and  $\gamma$ , we found the following partition of the parameter space:

$\lambda < 0.26$	$\gamma \in [0.02\lambda, 0.2\lambda]$	$P$ is stabilized by $K$
$\lambda = 0.26$	$\gamma \in [0.02\lambda, 0.12\lambda]$	$P$ is stabilized by $K$
$\lambda = 0.26$	$\gamma \in (0.12\lambda, 0.2\lambda]$	$P$ is destabilized by $K$
$\lambda > 0.26$	$\gamma \in [0.02\lambda, 0.2\lambda]$	$P$ is destabilized by $K$

When  $\bar{P}$  and  $P$  are controlled by  $K$  (designed for  $\lambda = 0.26$  to give minimum possible overshoot), the step responses are shown in Figure 5.4 to Figure 5.7. Observe that each of the designed step responses (Figures 5.4 and 5.5) has overshoot of about 40%. Furthermore, the actual step responses (Figures 5.6 and 5.7) clearly demonstrate that the closed-loop system resulting from the one step design approach is *highly sensitive* to high frequency unmodelled

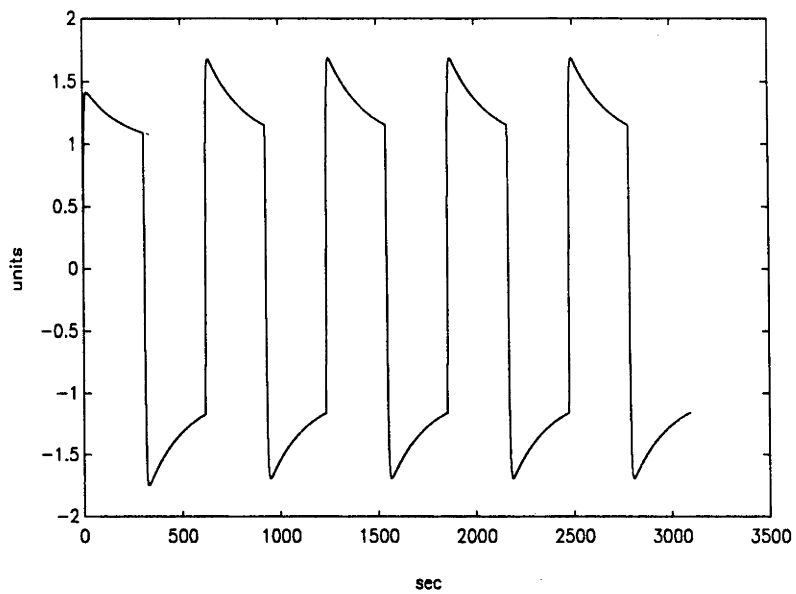


Figure 5.4: Designed closed-loop system response for a square wave input ( $\lambda = 0.26$ ,  $\gamma = 0.0052$ )

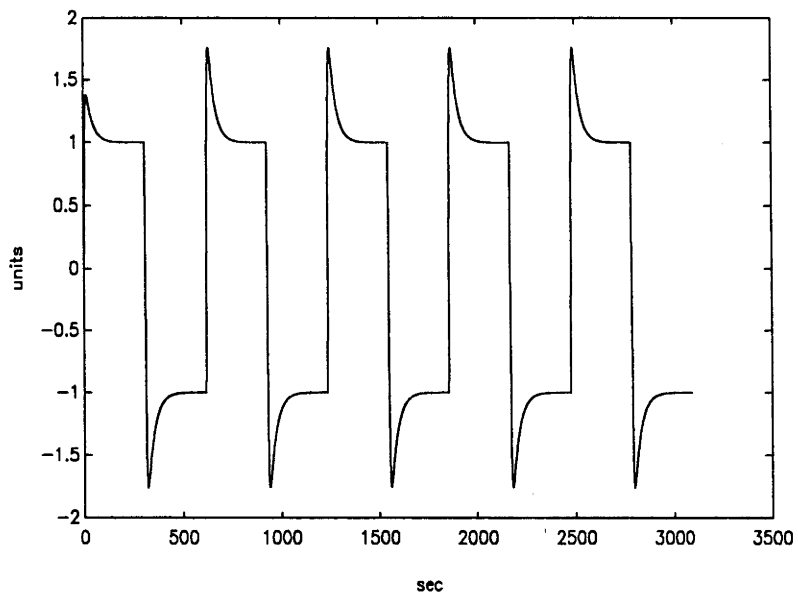


Figure 5.5: Designed closed-loop system response for a square wave input ( $\lambda = 0.26$ ,  $\gamma = 0.0312$ )

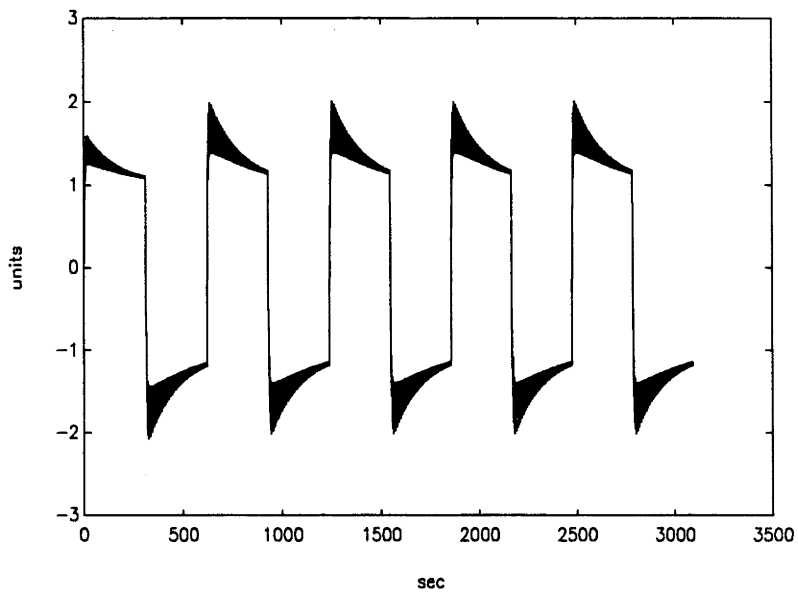


Figure 5.6: Actual closed-loop system response for a square wave input ( $\lambda = 0.26$ ,  $\gamma = 0.0052$ )

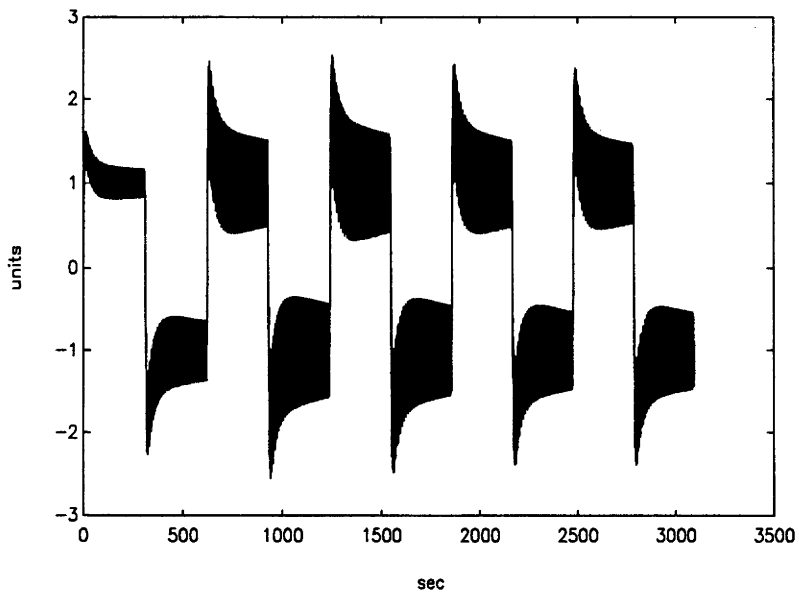


Figure 5.7: Actual closed-loop system response for a square wave input ( $\lambda = 0.26$ ,  $\gamma = 0.0312$ )

dynamics even when  $\lambda$  is well below 0.5 (the value of  $\lambda$  that is expected to keep the overshoot of the designed step response to within 10%).

**Remark 5.2.8** The last example clearly demonstrated that, when a controller is designed for an unstable plant by the one step approach, the limitation imposed on the closed-loop bandwidth by (relatively mild) high frequency unmodelled dynamics can prevent the overshoot from becoming acceptably small (say 10%).

By using the above plant and model, we will demonstrate in Section 5.4 that a two step control design approach (to be described in Section 5.3) can give better results.

## 5.3 A Two Step Iterative Identification and Control Design Approach for Unstable Plants

In Section 5.3.1 we outline a two step iterative identification and control design approach for unstable plants. Since the second step involves a direct application of the iterative identification and control design procedure to a stable plant or a Type 1 stable plant (or more exactly, a stabilized plant) as described in Chapter 3, the emphasis of Section 5.3.1 is on the first design step where the unstable plant is stabilized by a parallel feedback compensator. In Section 5.3.2 we discuss design guidelines for this stabilizer. The unstable model discussed in Section 5.2.2 will then be employed to illustrate the design procedure.

### 5.3.1 Outline of A Two Step Control Design Approach

In this subsection we shall outline a two step iterative identification and control design approach for unstable plants. The relevant system structure is depicted in Figure 5.1.

In the first step, we shall stabilize the unstable plant  $P$  by a parallel feedback compensator  $C$ . Obviously we have to design  $C$  on the basis of an approximate, presumably unstable model,  $\bar{P}$ , of  $P$ . For this purpose, we shall assume that  $P$  and  $\bar{P}$  have the same number of poles in the open right-half plane, and have no poles on the  $j\omega$ -axis. This assumption is



consistent with the conditions discussed in Remarks 5.2.2 and 5.2.3. In the second step we employ the standard IMC design method to design a sequence of series controllers,  $\{K_i^j ; j = 0, 1, 2, \dots\}$ , on the basis of a sequence of stable identified models,  $\{G_i ; i = 0, 1, 2, \dots\}$ , for the stabilized plant  $G = P/(1 + CP)$ . Since each of these IMC controllers is designed on the basis of a stable model, the two step iterative identification and control design approach completely avoids the problems that plague the one step control design approach.

**Remark 5.3.1** The idea of a two step control design approach (namely, employing a minor loop to stabilize an unstable plant before the major loop that includes the stabilized plant is designed for achieving performance) is not new. It was suggested as early as 1957 by Newton, Jr. *et al.* [1957] and more recently, in [Callier and Desoer 1982] and [Middleton and Goodwin 1990]. What is new are the introduction of a pole-placement procedure (albeit not thoroughly studied here) that takes into account the effects of high frequency modelling errors in the first design step and the application of the iterative identification and control design procedure in the second design step.

**Remark 5.3.2** The book by D'Azzo and Houpis [1988] contains extensive discussions on applying the two step approach to stable plants with poorly damped resonant poles (that is, plants with poor relative stability). In this case, the relative stability of the plant is improved effectively by a parallel output feedback compensator before a series controller is designed for the modified plant to achieve the overall closed-loop performance.

**Remark 5.3.3** The sole purpose of the first step is to stabilize  $P$  with  $C$  (designed on the basis of  $\bar{P}$ ). It is important to emphasize that, other than for the purpose of achieving stabilization, it is desirable that  $C$  has minimal adverse effects on the second design step, which is for achieving the overall control objective.

**Remark 5.3.4** The objective of the second (or iterative identification and control) design step is to achieve the desired closed-loop bandwidth and good step response. This is realized by designing appropriate series controllers  $K_i^j$  (on the basis of an existing model  $G_i$  for the stabilized plant  $G$ ) to increasing the closed-loop bandwidth progressively (in the face of model uncertainties) such that high frequency unmodelled dynamics are not overly excited.

If necessary, a better model  $G_{i+1}$  may be identified before the closed-loop bandwidth is increased further. This second design step, as it was emphasized in Section 5.1, is identical to the application of the iterative identification and control design procedure to a stable or a Type 1 stable plant discussed in Chapters 3 and 4.

**Remark 5.3.5** Since only stable (or Type 1 stable) models are involved in the second design step, designing for good overall closed-loop step responses that have small or no overshoot will become easier than the case where the models involve are unstable.

As the second step of the two step control design approach is similar to the application of the iterative identification and control design approach to a stable plant or a Type 1 stable plant (or an unstable plant that has already been stabilized by someone else) discussed in Chapters 3 and 4, in the remainder of this subsection, we shall only concentrate on the discussion of the first (or stabilization) step.

We shall now briefly delineate the considerations that lead to some of the guidelines for designing the parallel feedback compensator  $C$ .

In the two step design approach, since we do not like the solution of the first design step to cause unnecessary difficulties to the second design step, we would like the solution of the first step (that is, the parallel feedback stabilizer) to have the following properties:

1. The introduction of the parallel feedback stabilizer does not cause the noise disturbance to affect the stabilized plant  $G$  more than the way it affects the unstable plant  $P$ , so that iterative identification and control design (in the second design step) do not become more difficult than they should be.
2. The introduction of the parallel feedback stabilizer does not cause model uncertainties to make the design of the series controller (in the second design step) a more difficult problem than it should be.

We shall deal with the effects of disturbance (the first point) in the following discussion. Considerations with respect to model uncertainties (the second point) will be discussed later.

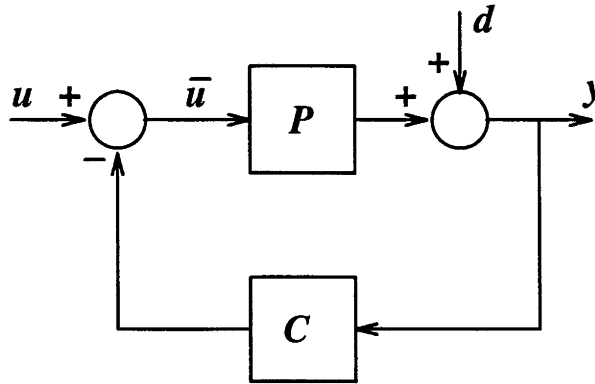


Figure 5.8: Parallel output feedback stabilization

With respect to Figure 5.8, we consider the simple situation where an unstable plant is

$$P(s) = \frac{1}{s - a}, \quad a > 0,$$

and we wish to use the parallel output feedback controller

$$C(s) = k$$

to stabilize  $P(s)$ . We assume for this discussion that the plant is perfectly known and we design  $C(s) = k$  on the basis of  $P$ .

The transfer function between the disturbance  $d$  and the closed-loop output  $y$  is given by

$$Z(s) = \frac{s - a}{s + k - a},$$

and the transfer function between the disturbance  $d$  and the input to the plant  $\bar{u}$  is

$$L(s) = -\frac{k(s - a)}{s + k - a}.$$

Obviously it is necessary that  $k > a$  for  $Z(s)$  and  $L(s)$  to be stable.

Firstly we consider the transfer function  $Z(s)$ . The magnitudes of the asymptotic frequency responses for  $Z(s)$  are shown in Figure 5.9 for various values of  $k$ . Observe from Figure 5.9 (a) that the effect of noise disturbance at the output of the plant is amplified at low frequencies by the introduction of the stabilizer for  $a < k < 2a$ . When the value of  $k$  approaches  $a$ , this noise amplification effect may become very serious. This may cause difficulty to the system identification process in the second design step.

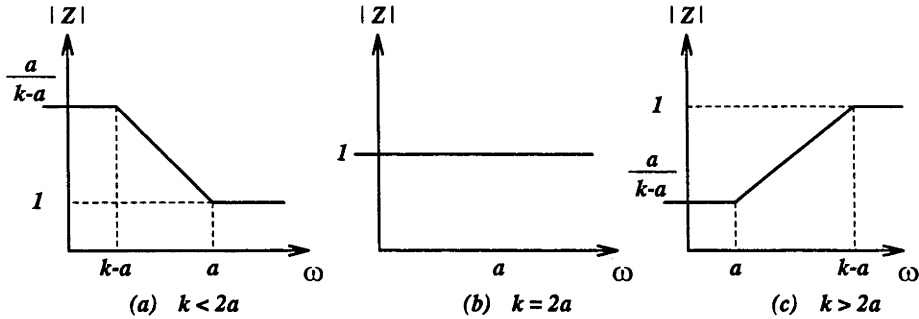


Figure 5.9: Magnitudes of  $|Z|$  for various values of feedback gain  $k$

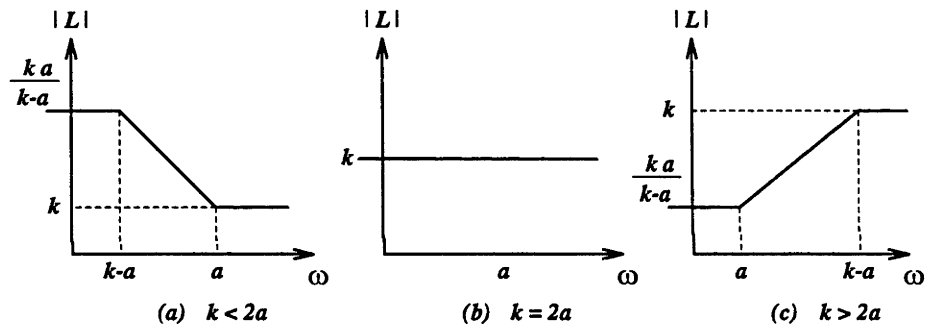


Figure 5.10: Magnitudes of  $|L|$  for various values of feedback gain  $k$

Now we consider the transfer function  $L(s)$ . The magnitudes of the asymptotic frequency responses for  $L(s)$  are shown in Figure 5.10 for various values of  $k$ . Observe from Figure 5.10 (c) that the effect of noise disturbance at the input of the plant will be amplified at high frequencies by the introduction of the stabilizer for  $k > 2a$ . Furthermore, this noise amplification effect may become very serious when the value of  $k$  is much larger than  $2a$ . This may cause the actuator of the plant to saturate. Likewise, if the plant transfer function  $P$  is replaced by  $P(1 + \Delta)$ , where  $\Delta$  models high frequency uncertainties, the sufficient condition for robust stability,

$$\left\| \Delta \frac{CP}{1 + CP} \right\|_{\infty} < 1 ,$$

will be harder to satisfy as  $k$  becomes larger than  $2a$ .

From the above discussions it appears that, if we consider the effects of the stabilizer  $C(s) = k$  on both  $Z$  and  $L$ , a reasonable tradeoff is to let  $k = 2a$ . Observe that this will lead to a stabilized plant  $G$  with a pole at  $s = -a$ , which is the mirror image of the unstable pole of  $P$  at  $s = a$ . Furthermore, under this condition, the magnitude of the frequency response for  $G = 1/(s+a)$  is the same as the magnitude of the frequency response for  $P = 1/(s-a)$ . In the sequel, we will use the above observation as one of the guidelines for the design of parallel output feedback stabilizer. Specifically, given an unstable model  $\bar{P}$ , we shall design the parallel output feedback stabilizer such that the model  $G_0 = \bar{P}/(1+C\bar{P})$  of the stabilized plant  $G$  retains the poles of  $\bar{P}$  in the *open* left-half plane and will have a pole at each of the mirror image locations (with respect to the imaginary axis) for the *open* right-half plane poles of  $\bar{P}$ . Other guidelines for designing  $C$  will be discussed in Section 5.3.2.

**Remark 5.3.6** Although the stabilization method that we are going to describe shortly shows encouraging results (as we shall illustrate with the examples in Section 5.4), we could not claim that this method is guaranteed to have the advantage of, other than stabilizing  $P$ , having minimal adverse effects on the second design step (where series controllers are designed).

**Remark 5.3.7** Note that  $C$  must have sufficiently large gain in appropriate frequencies to stabilize  $\bar{P}$  and  $P$ . In particular, if there is a pole of  $\bar{P}$  or  $P$  at  $s = a$ ,  $C$  will have to have significant magnitude at  $s = ja$ . However, in the high frequency range where  $\bar{P}$  may have significant unstructured model uncertainties,  $C$  must have a sufficiently small gain magnitude such that the unmodelled dynamics are not overly excited. Particularly, when  $\bar{P}$  has significant high frequency unstructured model uncertainties, it is helpful to have a strictly proper  $C$ .

**Remark 5.3.8** In order to have robust stability under singular perturbation [Kokotovic *et al.* 1986, Vidyasagar 1985b], it is necessary and sufficient that  $C$  is strictly proper.

In order to secure robustness against high frequency unstructured model uncertainties, we shall use a *strictly proper* parallel *output feedback* compensator to stabilize  $P$ . The order of  $G_0 = \bar{P}/(1+C\bar{P})$  will in general be higher than that of  $\bar{P}$ , and zeros in addition to those of  $\bar{P}$  may be introduced into  $G_0$  via the poles of  $C$ .

We shall next estimate the multiplicative model uncertainties associated with the initial model  $G_0$  for the stabilized plant  $G$  that is induced by the multiplicative model uncertainties associated with  $\bar{P}$  under the influence of the strictly proper parallel output feedback stabilizer.

By expressing the unstable plant transfer function as  $P = \bar{P}(1 + \Delta_P)$ , where  $\Delta_P$  denotes the multiplicative modelling error associated with  $\bar{P}$ , we can write the transfer function of the stabilized plant  $G = P/(1 + CP)$  as

$$G = G_0(1 + \Delta_G) ,$$

where

$$G_0 = \frac{\bar{P}}{1 + C\bar{P}}$$

is the model for  $G$  calculated on the basis of the model  $\bar{P}$  stabilized by the strictly proper parallel output feedback compensator  $C$ , and

$$\Delta_G = \frac{\Delta_P}{1 + C\bar{P}(1 + \Delta_P)}$$

is the multiplicative modelling error associated with  $G_0$  induced by  $\Delta_P$  under the influence of  $C$ .

Assume that the strictly proper parallel output feedback compensator  $C$  stabilizes the unstable plant  $P$  and its model  $\bar{P}$ . Observe that if  $C$  is designed to have the property that, in the high frequency region (to be denoted by  $\Omega$ ) where  $\Delta_P$  is significant and the controller gain is not necessary to be large for securing stabilization, the condition

$$\left| \frac{C(j\omega)\bar{P}(j\omega)}{1 + C(j\omega)\bar{P}(j\omega)} \Delta_P(j\omega) \right| \ll 1, \quad \forall \omega \in \Omega$$

is satisfied through requiring

$$|C(j\omega)\bar{P}(j\omega)| \ll 1, \quad \forall \omega \in \Omega ,$$

then

$$|\Delta_G(j\omega)| \approx |\Delta_P(j\omega)|, \quad \forall \omega \in \Omega .$$

**Remark 5.3.9** Roughly speaking, the above discussions shows that, to prevent  $\Delta_G$  from impinging upon the design of  $K_0^j$  more seriously than the manner that  $\Delta_P$  has impinged upon the design of  $C$ , it is sufficient that

$$|C(j\omega)\bar{P}(j\omega)| \ll 1, \quad \forall \omega \in \Omega .$$

In other words, outside the frequency range where  $|C(j\omega)|$  has to be sufficiently large for the purpose of stabilizing  $\bar{P}$ , we would like  $|C(j\omega)|$  to roll off quickly.

After a pole configuration is chosen for  $G_0$  (including those poles that disappear as stable pole-zero cancellations in  $P/(1 + CP)$ ), the characteristic polynomial  $W$  for  $G_0$  can be determined. (Guidelines for doing this will be discussed shortly in Section 5.3.2). We can then employ simple calculations to compute the strictly proper parallel output feedback compensator  $C$  such that the initial stable model  $G_0$  (corresponding to the stabilized but unknown plant  $G = P/(1 + CP)$ ) has the (monic) characteristic polynomial  $W(s)$ . We shall next describe a pole-placement technique for computing  $C$ .

**Remark 5.3.10** It is important to emphasize that the following pole-placement technique will not be employed as a stand alone procedure for the synthesis of  $C$ . It will instead be integrated into a design procedure, with additional guidelines to be developed in Section 5.3.2.

Consider the inner loop of the system structure shown in Figure 5.1. Assume that the model of  $P$  is given by  $\bar{P} = B/A$ , where

$$A(s) = s^n + A_1s^{n-1} + A_2s^{n-2} + \dots + A_n$$

and

$$B(s) = B_1s^{n-1} + B_2s^{n-2} + \dots + B_n$$

are, respectively, the *monic* denominator polynomial and the numerator polynomial of  $\bar{P}$ . We also assume that  $A$  and  $B$  are coprime. We would like to find a parallel feedback compensator  $C = N/D$  such that the compensated model  $G_0 = (\bar{P}/(1 + C\bar{P}))$  has the *monic* characteristic polynomial  $W$ . This pole-placement problem can be solved [Kailath 1980] by finding polynomials  $N$  and  $D$  that satisfy the Diophantine equation

$$A(s)D(s) + B(s)N(s) = W(s) \quad . \quad (5.5)$$

Recall that we want  $C$  to be *strictly proper*. However we do not like  $C$  to have unnecessarily high order. Let  $C$  have order  $m$  and a relative degree of one and let the polynomial

$D$  be monic, then equating the coefficients in equation (5.5) leads to  $m + n$  linear algebraic equations in the  $2m$  unknown coefficients of polynomials  $D$  and  $N$ . For a solution to exist, in general, we require  $m \geq n$ . For  $m = n$  we can rewrite the linear algebraic equations as

$$Mx = f \quad , \quad (5.6)$$

where

$$M = \begin{bmatrix} 1 & 0 & \cdots & 0 & 0 & 0 & \cdots & 0 \\ A_1 & 1 & \ddots & \vdots & B_1 & 0 & \ddots & \vdots \\ A_2 & A_1 & \ddots & 0 & B_2 & B_1 & \ddots & 0 \\ \vdots & \vdots & \ddots & 1 & \vdots & \vdots & \ddots & 0 \\ A_n & \vdots & \ddots & A_1 & B_n & \vdots & \ddots & B_1 \\ 0 & A_n & \ddots & \vdots & 0 & B_n & \ddots & \vdots \\ \vdots & \ddots & \ddots & \vdots & \vdots & \ddots & \ddots & \vdots \\ 0 & \cdots & 0 & A_n & 0 & \cdots & 0 & B_n \end{bmatrix}$$

is the  $2n \times 2n$  Sylvester matrix,

$$x = [ D_1 \ D_2 \ \cdots \ D_n \ N_1 \ N_2 \ \cdots \ N_n ]' \ ,$$

$$f = [ W_1 - A_1 \ W_2 - A_2 \ \cdots \ W_n - A_n \ Q_{n+1} \ Q_{n+2} \ \cdots \ Q_{2n} ]' \ ,$$

with

$$D(s) = s^n + D_1 s^{n-1} + D_2 s^{n-2} + \cdots + D_n$$

and

$$N(s) = N_1 s^{n-1} + N_2 s^{n-2} + \cdots + N_n \ ,$$

for

$$W(s) = s^{2n} + W_1 s^{2n-1} + W_2 s^{2n-2} + \cdots + W_{2n} \ .$$

Since  $A(s)$  and  $B(s)$  are coprime polynomials, by Sylvester's theorem [Kailath 1980], the matrix  $M$  is nonsingular and equation (5.6) has an unique solution.

**Remark 5.3.11** In the above discussions we assumed that the relative degree of  $C$  is one. In general, a strictly proper  $C$  could have relative degree  $q$  for  $1 \leq q \leq m$ . For a solution of the corresponding Diophantine equation to exist such that  $C$  has the minimum possible order, it is necessary that  $m = n + q - 1$ , where  $n$  is the order of the model  $\bar{P}$ . This will result in a closed-loop characteristic polynomial  $W(s)$  with a degree  $2n + q - 1$ . Observe that if we increase the relative degree for  $C$ , its order has to be increased correspondingly. This means a higher order  $C$  and more degrees of freedom in specifying the poles of  $W(s)$ .



### 5.3.2 Design Guidelines for Parallel Feedback Stabilizer

In this subsection we shall discuss design guidelines for  $C$ . These are mostly given in the form of rationales in choosing the poles of  $G_0$ . We will then give an example to illustrate the stabilization step of the two step control design approach.

Since the design of  $C$  will be carried out on the basis of the model  $\bar{P}$ , we shall begin with the consideration of the transfer function

$$G_0 = \frac{\bar{P}}{1 + C\bar{P}} . \quad (5.7)$$

Before further guidelines are developed for designing  $C$ , we shall first summarize the guidelines that we discussed in Section 5.3.1. These are

- Corresponding to the poles of  $\bar{P}$  in the open left-half plane, assign exactly the same poles for  $G_0$ .
- Corresponding to the poles of  $\bar{P}$  at  $\sigma_1 \pm j\omega_1$ ;  $\sigma_1 > 0$ , assign  $-\sigma_1 \pm j\omega_1$  as the poles of  $G_0$ .

In order to be able to use the IMC method for designing the series controller  $K_i^j$  in the second step, it is necessary that  $G_i$  and  $G$  cannot have poles on the imaginary axis other than those at the origin. Furthermore, in view of the ease of applying the IMC method for step reference input to stable plants or plants that, other than having a simple pole at the origin, are stable, we suggest the following guidelines:

- If  $\bar{P}$  has poles at the origin, one of these poles may be retained if so desired (for example, for the purpose of rejecting step disturbances that may enter the plant output). The remaining poles at the origin are to be assigned according to the next guideline for poles on the imaginary axis.
- Corresponding to poles of  $\bar{P}$  on the imaginary axis (say at  $\pm j\omega_2$ ;  $\omega_2 \neq 0$ ),  $-\sigma_2 \pm j\omega_2$ ;  $\sigma_2 > 0$  are to be assigned as the poles of  $G_0$  to achieve a degree of stability (measured by  $\sigma_2$ ) deemed appropriate by the designer's experience for the situation at hand.

**Remark 5.3.12** Note that in the last guideline, using a larger value for  $\sigma_2$  has the advantage of improving the relative stability for the pole (or pair of complex-conjugate poles) in question. However, this usually comes with an increase in the controller gain. In the presence of high frequency unstructured model uncertainties, increasing the controller gain may induce destabilizing effects. Therefore it is important to caution against increasing  $\sigma_2$  too aggressively.

From the point of view of designing (in the second step) series controllers  $K_i^j$ , it is desirable that the bandwidth of the overall closed-loop transfer function  $GK_i^j/(1 + GK_i^j)$  (where  $G = P/(1 + CP)$  is the stabilized plant) is not constrained by unnecessary unstable open-loop zeros. Therefore  $C$  should not unnecessarily introduce these unstable zeros into  $G$  and  $G_0$ . It is easy to show that

$$G_0 = \frac{BD}{AD + BN} \quad , \quad (5.8)$$

where the polynomials  $A$ ,  $B$ ,  $D$ , and  $N$  are defined in Section 5.3.1 when the solution of the Diophantine equation (equation (5.5)) is discussed. We observe from equation (5.8) that the zeros of  $G_0$  are given by the zeros of  $\bar{P}$  and the poles of  $C$  if they are not cancelled by the zeros of the desired characteristic polynomial  $W = AD + BN$ . Since the zeros of  $W$  are always in the open left-half plane or at the origin, all the unstable zeros of  $\bar{P}$  must appear as the unstable zeros of  $G_0$ . Furthermore,  $G_0$  will have additional unstable zeros at the locations where  $C$  has unstable poles. These additional unstable zeros in  $G_0$  may impose limitations on the achievable overall closed-loop performance when series controllers are designed in the second step. Therefore it is important to design a stable  $C$ , if possible. It is well known [Doyle *et al.* 1992, Vidyasagar 1985a, Youla *et al.* 1974] that, if the order of  $C$  is not constrained to some fixed, pre-selected value, then a stable stabilizing  $C$  exists if and only if the unstable real zeros and the unstable real poles of the strictly proper  $\bar{P}$  possess the parity interlacing property. That is, a stable stabilizing  $C$  (exists if and only if its order is not constrained and the strictly proper  $\bar{P}$  has an even number of real poles between every pair of its unstable real zeros). We have the following observations:

1. In the absence of the parity interlacing property, the stabilizing compensator  $C$  is unstable. In this situation, we should try (but there is no guarantee of success for a pre-selected order of  $C$ ) to design  $C$  such that its unstable poles are not closer to the origin than the minimum distance between the unstable zeros of  $\bar{P}$  and the origin.

This attempts to prevent  $C$  from introducing unnecessary limitations on the overall closed-loop performance.

2. If  $\bar{P}$  cannot be stabilized by a stable  $C$  and if the order of  $C$  is not constrained, then the unstable real poles in a  $C$  that are necessary for the stabilization of  $\bar{P}$  are those which, when augmented with the unstable real poles of  $\bar{P}$ , satisfy the parity interlacing property [Vidyasagar 1985a]. Clearly, the range of locations that each of these necessary unstable real poles of  $C$  should appear is constrained by the parity interlacing property. Particularly, it is apparent that the smallest unstable real pole in  $C$  that is necessary for satisfying the parity interlacing property has to be larger than the smallest unstable real zero of  $\bar{P}$ . Therefore the unstable real zero introduced into  $G_0$  (and  $G$ ) by the smallest necessary unstable real pole of  $C$  is always larger than the smallest unstable real zero of  $\bar{P}$  inherited by  $G_0$ . Hence, if  $C$  has unstable real poles only for satisfying the parity interlacing property, it is automatically guaranteed that no unnecessary limitations are imposed on the overall closed-loop performance by the unstable poles of  $C$ . We emphasize again that, if the order of  $C$  is pre-selected, the above results may not be achievable.

We summarize the above observations into the following guideline:

- After  $C$  is designed, examine whether its unstable poles are only those that, when taken together with the unstable poles of  $\bar{P}$ , are necessary for satisfying the parity interlacing property. Since we do not usually like the order of  $C$  to be excessively large (so that it can be implemented without too much difficulty using current technologies), we may not be able to find a reasonably low order  $C$  that has the above desirable property. In this situation, the locations of the offensive real unstable zeros introduced into  $G_0$  by  $C$  may be used to estimate the extent to which we may push the overall closed-loop bandwidth through iterative identification and control design in the second design stage.

After we have assigned  $n$  poles for  $G_0$  (recall that  $n$  is the order of  $\bar{P}$ ) according to the above considerations, there are still  $n$  more poles in  $G_0$  to be assigned. It was shown in [Leon de la Barra 1992] that if the stable zeros of  $P$  are located well to the right of the dominant poles of the transfer function  $CP/(1 + CP)$ , step-like disturbances at the input of

$P$  may cause the control signal at the actuator input of  $P$  to have large excursions. This may cause actuator saturation. Assuming that these stable zeros of  $P$  are also the zeros of  $\bar{P}$ , the problem can then be alleviated by cancelling these zeros by the poles of  $C$ . In this manner we obtain a stable pole-zero cancellations in  $CP/(1 + CP)$  at the locations of the problematic (open-loop) zeros of  $P$ . Since attempting to cancel poorly damped (although stable) zeros of  $\bar{P}$  by the poles of  $C$  may, due to modelling error, lead to an unstable  $G$ , we should only attempt to cancel well-damped stable zeros of  $\bar{P}$ . Summarizing, we have the following:

- It is desirable to cancel, via the poles of  $C$ , the stable well damped zeros of  $\bar{P}$  that are located within the expected overall designed closed-loop bandwidth. This can be accomplished by assigning the stable well damped zeros of  $\bar{P}$  as the zeros of the characteristic polynomial  $W = AD + BN$ . The zeros of  $W$  at these locations will then disappear as stable (well damped) pole-zero cancellations in  $C\bar{P}/(1 + C\bar{P})$  and in  $G_0 = \bar{P}/(1 + C\bar{P})$ .

**Remark 5.3.13** Note that  $G_0 = \bar{P}/(1 + C\bar{P})$  will still have zeros at the locations where  $\bar{P}$  has stable well damped zeros. However, these stable zeros in  $G_0$  are easily handled by the IMC method in the second design stage.

Finally, before we can assign the remaining poles for  $G_0$  (if there are any more left), it is helpful to consider the following.

In the guidelines for pole-placement that we have discussed so far, the high frequency unmodelled dynamics associated with  $\bar{P}$  have not been taken into account. In order to achieve robust stabilization, such that  $P$  is stabilized by the  $C$  designed on the basis of  $\bar{P}$ , we would like the open-loop gain  $|C(j\omega)\bar{P}(j\omega)|$  to become sufficiently small in the frequency range where the high frequency unmodelled dynamics may be significant (see Remark 5.3.9 regarding the advantage of having a quick high frequency roll off for  $|C(j\omega)\bar{P}(j\omega)|$ ). This implies that, from robust stability point of view, we would like  $|G_0(j\omega)|$  to roll off at a sufficiently low frequency. On the other hand, from the point of view of keeping  $|G_0(j\omega)|$  reasonably large for frequencies up to approximately twice the expected overall closed-loop bandwidth, it is desirable that  $|G_0(j\omega)|$  does not start to roll off at too low a frequency. Hence we need to compromise. This may be achieved by placing the remaining poles of

$G_0$  at locations between  $-2\omega_b$  and  $-10\omega_b$ , where  $\omega_b$  is the expected overall closed-loop bandwidth.

Now we list the guidelines for designing  $C$  as follows:

1. Retain all the poles of  $\bar{P}$  in the open left-half plane as the poles of  $G_0$ .
2. Corresponding to the poles of  $\bar{P}$  at  $\sigma_1 \pm j\omega_1$ ;  $\sigma_1 > 0$ , assign  $-\sigma_1 \pm j\omega_1$  as the poles of  $G_0$ .
3. If  $\bar{P}$  has poles at the origin, one of these poles may be retained if so desired (for example, for the purpose of rejecting step disturbances that may enter the plant output). The remaining poles at the origin are to be assigned according to the next guideline for poles on the imaginary axis.
4. Corresponding to the poles of  $\bar{P}$  at  $\pm j\omega_2$ , assign  $-\sigma_2 \pm j\omega_2$ ;  $\sigma_2 > 0$  as the poles of  $G_0$  to achieve a desirable degree of stability (measured by  $\sigma_2$ ) deemed appropriate by the designer's experience for the situation at hand. It is important to emphasize that increasing  $\sigma_2$  too aggressively may cause instability, especially in the face of high frequency unstructured model uncertainties.
5. Cancel stable, well damped zeros of  $\bar{P}$  by the poles of  $C$ . This is accomplished by assigning the stable well damped zeros of  $\bar{P}$  as the zeros of the characteristic polynomial  $W$ . The zeros of  $W$  at these locations will then disappear as stable (well damped) pole-zero cancellations in  $C\bar{P}/(1 + C\bar{P})$  and in  $G_0 = \bar{P}/(1 + C\bar{P})$ .
6. Assign the remaining poles of  $G_0$  at locations between  $-2\omega_b$  and  $-10\omega_b$ , where  $\omega_b$  is the expected overall closed-loop bandwidth.
7. Examine whether  $C$  is stable if the unstable real zeros and the unstable real poles of the strictly proper model  $\bar{P}$  possess the parity interlacing property. If this requirement is not met, it is necessary to modify the locations of the poles assigned on the basis of guideline (4) to guideline (6) and/or increase the assumed order of  $C$  and repeat the design procedure. Note that even after the assumed order of  $C$  is increased, there is no guarantee that the stabilizing  $C$  is stable. In the latter situation, the offensive real unstable zeros introduced into  $G_0$  by  $C$  may be used to estimate the extent to which we may push the overall closed-loop bandwidth through iterative identification and control design in the second design stage.

8. If the unstable real zeros and unstable real poles of the strictly proper model  $\bar{P}$  do not possess the parity interlacing property, examine whether  $C$  only has unstable poles for satisfying the parity interlacing property. If this requirement is not satisfied, it is necessary to modify the locations of the poles assigned on the basis of guideline (4) to guideline (6) and/or increase the assumed order of  $C$  and repeat the design procedure. There is no guarantee that a  $C$  with the above desirable property can be found, even after the order of  $C$  is increased. In this situation, the offensive real unstable zeros introduced into  $G_0$  by  $C$  may be used to estimate the extent to which we may push the overall closed-loop bandwidth through iterative identification and control design in the second design stage.
9. If the designed  $C$ , due to high frequency model uncertainties, does not stabilize  $P$ , it is necessary to modify the locations of the poles assigned on the basis of guideline (4) to guideline (6) and repeat the design procedure. This is usually accomplished by moving those poles of  $G_0$  that correspond to the poles of  $\bar{P}$  on the  $j\omega$ -axis nearer to the  $j\omega$ -axis (so that the controller gain is reduced), or by moving those poles of  $G_0$  between  $-2\omega_b$  and  $-10\omega_b$  nearer to the origin (so that the magnitude of the complementary-sensitivity function,  $CG_0$ , starts to roll off at a lower frequency).

**Remark 5.3.14** It is important to emphasize that what we have described are *neither synthesis procedures nor rigid design rules*. Just like any design method, *trial and error may very well be necessary* in the process of designing a  $C$  which stabilizes  $\bar{P}$  and  $P$ .

**Remark 5.3.15** The requirements on  $C$  stated in guidelines (7) and (8) may not be achievable if  $C$  is constrained to have the same order as  $\bar{P}$ . It may be necessary for the order of  $C$  to be higher than that of  $\bar{P}$  before the requirements set out in in guidelines (7) and (8) can be met. In this case, appropriate number of additional conditions have to be imposed on the basis of guideline (6) such that a Diophantine equation similar to equation (5.5) will have a unique solution. Furthermore we must warn that, because it is necessary to limit the order of  $C$  such that it is practically implementable with current technologies, it may not be possible to design a  $C$  that (together with  $\bar{P}$ ) satisfies the parity interlacing property under such constraints.

**Remark 5.3.16** Before a  $C$  that is designed on the basis of  $\bar{P}$  can stabilize  $P$ , it is necessary that modelling errors associated with  $\bar{P}$  are sufficiently small at the critical frequencies

corresponding to the unstable poles of  $\bar{P}$ .

To illustrate the design method described, we shall use the model,

$$\bar{P} = \frac{s - 1}{(s + 0.5)(s - 2)},$$

that we have discussed in one of the examples of Section 5.2.2. Observe that the unstable real zero and unstable real pole of  $\bar{P}$  do not possess the parity interlacing property. Therefore an unstable  $C$  is necessary for the stabilization of  $\bar{P}$ .

Since the order of  $\bar{P}$  is two, the minimum required order for a strictly proper  $C$  is two. This will result in a fourth order characteristic polynomial  $W$ . Following the guidelines given in the above discussions, we shall retain the pole of  $\bar{P}$  at  $s = -0.5$  in  $G_0$ . Corresponding to the pole of  $\bar{P}$  at  $s = 2$ , we assign a pole of  $G_0$  to  $s = -2$ . To cancel the effect of the unstable zero (of both  $\bar{P}$  and  $G_0$ ) at  $s = 1$  on  $|G_0(j\omega)|$ , we assign a pole of  $G_0$  to  $s = -1$ . Since the unstable zeros in  $\bar{P}$  and  $G_0$  are at  $s = 1$ , under the assumption that the unstable poles of  $C$  that we are going to design are further from the origin than  $s = 1$  is from the origin, we would design an overall closed-loop system to have a bandwidth not exceeding 2 rad/s. We therefore assign the remaining pole of  $G_0$  to  $s = -4$ . Therefore the desired characteristic polynomial of  $G_0$  become

$$W(s) = (s + 0.5)(s + 2)(s + 1)(s + 4).$$

By solving an appropriate Diophantine equation as described in Section 5.3.1, we obtain

$$C(s) = \frac{72(s + 0.5)}{(s - 3.2621)(s + 12.2621)},$$

and

$$G_0(s) = \frac{(s - 3.2621)(s + 12.2621)}{(s + 0.5)(s + 2)(s + 4)} \left[ \frac{s - 1}{s + 1} \right].$$

The frequency responses of the parallel output feedback stabilizer  $C(s)$  and the complementary-sensitivity function  $C(s)G_0(s)$  are shown, respectively, in Figure 5.11 and Figure 5.12.

**Remark 5.3.17** It is apparent that the unstable real pole of  $C$  at  $s = 3.2621$  is further away from the origin than the unstable real zero of  $\bar{P}$  at  $s = 1$  is away from the origin. Therefore the unstable real zero of  $G_0$  introduced by  $C$  at  $s = 3.2621$  does not impose unnecessary

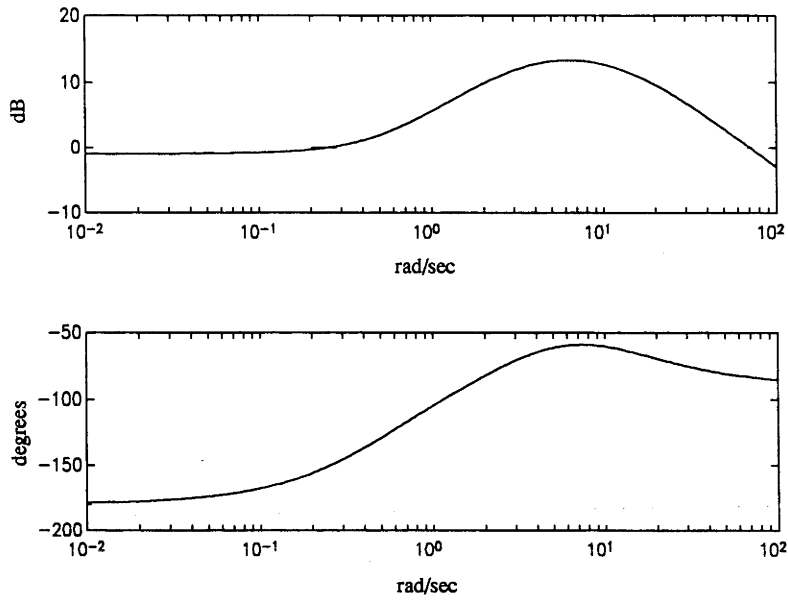


Figure 5.11: Frequency response of the parallel feedback stabilizer  $C(s)$

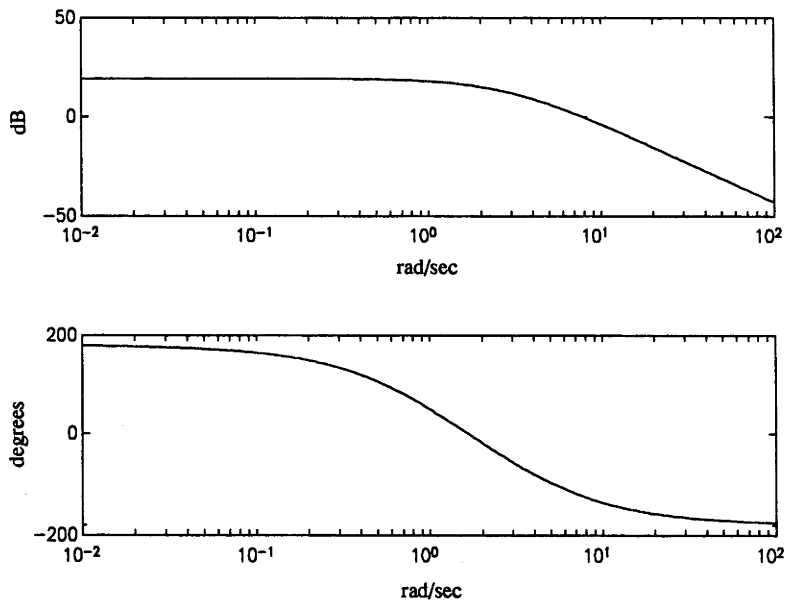


Figure 5.12: Frequency response of the complementary-sensitivity function  $C(s)G_0(s)$



limits on the overall closed-loop performance, as compared to the unstable real zero at  $s = 1$  inherited from  $\bar{P}$ .

**Remark 5.3.18** The system  $G = P/(1 + CP)$  is guaranteed to be stable if the designed complementary-sensitivity-function weighted multiplicative modelling errors associated with  $\bar{P}$  satisfies

$$\left| \frac{P(j\omega) - \bar{P}(j\omega)}{\bar{P}(j\omega)} C(j\omega) G_0(j\omega) \right| < 1 .$$

From Figure 5.12, we can obtain an estimate of the size of tolerable multiplicative *unstructured* modelling errors associated with  $\bar{P}$  at various frequencies.

Before we end the discussions of the two step iterative identification and control design approach, it suffices to say that after  $\bar{P}$  is stabilized by  $C$ , all stabilizing series controllers  $K_i^j$  for the overall designed closed-loop system are described by the parametrization

$$K_i^j = \frac{Q_i^j}{1 - G_i Q_i^j} ,$$

where  $G_i$  are stable models for the stabilized plant

$$G = \frac{P}{1 + CP} .$$

## 5.4 Simulation Results

We shall present the results of two simulation examples in this section. In both examples, the noise disturbance at the output of  $P$  has a constant energy density of 0.0025 over the frequency range of interest. Example 1 illustrates the situation where the effect of high frequency unmodelled dynamics associated with the initial model of an unstable plant is the main obstacle to achieving a large closed-loop bandwidth. By using the two step iterative identification and control design approach described in Section 5.3, we successfully increased the bandwidth of the overall closed-loop system. In Example 2, the initial model of the unstable plant  $P$  is identical to the transfer function  $\bar{P}$  used in the examples of Section 5.2.2 and Section 5.3.2. It should be realized that in this situation, where  $\bar{P}$  and

$P$  have unstable real poles larger than unstable real zeros, serious fundamental limitations [Doyle *et al.* 1992, Freudenberg and Looze 1985, Middleton and Goodwin 1990] are imposed on the achievable closed-loop performance. The system response will be sensitive to noise disturbances when the closed-loop bandwidth is smaller than the largest magnitude of the unstable poles, and will have large undershoot when the closed-loop bandwidth is larger than the smallest magnitude of the unstable zeros. Furthermore, because the unstable real poles are larger than the unstable real zeros, it is impossible to achieve low sensitivity to noise disturbances while having a small undershoot in the system response. It is important to emphasize that we *do not* claim to be able to overcome the above-mentioned fundamental limitations. The *sole objective* of Example 2 is to show that, under this adverse situation, it is still possible to alleviate the effect of initial modelling errors through the two step iterative identification and control design approach where the second step involves the iterative identification and control design procedure. The graphs for Example 1 and Example 2 are documented in Appendix 5.1 and Appendix 5.2, respectively, at the end of the chapter.

### 5.4.1 Example 1

In this example we consider an unstable plant with

$$P(s) = \frac{0.1(s - 4)}{(s - 0.1)(s^2 + 0.2s + 4)}$$

and

$$H_1(s) = 1 .$$

The noise disturbance  $e$  is zero mean and has a constant energy density of 0.0025 within the bandwidth of interest.

It is given that a model of  $P(s)$  is

$$\bar{P}(s) = \frac{0.1}{-s + 0.1} .$$

The frequency responses of  $P$  and  $\bar{P}$  are shown in Figure 5.13.

Assuming that it is desirable to have a closed-loop bandwidth of at least 0.5 rad/s. We shall show that this design objective can be achieved by the two step control design approach.

In the first step we stabilize  $\bar{P}$  with a strictly proper parallel output feedback compensator  $C$ . Following the design guidelines of Section 5.3.2, we assign the characteristic polynomial of  $G_0 = \bar{P}/(1+C\bar{P})$  as  $(s+0.1)(s+1)$ . The required  $C$  and  $G_0$  are found to be, respectively,

$$C(s) = -\frac{2.2}{s+1.2}$$

and

$$G_0(s) = -\frac{0.1(s+1.2)}{(s+0.1)(s+1)}.$$

Note that  $C$  is stable.

It can easily be shown that the transfer function of the stabilized plant is

$$G(s) = \frac{0.1(s^2 - 2.8s - 4.8)}{s^4 + 1.3s^3 + 4.1s^2 + 4.156s + 0.4}$$

with poles at  $s = -0.1072$ ,  $s = -0.9892$  and  $s = -0.1018 \pm j1.939$ , and zeros at  $s = -1.2$  and  $s = 4.0$ . Note that the unstable zero at  $s = 4.0$  is inherited from  $P$ . The corresponding noise transfer function  $H = H_1/(1+CP)$  becomes

$$H(s) = \frac{s^4 + 1.3s^3 + 4.1s^2 + 4.376s - 0.48}{s^4 + 1.3s^3 + 4.1s^2 + 4.156s + 0.4}.$$

Since the negative signs in  $G_0$  and  $G$  can be eliminated easily by cascading an inverter with each of these transfer functions, we shall omit them in the following discussions and assume that

$$G_0(s) = \frac{0.1(s+1.2)}{(s+0.1)(s+1)}$$

and

$$G(s) = \frac{0.1(-s^2 + 2.8s + 4.8)}{s^4 + 1.3s^3 + 4.1s^2 + 4.156s + 0.4}.$$

The frequency responses of  $G$  and  $G_0$  are shown in Figure 5.14.

To begin the second design step, we apply the standard IMC design method to design, on the basis of the initial model  $G_0$  for the stabilized plant  $G$ , a sequence of series controllers  $\{K_0^j; j = 0, 1, \dots, f\}$  (corresponding to a sequence of increasing overall designed closed-loop bandwidth  $\{\lambda_0^j; j = 0, 1, \dots, f\}$ , where  $\lambda_0^f$  is the final achievable bandwidth before a better model  $G_1$  is necessary). To avoid exciting high frequency modelling errors associated with  $G_0$ , we start with an overall designed closed-loop bandwidth of  $\lambda_0^0 = 0.1$  rad/s. For such a small bandwidth, we cannot find any perceptible effects of high frequency modelling

errors associated with  $G_0$  on the closed-loop step responses. We then progressively increase the overall designed closed-loop bandwidth by re-designing  $K_0^j$ . When the overall designed closed-loop bandwidth reaches  $\lambda_0^f = 0.75$  rad/s, it was found, by using the model validation methods described in Section 4.6 that effects of high frequency modelling errors associated with  $G_0$  on the closed-loop step response have become significant. The designed closed-loop step response and the corresponding actual closed-loop step response (with and without noise disturbances) are shown in Figure 5.15 to Figure 5.17.

By using the control-relevant closed-loop system identification procedure summarized in Section 4.8, we set the bandwidth of the low-pass data filter to 2 rad/s, and  $N_n = [3\ 6\ 6\ 3\ 1]$ . The identification results in

$$\hat{R}_0^f = \frac{-1.2291s^2 + 0.1531s - 0.0026}{s^3 + 0.174s^2 + 3.1384s + 0.133} ,$$

$$\hat{R}_0^f = \left( \begin{array}{c} -0.1229s^4 - 0.2244s^3 \\ -0.081s^2 + 0.0133s - 0.0002 \end{array} \right) \Bigg/ \left( \begin{array}{c} s^5 + 1.274s^4 + 3.4298s^3 \\ +3.6027s^2 + 0.4602s + 0.0133 \end{array} \right) ,$$

and

$$G_1 = \left( \begin{array}{c} -0.0229s^5 - 0.1041s^4 + 0.2576s^3 \\ +0.6678s^2 + 0.3079s + 0.012 \end{array} \right) \Bigg/ \left( \begin{array}{c} s^6 + 2.024s^5 + 5.0767s^4 \\ +6.8494s^3 + 3.1381s^2 \\ +0.3514s + 0.0101 \end{array} \right) .$$

After performing model reduction, a new reduced-order model<sup>4</sup> for  $G$  is validated as

$$G_1(s) = \frac{-0.0102s^2 - 0.0939s + 0.4537}{s^3 + 0.3879s^2 + 3.805s + 0.3657} .$$

The frequency responses of  $G$  and  $G_1$  are compared in Figure 5.18.

On the basis of  $G_1$  we design the sequence of controllers  $\{K_1^j ; j = 0, 1, 2, \dots\}$ . We start with  $\lambda_1^0 = 0.75$  rad/s. The resulting step responses are presented in Figure 5.19 to Figure 5.21. When the overall designed closed-loop bandwidth is increased to  $\lambda_1^f = 3.0$  rad/s, it was found that a more accurate model is necessary for increasing the closed-loop bandwidth further. At this stage, the step responses are shown in Figure 5.22 to Figure 5.24.

For the identification, the bandwidth of the low-pass data filter is 3 rad/s and  $N_n = [4\ 6\ 6\ 6\ 1]$ . The identification results in

$$\hat{R}_1^f = \frac{-0.0948s^3 + 0.01185s^2 - 0.2783s + 0.06134}{s^4 + 1.842s^3 + 6.018s^2 + 6.685s + 6.2019} ,$$

<sup>4</sup>Model reduction was achieved by the method of frequency weighted balanced truncation as mentioned in Remark 3.3.4.

$$\widehat{R}_1^f = \left( \begin{array}{l} -0.00021s^9 - 0.011s^8 \\ -0.0796s^7 - 0.2332s^6 \\ -0.5497s^5 - 1.084s^4 \\ -1.075s^3 - 1.386s^2 \\ +0.4067s - 0.1648 \end{array} \right) / \left( \begin{array}{l} s^{10} + 2.8045s^9 + 15.039s^8 \\ +31.566s^7 + 80.018s^6 + 121.58s^5 \\ +178.74s^4 + 175.16s^3 + 141.65s^2 \\ +56.272s + 4.3212 \end{array} \right),$$

and

$$G_2 = \left( \begin{array}{l} -0.0104s^{17} - 0.1839s^{16} \\ -0.8227s^{15} - 2.899s^{14} \\ -5.722s^{13} - 0.9168s^{12} \\ +39.96s^{11} + 197.24s^{10} \\ +580.02s^9 + 1339.5s^8 \\ +2444.4s^7 + 3711.8s^6 \\ -4531.9s^5 + 4508.1s^4 \\ +3378.4s^3 + 1812.6s^2 \\ +520.85s + 36.548 \end{array} \right) / \left( \begin{array}{l} s^{18} + 8.0342s^{17} \\ +47.786s^{16} + 209.15s^{15} \\ +739.54s^{14} + 2208.3s^{13} \\ +5579.1s^{12} + 12270s^{11} \\ +23276s^{10} + 38565s^9 \\ +55043s^8 + 67743s^7 \\ +70066s^6 + 60113s^5 \\ +40377s^4 + 19988s^3 \\ +5934.8s^2 + 713.79s + 28.526 \end{array} \right).$$

After performing frequency weighted model reduction, a new model for  $G$  is validated as

$$G_2 = \frac{-0.0106s^4 - 0.1086s^3 + 0.3092s^2 + 0.3612s + 0.0125}{s^5 + 1.0896s^4 + 4.0596s^3 + 3.2852s^2 + 0.3924s + 0.0096}$$

Its frequency response is compared to that of  $G$  in Figure 5.25. At  $\lambda_2^0 = 3.0$ , the step responses for the closed-loop system designed on the basis of  $G_2$  are shown in Figure 5.26 to Figure 5.28.

With  $G_2$ , we can easily increase the overall closed-loop bandwidth to 6.0 rad/s. The closed-loop step responses when the overall closed-loop bandwidth is 6.0 rad/s are shown in Figure 5.29 to Figure 5.31.

## 5.4.2 Example 2

In this example, the unstable plant is described by

$$P(s) = \frac{400(s-1)}{(s+0.5)(s^2+25s+400)(s-2)}$$

and

$$H_1(s) = 1.$$

The noise disturbance  $e$  is zero mean and has a constant energy density of 0.0025 within the bandwidth of interest.

A given model of  $P$  is

$$\bar{P}(s) = \frac{s - 1}{(s + 0.5)(s - 2)}$$

The frequency responses of  $P$  and  $\bar{P}$  are shown in Figure 5.32.

Note that  $\bar{P}$  is the same as the unstable model employed in the examples of Section 5.2.2 and Section 5.3.2. In Section 5.3.2 we have found that, in the first design step, a strictly proper parallel output feedback stabilizer for  $\bar{P}$  is given by

$$C(s) = \frac{72(s + 0.5)}{(s - 3.2621)(s + 12.2621)}$$

The resulting stabilized plant and the corresponding model are given, respectively, by

$$G(s) = \frac{400(s^3 + 8s^2 - 49s + 40)}{s^6 + 32.5s^5 + 533s^4 + 1688.5s^3 + 8315s^2 + 7000s + 1600}$$

and

$$G_0(s) = \frac{(s - 3.2621)(s + 12.2621)}{(s + 0.5)(s + 2)(s + 4)} \left[ \frac{s - 1}{s + 1} \right]$$

The noise transfer function  $H = H_1/(1 + CP)$  is given by

$$H(s) = \left( \begin{array}{c} s^6 + 32.5s^5 + 533s^4 + 1688.5s^3 \\ -20485s^2 + 21400s + 16000 \end{array} \right) \bigg/ \left( \begin{array}{c} s^6 + 32.5s^5 + 533s^4 + 1688.5s^3 \\ +8315s^2 + 7000s + 1600 \end{array} \right)$$

Note that both  $G$  and  $G_0$  are stable. The frequency responses of  $G$  and  $G_0$  are shown in Figure 5.33.

Following the idea of the iterative identification and control design approach, we start with a small overall designed closed-loop bandwidth of  $\lambda_0^0 = 0.1$  rad/s and design the series controller  $K_0^0$ , on the basis of  $G_0$ , by the standard IMC design method. The step responses of the resulting closed-loop system are shown in Figure 5.34 to Figure 5.36. It was verified by the methods described in Section 4.6 that the model errors associated with  $G_0$  have negligible effects on the closed-loop response for  $\lambda_0^0 = 0.1$  rad/s. In fact it was not until  $\lambda_0^f = 4.0$  rad/s that the model errors associated with  $G_0$  has significant effects on the closed-loop response. The step responses at this stage is presented in Figure 5.37 to Figure 5.39. Note that the actual closed-loop responses are highly oscillatory. To identify a new model, we set the bandwidth of the low-pass data filter to 8 rad/s and  $N_n = [5 \ 6 \ 6 \ 5 \ 1]$ . The identified transfer functions are

$$\hat{R}_0^f = \left( \begin{array}{c} -0.6351s^4 + 8.909s^3 - 29.236s^2 \\ +37.011s - 22.298 \end{array} \right) \bigg/ \left( \begin{array}{c} s^5 + 9.257s^4 + 78.855s^3 \\ +231.77s^2 + 504.14s + 789.33 \end{array} \right)$$

and

$$G_1 = \left( \begin{array}{c} 0.3649s^{16} + 18.881s^{15} \\ +452.093s^{14} + 5982.2s^{13} \\ +49363.6s^{12} + 276796.4s^{11} \\ +906122s^{10} + 1509733.7s^9 \\ -2939725.8s^8 - 25276457s^7 \\ -79918053s^6 - 165528014s^5 \\ -189827015s^4 - 88284308s^3 \\ +76724424s^2 + 244295487s \\ +99687505 \end{array} \right) / \left( \begin{array}{c} s^{17} + 32.51s^{16} + 590.01s^{15} \\ +7029.71s^{14} + 61401.4s^{13} \\ +409165.4s^{12} + 2147784.8s^{11} \\ +9104396.9s^{10} + 31355509.7s^9 \\ +87846147.1s^8 + 200230435.5s^7 \\ +367631228.7s^6 + 533105850.3s^5 \\ +594271053s^4 + 485388286s^3 \\ +265346513s^2 + 83420902s \\ +11095195 \end{array} \right).$$

After performing frequency weighted model reduction and model validation, we have the new model

$$G_1(s) = \left( \begin{array}{c} 0.3785s^{11} + 14.58s^{10} \\ +290.521s^9 + 2114.88s^8 \\ +11796.6s^7 + 4867.14s^6 \\ -48554.3s^5 - 309692s^4 \\ -581936.1s^3 - 195981.1s^2 \\ -340906.2s + 1210046.8 \end{array} \right) / \left( \begin{array}{c} s^{12} + 22.156s^{11} + 312.05s^{10} \\ +2556.3s^9 + 16457s^8 + 66104.6s^7 \\ +248183s^6 + 536823.3s^5 \\ +1135468s^4 + 1227317.3s^3 \\ +1378618.5s^2 + 569837.6s \\ +133434 \end{array} \right).$$

The frequency responses of  $G$  and  $G_1$  are compared in Figure 5.40.

On the basis of  $G_1$ , we design  $K_1^0$  while keeping the overall designed closed-loop bandwidth as  $\lambda_1^0 = 4.0\text{rad/s}$ . The resulting step responses are shown in Figure 5.41 to Figure 5.43. Notice that the oscillations in the actual responses due to model errors associated with  $G_0$  are almost eliminated for the controller designed on the basis of  $G_1$ .

## 5.5 Summary and Discussions

In this chapter we have reviewed some difficulties of designing closed-loop systems for unstable plants by the one step control design methods discussed in [Campi *et al.* 1994] and [Morari and Zafriou 1989]. To overcome these difficulties, we have presented a two step iterative identification and control design approach for unstable plants. We have shown that, after stabilizing the unstable plant with a strictly proper parallel output feedback compensator, it is possible to apply the iterative identification and control design methodology (embedded with the standard IMC design method and a control-relevant closed-loop system identification procedure) to extend the overall closed-loop bandwidth progressively. The proposed approach is illustrated with two simulation examples. These examples represent

two different scenarios. Example 1 has shown that the approach produces very encouraging results when high frequency modelling errors associated with the initial model are the main constraints to a large overall closed-loop bandwidth. Example 2 indicated that, although *fundamental limitations* imposed on the closed-loop performance by the plant's undesirable unstable pole-zero structure cannot be overcome by any control design method (including our two step iterative identification and control design approach), the adverse conditions do not prevent the iterative identification and control design methodology from successfully alleviating the oscillatory behaviour in the closed-loop response that is due to high frequency modelling errors.

Finally we emphasize that, although the two step iterative identification and control design approach shows promising results, the following issues have not been investigated thoroughly and should be considered for future research:

- We have highlighted in Remark 5.1.4 that, due to the fundamental limitations imposed by the plant's unstable poles on the area under the logarithmic magnitude of the sensitivity function, the effects of noise disturbance at the plant output may be accentuated in the process of stabilization and may cause the problem of identifying the stabilized plant to become more difficult. This effect will depend on the choice of stabilization schemes and control design methods. This is an important issue that has to be investigated carefully. We believe that  $\mathcal{H}_\infty$  control theory has a big role to play here.
- Although the pole-placement technique embedded in the two step iterative identification and control design approach shows encouraging results, we must emphasize that the question of how to design a low order stabilizer (for example, comparable to the order of a given unstable model), not limited to the method introduced here, such that it satisfies (together with a given model) the parity interlacing property is still far from resolved. This is a very challenging problem that is of major interest in its own right.



Appendix 5.1: Graphs for Simulation Example 1

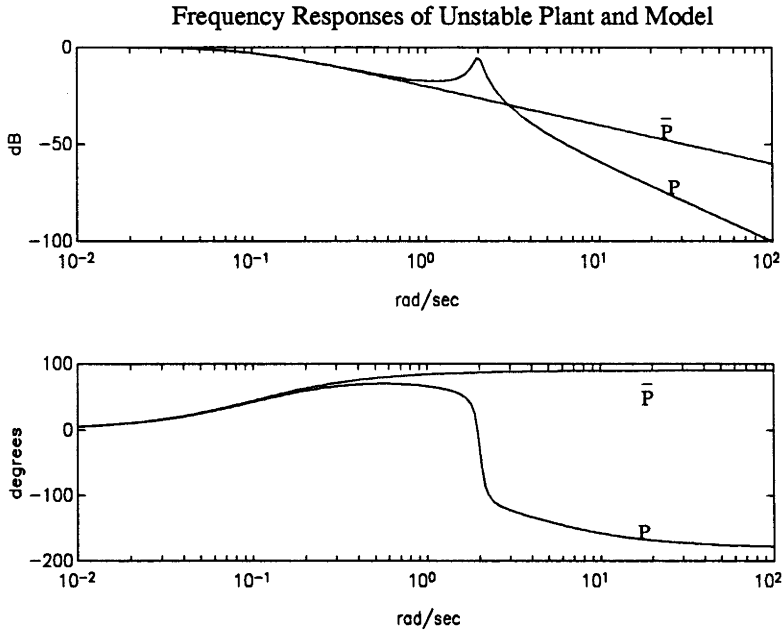


Figure 5.13: Frequency responses of  $P$  and  $\bar{P}$

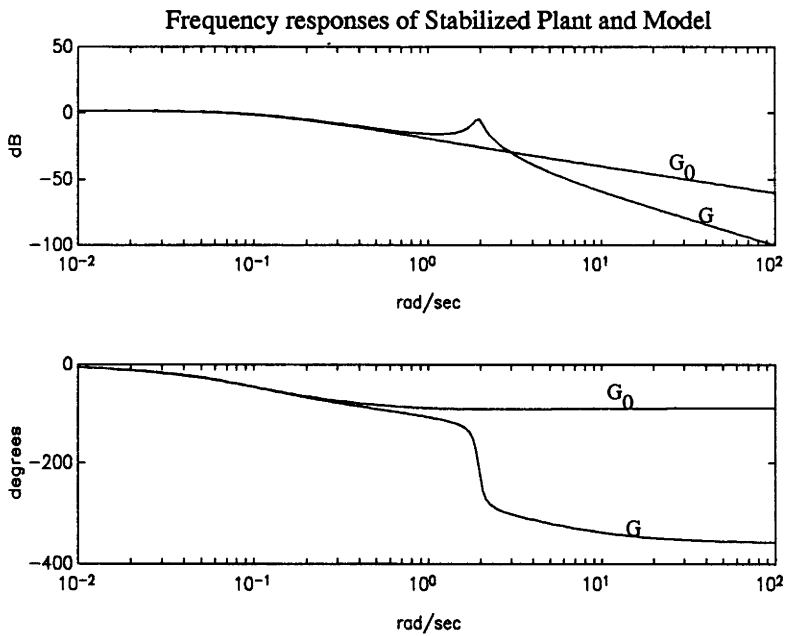


Figure 5.14: Frequency responses of  $G$  and  $G_0$

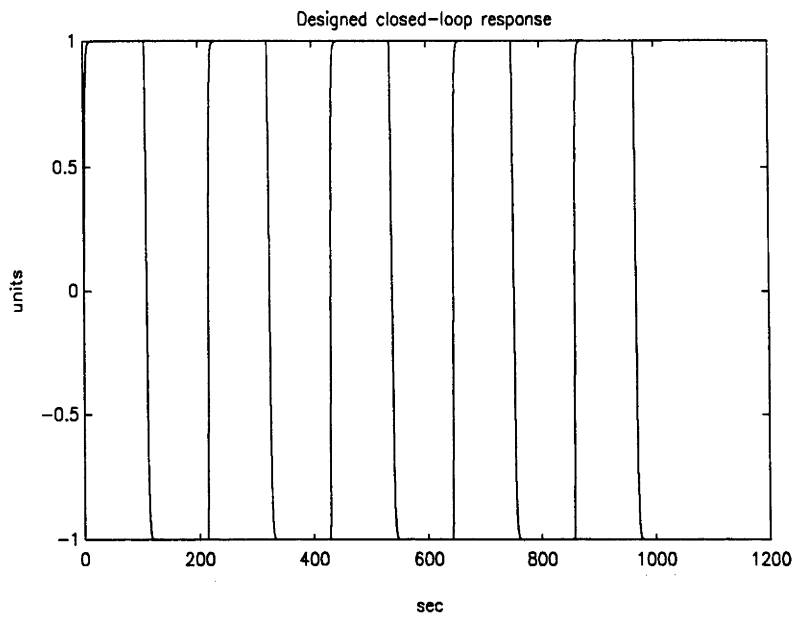


Figure 5.15: Response of designed closed-loop for a square wave input ( $\lambda_0^f = 0.75$ )

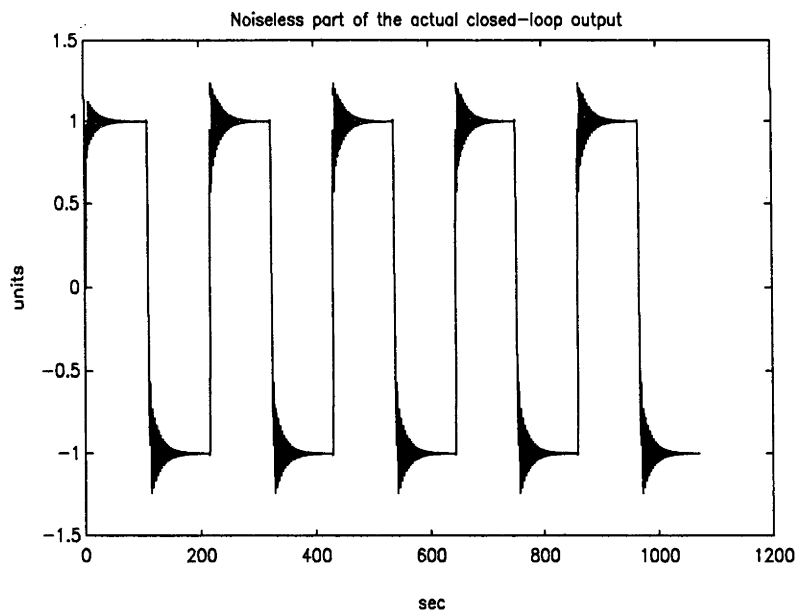


Figure 5.16: Noiseless response of actual closed-loop for a square wave input ( $\lambda_0^f = 0.75$ )

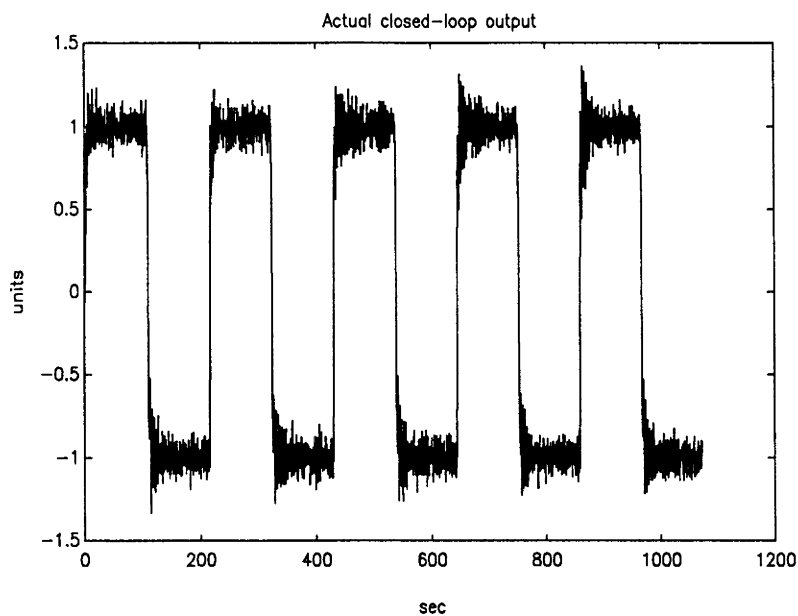


Figure 5.17: Noisy response of actual closed-loop for a square wave input ( $\lambda_0^f = 0.75$ )

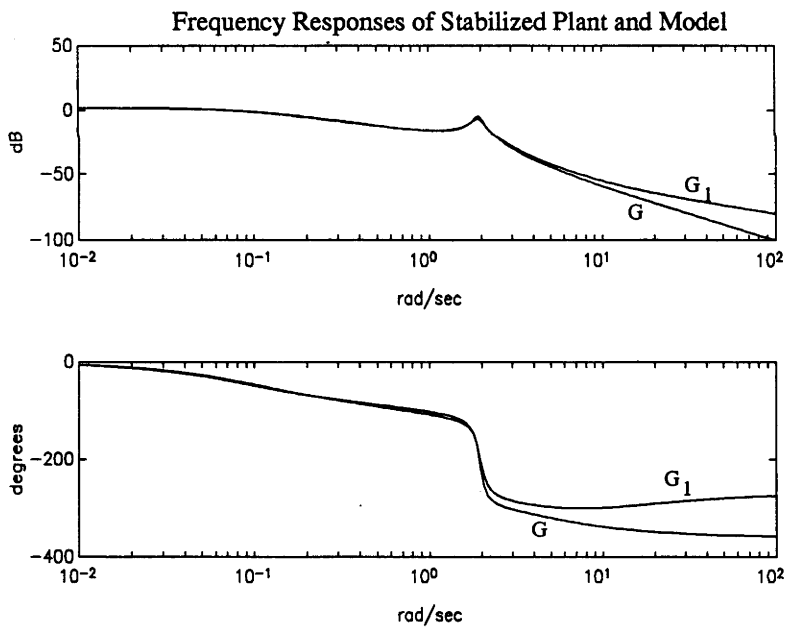


Figure 5.18: Frequency responses of  $G$  and  $G_1$

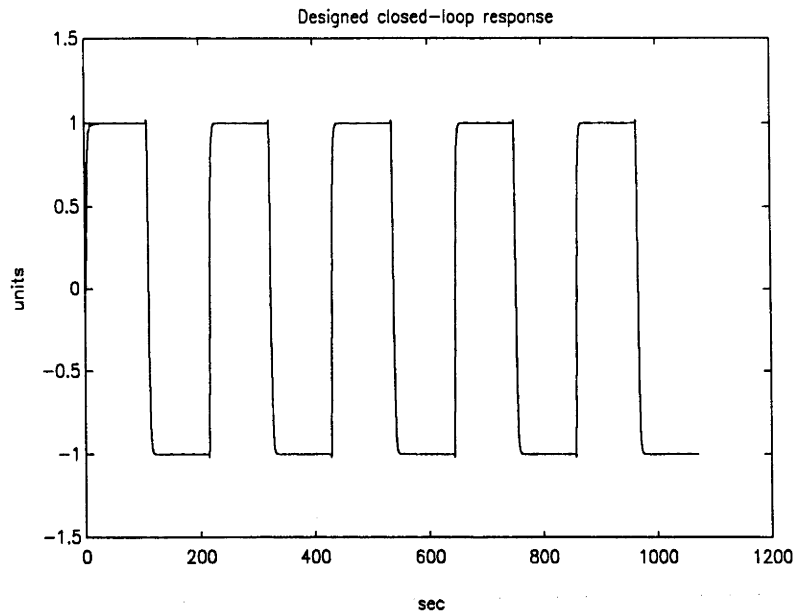


Figure 5.19: Response of designed closed-loop for a square wave input ( $\lambda_1^0 = 0.75$ )

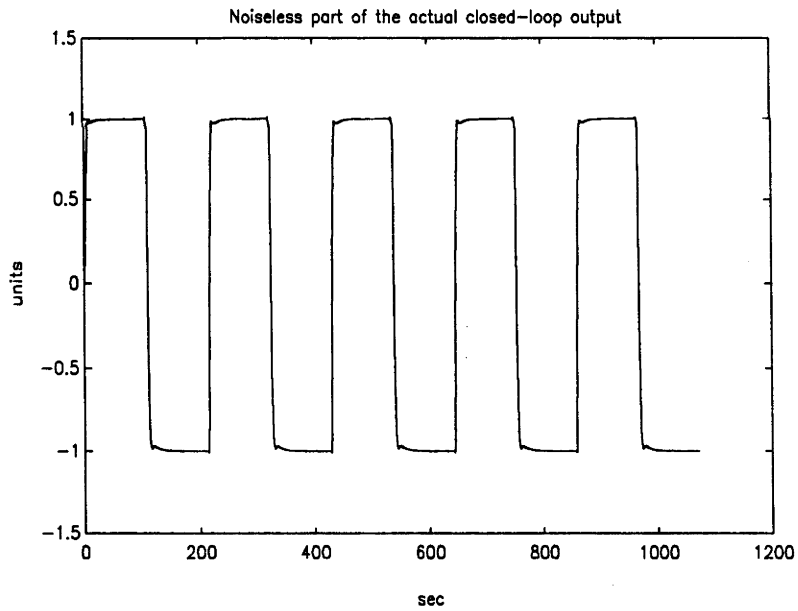


Figure 5.20: Noiseless response of actual closed-loop for a square wave input ( $\lambda_1^0 = 0.75$ )

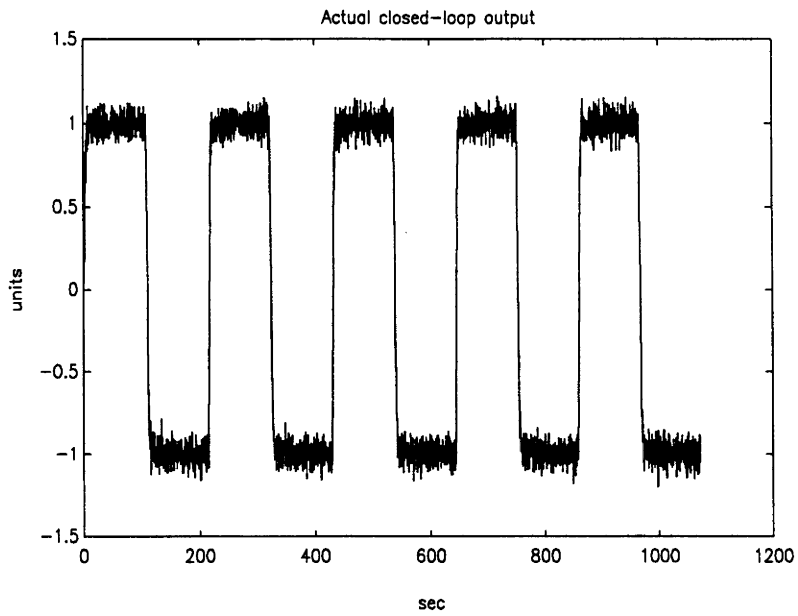


Figure 5.21: Noisy response of actual closed-loop for a square wave input ( $\lambda_1^0 = 0.75$ )

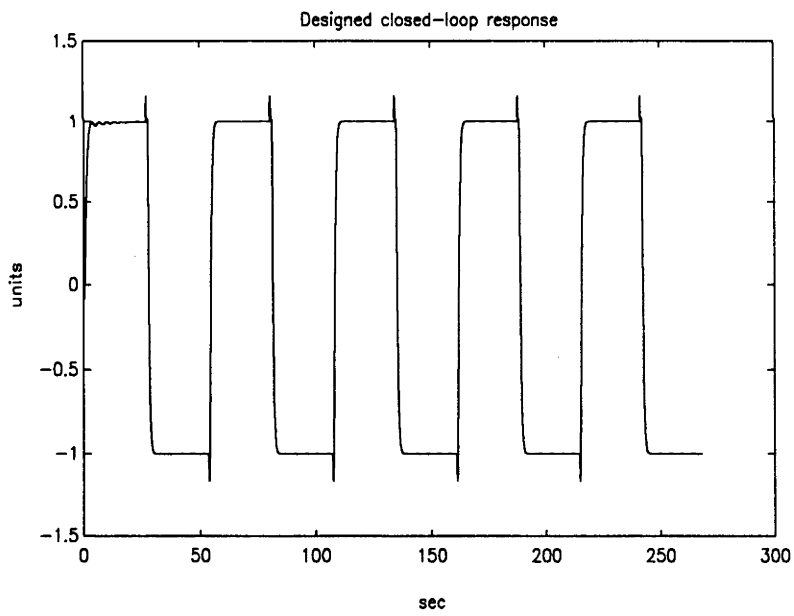


Figure 5.22: Designed response of closed-loop for a square wave input ( $\lambda_1^f = 3.0$ )

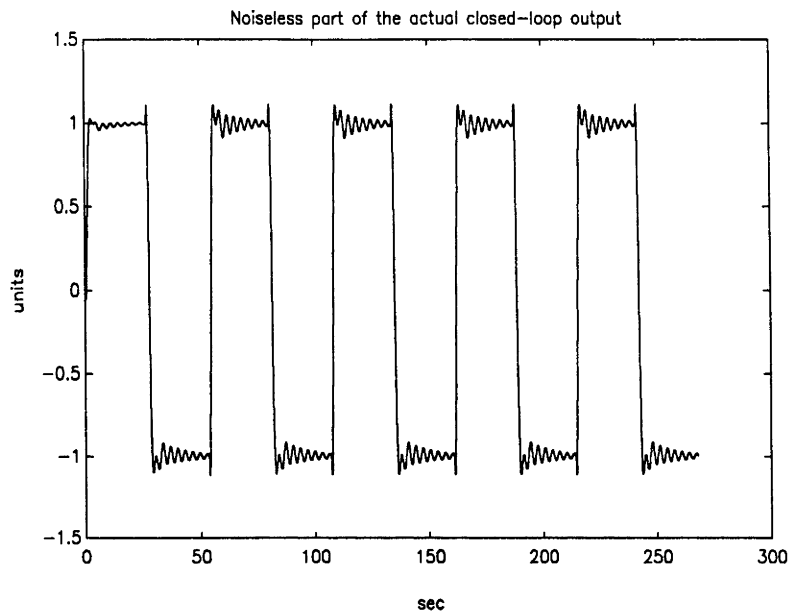


Figure 5.23: Noiseless response of actual closed-loop for a square wave input ( $\lambda_1^f = 3.0$ )

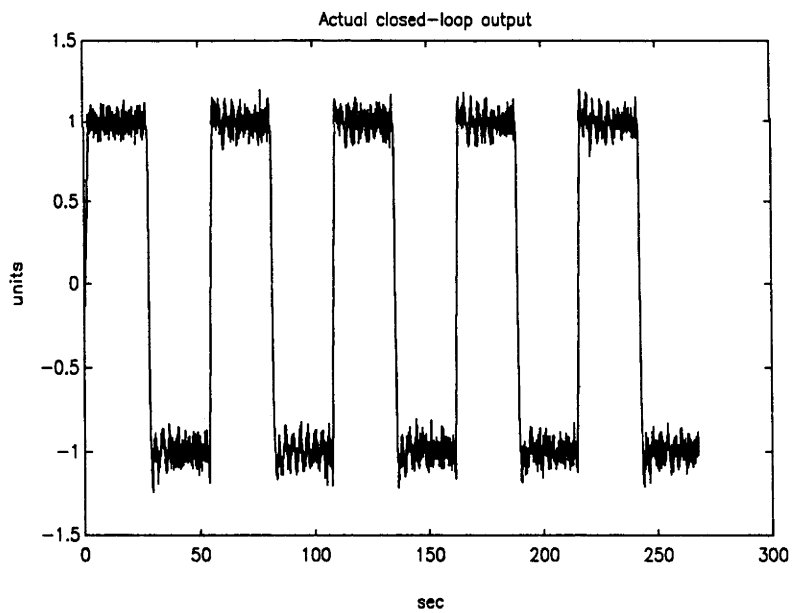


Figure 5.24: Noisy response of actual closed-loop for a square wave input ( $\lambda_1^f = 3.0$ )

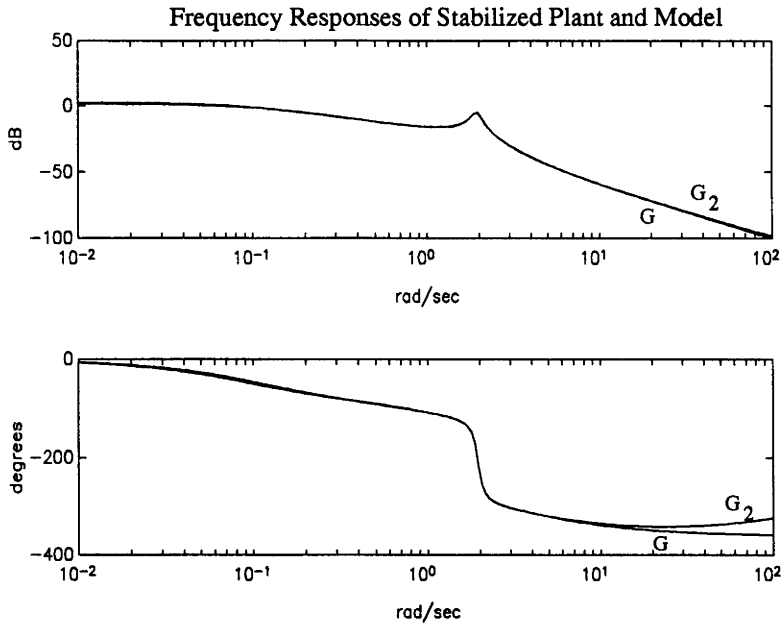


Figure 5.25: Frequency responses of  $G$  and  $G_2$

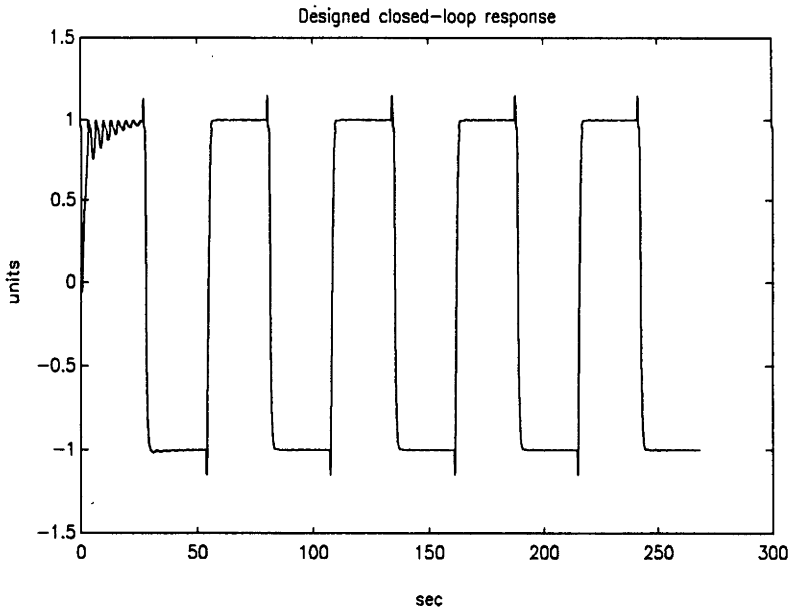


Figure 5.26: Response of designed closed-loop for a square wave input ( $\lambda_2^0 = 3.0$ )

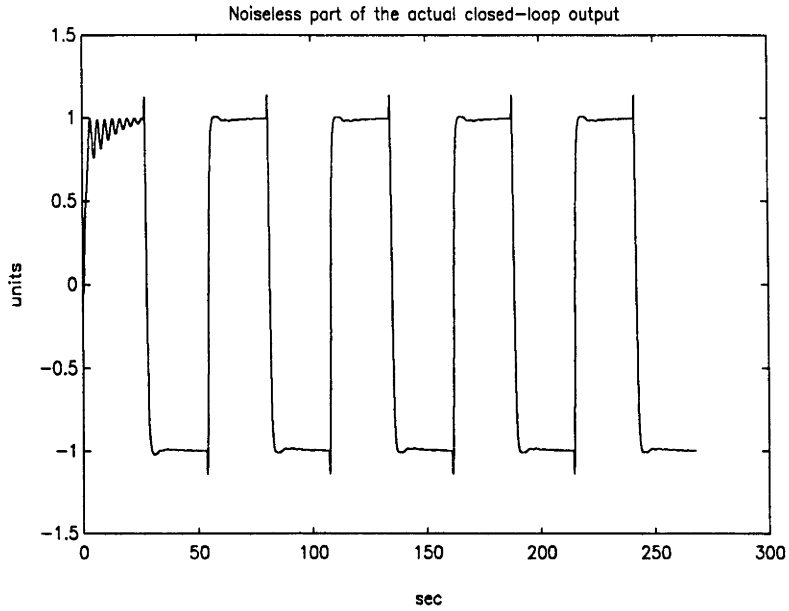


Figure 5.27: Noiseless response of actual closed-loop for a square wave input ( $\lambda_2^0 = 3.0$ )

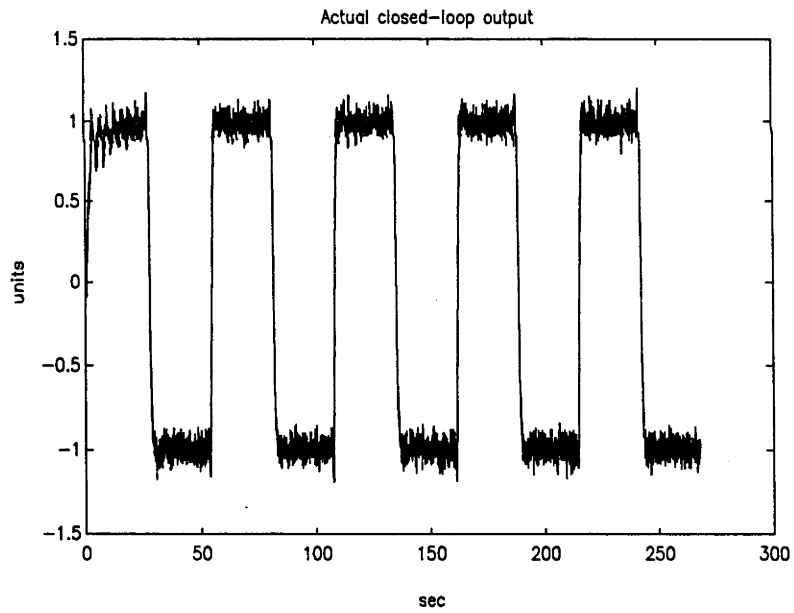


Figure 5.28: Noisy response of actual closed-loop for a square wave input ( $\lambda_2^0 = 3.0$ )



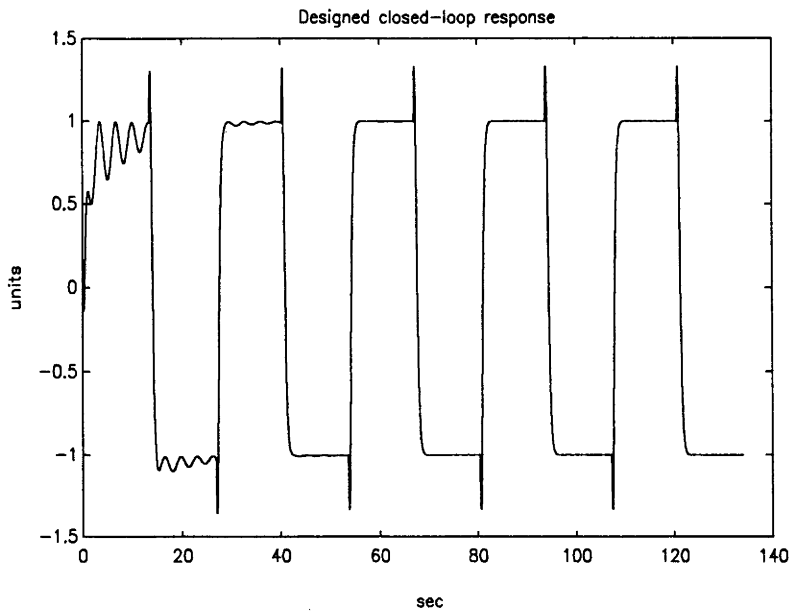


Figure 5.29: Response of designed closed-loop for a square wave input ( $\lambda_2 = 6.0$ )

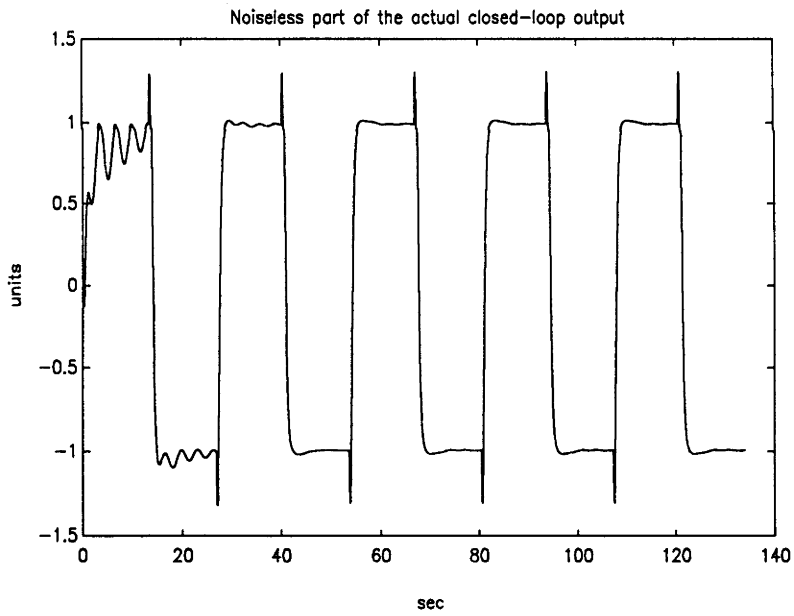


Figure 5.30: Noiseless response of actual closed-loop for a square wave input ( $\lambda_2 = 6.0$ )

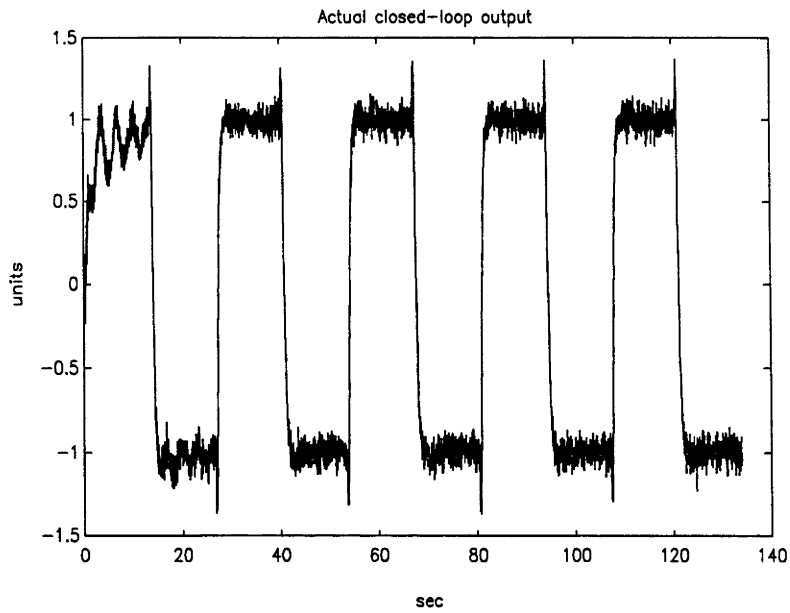


Figure 5.31: Noisy response of actual closed-loop for a square wave input ( $\lambda_2 = 6.0$ )

**Appendix 5.2: Graphs for Simulation Example 2**

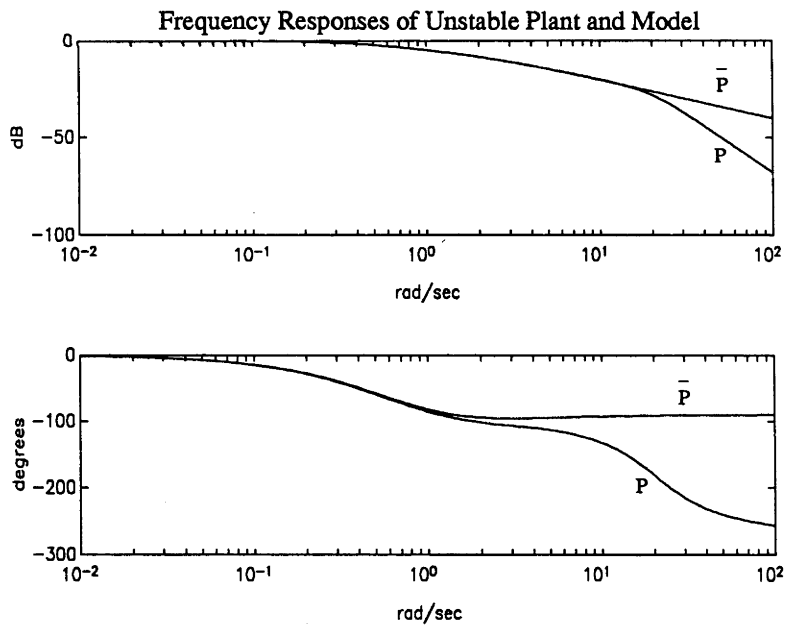


Figure 5.32: Frequency responses of  $P$  and  $\bar{P}$

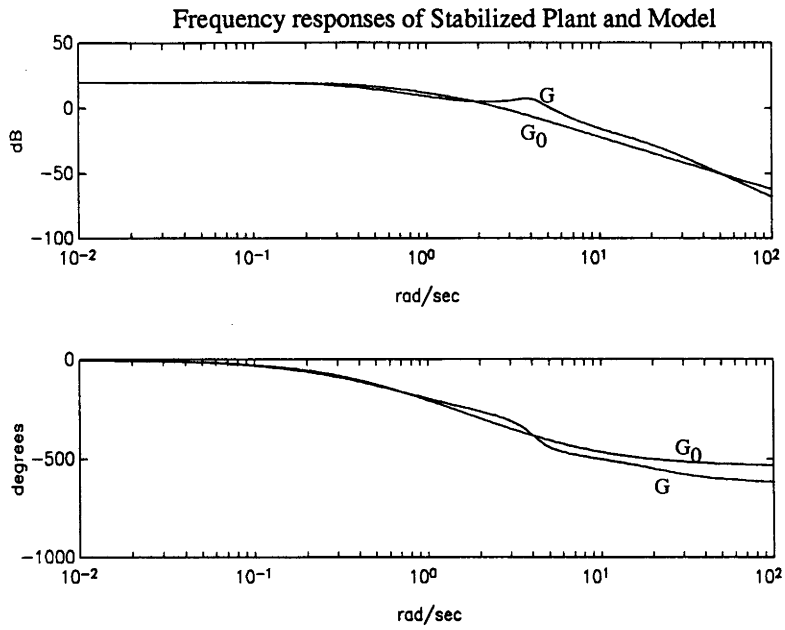


Figure 5.33: Frequency responses of  $G$  and  $G_0$

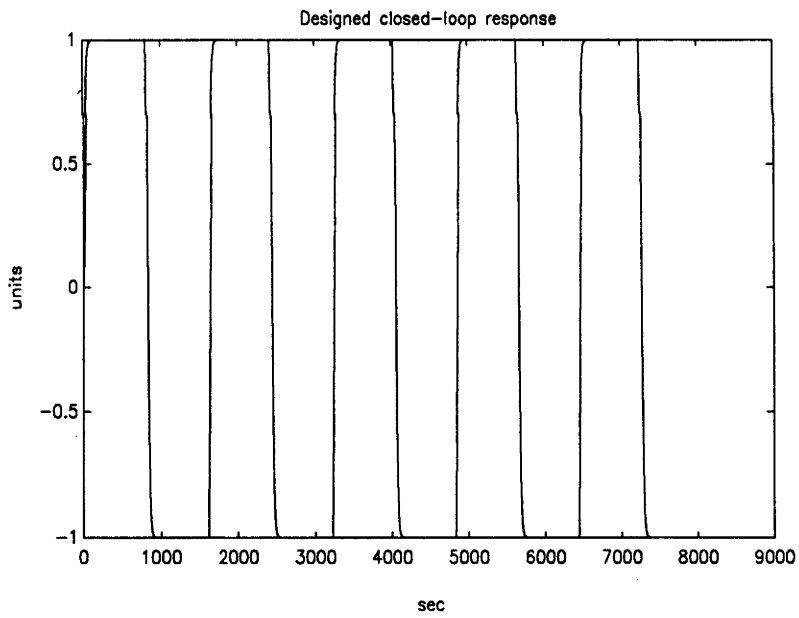


Figure 5.34: Response of designed closed-loop for a square wave input ( $\lambda_0^0 = 0.1$ )

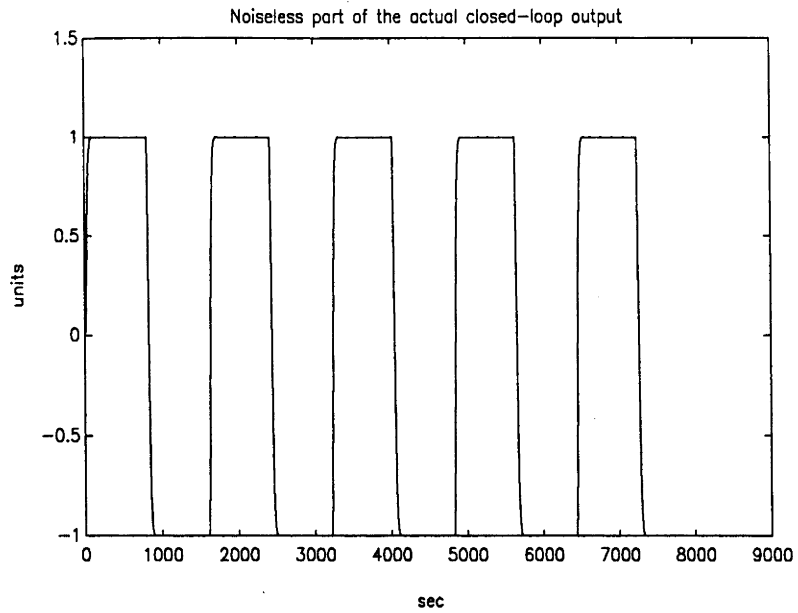


Figure 5.35: Noiseless response of actual closed-loop for a square wave input ( $\lambda_0^0 = 0.1$ )

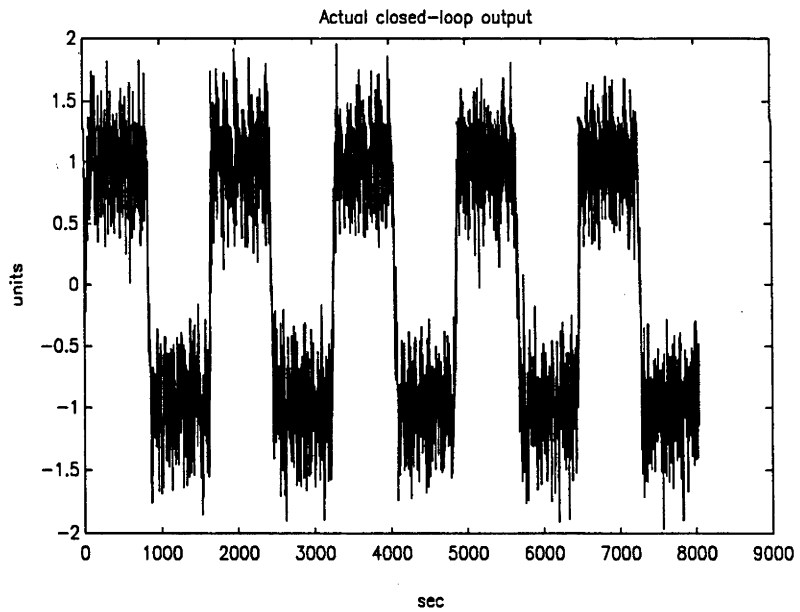


Figure 5.36: Noisy response of actual closed-loop for a square wave input ( $\lambda_0^0 = 0.1$ )

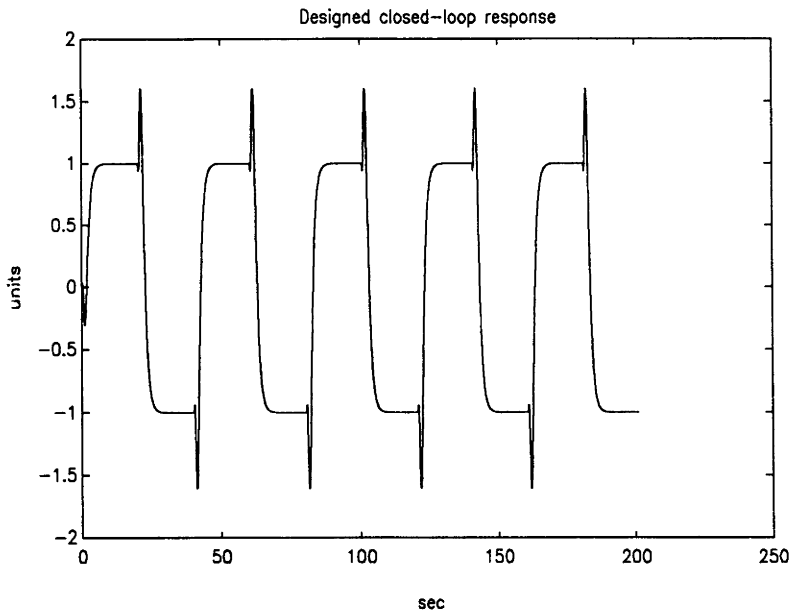


Figure 5.37: Response of designed closed-loop for a square wave input ( $\lambda_0^f = 4.0$ )

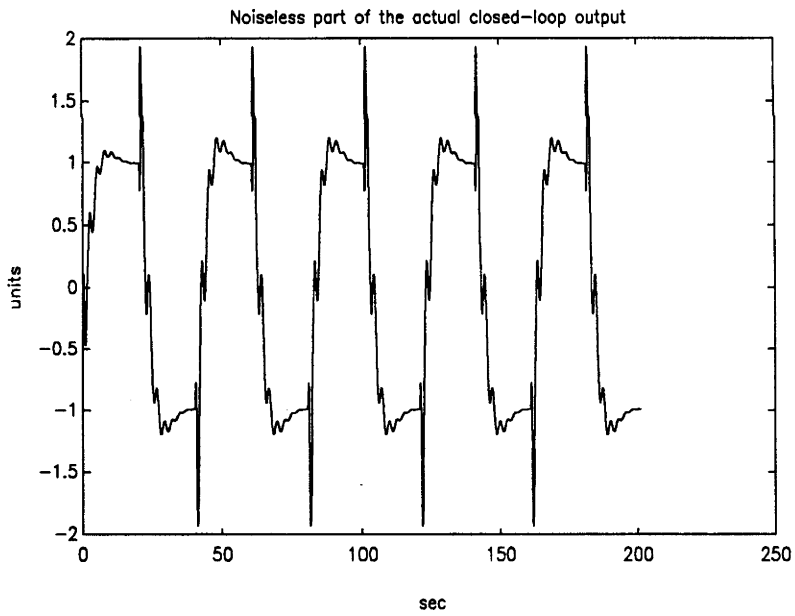


Figure 5.38: Noiseless response of actual closed-loop for a square wave input ( $\lambda_0^f = 4.0$ )

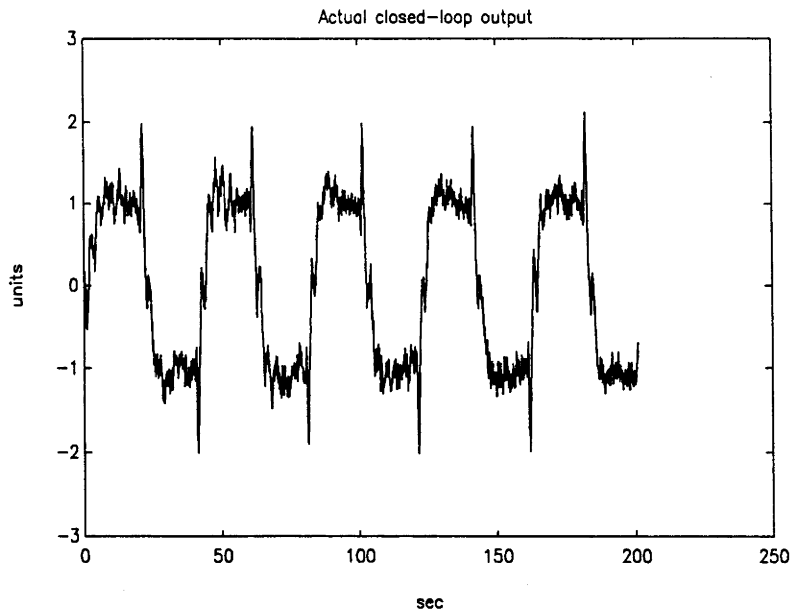


Figure 5.39: Noisy response of actual closed-loop for a square wave input ( $\lambda_0^f = 4.0$ )

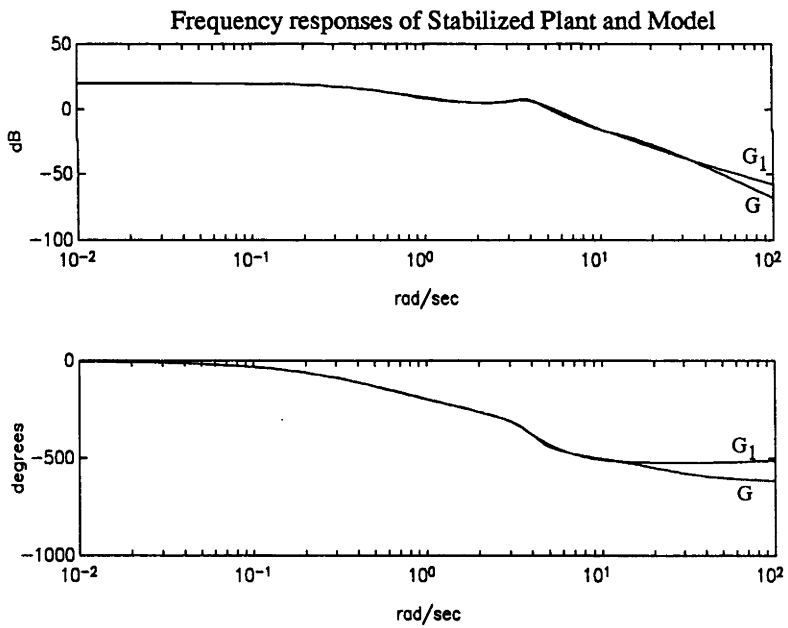


Figure 5.40: Frequency responses of  $G$  and  $G_1$

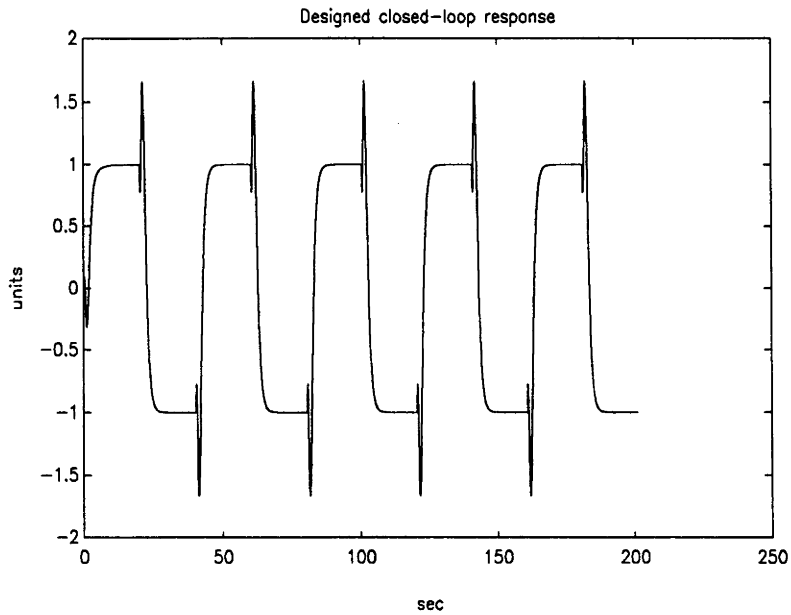


Figure 5.41: Response of designed closed-loop for a square wave input ( $\lambda_1^0 = 4.0$ )

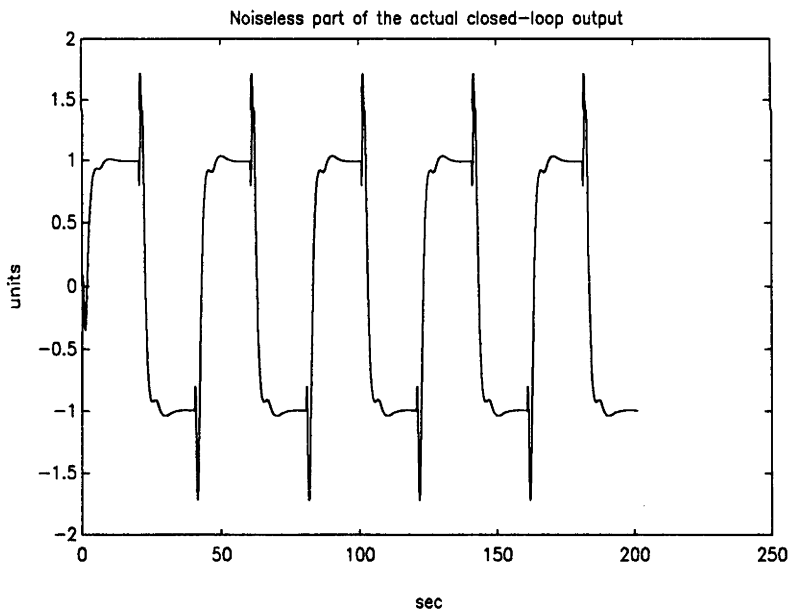


Figure 5.42: Noiseless response of actual closed-loop for a square wave input ( $\lambda_1^0 = 4.0$ )

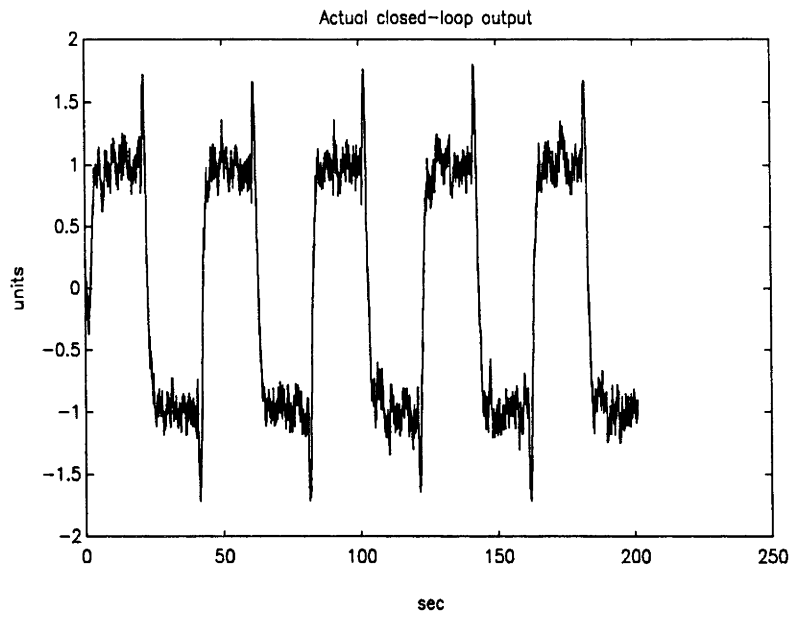


Figure 5.43: Noisy response of actual closed-loop for a square wave input ( $\lambda_1^0 = 4.0$ )



## Chapter 6

# Conclusions and Future Research Directions

### 6.1 Conclusions

In this thesis we have systematically studied an iterative identification and control design methodology that has the adaptive robust control design philosophy propounded by Anderson and Kosut [1991] as its foundation.

Through a brief review of robust control and traditional adaptive control, we have established in Chapter 1 the need of blending robust control and adaptive control harmoniously such that, in the face of significant initial modelling error, a specified nominal closed-loop performance and performance robustness may be achieved progressively. We have reported in Chapter 2 a preliminary study of an iterative identification and control design paradigm for achieving the above mentioned objective in the ideal situation where an infinite number of noiseless measurements are available for the plant input and output. This takes the form of an iterative model approximation and control design algorithm and for which encouraging simulation results are obtained. We have investigated in Chapter 3 the iterative identification and control design methodology under realistic situations where only a finite number of noisy input-output measurements are available. We have shown that the controller design equations and the control-relevant system identification procedure are the same for stable plants and Type 1 stable plants. Good simulation results are obtained when the iterative

identification and control design algorithm is applied to stable plants and Type 1 stable plants. These results have shown that control-relevant frequency weighting on the identification criterion (or equivalently, appropriate data filtering) is instrumental to the matching of identified models to the overall control performance objective. In Chapter 4 we have shown that, given a stable strictly proper model of a stable strictly proper plant, we can improve the performance robustness of the closed-loop system through iterative identification and control design if the plant and the existing model has no unstable zeros within the designed closed-loop bandwidth and if the deterioration in performance robustness caused by increasing the closed-loop bandwidth results in a sufficiently high signal-to-noise ratio for the closed-loop output error. Situations that may cause the iterative identification and control design process to terminate prematurely are also indicated. An important contribution of this chapter is the incorporation of model validation procedures into the iterative identification and control design methodology. This has improved the reliability of the iterative process significantly. In Chapter 5 we have extended the applications of iterative identification and control design to unstable plants by embedding the iterative identification and control design procedure for stable plants into a two step control design approach. Specifically, we have shown that by first stabilizing the unstable plant with a strictly proper parallel output feedback compensator, it is possible to design the overall closed-loop system systematically through applying the iterative identification and control design methodology to the stabilized plant. This allows the overall closed-loop system to maintain good step responses with little overshoot (that is, performance robustness) while its bandwidth is widened progressively.

The analyses and encouraging results presented in this thesis have demonstrated succinctly the effectiveness of the iterative identification and control design methodology in robust performance improvement. However, it is important to emphasize that a rigorous theory is still lacking. We wish the investigations reported in this thesis will stimulate further research interests of the control engineering community. In the next section we shall suggest some possible directions for future research in this exciting area of control engineering.

## 6.2 Future Research Directions

It is well known that the solution to a problem is the beginning of other problems. We shall now discuss some future research directions. For this purpose, it is convenient to group them

under the following categories:

1. Immediate extensions
2. Theoretical issues
3. Practical investigations
4. Model error characterization
5. Adaptive control design framework

### 6.2.1 Immediate extensions

- In the tracking problem that we have studied in the thesis, the main objective is to increase the closed-loop bandwidth of a system robustly. Since the closed-loop transfer function for the unity feedback structure adopted is the same as the complementary sensitivity function, the sensitivity function will be small in the passband of the closed-loop system. This implies that widening the closed-loop bandwidth will increase the frequency range where the system will have good disturbance rejection property. Notwithstanding the last observation, it is sometimes desirable to be more frequency selective in the design of the sensitivity function. This is especially the case when plant output measurement noise and control input energy consideration may prevent a closed-loop system with wide bandwidth from being implemented. These requirements not only will affect the control design but also will influence the system identification process. This can be a very interesting problem to investigate.
- We emphasize that the Internal Model Control design method is very effective in the iterative identification and control design paradigm presented because it is well suited for adjusting the design closed-loop bandwidth. The lesson learned is that the control design method chosen for an iterative identification and control design methodology should be matched to the control problem at hand. As the class of problems considered is widened, we should not confine ourselves to the Internal Model Control design method. More powerful robust control design paradigms like Generalized Predictive Control and  $\mathcal{H}_\infty$ -optimization should also be considered.

### 6.2.2 Theoretical issues

- We have pointed out at the end of Chapter 5 that the applications of iterative identification and control design to unstable plants have *merely been touched upon* in this thesis by employing a two step iterative identification and control design approach, where the unstable plant is first stabilized by a strictly proper parallel output feedback stabilizer before the iterative identification and control design methodology is applied to the stabilized plant. In particular, we recognize that:
  - Due to the fundamental limitations imposed by the plant's unstable poles on the area under the logarithmic magnitude of the sensitivity function, the effects of noise disturbance at the plant output may be accentuated in the process of stabilization and may cause the problem of identifying the stabilized plant to become more difficult. This effect will depend on the choice of stabilization schemes and control design methods. This is an important issue that has to be investigated carefully. We anticipate that  $\mathcal{H}_\infty$  robust control techniques may have a big role to play here.
  - Although the pole-placement technique embedded in the two step iterative identification and control design approach shows encouraging results, the question of how to design a stabilizer whose order is comparable to or lower than the order of a given unstable model, such that it satisfies (together with a given model) the parity interlacing property, is still far from resolved. This is a very challenging problem that is of major interest in its own right.
- We have observed that models updated through estimating their respective  $R$  parametrization tend to have excessively high order. This difficulty has not been completely overcome by the incorporation of frequency weighted model reduction procedure. To solve the problem at the root, it is important to seek effective and efficient parametrization of the  $R$  transfer function. We may start this direction of research by considering the orthogonal function approach [Wahlberg and Lindskog 1991].
- Schrama [1992b] has observed that, when a model leads to the design of a high performance (both nominal and robust) closed-loop system, the frequency response of the model is often a poor representation of the plant under open-loop conditions. Our simulation experience does not support Schrama's observation. In fact, we often find that frequency responses of models approach the frequency response of the open-

loop plant while the actual closed-loop performance is improved through iteration. We have observed that for the iterative identification and control design methodology considered in this thesis, good control performance and good identified models go hand in hand. Further research should be directed to resolve these seemingly contradictory observations of Schrama and ours. We believe that better understanding of **iterative identification and control design in general** can be gained by studying this problem.

- Due to the complexity of the algorithm, it is very difficult to prove its convergence. A less daunting but equally important task is to establish conditions that guarantee robust stabilization is achieved by the controller re-designed on the basis of an updated model.

### 6.2.3 Practical investigations

- It was indicated by analysis (see Remark 4.5.1 and the fourth observation in Section 4.6.3) and simulation experience that unstable zeros of the existing model that are within the designed closed-loop bandwidth may hinder closed-loop identification of a new model. However there is also simulation evidence (see the simulation example in Section 4.8) that this may not be always the case. It is therefore important to clarify the condition (or conditions) that may hinder closed-loop identification. Our experience with this problem seems to indicate that, other than theoretical analysis, extensive careful simulation studies are necessary for finding a clue to this puzzle.
- Despite the encouraging results obtained for the iterative identification and control design paradigm investigated in this thesis, it is important to study how it performs in actual applications like those reported by de Callafon *et al.* [1993] and Partanen and Bitmead [1993*b*].
- An excellent survey has been conducted recently by Van den Hof and Schrama [1994] in the area of approximate identification and model-based control design. Iterative identification and control design paradigms that are currently available were also reviewed critically in this survey. It will be interesting to take this step further by comparing the various paradigms (including [Partanen *et al.* 1994], [Van den Hof *et al.* 1993], [Skellton *et al.* 1994] and ours) on the basis of a common set of plants, initial models, and specifications. These benchmark problems and case studies should facilitate further interactions and cooperations between researchers interested in this area.

### 6.2.4 Model error characterization

- In the face of significant model uncertainties, it is not sure whether an unstable plant could be stabilized unless the associated model error is appropriately characterized. Furthermore, if we can characterize the modelling error associated with each of the identified models in the iterative identification and control design process, the control design step could possibly be made more efficient because we could then design, in a single step, the most ambitious controller which does not cause instability. Significant progress has already been made in model error characterization. (See [Parker and Bitmead 1987], [LaMaire *et al.* 1991], [Partington 1991], [Helmicki *et al.* 1991], [Kosut 1986], [Kosut *et al.* 1992], [Goodwin *et al.* 1992], [De Vries and Van den Hof 1993] and [De Vries and Van den Hof 1994].) Initial attempts to apply some of these results were reported by Graebe and Goodwin [1993] and Kosut [1994]. We believe further research in applications of model error characterization to iterative identification and control design could lead to very fruitful outcomes.

### 6.2.5 Adaptive control design framework

- It is important to observe that the iterative identification and control design paradigm that we have studied (and others that are depending on coprime fractional representations) tends to result in excessively high order model. This could be a hindrance for its direct applications as an on-line adaptive control algorithm. However it could be employed as a platform for designing adaptive control systems through its capability in model refinement and the matching of models with the underlying control design paradigm.

## 6.3 Epilogue

It has been a very exciting and satisfying experience to transform the iterative identification and control design methodology from an initial concept to its present form. More importantly, it is hoped that, together with other *iterators*<sup>1</sup>, we have moved a step closer to the objective

---

<sup>1</sup>We borrow this term from Van den Hof and Schrama [1994].

of providing convenient and practical tools for tradeoff among the competing design goals of stability, performance and sensitivity<sup>2</sup>, while we attempt to convince control theoreticians that control-relevant system identification and modelling are integral parts of the general control design problem and therefore deserve serious attentions from the control research community at large.

Our final message is:

Control engineering is very much an experimental science. In practical control applications, it is very likely that we have to get involved with poor initial models (from the point of view of control design), noisy plant measurements, and ambitious nominal and robust performance requirements. In these situations, we have demonstrated that iterative identification and control design is a promising approach for refining the model and the controller in closed-loop (with appropriately filtered plant measurements acting as the vehicle through which they interact) such that a robust high performance closed-loop system can be designed progressively.

---

<sup>2</sup>It was pointed out succinctly by Skelton [1989] that modelling and control theory has not yet provide a convenient and practical tradeoff among the competing design goals of stability, performance and sensitivity.

## Appendix A

### Proof of Theorem 2.4.2 in Chapter 2

Since the controller

$$K_i^f = \frac{X_i^f}{Y_i^f} \quad (\text{A.1})$$

stabilizes the model

$$G_i = \frac{N_i}{D_i} ,$$

and

$$N_i X_i^f + D_i Y_i^f = 1 , \quad (\text{A.2})$$

solving equations (A.1) and (A.2) simultaneously, we get

$$X_i^f = \frac{K_i^f}{D_i + N_i K_i^f} , \quad (\text{A.3})$$

and

$$Y_i^f = \frac{1}{D_i + N_i K_i^f} ; \quad (\text{A.4})$$

or

$$Y_i^f = \frac{1 - N_i X_i^f}{D_i} .$$

Substituting  $X_i^f$  and  $Y_i^f$  into

$$G_{i+1} = \frac{N_i + \hat{R}_i^f Y_i^f}{D_i - \hat{R}_i^f X_i^f}$$

will result in

$$G_{i+1} = G_i + \frac{\hat{R}_i^f}{D_i(D_i - \hat{R}_i^f X_i^f)} .$$



Solving for  $\widehat{R}_i^f$ , we get

$$\widehat{R}_i^f = \frac{D_i^2(G_{i+1} - G_i)}{1 + D_i X_i^f(G_{i+1} - G_i)} . \quad (\text{A.5})$$

From Figure 2.2 of Section 2.4, with  $r_2 = 0$ , we can write for the closed-loop system (when  $j = f$ ),

$$y_i^f = \frac{GK_i^f}{1 + GK_i^f} r_1 + \frac{1}{1 + GK_i^f} He ,$$

and

$$u_i^f = \frac{K_i^f}{1 + GK_i^f} r_1 - \frac{K_i^f}{1 + GK_i^f} He .$$

Therefore we can write

$$\beta = D_i y_i^f - N_i u_i^f$$

as

$$\beta = \frac{D_i K_i^f (G - G_i)}{1 + GK_i^f} r_1 + \frac{D_i (1 + G_i K_i^f)}{1 + GK_i^f} He , \quad (\text{A.6})$$

and

$$\alpha = X_i^f r_1$$

as

$$\alpha = \frac{K_i^f}{D_i (1 + G_i K_i^f)} r_1 . \quad (\text{A.7})$$

If we form the output error defined by

$$\epsilon = \beta - \widehat{R}_i^f \alpha , \quad (\text{A.8})$$

then by substituting equations (A.5), (A.6), and (A.7) into equation (A.8), and using the expression of  $X_i^f$  given by equation (A.3), we can obtain

$$\epsilon = \frac{D_i (1 + G_i K_i^f) K_i^f (G - G_{i+1})}{(1 + GK_i^f)(1 + G_{i+1} K_i^f)} r_1 + \frac{D_i (1 + G_i K_i^f)}{1 + GK_i^f} He .$$

Since equation (A.4) can also be written as

$$Y_i^f = \frac{1}{D_i (1 + G_i K_i^f)} ,$$

it is clear that if we define the filtered output error as

$$\xi_1 = Y_i^f \epsilon ,$$

then

$$\xi_1 = \frac{K_i^f(G - G_{i+1})}{(1 + GK_i^f)(1 + G_{i+1}K_i^f)} r_1 + \frac{1}{1 + GK_i^f} He ,$$

or

$$\xi_1 = \left( \frac{GK_i^f}{1 + GK_i^f} - \frac{G_{i+1}K_i^f}{1 + G_{i+1}K_i^f} \right) r_1 + \frac{1}{1 + GK_i^f} He .$$

## Appendix B

### Proof of Theorem 2.6.1 in Chapter 2

Using the notations established in Chapter 2, we have

$$R_i^f = \frac{G - G_i}{1 + Q_i^f(G - G_i)},$$

and

$$Q_i^f = \frac{K_i^f}{1 + G_i K_i^f}.$$

Therefore we can write

$$R_i^f = \frac{1 + G_i K_i^f}{1 + G_i K_i^f} (G - G_i). \quad (\text{B.1})$$

We also have

$$G_i = [G_i]_m [G_i]_a,$$

where

$$[G_i]_m = \frac{\tilde{n}_{G_i} \prod_i (z_i^* + s)}{d_{G_i}},$$

and

$$[G_i]_a = \frac{\prod_i (z_i - s)}{\prod_i (z_i^* + s)}.$$

Since  $Q_i^f = [G_i]_m^{-1} F_i^f$ , we can therefore rewrite the equation

$$K_i^f = \frac{Q_i^f}{1 - Q_i^f G_i}$$

as

$$K_i^f = \frac{d_{G_i} n_{F_i^f}}{\tilde{n}_{G_i} [\prod_i (z_i^* + s) d_{F_i^f} - \prod_i (z_i - s) n_{F_i^f}]}.$$

Hence, we can write

$$1 + G_i K_i^f = \frac{\prod_i (z_i^* + s) d_{F_i^f}}{\prod_i (z_i^* + s) d_{F_i^f} - \prod_i (z_i - s) n_{F_i^f}} . \quad (\text{B.2})$$

By substituting equation (B.2) into equation (B.1) and noting that

$$d_{F_i^f} = (s + \lambda_i^f)^n ,$$

(Note that by having  $n$ , the relative degree of  $G_i$ , as the relative degree of  $F_i^f$ , the transfer function  $Q_i^f$  will be bi-proper.)

$$1 + G K_i^f = \frac{d_G d_{K_i^f} + n_G n_{K_i^f}}{d_G d_{K_i^f}} ,$$

and

$$G - G_i = \frac{d_{G_i} n_G - d_G n_{G_i}}{d_G d_{G_i}} ,$$

we obtain

$$R_i^f = \tilde{R}_i^f \check{R}_i^f ,$$

where

$$\tilde{R}_i^f = [G_i]_m (s + \lambda_i^f)^n ,$$

is a *known* stable proper transfer function and

$$\check{R}_i^f = \frac{d_{G_i} n_G - d_G n_{G_i}}{d_{K_i^f} d_G + n_{K_i^f} n_G} . \quad (\text{B.3})$$

is an *unknown* stable strictly-proper transfer function.

## Appendix C

# Proof of Theorem 2.6.2 in Chapter 2

To obtain the results on the order and relative degree of  $\check{R}_i^f$ , we shall write

$$[G_i]_m = \frac{\eta_i(s)}{\pi_i(s)} ,$$
$$[G_i]_a = \frac{\rho_i(-s)}{\rho_i(s)} ,$$

where each of the polynomials  $\eta_i(s)$ ,  $\pi_i(s)$ , and  $\rho_i(s)$  has degree  $r$ ,  $n+r$ , and  $m$ , respectively.

We can then obtain

$$K_i^f = \frac{(\lambda_i^f)^n \pi_i(s) \rho_i(s)}{\eta_i(s) [(s + \lambda_i^f)^n \rho_i(s) - (\lambda_i^f)^n \rho_i(-s)]} .$$

If we also write  $G$  as

$$G = \frac{\alpha(s)}{\beta(s)} ,$$

where  $\alpha(s)$  has degree  $p$ , and  $\beta(s)$  has degree  $q$ , then by substituting all these into equation (B.3), we get

$$\check{R}_i^f = \frac{\alpha(s) \pi_i(s) \rho_i(s) - \eta_i(s) \rho_i(-s) \beta(s)}{\beta(s) \eta_i(s) [(s + \lambda_i^f)^n \rho_i(s) - (\lambda_i^f)^n \rho_i(-s)] + (\lambda_i^f)^n \alpha(s) \pi_i(s) \rho_i(s)} . \quad (C.1)$$

By counting the degrees of the resulting numerator and denominator polynomials of  $\check{R}_i^f$  given by equation (C.1), the required results are established immediately.

## Appendix D

# Proof of Theorem 3.2.2 in Chapter 3

By using the  $K_0^0(s)$  and the  $G(s)$  given in Theorem 3.2.2, we can write the characteristic polynomial of the actual closed-loop system as

$$s^2(s + 2\lambda_0^0)\tilde{d}_G(s) + \frac{(\lambda_0^0)^2}{\kappa\tau}(\tau s + 1)n_G(s) .$$

As  $\lambda_0^0$  approaches zero, all but three poles of the actual closed-loop system approach the zeros of  $\tilde{d}_G(s)$ . The stability of the actual closed-loop will therefore depend on the remainder three poles that are approaching the origin.

Let  $s_0$  denote the poles of the actual closed-loop system that are approaching the origin as  $\lambda_0^0$  approaches zero. After approximating  $\tilde{d}_G(s)$  and  $n_G(s)$  in the characteristic polynomial of the actual closed-loop system by the constant term of their respective Taylor series expansions at the origin, we consider the stability of the following third order polynomial,

$$s^3 + 2\lambda_0^0 s^2 + (\lambda_0^0)^2 \frac{n_G(0)}{\kappa\tilde{d}_G(0)} s + \frac{(\lambda_0^0)^2}{\tau} \frac{n_G(0)}{\kappa\tilde{d}_G(0)} ,$$

whose zeros are  $s_0$ . By applying Routh-Hurwitz criterion to the last polynomial, we immediately see that the actual closed-loop system is stable if

$$\kappa \quad \text{and} \quad \frac{n_G(0)}{\tilde{d}_G(0)}$$

have the same sign, and if

$$\lambda_0^0 > \frac{1}{2\tau}$$

is suitably small.

## Appendix E

### Proof of Theorem 3.3.1 in Chapter 3

Using equations (3.3),(3.4) and (3.5), we can obtain

$$R_i^f = \frac{D_i^2(G - G_i)}{1 + D_i X_i^f(G - G_i)} . \quad (\text{E.1})$$

By substituting equation (3.3) into equation (E.1), and noting that  $G_i = N_i/D_i$ , we can obtain

$$R_i^f = D_i^2 \frac{1 + G_i K_i^f}{1 + G K_i^f} (G - G_i) . \quad (\text{E.2})$$

Now from Theorem 2.5.1, we have (for  $q = 1$ )

$$Q_i^f = s [D_i]_a [G_i]_m^{-1} \left\{ [D_i]_a^{-1} [G_i]_a^{-1} \frac{1}{s} \right\}_* F_i^f .$$

By using the equations

$$[D_i]_a = \frac{\prod_{i=1}^k (p_i - s)}{\prod_{i=1}^k (p_i^* + s)} ,$$

and

$$[G_i]_a = \frac{\prod_i (z_i - s)}{\prod_i (z_i^* + s)} ,$$

direct calculation gives

$$\left\{ [D_i]_a^{-1} [G_i]_a^{-1} \frac{1}{s} \right\}_* = \frac{n_*}{s \prod_{i=1}^k (p_i - s)} ,$$

where  $n_*$  represents the resulting numerator polynomial. Therefore we can write

$$Q_i^f = \frac{d_{G_i}}{\tilde{n}_{G_i} \prod_i (z_i^* + s)} \frac{n_*}{\prod_{i=1}^k (p_i^* + s)} \frac{n_{F_i^f}}{d_{F_i^f}}$$

and

$$G_i Q_i^f = \frac{\prod_i (z_i - s)}{\prod_i (z_i^* + s)} \frac{n_*}{\prod_{i=1}^k (p_i^* + s)} \frac{n_{F_i^f}}{d_{F_i^f}} .$$

Now by using

$$K_i^f = \frac{Q_i^f}{1 - G_i Q_i^f}$$

we obtain

$$K_i^f = \frac{d_{G_i} n_* n_{F_i^f}}{\tilde{n}_{G_i} [\prod_i (z_i^* + s) \prod_{i=1}^k (p_i^* + s) d_{F_i^f} - \prod_i (z_i - s) n_* n_{F_i^f}]} ,$$

which in turn allow us to write

$$1 + G_i K_i^f = \frac{\tilde{n}_{G_i} [\prod_i (z_i^* + s) \prod_{i=1}^k (p_i^* + s) d_{F_i^f}]}{d_{K_i^f}} .$$

The last equation together with

$$1 + G K_i^f = \frac{d_G d_{K_i^f} + n_G n_{K_i^f}}{d_G d_{K_i^f}} ,$$

$$G - G_i = \frac{d_{G_i} n_G - d_G n_{G_i}}{d_G d_{G_i}} ,$$

$$d_{F_i^f} = (s + \lambda_i^f)^{k+n+1} , \quad (\text{since } q = 1 \text{ and } N = n + 1) ,$$

and equation (E.2) leads to

$$R_i^f = \tilde{R}_i^f \check{R}_i^f ,$$

with

$$\check{R}_i^f = (s + \lambda_i^f)^{k+1} \left[ \prod_{i=1}^k (p_i^* + s) \right] \frac{d_{G_i} n_G - d_G n_{G_i}}{d_G d_{K_i^f} + n_G n_{K_i^f}} ,$$

and

$$\tilde{R}_i^f = D_i [N_i]_m (s + \lambda_i^f)^n .$$



## Appendix F

### Proof of Theorem 4.7.2 in Chapter 4

By direct substitution we can write

$$\frac{\left(\frac{G-G_1}{G_1}\right) \bar{T}_1^0}{\left(\frac{G-G_0}{G_0}\right) \bar{T}_0^f} = \frac{Q_1^0}{Q_0^f} \left(\frac{G-G_1}{G-G_0}\right). \quad (\text{F.1})$$

Now equations (4.21), (4.22), and (4.23) allow us to write

$$\frac{R_0^f}{[G_0]_m} = \frac{G-G_0}{[G_0]_m + (G-G_0)F_0^f},$$

and

$$\frac{\hat{R}_0^f}{[G_0]_m} = \frac{G_1-G_0}{[G_0]_m + (G_1-G_0)F_0^f}.$$

Direct calculation with the last two equations give

$$\frac{\hat{R}_0^f - R_0^f}{R_0^f} = - \frac{(G-G_1)[G_0]_m}{(G-G_0)\{[G_0]_m + (G_1-G_0)F_0^f\}}. \quad (\text{F.2})$$

Recall that  $G_0 = [G_0]_m[G_0]_a$ , and  $\bar{T}_0^f = F_0^f[G_0]_a$ , we can therefore rewrite equation (F.2) as

$$- \left(\frac{G-G_1}{G-G_0}\right) = \left[1 + \left(\frac{G_1-G_0}{G_0}\right) \bar{T}_0^f\right] \frac{\hat{R}_0^f - R_0^f}{R_0^f}. \quad (\text{F.3})$$

Substituting equation (F.3) into equation (F.1) allows us to write

$$\left| \frac{\left(\frac{G-G_1}{G_1}\right) \bar{T}_1^0}{\left(\frac{G-G_0}{G_0}\right) \bar{T}_0^f} \right| = \left| \frac{Q_1^0}{Q_0^f} \right| \left| 1 + \left(\frac{G_1-G_0}{G_0}\right) \bar{T}_0^f \right| \left| \frac{\hat{R}_0^f - R_0^f}{R_0^f} \right|.$$

Since  $G_1$  and  $G_0$  are strictly proper stable transfer function, and  $\bar{T}_0^f = G_0 Q_0^f$  with  $Q_0^f$  proper and stable, it follows from Lemma 4.7.2 that

$$\sup_{\omega_1 \leq \omega \leq \omega_2} \left| \left[ \frac{G_1(j\omega) - G_0(j\omega)}{G_0(j\omega)} \right] \bar{T}_0^f(j\omega) \right| = \eta$$

and

$$\sup_{\omega_1 \leq \omega \leq \omega_2} \left| 1 + \left[ \frac{G_1(j\omega) - G_0(j\omega)}{G_0(j\omega)} \right] \bar{T}_0^f(j\omega) \right| \leq 1 + \eta.$$

Furthermore, from Lemma 4.7.1, we have

$$\sup_{\omega_1 \leq \omega \leq \omega_2} \left| \frac{Q_1^0(j\omega)}{Q_0^f(j\omega)} \right| = \delta.$$

Therefore

$$\frac{\left| \left[ \frac{G(j\omega) - G_1(j\omega)}{G_1(j\omega)} \right] \bar{T}_1^0(j\omega) \right|^2}{\left| \left[ \frac{G(j\omega) - G_0(j\omega)}{G_0(j\omega)} \right] \bar{T}_0^f(j\omega) \right|^2} \leq \delta^2 (1 + \eta)^2 \left| \frac{\hat{R}_0^f(j\omega) - R_0^f(j\omega)}{R_0^f(j\omega)} \right|^2$$

for  $\omega_1 \leq \omega \leq \omega_2$ .

## Appendix G

# Proof of Theorem 4.7.3 in Chapter 4

It can be shown easily that the tracking error induced by the model error associated with  $G_1$  and when the designed closed-loop transfer function is  $\bar{T}_1^0$  is given by

$$v_1^0 = \frac{\frac{G-G_1}{G_1} \bar{T}_1^0}{1 + \left(\frac{G-G_1}{G_1}\right) \bar{T}_1^0} (1 - \bar{T}_1^0) r .$$

Therefore

$$\Phi_{v_1^0}(\omega) = \frac{\left| \frac{G(j\omega) - G_1(j\omega)}{G_1(j\omega)} \bar{T}_1^0(j\omega) \right|^2}{\left| 1 + \left[ \frac{G(j\omega) - G_1(j\omega)}{G_1(j\omega)} \right] \bar{T}_1^0(j\omega) \right|^2} \left| 1 - \bar{T}_1^0(j\omega) \right|^2 \Phi_r(\omega) .$$

Since

$$\left| \frac{\hat{R}_0^f(j\omega) - R_0^f(j\omega)}{R_0^f(j\omega)} \right|^2 \ll \frac{1}{\delta^2(1+\eta)^2} \left| \left[ \frac{G(j\omega) - G_0(j\omega)}{G_0(j\omega)} \right] \bar{T}_0^f(j\omega) \right|^{-2}$$

for  $\omega_1 \leq \omega \leq \omega_2$ , we have, from Theorem 4.7.2,

$$\left| \left[ \frac{G(j\omega) - G_1(j\omega)}{G_1(j\omega)} \right] \bar{T}_1^0(j\omega) \right| \ll 1$$

for  $\omega_1 \leq \omega \leq \omega_2$ . It follows that

$$\Phi_{v_1^0}(\omega) \approx \left| \left[ \frac{G(j\omega) - G_1(j\omega)}{G_1(j\omega)} \right] \bar{T}_1^0(j\omega) \right|^2 \left| 1 - \bar{T}_1^0(j\omega) \right|^2 \Phi_r(\omega)$$

for  $\omega_1 \leq \omega \leq \omega_2$ .

## Appendix H

# Programs and Information for Simulations

In the following we describe the programs (or MATLAB™ m-files) used for simulation studies of the iterative identification and control design paradigm discussed in this thesis. These m-files run under MATLAB™ version 4.2. This set of programs also requires the supports of the Control System Toolbox, the Robust-Control Toolbox, the System Identification Toolbox, and the Signal Processing Toolbox. Hints for choices of experimental variables will also be given. We proceed chapter by chapter and will start with Chapter 2. This allows systematic presentation because many of these programs are shared by simulations in the chapters.

The discussions will proceed in the following fashion. We briefly explain the function for each of the m-files (from user's point of view) when they are first encountered. This will be followed by a discussion on how the relevant set of m-files can be executed in the appropriate sequence to accomplish the simulations. We follow the notations for transfer functions and signals that are defined in the various chapters.

## Chapter 2

### Program Descriptions

#### 1. **plant.m**

This m-file is mainly used to define the plant transfer function  $G$  and the noise transfer function  $H$ . This is accomplished by defining (or re-defining) the vectors **nG** and **dG** in the program code that contain, respectively, the coefficients (in descending order) of the numerator and denominator polynomials of  $G$ . (The noise transfer function  $H$  is also defined likewise in the program code by **nH** and **dH**.) This m-file, when executed, also initializes (or re-initializes) the vectors that store data for graph plotting.

To ensure that graphs are plotted nicely with the scale to be set up by the **init.m** program (to be discussed later), it is a good practice to appropriately scale the plant transfer function such that its dominant time-constant is about 1 second.

Noise disturbances (which are defined partially by  $H$ ) are not considered in the simulations of Chapter 2.

#### 2. **target.m**

This m-file is used to define a transfer function of the form  $\lambda/(s + \lambda)$ . Subsequently (for example, in **q\_control.m** to be described later), this transfer function will be used to define the IMC filter.

The variable  $\lambda$  defines the designed closed-loop bandwidth. It should be defined, for example, by executing the statement **lambda=0.1** (which defines the designed closed-loop bandwidth to be 0.1 rad/s) before **target.m** is executed.

#### 3. **model.m**

This m-file is mainly used to define the transfer function of the *initial model*  $G_0$ . This is accomplished by defining (or re-defining) the vectors **nGi** and **dGi** in the program code that contain, respectively, the coefficients (in descending order) of the numerator and denominator polynomials of  $G_0$ .

We emphasize that  $nG_i$  and  $dG_i$  are actually associated with the *current or existing model*  $G_i$ . They only represent  $G_0$  (after **model.m** is executed) before the first model update.

Whenever **model.m** is executed, the current or existing model is reset to  $G_0$ . This is usually used to prepare for repeating the simulation from the beginning.

#### 4. **q\_control.m**

This m-file calculates the *bi-proper*  $Q$  transfer function that parametrizes the controller on the basis of the existing model  $G_i$ . *Its execution will be aborted if  $G_i$  is found to be unstable.*

#### 5. **k\_control.m**

This m-file calculates the controller  $K$  by using the  $Q$ -parametrization found by **q\_control.m**. The coprime factors of  $K$  defined by  $X = Q$  and  $Y = 1 - G_i Q$  are also calculated for later use.

#### 6. **init.m**

This m-file is for initializing auxiliary variables that are used, for example, to set up the scale of frequency response plots and the grids in the parameter space where the search for the optimal approximation of  $R$  is conducted. This program also calculates frequency responses of the plant and the current model, the designed closed-loop transfer function and the actual closed-loop transfer function.

#### 7. **time\_plot.m**

This program calculates and plots the (noiseless) step response of the actual closed-loop system. To be executed after **init.m** is executed.

#### 8. **rhat\_iter.m**

This program performs the optimal frequency weighted rational approximation for the  $R$  transfer function described in Chapter 2. The calculations use the fact that  $R$  can be factorized as the product of a transfer function known by design and an unknown transfer function. In this program a second order transfer function with a relative degree of one is assumed for estimating the unknown part of  $R$  (as explained in Chapter 2). The vectors **nfilter** and **dfilter** describe the numerator and denominator of the known part of  $R$ , and the vectors **nR** and **dR** describe the numerator and denominator of  $R$  as

a result of executing this program. These vectors are calculated when the controller is designed.

This program takes time to run. Please be patient.

#### 9. **update.m**

This program updates the current model to a new model through the rational approximation of  $R$  produced by `rhat_iter.m`. It then performs frequency weighted model reduction on the new model. It shows the Hankel singular values in decreasing magnitudes. The user will response by entering through the keyboard the number of states to be retained. This defines the order of the reduced-order model.

Model update will not be conducted if  $R$  is unstable or if it will result in an unstable model. Warnings will be given under these conditions.

This program calls the function `fwbalred.m`. Therefore it will not be executed unless the `fwbalred.m` function is present.

#### 10. **mfres\_plot.m**

This program plots the frequency responses of the plant and the models on the same graph for comparison.

This program can be executed at any time after `init.m` is executed, provided that  $G$  and  $G_i$  are defined.

### Simulation Information

To perform the type of simulations described in Chapter 2, we do the following according to the sequence in which it is described.

1. Modify the vectors **nG** and **dG** in **plant.m** to reflect the plant of interest.
2. Modify the vectors **nGi** and **dGi** in **model.m** to describe the initial model of the plant.
3. Choose a small value for  $\lambda$  so that robust stability can be achieved. Trial and error may be necessary to find a suitable  $\lambda$  to begin with. The chosen value of  $\lambda$  will be entered through the keyboard by defining the variable **lambda**.
4. Set the value of **nm** to 0 (through the keyboard) follows by executing **model.m**.

5. Execute the m-files in the following sequence:

**plant, target, q\_control, k\_control, init, time\_plot**

and print (or store) the required graphs for record.

6. If the step response does not show excessive oscillations or overshoot, increase the value of **lambda** and repeat Step 6. Otherwise, execute **rhat\_iter.m** to perform frequency weighted model approximation for  $R$ .
7. Execute **update.m** to obtain the reduced-order updated model. We usually truncate the order of the model at the point where the Hankel singular value is small and where a large decrease (usually by an order) occurs in the Hankel singular values. The resulting values for **nGi** and **dGi** will be displayed.
8. Perform the iteration by repeating the sequence of program executions starting from Step 6. Continue until the desired value of **lambda** is achieved or until no further improvement can be made.



## Chapter 3

### Program Descriptions

#### 1. **mq\_controlss.m**

Its function is similar to that of **q\_control.m**, except that a  $Q$  transfer function of relative degree one (instead of bi-proper) will be calculated.

#### 2. **k\_controlss.m**

Its function is similar to that of **k\_control.m**. To be used with **mq\_controlss.m**.

#### 3. **initss.m**

Its function is similar to that of **init.m**. To be used with **mq\_controlss.m** and **k\_controlss.m**.

#### 4. **deress1.m**

This program calculates and plots the noiseless step response of the designed closed-loop system. The variable **probe** is used to turn on (when sets to 1) or turn off (when sets to 0) the low amplitude sinusoids that are superimposed on the unit step input to the actual closed-loop system. The vector **efm** defines the amplitude for each of the sinusoids. The vector **ef** defines the angular frequency for each of the sinusoids.

It is necessary to make sure that the vectors **efm** and **ef** have the same length. The variable **probe** has to be defined for example, by executing the statement **probe=1** (which turns on the sinusoidal probing signals) before **deress1.m** is executed.

#### 5. **time\_plotss.m**

Its function is similar to that of **time\_plot.m**, except that its output will depend on whether **deress1.m** or **deress2.m** (to be described later for performing simulations that are related to Chapter 4) was executed. If **deress1.m** was executed, **time\_plotss.m** will calculate and plot the noiseless actual *step response*. If **deress2.m** was executed, **time\_plotss.m** will calculate and plot the noiseless actual *square wave response*.

## 6. `noisy_t_plotss.m`

This program plots the noisy response of the actual closed-loop system. The type of response produced will depend on whether `deress1.m` or `deress2.m` was executed (similar to the way that `time_plotss.m` responds to `deress1.m` and `deress2.m`). The variable `nm` defines the square root of the variance of the zero mean Gaussian white noise disturbance  $e$ . This noise disturbance passes through the transfer function  $H$  before it is added to the plant output.

The variable `nm` has to be defined, for example by executing the statement `nm=0.05` (which results in a noise energy density of 0.0025) before `noisy_t_plotss.m` is executed.

## 7. `siggenss.m`

This program generates the signals needed in closed-loop system identification by Hansen's framework. A low-pass data filter is included. The bandwidth of the data filter is defined by the variable `bw`. The signals generated is suitable for the identification of the unknown part of  $R$ .

We usually (but not always) set the value of the variable `bw` from two to ten times of the value of `lambda`.

## 8. `mrhat_idenss.m`

This program identifies  $R$  indirectly by identifying the unknown part of  $R$ . Output Error or Box-Jenkins model can be selected by making simple (and obvious) modifications to this program. The vector `Nn` defines the structure of the plant model  $\hat{R}_i^f$ , and the corresponding noise model  $\hat{\Psi}_i^f$ .

The vector `Nn` has to be defined, for example, by executing the statement `Nn= [4 6 6 4 1]` if Box-Jenkins model structure is assumed (or the statement `Nn= [4 4 1]` if Output Error model structure is assumed). Note that  $\hat{\Psi}_i^f = 1$  if Output Error model structure is assumed. (See MATLAB™ System Identification Toolbox user's guide for details.)

## 9. `tupdatess.m`

This program updates the current model to a new model through the identified model of  $R$  produced by `mrhat_idenss.m`. Model update will not be conducted if  $R$  is unstable or if it will result in an unstable model. Warnings will be given under these conditions.

The current model are saved before model updating is performed. This will allow resetting if the updated model is found to be inaccurate.

The possibility of resetting the model from a poor updated model back to the model before updating is not used in the simulations of Chapter 3. This will be useful in Chapter 4 when model validation methods become available.

#### 10. **mreducss.m**

This program performs frequency weighted balanced truncation model reduction on the updated model. It shows the Hankel singular values in decreasing magnitudes. The user will response by entering through the keyboard the number of states to be retained. This defined the order of the reduced-order model.

This program calls the function **fwbalred.m**. Therefore it will not be executed unless the **fwbalred.m** function is present.

### Simulation Information

To perform the type of simulations described in Chapter 3, we do the following according to the sequence in which it is described.

1. Modify the vectors **nG**, **dG**, **nH**, and **dH** in **plant.m** to describe the plant (including the noise transfer function  $H$ ) of interest. For the simulations in Chapter 3, we have set  $H = 1$ .
2. Modify the vectors **nGi** and **dGi** in **model.m** to describe the initial model of the plant.
3. Choose a small value for  $\lambda$  so that robust stability can be achieved. Trial and error may be necessary to find a suitable  $\lambda$  to begin with. The chosen value of  $\lambda$  will be entered through the keyboard by defining the variable **lambda**.
4. Choose the value of the noise variance to reflect the situation at hand. The value of **nm** should then be entered through the keyboard. For the simulations in Chapter 3, we use a noise variance (energy density) of 0.0025. This is accomplished by setting **nm=0.05**.
5. Execute the program **model.m**.
6. Execute the m-files in the following sequence:

---

**plant, target, mq\_controlss, k\_controlss, initss, deress1, time\_plotss,  
noisy\_t\_plotss**

and print (or store) the required graphs for record.

7. If the step response does not show excessive oscillations or overshoot, increase the value of **lambda** and repeat Step 7. Otherwise, execute **siggenss.m** to prepare for the identification of  $R$ . (We may repeat the previous steps with sinusoids superimposed on the step reference input to improve the excitation conditions before **siggenss.m** is executed. The adding of sinusoidal excitations to the step reference input can be accomplished by modifying the vectors **efm** and **ef** in **deress1.m**.)
8. Execute **mrhat\_idenss.m** to identify  $R$ .
9. Execute **tupdatess.m** followed by **mreducss.m** to obtain the reduced-order updated model. We usually truncate the order of the model at the point where the Hankel singular value is small and a large decrease (usually by an order) occurs in the Hankel singular values occurs. The resulting values of **nGi** and **dGi** will be displayed.
10. Perform the iteration by repeating the sequence of program executions starting from Step 7. Continue until the desired value of **lambda** is achieved or until no further improvement can be made.

## Chapter 4

### Program Descriptions

#### 1. **deress2.m**

This program calculates and plots five periods of the noiseless square wave response. The variable **switch** is used to turn on (when sets to 1) or turn off (when sets to 0) the square wave reference input to the designed and actual closed-loop systems.

When the square wave input is turned off, the closed-loop output error is purely due to the noise disturbance. When the square wave input is turned on, the closed-loop output error is due to both the reference excitation and the noise disturbance. By comparing the power spectra of these closed-loop output errors (under the two different conditions that we have just described), we can validate the model in question in the frequency domain under closed-loop conditions.

#### 2. **testrs.m**

This program performs the time domain method of model validation. It calls the function **mresid.m**. This is accomplished by residual analysis as described in [Ljung 1987], except that it is performed within the Hansen's framework.

This program will not be executed if the **mresid.m** function is absent.

#### 3. **preset.m**

This program resets  $\hat{R}_i^f$  to 0 and  $\hat{\Psi}_i^f$  to 1. (These notations are defined in Chapter 4.) This will allow the current model to be updated.

It is a good practice to execute this program once an accurate reduced order updated model is found, and the recent estimated values of  $\hat{R}_i^f \neq 0$  and  $\hat{\Psi}_i^f \neq 1$  are no longer needed.

#### 4. **snrchk1.m**

This program calculates the power spectrum of the closed-loop output error. This will be useful for performing the frequency domain model validation when it is combined with the **switch** variable that was described with **deress2.m**.

When the current model is falsified by the frequency domain model validation test, the range of frequency where there are significant signal-to-noise ratio for identifying  $\check{R}_i^f$  can be estimated. We usually select the bandwidth of the (low-pass) data filter to be this frequency range.

#### 5. **cloe.m**

This program is used to calculate the closed-loop output error before **snrchk1.m** is executed to validate models in the frequency domain.

To prepare for validating an updated or reduced order model, **initss.m** and **deress2.m** should be executed before **cloe.m** is executed.

To prepare for validating the current model, execute **cloe.m** after **noisy\_t\_plotss.m** is executed.

#### 6. **recover.m**

This program resets the model back to the one before the latest model update was carried out. It is used, for example, to prepare for model re-updating after an updated model (before or after model reduction) is found to be inaccurate by the frequency domain model validation method.

### Simulation Information

To perform the type of simulations described in Chapter 4, we do the following according to the sequence in which it is described.

1. Modify the vectors **nG**, **dG**, **nH**, and **dH** in **plant.m** to reflect the plant (including the noise transfer function  $H$ ) of interest. For the simulations in Chapter 4, we have set  $H = 1$ .
2. Modify the vectors **nGi** and **dGi** in **model.m** to describe the initial model of the plant.
3. Choose a small value for  $\lambda$  so that robust stability can be achieved. Trial and error may be necessary to find a suitable  $\lambda$  to begin with. The chosen value of  $\lambda$  will be entered through the keyboard by defining the variable **lambda**.

4. Choose the value of the noise variance to reflect the situation at hand. The value of **nm** should then be entered through the keyboard. For the simulations in Chapter 3, we use a noise variance (energy density) of 0.0025. This is accomplished by setting **nm=0.05**.
5. Execute the program **model.m**.
6. Set the variable **switch** to 1.
7. Execute the m-files in the following sequence:  
  
**plant, target, mq\_controlss, k\_controlss, initss, deress2, time\_plotss,  
noisy\_t\_plotss**  
  
and print (or store) the required graphs for record.
8. Define the bandwidth **bw** of the low-pass data filter. (We usually choose **bw=10\*lambda** at the beginning stage of simulation.)
9. Perform the time domain model validation test (by executing **siggenss.m** and **testrs.m**) to check the validity of the current model. If the current model passes the time domain model validation test, increase the value of **lambda** and repeat Step 7. If the current model fails the time domain model validation test, increase the value of **lambda** and repeat from the previous step. The frequency domain model validation test should be carried out and the results should be closely monitored. (This will require the execution of **cloe.m** and **srchk1.m** on the basis of data obtained in Step 7 when the variable **switch** is set to 1, and the execution of **cloe.m** and **srchk1.m** on the basis of data obtained by repeating Step 7 but with the variable **switch** set to 0, so that the power spectra of the closed-loop output errors with and without the square wave reference input can be compared.) Proceed to the next step when the current model fails the frequency domain model validation test.
10. To prepare for the identification of  $R$ , use the results of frequency domain model validation test obtained in the last step as a guide to set the value of **bw**, such that the bandwidth of the data filter includes only frequency range where the closed-loop output error has good signal-to-noise ratio. Then execute **siggenss.m** to prepare for the identification of  $R$ . The signals to be employed in this step are obtained by executing **initss.m**, **deress2.m**, **time\_plotss.m**, and **noisy\_t\_plot.m** in the given order and under the conditions where **switch** is set to 1.

11. Execute **mrhat\_idenss.m** to identify  $R$ . (It is actually the unknown part of  $R$  that is estimated.) Once an estimate of  $R$  is found, execute **testrs.m** immediately to validate the estimate of  $R$  in the time domain. It is often necessary to experiment with different model structures (by defining the vector  $\mathbf{Nn}$  accordingly) before an estimate of  $R$  that passes the time domain model validation test can be found. If the identified model for  $R$  passes the time domain model validation test, proceed to the next step.

If extensive experimentation with different choices of model structures did not produce good models, it may be necessary to increase the value of **lambda** in an attempt to improve the signal-to-noise ratio of the closed-loop output error (assuming the data record length remain fixed) before repeating the identification step. This has to be performed carefully to prevent instability. If this action still does not improve the results of identification, the iterative process may have to be terminated.

In performing simulation experiments, we can estimate the order of the unknown part of  $R$  (usually about twice that of the plant) because we know the plant exactly. (This is of course not true for a real plant in practice.) In our simulation experience, we have never need to use such a high order transfer function for estimating the unknown part of  $R$ . For example, in the simulation example presented in Section 4.8, where the plant is sixth order, using a fourth order model structure for the unknown part of  $R$  (with  $\mathbf{Nn} = [4 \ 5 \ 5 \ 4 \ 1]$ ) gave very good results.

12. Execute **tupdatess.m** to update the model. Verify the updated model by executing **plant.m**, **deress2.m**, **cloe.m**, and **snrchk1.m** in the given order. This checks whether the closed-loop output error is now mainly due to the effects of the noise disturbance. If the updated model fails the above frequency domain model validation test, reset the model back to the one before the latest model update was performed (this will require you to save the model before **tupdatess.m** was executed) and repeat the system identification exercise as it was described previously. (Collection of new data for a larger designed closed-loop bandwidth may be necessary.) If the updated model passes the frequency domain model validation test, proceed to the next step.
13. Perform model reduction by executing **mreducss.m**. We usually truncate the order of the model at the point where the Hankel singular value is small and a large decrease (usually by an order) occurs in the Hankel singular values. The resulting values of  $\mathbf{nGi}$  and  $\mathbf{dGi}$  will be displayed.



Perform frequency domain model validation test on the reduced-order model exactly like the way the updated model (before model order reduction was performed) was tested. It may be necessary to reset the model to the one before the latest system identification was carried out (use **recover.m**), re-update the model (use **tupdatess.m**), and re-perform model reduction (use **mreducss.m**) if the frequency domain model validation test indicates that the model order truncation was too drastic.

If the reduced order model is validated by the frequency domain model validation test, execute **preset.m** before proceed to the next step.

14. Perform the iteration by repeating the sequence of program executions starting from Step 7. Continue until the desired value of **lambda** is achieved or until no further improvement can be made.

## Chapter 5

### Program Descriptions

#### 1. **usqwnf1.m**

This program calculate the  $Q$  transfer function for the situation of unstable plants. The IMC filter used in this program is the one proposed in [Campi *et al.* 1994]. A summary of the main points for this design method is given in Chapter 5. The design parameters are  $\lambda$  (which defines the designed closed-loop bandwidth) and  $\gamma$  (which control the tradeoff between the overshoot and the recovery time after the overshoot has occurred).

The variables  $\lambda$  and  $\gamma$  must be defined before this program can be executed.  $\lambda$  is defined through the variable **lambda** as we have described in the **target.m** program for Chapter 2. The parameter  $\gamma$  can be defined, for example, by executing the statement **gamma=0.01\*lambda**.

#### 2. **usk\_control.m**

This program calculate the controller for the situation of unstable plants.

#### 3. **usk\_initss.m**

This program performs the same function as **initss.m** but for the situation of unstable plants.

### Simulation Information

1. The programs **usqwnf1.m**, **usk\_control.m**, and **usk\_initss.m** are useful for performing simulations for one step design approach in the situation of unstable plants.

For this purpose, we proceed by executing **plant.m**, **model.m** target, **usqwnf1**, **usk\_control**, **initss**, **deress2.m** (after making appropriate modifications to the m-files like **plant.m** and **model.m**, and initializing the relevant variables like **lambda** and **gamma**) to obtain results similar to those presented in Figures 5.4 to 5.7.

2. To perform simulations for the two step iterative identification and control design approach in the situation of unstable plants, we first design a parallel feedback stabilizer

$C$  on the basis of a given unstable model  $\bar{P}$  for the unstable plant  $P$  (as it was described in Chapter 5). The designed parallel feedback stabilizer  $C$  will then allow us to calculate the stabilized plant  $G$ , the noise transfer function  $H$  (which includes the effects of the unstable plant  $P$ , the stabilizer  $C$ , and the original noise transfer function  $H_1$ ), and the stable initial model  $G_0$ . (Note that we use the notations defined in Chapter 5.) These transfer functions will be used to set up the  $G$  and  $H$  in **plant** and the  $G_i$  in **model.m**. We can now start the simulation of the second step where iterative identification and control design is applied to the stabilized plant  $G$  (on the basis of the stable models  $G_i$  of  $G$ ). Starting from here, the simulation procedure is the same as what we have described for Chapter 4 and we will not elaborate further.

# Bibliography

- ANDERSON B.D.O. (1985). Adaptive systems, lack of persistency of excitation and bursting phenomena. *Automatica* Vol. 21, pp. 247-258.
- ANDERSON B.D.O. AND R.L. KOSUT (1991). Adaptive robust control: On-line learning. *Proc. IEEE CDC'91* pp. 297-298.
- ANDERSON B.D.O. AND Y. LIU (1989). Controller reduction: Concepts and approaches. *IEEE Trans. Automat. Contr.* Vol. 34, pp. 802-812.
- ANDERSON B.D.O., R.R. BITMEAD, C.R. JOHNSON, JR., P.V. KOKOTOVIC, R.L. KOSUT, I.M.Y. MAREELS, L. PRALY AND B.D. RIEDLE (1986). *Stability of Adaptive Systems: Passivity and Averaging Analysis*. MIT Press. Cambridge MA., USA.
- ASTRÖM K.J. (1993). Matching criteria for identification and control. *Proc. 2<sup>nd</sup> European Control Conference* pp. 248-251.
- ASTRÖM K.J. AND B. WITTENMARK (1989). *Adaptive Control*. Addison-Wesley. Reading MA., USA.
- BITMEAD R.R., M. GEVERS AND V WERTZ (1990). *Adaptive Optimal Control: The Thinking Man's GPC*. Prentice Hall. VIC., Australia.
- BODSON M. (1993). Pseudo-burst phenomenon in ideal adaptive systems. *Automatica* Vol. 29, pp. 929-940.
- BONGERS P.M.M. AND O.H. BOSGRA (1990). Low order robust  $calH_{\infty}$  controller synthesis. *Proc. IEEE CDC'90* pp. 194-199.
- BOYD S.P. AND C.H. BARRATT (1989). *Linear Controller Design: limits on performance*. Prentice-Hall. Englewood Cliffs NJ., USA.

- BOYD S.P. AND J.C. DOYLE (1987). Comparison of peak and rms gains for discrete-time systems. *Syst. Control Letters* Vol. 9, pp. 1–6.
- CALLIER F.M. AND C.A. DESOER (1982). *Multivariable Feedback Systems*. Springer-Verlag. NY., USA.
- CAMPI M., W.S. LEE AND B.D.O. ANDERSON (1994). New filters for internal model control design. *to appear in Int. J. Robust and Nonlinear Control*.
- D'AZZO J.J. AND C.H. HOUPIS (1988). *Linear Control System Analysis and Design: Conventional and Modern*. McGraw-Hill. NY., USA.
- DE CALLAFON R.A., P.M.J. VAN DEN HOF AND M. STEINBUCH (1993). Control relevant identification of a compact disc pickup mechanism. in *Selected Topics in Identification, Modelling and Control* (O.H. Bosgra and P.M.J. Van den Hof, Eds.). Vol. 6. pp. 11–19. Delft University Press. Delft, The Netherlands.
- DE VRIES D.K. AND P.M.J. VAN DEN HOF (1993). Quantification of uncertainty in transfer function estimation: a mixed deterministic-probabilistic approach. *Preprints IFAC 12<sup>th</sup> Triennial World Congress* Vol. 8, pp. 157–160.
- DE VRIES D.K. AND P.M.J. VAN DEN HOF (1994). Quantification of model uncertainty from data. *Int. J. Robust and Nonlinear Control* Vol. 4, pp. 301–319.
- DORATO P. (1986). Robust control: A historical review. *Proc. IEEE CDC'86* pp. 346–349.
- DOYLE J.C. (1984). *Lecture Notes*. ONR/Honneywell Workshop on Advances on Multivariable Control. Minneapolis MN., USA.
- DOYLE J.C. AND G. STEIN (1981). Multivariable feedback design: Concepts for a classical/modern synthesis. *IEEE Trans. Automat. Contr.* Vol. 26, pp. 4–16.
- DOYLE J.C., B.A. FRANCIS AND A.R. TANNENBAUM (1992). *Feedback Control Theory*. Macmillan. NY., USA.
- FRANCIS B.A. AND W.M. WONHAM (1976). The internal model principle of control theory. *Automatica* Vol. 12, pp. 457–465.
- FRANKLIN G.F., J.D. POWELL AND A. EMAMI-NAEINI (1986). *Feedback Control of Dynamic Systems*. Addison-Wesley. Reading MA., USA.

- FREUDENBERG J.S. AND D.P. LOOZE (1985). Right half plane poles and zeros and design tradeoffs in feedback systems. *IEEE Trans. Automat. Contr.* Vol. 30, pp. 555–565.
- GEVERS M. (1993). Towards a joint design of identification and control?. in *Essays on Control: Perspectives in the Theory and its Applications* (H.L. Trentelman and J.C. Willems, Eds.). pp. 111–151. Birkhäuser. Boston MA., USA.
- GEVERS M. AND L. LJUNG (1986). Optimal experiment designs with respect to the intended model application. *Automatica* Vol. 22, pp. 543–554.
- GOODWIN G.C. AND K.S. SIN (1984). *Adaptive Filtering, Prediction and Control*. Prentice-Hall. Englewood Cliffs NJ., USA.
- GOODWIN G.C., D.J. HILL AND N. PALANISWAMI (1985). Towards an adaptive robust controller. *Proc. IFAC Symposium on Identification and System Parameter Estimation* pp. 997–1002.
- GOODWIN G.C., M. GEVERS AND B.M. NINNESS (1992). Quantifying the error in estimated transfer functions with application to model order selection. *IEEE Trans. Automat. Contr.* Vol. 37, pp. 913–928.
- GRAEBE S.F. AND G.C. GOODWIN (1993). An incremental estimation technique for predicting a bandwidth of robust performance. *Proc. IEEE CDC'93* pp. 2260–2265.
- HAKVOORT R.G., R.J.P. SCHRAMA AND P.M.J. VAN DEN HOF (1994). Approximate identification with closed-loop performance criterion and application to LQG feedback design. *Automatica* Vol. 30, pp. 679–690.
- HANSEN F.R. (1989). A Fractional Representation Approach to Closed-loop System Identification and Experiment Design. PhD thesis. Stanford University. Stanford CA., USA.
- HANSEN F.R. AND G.F. FRANKLIN (1988). On a fractional representation approach to closed-loop experiment design. *Proc. ACC'88* pp. 1319–1320.
- HANSEN F.R., G.F. FRANKLIN AND R.L. KOSUT (1989). Closed-loop identification via the fractional representation: Experiment design. *Proc. ACC'89* pp. 1422–1427.
- HELMICKI A.J., C.A. JACOBSON AND C.N. NETT (1991). Control oriented system identification: A worst-case/deterministic approach in  $\mathcal{H}_\infty$ . *IEEE Trans. Automat. Contr.* Vol. 36, pp. 1167–1176.

- IGLESIAS P.A. (1990). On the use of robust regulators in adaptive control. *Proc. IFAC 11<sup>th</sup> Triennial World Congress* pp. 369–374.
- KAILATH T. (1980). *Linear Systems*. Prentice Hall. Englewood Cliffs NJ., USA.
- KOKOTOVIC P.V., H.K. KHALIL AND J. O'REILLY (1986). *Singular Perturbation Methods in Control: Analysis and Design*. Academic Press. London, UK.
- KOSUT R.L. (1986). Adaptive calibration: An approach to uncertainty modeling and on-line robust control design. *Proc. IEEE CDC'86* pp. 455–461.
- KOSUT R.L. (1994). Adaptive control via parameter set estimation. *Int. J. Adaptive Control and Signal Processing* Vol. 2, pp. 371–399.
- KOSUT R.L., I.M.Y. MAREELS, B.D.O. ANDERSON, R.R. BITMEAD AND C.R. JOHNSON, JR. (1987). Transient analysis of adaptive control. *Proc. IFAC 10<sup>th</sup> Triennial World Congress* pp. 127–132.
- KOSUT R.L., M.K. LAU AND S.P. BOYD (1992). Set-membership identification of systems with parametric and nonparametric uncertainty. *IEEE Trans. Automat. Contr.* Vol. 37, pp. 929–941.
- KWAKERNAAK H. (1993). Robust control and  $\mathcal{H}_\infty$ -optimization- tutorial paper. *Automatica* Vol. 29, pp. 255–273.
- LAMAIRE R.O., L. VALAVANI, M. ATHANS AND G. STEIN (1991). A frequency domain estimator for use in adaptive control systems. *Automatica* Vol. 27, pp. 23–38.
- LEE W.S., B.D.O. ANDERSON, R.L. KOSUT AND I.M.Y. MAREELS (1993). A new approach to adaptive robust control. *Int. J. Adaptive Control and Signal Processing* Vol. 7, pp. 183–211.
- LEON DE LA BARRA B.A. (1992). Zeros and Their Influence on Time and Frequency Domain Properties of Scalar Feedback Systems. PhD thesis. University of Newcastle. Newcastle NSW., Australia.
- LIU K. AND R.E. SKELTON (1990). Closed-loop identification and iterative control design. *Proc. IEEE CDC'90* pp. 482–487.
- LJUNG L. (1985). Asymptotic variance expressions for identified black-box transfer models. *IEEE Trans. Automat. Contr.* Vol. 30, pp. 834–844.

- LJUNG L. (1987). *System Identification: Theory for the user*,. Prentice-Hall. Englewood Cliffs NJ., USA.
- LJUNG L. (1988). *System Identification Toolbox for use with MATLAB<sup>TM</sup>: User's Guide*,. The Math Works, INC.. South Natick, MA., USA.
- LJUNG L. AND B.D.O. ANDERSON (1984). Adaptive control, where are we?. *Automatica* Vol. 20, pp. 499–500.
- LJUNG L., B. WAHLBERG AND H. HJALMARSSON (1991). Model quality: The roles of prior knowledge and data information. *Proc. IEEE CDC'91* pp. 273–278.
- MAREELS I.M.Y. AND R.R. BITMEAD (1987). Nonlinear dynamics in adaptive control: chaotic and periodic stabilization. *Automatica* Vol. 22, pp. 641–665.
- McFARLANE D. AND K. GLOVER (1990). *Robust Controller Design Using Normalized Coprime Factor Plant Descriptions*. Springer-Verlag. Berlin, Germany.
- MIDDLETON R.H. AND G.C. GOODWIN (1990). *Digital Control and Estimation - A Unified Approach*. Prentice-Hall. Englewood Cliffs NJ., USA.
- MORARI M. AND E. ZAFIRIOU (1989). *Robust Process Control*. Prentice-Hall. Englewood Cliffs NJ., USA.
- NEWTON, JR. G.C., L.A. GOULD AND J.F. KAISER (1957). *Analytical Design of Linear Feedback Controls*. John Wiley and Sons. NY., USA.
- ORTEGA R. AND Y TANG (1989). Robustness of adaptive controllers - a survey. *Automatica* Vol. 25, pp. 651–677.
- OWENS D.H. AND R.E. SKELTON (1985). Workshop Editorial. *IFAC Workshop on Model Error Concepts and Compensation* pp. ix–xi.
- PARKER P.J. AND R.R. BITMEAD (1987). Adaptive frequency response identification. *Proc. IEEE CDC'87* pp. 348–353.
- PARTANEN A.G. AND R.R. BITMEAD (1993a). Closed-loop identification for disturbance rejection in a sugar cane crushing mill. *submitted to Automatica in 1993*.
- PARTANEN A.G. AND R.R. BITMEAD (1993b). Excitation versus control issues in closed-loop identification of plant models for a sugar cane crushing mill. *Preprints IFAC 12<sup>th</sup> Triennial World Congress* Vol. 9, pp. 49–52.



- PARTANEN A.G. AND R.R. BITMEAD (1993c). Two stage iterative identification/control design and direct experimental controller refinement. *Proc. IEEE CDC'93* pp. 2833–2838.
- PARTANEN A.G., Z. ZANG, R.R. BITMEAD AND M. GEVERS (1994). Experimental restricted complexity controller design. *Proc. 10<sup>th</sup> IFAC Symposium on System Identification* Vol. 2, pp. 177–182.
- PARTINGTON J.R. (1991). Robust identification and interpolation in  $\mathcal{H}_\infty$ . *Int. J. Control* Vol. 54, pp. 1281–1290.
- RIVERA D.E. (1991). Control-relevant parameter estimation: A systematic procedure for prefilter design. *Proc. ACC'91* pp. 237–241.
- SASTRY S. AND M. BODSON (1989). *Adaptive Control: Stability, Convergence, and Robustness*. Prentice-Hall. Englewood Cliffs NJ., USA.
- SCHRAMA R.J.P. (1992a). Accurate identification for control: The necessity of an iterative scheme. *IEEE Trans. Automat. Contr.* Vol. 37, pp. 991–994.
- SCHRAMA R.J.P. (1992b). Approximate Identification and Control Design. PhD thesis. Delft University of Technology. Delft, Netherlands.
- SCHRAMA R.J.P. AND P.M.J. VAN DEN HOF (1992). An iterative scheme for identification and control design based on coprime factorizations. *Proc. ACC'92* pp. 2842–2846.
- SHIMKIN N. AND A. FEUER (1988). On the necessity of "block invariance" for the convergence of adaptive pole-placement algorithms with persistently exciting input. *IEEE Trans. Automat. Contr.* Vol. 33, pp. 775–780.
- SKELTON R.E. (1985). On the structure of modeling errors and the inseparability of the modeling and control problems. *IFAC Workshop on Model Error Concepts and Compensation* pp. 13–20.
- SKELTON R.E. (1989). Model error concepts in control design. *Int. J. Control* Vol. 49, pp. 1725–1753.
- SKELTON R.E., K.M. GRIGORIADIS AND G. ZHU (1994). An algorithm for iterative identification and control design using an improved Q-markov cover. *Proc. 10<sup>th</sup> IFAC Symposium on System Identification* Vol. 2, pp. 183–188.

- SÖDERSTRÖM T. AND P. STOICA (1988). *System Identification*. Prentice-Hall International. Hemel Hempstead, UK.
- TAY T.T., J.B. MOORE AND R. HOROWITZ (1989). Indirect adaptive techniques for fixed controller performance enhancement. *Int. J. Control* Vol. 50, pp. 1941–1989.
- VAN DEN HOF P.M.J. AND R.J.P. SCHRAMA (1993). An indirect method for transfer function estimation from closed-loop data. *Automatica* Vol. 29, pp. 1523–1527.
- VAN DEN HOF P.M.J. AND R.J.P. SCHRAMA (1994). Identification and control - closed loop issues. *Proc. 10<sup>th</sup> IFAC Symposium on System Identification* Vol. 2, pp. 1–13.
- VAN DEN HOF P.M.J., R.J.P. SCHRAMA, O.H. BOSGRA AND R.A. DE CALLAFON (1993). Identification of normalized coprime plant factors for iterative model and controller enhancement. *Proc. IEEE CDC'93* pp. 2839–2844.
- VIDYASAGAR M. (1985a). *Control System Synthesis: A Factorization Approach*. MIT Press. Cambridge MA., USA.
- VIDYASAGAR M. (1985b). Robust stabilization of singularly perturbed systems. *Systems and Control Letters* Vol. 5, pp. 413–418.
- WAHLBERG B. AND L. LJUNG (1986). Design variables for bias distribution in transfer function estimation. *IEEE Trans. Automat. Contr.* Vol. 31, pp. 134–144.
- WAHLBERG B. AND P. LINDSKOG (1991). Approximate modeling by means of orthogonal functions. in *Modeling, Estimation and Control of Systems with Uncertainty* (G.B. Di Masi, A. Gombani and A.B. Kurzhansky, Eds.). pp. 449–467. Birkhäuser. Boston MA., USA.
- YOULA D.C., J.J. BONGIORNO AND C.N. LU (1974). Single-loop feedback-stabilization of linear multivariable dynamical plants. *Automatica* Vol. 10, pp. 159–173.
- ZAMES G. (1981). Feedback and optimal sensitivity: Model reference transformations, multiplicative seminorms, and approximate inverses. *IEEE Trans. Automat. Contr.* Vol. 26, pp. 301–320.
- ZAMES G. AND L.Y. WANG (1992). Adaptive vs robust control: Information based concepts. *Proc. IFAC Adaptive Systems in Control and Signal Processing* pp. 187–190.

- ZANG Z. (1992). Performance Analysis and Enhancement of Adaptive Control Systems. PhD thesis. The Australian National University. Canberra ACT., Australia.
- ZANG Z. AND R.R. BITMEAD (1990). Transient bounds for adaptive control systems. *Proc. IEEE CDC'90* pp. 2724–2729.
- ZANG Z. AND R.R. BITMEAD (1994). Transient bounds for adaptive control systems. *IEEE Trans. Automat. Contr.* Vol. 39, pp. 171–175.
- ZANG Z., R.R. BITMEAD AND M. GEVERS (1991).  $\mathcal{H}_2$  iterative model refinement and control robustness enhancement. *Proc. IEEE CDC'91* pp. 279–284.
- ZANG Z., R.R. BITMEAD AND M. GEVERS (1992). Disturbance rejection: On-line refinement of controllers by closed loop modelling. *Proc. ACC'92* pp. 1829–1833.